A two-stage biorefinery for renewable industrial chemical production



Nicholas A. Tenci

Linacre College
University of Oxford

A thesis submitted for the degree of
Doctor of Philosophy in Engineering Science
Trinity Term 2024

This thesis is dedicated to Patricia Poff and Fedora Tenci.

Statement

The following thesis includes both published and unpublished work. Several chapters are thus presented in manuscript format, consistent with the 'integrated thesis' format as defined by the relevant rules of the Department of Engineering Science at the University of Oxford. **Chapters 3**, **4**, **5** and **Section 7.1** of **Chapter 7** are in manuscript format.

For specific information, please refer to the introductory disclaimer provided to each chapter which details the publication status of the data therein.

Acknowledgements

I must firstly thank my supervisors Professors Ian P. Thompson and Wei E. Huang, without whom this thesis would not have been possible. Ian, I must extend particular thanks to you for the huge assistance you have provided me across every facet of this D.Phil., from your help navigating the complexities of funding this project, to your assistance in managing uncooperative bacteria. I have thoroughly enjoyed our regular Friday meetings, both as an opportunity to resolve lab-related frustrations and to chat about the state of the world. I consider myself very fortunate to have been under your tutelage. Wei, thank you for your enthusiastic feedback in our meetings and for the employment opportunities offered by your spinout companies, these provided a particularly novel angle to my D.Phil. experience.

I must also extend huge thanks to the organisations whose generous financial assistance made this D.Phil. possible: East Alpha LLP. for their generous funding of my course fees and Rotary International, for their provision of a stipend. In particular I must thank Claire Ramsay for her effort in making this latter scholarship possible and Rev. Dr. Derek Spears for receiving me so warmly at Rotary Pangbourne, and for his camaraderie as a fellow D.Phil. student.

Perhaps most of all, I would like to thank my family for their unwavering support of me in this daunting and often lonely undertaking. To my fiancé, Emanuele, I thank you for your unshakeable belief in me over the past few years and for your constant encouragement. To my family back in New Zealand, my parents Silvio and Bernadette and my sisters, Sophie and Polly, thank you for your constant moral, emotional, and in the case of my parents, financial support.

I would also like to acknowledge the many people who made my time at Oxford what it was, from May Sin Ke and Gulsah Albayrak, among the first friends I made upon arriving in Oxford, and with whom I share fond memories of our work in the Covid testing labs at Luton Airport, to Charlotte Ball, Mala Gunadasa-Rohling, Pete Young, Gerardo Montalvo, and many others for making Linacre College a home away from home, and to Simon Marchant, Morgan Wade, Vinayak Dewan, and Surbhi Sachdeva. I must also acknowledge my fellow lab members in Lab 43 and at Begbroke Science Park: Jochem Nielsen, Haris Saeed, Reza Rohani, Yutong Yin, Weiming Tu and my postdocs Dr. Fariza Ammam and Dr. Nichola Austen. A particularly special mention must be given to Laura Martin for being my closest collaborator over these past few years.

Declaration

I declare that the work in this thesis is entirely my own with the exception of the following contributions:

Chapter 3

Dr. Fariza Ammam assisted with the setup of the batch experiments in this chapter and with the revision of the resulting manuscript, of which she is a co-author.

Chapter 4

The work in this chapter and the manuscript arising therefrom was undertaken in collaboration with Dr. Nichola Austen, who contributed equally to the experimental and writing work and who accordingly shares co-first authorship of this manuscript.

Chapter 5

The experimental setup of the batch experiments in this chapter was assisted by Dr. Fariza Ammam. Dr. Nichola Austen assisted with the processing of samples. Both provided feedback on the resulting manuscript and are listed as co-authors.

Chapter 6

The agave fermentates used for several of the experiments in this chapter were provided by Dr. Fariza Ammam.

Chapter 7

Assistance with the optimisation of the organic extraction, derivatisation, and quantification of PHA monomers was provided by Weiming Tu.

Abstract

The concept of the 'biorefinery', in which biomass is converted into fuels, chemicals, and other products, holds promise for the transition from a fossil-carbon economy to a more sustainable paradigm based on biological carbon sources. However, while biological alternatives to some conventional petroleum products already exist, their deployment is hampered by their high-cost relative to their conventional fossil-based alternatives. Feedstocks, often taking the form of pure sugars, can represent a major source of this cost. Purification and intermediate processing steps add yet further cost. This thesis thus focused on the acidogenic fermentation of biomass to produce low-cost volatile fatty acids (VFA) and on refining of these to polyhydroxyalkanoate (PHA) bioplastics. The chapters of this thesis accordingly correspond to the nodes along this bioproduction process, from the fermentation of biomass to VFA, post-treatment of the fermentates, and finally bioproduction of PHA, with each endeavouring to yield process improvements which may contribute to overall process efficiency.

The acidogenic fermentation of the dryland Crassulacean Acid Metabolism (CAM) crop *Euphorbia tirucalli* is analysed in a co-fermentation format with a high protein substrate – pig blood. Co-fermentation was found to produce little improvement in overall VFA production, with the highest VFA titres found in blood mono-digestions (38 ±2 g/L), from an initial substrate concentration of 60 g/L volatile solids. The use of a co-substrate did however have a significant impact on acetate titres however, with acetic acid titres in a mixed fermentation of 25% *E. tirucalli* with 75% blood calculated as 40.8% ($p < 0.001$) and 30.8% ($p = 0.001$) higher than levels seen in mono-digestions of *E. tirucalli* and blood, respectively. This suggested that where acetate is the desired product, inclusion of blood as a co-substrate offered significant benefit for acidogenic fermentation of *E. tirucalli*.

Subsequent experiments more broadly analysed the fermentation characteristics of several of the most economically relevant CAM crops and compared these to more conventional agricultural residues and energy crops from non-CAM sources. VFA yields were in the ranges of (0.41 ±0.01 - 0.48 ±0.02 g/gvs) for CAM as opposed to (0.213 ±0.009 - 0.38 ±0.01 g/gvs) for the non-CAM substrates, when fermented with a standard AD sludge inoculum. Regression of fermentation rates and VFA yields against bulk biomass parameters found the overall content of lignocellulose to best explain the divergence in performance between CAM and non-CAM crops, with the latter found to have a higher content of recalcitrant lignocellulosic material. These results suggest the suitability of CAM feedstocks as biorefinery substrates.

While the above experiments use the standard small molecule methanogenesis inhibitor bromoethane sulfonate to prevent methanogenic consumption of VFA, experiments were also undertaken to identify whether red seaweed (*Asparagopsis taxiformis*) could provide a renewable, scalable alternative inhibitor to establish and maintain bioreactor control at industrial scale. Effective control was found in reactors inoculated with rumen fluid, with *Asparagopsis* treatments of ≥5% of substrate (volatile solids basis) found to provide complete inhibition at retention times below 30 days (Gompertz lag phase of 5% treatment 30.3 ±0.8, lag phase of untreated control 9 ±1, days). *Asparagopsis* was not found to provide effective inhibition in reactors inoculated with anaerobic digestion sludge at the doses tested.

In order to valorise the VFA-rich fermentates arising from the above processes for the production of polyhydroxyalkanoate (PHA) bioplastics, a novel pre-treatment process was developed. This involved the use of zeolites to strip ammonium nitrogen from fermentates, increasing the fermentate carbon to nitrogen ratio and thereby inducing conditions of 'nutrient starvation' required for effective PHA accumulation. Zeolites were found to have a binding capacity of 4.91 mg NH_4^+-N/ g zeolite, and to provide near total removal of fermentate ammonium at higher doses >25% zeolite (w/v), in batch format. Zeolites were also shown to provide effective ammonium removal when used as the stationary phase in an ion-exchange chromatography system, suggesting a scalable format for industrial biorefinery.

The direct production of PHA bioplastics on zeolite-treated fermentates was demonstrated in two industrially relevant PHA accumulating species, *Pseudomonas putida* KT2440 and *Cupriavidus necator* H16. *P. putida* showed an increase in titre from 80 ±10 to 270 ±20 mg/L ($p<0.0001$), and in yield from 10.0 ±0.8 to 40 ±7 %CDW ($p<0.0001$) between untreated and zeolite treated conditions. *C. necator* showed an increase in PHA titres from 192 ±3 to 247 ±5 mg/L ($p=0.0002$), and in yields from 49 ±4 to 94 ±2 % PHA/CDW, between the control and best-performing zeolite treatment respectively.

Taken together this experimental work offers novel insights at many levels of the bioproduction process for the conversion of biomass to PHA, offering several routes by which to render this process both more economically feasible, or environmentally sustainable.

Table of Contents

Statement ..... **ii**

Acknowledgements ..... **iii**

Declaration ..... **iv**

Abstract ..... **v**

Table of Contents ..... **vii**

List of Abbreviations ..... **xiii**

Chapter 1. Introduction **1**

1.1 The structure of this thesis *4*

Chapter 2. Literature review **7**

2.1 Volatile fatty acid production through acidogenic fermentation *7*

2.1.1 Comparing feedstocks: Fossil vs. biological carbon 7

2.1.2 Strategies to reduce biomass heterogeneity and insolubility 10

2.1.3 Acidogenic fermentation – Hydrolysis 13

2.1.4 Acidogenic fermentation – Acidogenesis 16

2.1.5 VFA post processing – Acetogenesis and chain elongation 20

2.1.6 Methanogenesis and its inhibition 21

2.2 Crassulacean acid metabolism crops as biomass sources for biorefinery *22*

2.3 Microbial production of industrially relevant storage lipids *25*

2.3.1 Microbial storage lipids as substitutes to high-value petroleum products 25

2.3.2 Polyhydroxyalkanoates as alternatives to conventional plastics 26

2.4 Use of aluminosilicates to remove fermentate nitrogen *31*

2.5 Research gap *37*

2.6 Aims and Objectives *39*

Chapter 3. Anaerobic co-digestion of *Euphorbia tirucalli* with pig blood for volatile fatty acid production **40**

Disclaimer *40*

Abstract: *41*

3.1 Introduction: ... *42*

3.2. Materials and methods ... *44*

3.2.1 Biomass and inoculum ... 44

3.2.2 Anaerobic batch assays ... 44

3.2.3 Analytical methods ... 45

3.2.4 Statistical analysis ... 46

3.3 Results and Discussion ... *46*

3.3.1 Characterisation of substrates and inoculum ... 46

3.3.2 Acidogenic anaerobic digestion of *Euphorbia* and blood by AD sludge ... 48

3.2.2 Total VFA production ... 50

3.2.3 Responses of individual VFA titres over the co-digestion parameter space ... 53

3.4. Conclusion ... *58*

3.5 Acknowledgements ... *58*

3.6 References ... *58*

Chapter 4. Biorefinery for a circular carbon economy: process benefits to the use of dryland CAM crops for anaerobic volatile fatty acid production ... 63

Disclaimer ... *63*

Biorefinery for a circular carbon economy: process benefits to the use of dryland (CAM) crops for anaerobic volatile fatty acid production ... *64*

Abstract ... *64*

4.1. Background ... *65*

4.2. Methods ... *67*

4.2.1 Biomass and inoculum ... 67

4.2.2 Anaerobic batch assays ... 68

4.2.3 Analytical methods ... 69

4.2.4 Metagenomic analyses ... 69

4.2.5 Statistical analysis and modelling ... 70

4.3 Results ... *70*

4.3.1 Characterisation of feedstock and inocula for VFA production ... 70

4.3.2 VFA yield comparison of two inocula with novel feedstocks ... 73

4.3.3 Relationship between substrate solubility and acidification rate ... 76

4.3.4 Relationship between substrate structural characteristics and total VFA yield ... 77

4.4. Discussion ... *79*

4.4.1 Characterisation of VFA yield ... 79

4.4.2 Hydrolysis rates are faster when CAM biomass is used as a substrate in methanogenesis-inhibited AD sludge 80
4.4.3 Yield performance of AD sludge is inhibited by high Neutral Detergent Fibre (NDF) from traditional biofuel feedstock 81
4.4.4 Implications for biorefinery 82

4.5 Conclusion *83*

Acknowledgements *83*

References *84*

Chapter 5. Red seaweed as an abundant, natural methanogenesis inhibitor for industrial biorefinery 90

Disclaimer *90*

Red seaweed as an abundant, natural methanogenesis inhibitor for industrial biorefinery *91*

Abstract *91*

5.1. Introduction *92*

5.2. Materials and methods *93*
5.2.1. Biomass and inoculum 93
5.2.2. Anaerobic batch assays 94
5.2.3. Analytical methods 95
5.2.4. Statistical analysis and modelling 96

5.3. Results *97*
5.3.1. Characterisation of feedstock and inocula 97
5.3.2. Response of biomethane production to *Asparagopsis* and BES treatment 97
5.3.3. Response of VFA production to *Asparagopsis* and BES treatment 99
5.3.4 Microbial communities of initial inocula and community response to *Asparagopsis* treatment 101

5.4. Discussion *102*
5.4.1. Efficacy of Asparagopsis as a methanogenesis inhibitor in rumen and AD sludge inocula 102
5.4.2. Effect of Asparagopsis treatment on volatile fatty acid production and biorefinery 104
5.4.3. Interplay of Asparagopsis and rumen microbial community 104

5.5. Conclusion *106*

CRediT authorship contribution statement *106*

Declaration of competing interest *106*

Acknowledgements *106*

Data availability *107*

References *107*

Chapter 6. Zeolite treatment of acidogenic fermentates for accurate control of C:N ratio 112

Disclaimer *112*

6.1 Introduction *113*

6.2 Materials and Methods *114*

6.2.2.1 Quantification of ammonium nitrogen – Hach Lange LCK303 115

6.2.2.2 Quantification of ammonium nitrogen – Salicylate method 115

6.2.2.3 Quantification of VFA and determination of carbon to nitrogen ratios 115

6.3 Results and discussion *116*

6.3.1 Ammonium depletion with bentonite and zeolite 116

6.3.2 Establishing the zeolite dose-response relationship and binding kinetics 118

6.3.3 Determining zeolite binding specificity and ability to manipulate C:N ratios 119

6.4 Development and optimisation of a zeolite-chromatography process for in-line digestate treatment *121*

6.5 Recovery of bound ammonium as fertiliser *124*

6.6 Conclusion and future directions *127*

Chapter 7. A two-stage biorefinery for renewable industrial chemical production 129

Disclaimer *129*

Section 7.1 – Manuscript "A two-stage bioreactor for renewable industrial chemical production" 130

Abstract *130*

7.1.2 Introduction *130*

7.1.3 Methods *132*

7.1.3.1 Materials 132

7.1.3.2 Preparation of sodium-zeolite 133

7.1.3.3 Preparation of VFA-rich fermentate 133

7.1.3.4 Preparation of fermentate growth medium 133

7.1.3.4 *Pseudomonas putida* growth time-courses 134

7.1.3.5 Analytical methods 134

7.1.3.6 Extraction and quantification of PHA 135

7.1.3 Results *135*

7.1.3.1 Characterisation of AF substrate and feedstock 135

7.1.3.2 Characterisation of bulk VFA-rich fermentates, with and without zeolite treatment 136

7.1.3.3 Growth characteristics of *P. putida* on fermentates 138

7.1.3.4 Effect of zeolite treatment on *P. putida* polyhydroxyalkanoate production on fermentate 138
7.1.3.4 Composition of *P. putida* PHAs across the time / C:N parameter space 140

7.1.4 Discussion: *142*
7.1.4.1 Zeolite treatment of *Opuntia* fermentate 142
7.1.4.2 Response of *P. putida* PHA production to zeolite-induced nitrogen limitation 142

7.5 Conclusion *145*

References *145*

7.2 – Additional Bioproduction Experiments 149

7.2.1 Introduction *149*

7.2.2 Materials and methods *151*
7.2.2.1 Materials 151
7.2.2.3 Preparation of zeolites 151
7.2.2.4 Preparation of fermentate 151
7.2.2.5 Zeolite treatment of acidogenic fermentates 152
7.2.2.6 Preparation of fermentate-based microbial growth media for *P. putida* and *C. necator* 152
7.2.2.7 Preparation of *Opuntia* Liquid Extract and media thereof 153
7.2.2.8 Culture conditions *P. putida* and *C. necator* 153
7.2.2.9 Growth experiments 154
7.2.2.10 Analytical methods 154

7.2.3 Results *155*
7.2.3.1 Utilisation of fermented and non-fermented *Opuntia* media by *P. putida* 155
7.2.3.2 Utilisation of *Opuntia* and blood-based fermentates by *P. putida* and associated PHA accumulation 156
7.2.3.3 Growth and PHA accumulation of C. necator on *Opuntia* fermentates subjected to various zeolite treatments 159
7.2.3.4 Growth and PHA accumulation of *C. necator* on molasses fermentates subjected to various zeolite treatments 162

7.2.4 Discussion *165*

7.2.4.1 P. putida growth on OLE and Opuntia fermentate *165*

7.2.4.2 P. putida PHA production on Opuntia and blood-derived fermentates *166*

7.2.4.3 C. necator PHA production on zeolite treated Opuntia fermentates *167*

7.2.4.4 C. necator PHA production on zeolite-treated molasses fermentates *168*

7.2.5 Conclusion *171*

Chapter 8. Future directions 173

8.1.1 Chapter 3 and the "Acetate Parabola" 173

8.1.2 Matters arising from Chapter 4 174

8.1.2.1 Expansion of the CAM question – Employing a targeted "biorefinery" approach 174

8.1.2.2 Exploring the basis of observed yield differences between inocula 175

8.1.3 Exploring Asparagopsis inhibition of sludge methanogenesis 176

8.1.4 Matters arising from Chapter 6 177

8.1.5 Matters arising from Chapter 7 181

8.1.5.1 Systematic evaluation of three key PHA species (*P. putida, C. necator, V. natriegens*) 181

8.1.5.2 Expansion to alternative MSL species 182

8.1.5.2 Cation sensitivity of MSL accumulation – toward a two-directional zeolite process 182

8.1.5.3 Utilising Vibrio natriegens for a non-sterile 'pure culture' bioproduction process. 183

8.1.6 Unifying these processes 184

References 186

Appendices 200

Appendix to Chapter 3 201

Appendix to Chapter 4 203

Appendix to Chapter 5 207

Appendix to Chapter 6 209

Appendix to Chapter 7 210

List of Abbreviations

Abs_n	Absorbance at a wavelength of 'n' nanometres
AD	Anaerobic digestion
AF	Acidogenic fermentation
CAM	Crassulacean acid metabolism
CDW	Cell dry weight
C:N	Carbon: nitrogen ratio
COD	Chemical oxygen demand
• SCOD	Soluble chemical oxygen demand
FW	Fresh weight
GC	Gas Chromatography
• GC-FID	GC with Flame Ionisation Detection
• GC-TCD	GC with Thermal Conductivity Detection
LCFA	Long Chain Fatty Acid(s)
MSL	Microbial Storage Lipid(s)
OD_{600}	Optical density at 600 nm
PBS	Phosphate buffered saline
PHA	Polyhydroxyalkanoate
• scPHA	Short-chain PHA
• mcPHA	Medium-chain PHA
• lcPHA	Long-chain PHA
• 3HP	3-Hydroxypropanoate
• 3HB	3-Hydroxybutyrate
• 3HV	3-Hydroxyvalerate
• 3HH	3-Hydroxyhexanoate

• 3HHep	3-Hydroxyheptanoate
• 3HO	3-Hydroxyoctanoate
• 3HN	3-Hydroxynonanoate
• 3HD	3-Hydroxydecanoate
• 3HU	3-Hydroxyundecanoate
• 3HDD	3-Hydroxydodecanoate
• 3HTD	3-Hydroxytetradecanoate
PHB	Polyhydroxy butyrate
SDG	United Nations Sustainable Development Goal
TAG	Triacylglycerides
TN	Total nitrogen
TOA	Total organic acids
TOC	Total organic carbon
TS	Total solids
VFA	Volatile fatty acid(s)
VS	Volatile solids

Chapter 1. Introduction

The First Agricultural Revolution, commonly understood to have occurred around 10,000 BC, saw the simultaneous rise of static agricultural societies in multiple regions, which represented a fundamental shift from the nomadic, hunter-gatherer societies which had defined human existence from the origin of the species several hundred thousand years earlier. These novel societal organisations were enabled by a global climatic shift to a period of relative warmth and stability. This period, the Holocene, persists to the present [1]. Agricultural societies allowed individual farmers to produce calories in excess of their own need. This surplus provided both a necessary precondition to the development of the first cities and freed a fraction of society to engage in non-agricultural activities, thereby spurring both cultural and technological innovation. Human populations thus began to cluster and expand in regions favourable to agriculture, particularly the flood plains of major rivers such as the Tigris and Euphrates, the Nile, Indus, Brahmaputra, Yellow, and Yangtze - regions which support a significant fraction of the human population to this day. In areas of the world in which agriculture remained unfeasible, hunter-gatherer social organisations, reminiscent of the pre-Holocene, continue to the present, such as among the Khoisan people of Southern Africa's Kalahari Desert [2]. These millennia of stable climatic conditions have been enabled in large part by similarly stable atmospheric CO_2 levels, which have remained in the range of 260-280 ppm for the past 12,000 years [3]. This equilibrium is now being disrupted by the large-scale emission of anthropogenic CO_2 from the burning of fossil carbon reserves. Such activities thus threaten to disrupt the environmental conditions upon which our current agricultural paradigm and the relatively stable society it supports are delicately perched. It is understood for example that a three-year drought of record proportions destabilised agriculture in the Levant and contributed to the outbreak of the 2011 Syrian Civil War [4]. Continued warming threatens to make such events more commonplace.

The role of atmospheric gases in regulating planetary temperatures was elucidated by Joseph Fourier in the early 1800s [5] and the insulative capacity of carbon dioxide was elucidated soon thereafter [6, 7]. Fears over the danger of human interference with this equilibrium followed; in 1912, the New Zealand newspaper, the Rodney and Otamatea Times, ran an article titled "Coal Consumption Affecting Climate", which raised this very issue as a potential consideration for future generations [8]. Climate models produced as early as the 1970s, such as those produced and circulated internally by Exxon Corporation scientists, can be

said in retrospect to have provided highly accurate predictions of the rate and magnitude of this development [9]. Concerted efforts to obfuscate and sow doubt as to the origin of and solutions to this warming however stymied political efforts to combat this process, and continue to do so. Despite this, global action was ultimately taken in the form of the United Nations Framework Convention on Climate Change, signed in 1992, which aimed to prevent "dangerous human interference with the climate system" [10]. This framework gave rise to the Kyoto Protocol in 1997 and the Paris Agreement of 2015, the latter of which aimed to hold global warming to "well below 2 degrees C" and stated that the increase should be preferably kept to within 1.5 ºC of warming [11]. The annual "Conference of the Parties" (COP), is convened to review progress towards the targets established within these agreements, as most recently occurred in 2023 in Dubai, under the presidency of Dr. Sultan Al Jaber, head of the Abu Dhabi National Oil Company. **Figure 1.1** plots publicly available data for historic atmospheric carbon dioxide, and the annual global temperature change against the 1880-1900 average. The signatory dates of these key agreements are superimposed over these historical data.

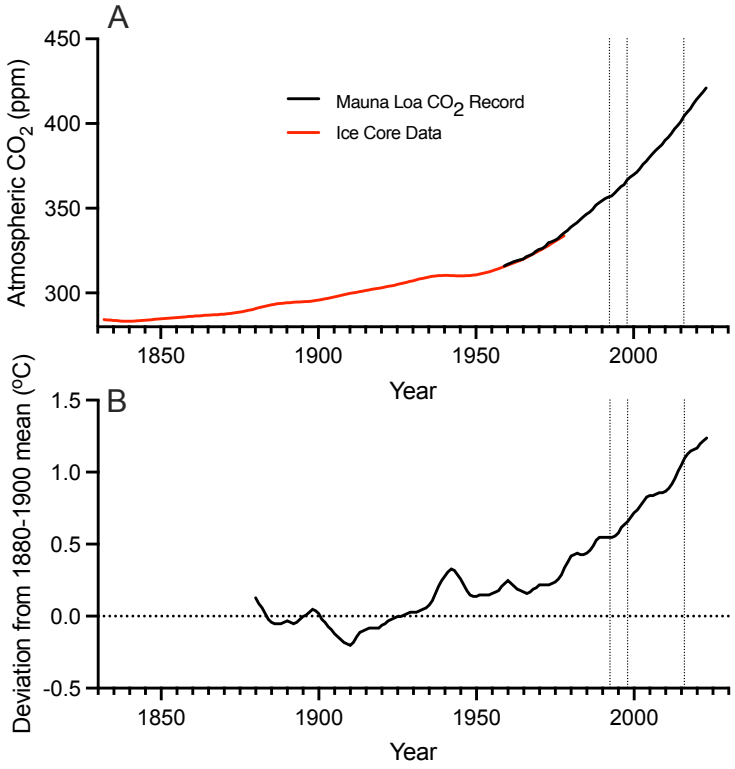


Figure 1.1: Atmospheric carbon dioxide levels 1830-2024 and global temperature anomaly 1880-2023. **A**) Atmospheric CO_2 levels 1830-1973 as measured from ice-core measurements [12], and 1958-2024 as measured directly at the Mauna Loa Observatory, Hawaii [13]. Graph origin set to 280 ppm, i.e., pre-industrial CO_2 levels. **B**) Global surface temperature anomaly against 1880-1900 mean temperature [14]. [Original figure - data sources in legend]

The vast majority of fossil fuels are consumed as fuels for electricity generation in transportation. Large, stationary infrastructure such as that required for electricity generation is proving somewhat amenable to decarbonisation, and many renewable and low-carbon alternatives already exist, such as generation from hydroelectric, geothermal, wind, biomass, and nuclear sources. These are rapidly increasing in their share of the global energy mix [15]. The decarbonisation of any transportation infrastructure directly dependent on this electrical grid, such as many mass transit systems and high-speed rail, proceeds axiomatically from this development, while other areas of transportation are more resistant to decarbonisation. Personal vehicles are perhaps the most significant such example, though the sector has seen gains for low-emissions vehicles with approximately 18% of cars sold in 2023 being electric. China alone represented over half of these sales [16].

A significant fraction of petrochemical demand is in non-fuel applications, as feedstocks for the production of chemicals and materials used in products as diverse as pharmaceuticals, textiles, packaging, and electronics. The manufacture of such products from petrochemical substrates nonetheless introduces lithospheric carbon into the carbon cycle, either to be released to the atmosphere upon incineration, or to otherwise accumulate in landfills or the environment [17]. The transition to a fully circular carbon economy demands that such products instead be derived through the fixation of atmospheric carbon. This may be achieved through processes which directly fix atmospheric CO_2 such as “Direct Air Capture” technologies or those which make use of biomass. This latter option currently has more precedent at scale, with the vast biofuel industries of the United States and Brazil being perhaps the most obvious examples [18]. Ongoing investigation into new-generation biomass feedstocks, such as those cultivable on marginal lands, suggests that these offer a considerable resource for this purpose. A study by Mason et al. [19] suggests that cultivation of 100-380 million hectares of such semi-arid land with dryland crops could provide sufficient resource to substitute for all gas use in electricity generation. Assuming such energy production can be decarbonised by other means, this resource could instead provide the carbon source for a biomass-based petrochemical industry. Significant sources of renewable biomass can be found also in the waste products of existing activities, such as agricultural residues, sewage sludge, and municipal organic waste, and recycling these back into the productive economy as raw materials could serve a double function of offsetting fossil-fuel demand, and minimising pollution.

While multiple promising technologies exist which offer alternatives to fossil-fuels, care needs to be taken not to frame the question of sustainability as a solely technological

problem. Many common practices, from the manufacture of low-quality "fast-fashion" products, the planned obsolescence of consumer electronics, and car-centric city planning all increase demand for fossil fuels greatly above what it might otherwise be, in a more rationally organised system which would nonetheless still fulfil this demand for clothing, electronics, and transportation. The fetishization of technological solutions should not feed complacency around addressing these problems. The sustainable production of high-value, carbon-based products from renewable feedstocks, much like electrified transportation or recycling, is a necessary precondition for a renewable economy, not a *deus ex machina* that cancels all environmental sins.

1.1 The structure of this thesis

Chapter 2 "Literature review" provides an overview of the relevant processes, state of the field, and key process obstacles across the various distinct fields covered by this project, in its attempt to chart a course from raw biomass to renewable bioplastic. It covers the complexities of biomass as a substrate for biorefinery, and the use of fermentative processes to reduce it to volatile fatty acids (VFA) for subsequent upgrading. It also introduces the various obstacles posed to acidogenic fermentation by the lignocellulosic structure of much biomass and suggests the use of Crassulacean Acid Metabolism crops as feedstocks to minimise this process obstacle, as well as briefly introducing their agricultural benefits over conventional energy crops.

Microbial storage lipids, and particularly the thermoplastic polyhydroxyalkanoates, are introduced as high-value target chemicals to be produced from this VFA. The biology, chemistry, and preconditions of PHA accumulation are introduced, with particular focus on the need for nutrient limitation. Finally, the zeolites are introduced as a potential tool to induce nutrient limitation and improve this flux of carbon from VFA to PHA.

Chapter 3 "Anaerobic co-digestion of *Euphorbia tirucalli* with pig blood for volatile fatty acid production" consists of a published, first-author article of the same name [20], which describes an experiment undertaken to explore the effect of organic loading rate, and on inclusion of a high-nitrogen co-substrate (pig blood) on the acidogenic fermentation of a dryland energy crop *E. tirucalli*.

The finding of this study was that overall VFA yields did not to benefit from co-fermentation, however, higher reactor loadings, which improve reactor energy density were found not to significantly reduce yields as might have been expected, suggesting dense reactor configurations

could be used for efficient conversion to VFA. Co-digestion was found to significantly improve acetate yields, with this synergistic effect increasing with greater substrate loading.

Chapter 4 "Biorefinery for a circular carbon economy: process benefits to the use of dryland CAM crops for anaerobic volatile fatty acid production" consists of a co-first author manuscript which is currently under review for publication. This study analysed the acidogenic fermentation kinetics of several CAM crops and sub-fractions thereof, and of common energy crops and agricultural residues, with two distinct microbial inocula. First-order models were fit to fermentation data to extract kinetic parameters and standardise comparisons. Consistent with expectation, CAM substrates outperformed the non-CAM substrates tested, though the specific nature of this outperformance was dependent on the microbial community, one showing higher reaction rates, and the other showing higher yields. The relative overperformance of CAM crops was not found to be explained by their lower lignin content, as was expected, but rather by their lower content of overall lignocellulosic material.

Chapter 5 "Red seaweed as an abundant natural methanogenesis inhibitor for industrial biorefinery" consists of a published, first-author article of the same name [21], which describes an experiment undertaken to evaluate the capacity of the red seaweed *Asparagopsis taxiformis* to act as a methanogenesis inhibitor in industrial biorefinery, in which various doses of this seaweed are tested for the efficacy of their methanogenesis inhibition against doses of the standard inhibitor bromoethane sulfonate, in two distinct microbial communities (the same as those used in **Chapter 4**). *Asparagopsis* had previously been demonstrated as an effective inhibitor in rumen fluid over short retention times, but not been evaluated for reactor applications or the longer retention times this would entail. *Asparagopsis* was found to provide effective inhibition of methanogenesis in rumen fluid, effectively replicating the literature on this point, up to retention times of 30 days, which is sufficient for most AF applications. It was not found to provide effective inhibition in commercial anaerobic digester sludge.

Chapter 6 "Zeolite treatment of acidogenic fermentates for accurate control of C:N ratio" details initial validation of the application of aluminosilicates (bentonite and zeolite) to remove ammonium from both acidogenic fermentates and from ammonium chloride solutions. Zeolites were found to offer improved properties over bentonites and so were further evaluated for their ability to specifically deplete nitrogen, but not carbon in fermentates. Their specificity for nitrogen was found to be high, and they were demonstrated to increase fermentate C:N ratios to well in excess of those reported in the literature as being required for PHA production. Various

zeolite doses and treatment times were tested to obtain a response surface for the depletion of fermentate ammonium. These experiments were performed in batch format.

Finally, a chromatography device was constructed, with the zeolite acting as a stationary, ion-exchange medium, to validate this more scalable approach. This device was used to explore binding and elution dynamics, and to optimise eluate concentrations. Finally, a novel eluent was tested in order to recover immobilised ammonium in a usable format – as the fertiliser ammonium phosphate.

Chapter 7 "A two-stage biorefinery for industrial chemical production" consolidates the findings of the above chapters into a linear process, in which CAM biomass was fermented to VFA, the fermentate treated with zeolite to various C:N ratios, and these fermentates used as the feedstock for mcPHA production in *Pseudomonas putida*. These findings are presented in the form of a first-author manuscript of the same name in **Section 7.1**, the primary finding of which is that zeolite treatment leads to a roughly 3-fold increase in PHA titres in this species.

A series of follow up experiments in both *P. putida* and *C. necator* are subsequently detailed in **Section 7.2** to address a series of relevant questions arising from these promising initial results. The most striking result presented in this section is the demonstration that zeolite treatment also increases PHA titres in *Cupriavidus necator*, with an approximately 2-fold increase registered – suggesting its use will broadly apply across PHA accumulating species. Further experiments in *P. putida* then aim to use the findings of **Chapter 3**, in which distinct VFA profiles were produced from different feedstocks, to see whether customising the VFA profile can allow for customised PHA compositions. This demonstrated some limited success but encountered several fundamental barriers which are discussed in more detail in this chapter.

Chapter 8 outlines the key findings of the previous results chapters and comments on their overall significance and contribution to answering the research gaps outlined in **Chapter 2**. It addresses the partial failure of the attempt to modify PHA compositions in *P. putida* (**Chapter 6**) by proposing a slightly less ambitious alternative project using *C. necator* which might be able to use custom VFA profiles to achieve PHAs with desirable properties. It also outlines several other key questions arising from this work and potential future avenues of investigation, ongoing experiments which aim to address these, and suggestions for longer-term work well beyond the scope of this study for anyone potentially wishing to pursue this avenue of investigation in future.

Chapter 2. Literature review

2.1 Volatile fatty acid production through acidogenic fermentation

2.1.1 Comparing feedstocks: Fossil vs. biological carbon

Crude oil and natural gas represent the feedstocks from which the vast majority of non-fuel petrochemicals are currently derived. Crude oil, while varying in composition between deposits, consists primarily of paraffins (i.e., linear and branched alkanes), naphthenes (i.e., cycloalkanes) and aromatic compounds with smaller fractions of other residues [22, 23]. Natural gas consists mainly of methane though it may contain smaller amounts of higher (C2+) alkanes such as ethane and propane [24]. The simple composition of these feedstocks means they may be fractionated by simple mechanical and thermal processes, such as distillation, to yield pure fractions for downstream processing. The higher alkanes in natural gas (ethane and propane) for example, may be converted through the process of steam cracking, to their corresponding alkenes: ethylene and propylene, which represent the monomeric units for production of the most common plastic polymers, polyethylene and polypropylene. Accordingly, in the United States, natural gas treated through this simple process represents the primary feedstock for plastic production [25]. This combination of a cheap raw material and ease of processing have resulted in a profusion of inexpensive plastic and petroleum products throughout the globe [26]. This imposes a daunting price constraint on any renewable processes which might seek to acquire market share.

In contrast to fossil carbon sources, biomass may be highly chemically and structurally complex and thus not amenable to simple fractionation; while crude oil and natural gas consist primarily of alkanes, biological carbon is mainly present as carbohydrates, proteins, and fats. Significant chemical and structural variability exist even within these broad macronutrient categories which can have implications on the amenability of biomass to refining. Carbohydrates may be present as soluble mono or disaccharides, or as complex plant polysaccharides such amylose, amylopectin, hemicellulose, and cellulose, the latter of which is the most abundant organic polymer in nature [27]. While highly pure plant mono and disaccharides may be directly used for bioproduction of high value products, the more complex polymeric fractions will likely require some form of hydrolysis to render them suitable for bioproduction. Cellulose is a linear polysaccharide of hundreds to thousands of D-glucose subunits via ß(1-4) glycosidic linkages [28]. Hemicelluloses, conversely, are a heterogeneous class of typically short-chain polysaccharides, consisting of monomers of D-mannose, D-xylose,

D-glucose, D-galactosyl, glucuronic and galacturonic acids, and L-arabinose, the composition of which can depend on many factors including species and growth conditions [29]. Unlike cellulose, hemicellulose may be linear or branched. Hemicellulose and cellulose latter most commonly occur in complex 'lignocellulosic' organisations with lignin, the third major component of this lignocellulosic structure, which is a class of complex phenolic polymers consisting of phenyl-propane units. Lignin polymers display five linkage patterns, among which the ß-O-4 ether linkage is particularly common and is thus seen as key to lignin degradation and valorisation [30].

Lignocellulose is the most abundant natural material on Earth [28], and it is the major constituent of almost all plant biomass[1]. This abundance and near ubiquity across plant species [31] means it is a major constituent of almost all plant materials considered for refining, and that the efficiency of its degradation will be key to the economic feasibility of biorefinery processes utilising plant substrates. It is abundant in agricultural residues, such as those from rice, wheat, corn, sugar cane, and pineapple, which may be obtained at nearly no cost as wastes of existing economic activities, as well as in key species of 'second generation' energy crops such as *Miscanthus* [31, 32]. These offer abundant feedstocks for potential conversion to high value products. However *in vivo,* cellulose polymers are organised into rigid microfibres to form the skeleton of the plant cell wall, between which is organised a complex mixture of lignin and hemicelluloses [29]. This complex structure is resistant to degradation by physical, chemical, and biological means, and this recalcitrance presents a primary obstacle to biorefinery. The relative abundance and particular organisation of each of these polymers can vary considerably between species, and in response to growth conditions [28, 31]. A model of this organisation is shown in **Figure 2.1**.

[1] This caveat is included to account for several species of microalgae reported as containing either no lignin and/or no cellulose.

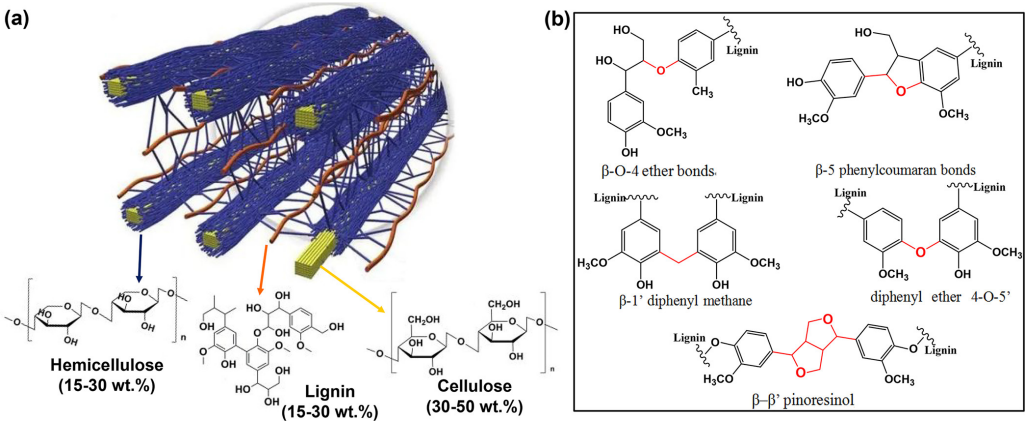


Figure 2.1: Indicative 3D spatial and chemical organisation of cellulose, hemicellulose, and lignin polymers within lignocellulosic biomass. A) Location and general structures of cellulose, hemicellulose, and lignin in lignocellulosic biomass, B) Typical bonding patterns in lignin matrix. Figure reproduced from Liu and Yu [33], licensed under CC-BY-NC-ND 4.0.

Carbohydrates constitute just one of the three broad macronutrient categories found in biomass, and while they typically are the predominant macronutrient in plant materials, in other biomass sources, proteins instead can represent a majority of biomass carbon. Examples of such sources include wastes from the meat, diary, and legume processing industries (e.g. blood, cheese whey, and tofu whey), as well as the enormous quantities of sludge arising from sewage processing, in which up to 60-90 % of COD may be present as protein [34]. Proteins vary from each other in their amino acid composition, i.e., in the relative abundance of each of the 20 proteinogenic amino acids. They further vary in their 3-dimensional organisation, from soluble, globular proteins (e.g., albumin), to insoluble structural proteins such as keratin, which may be more resistant to degradation in a biorefinery [35]. Unlike carbohydrates, proteins also contains a large nitrogen fraction (about 16% w/w), which may or may not be desirable depending on the specifics of the biorefinery process.

Due to the nature of the feedstocks employed in the latter chapters of this thesis, lipids are of the least relevance to this study, but as the third of the major groups of biological macromolecules nonetheless deserve a brief mention. Lipid-rich biomass may be found in oleaginous microbes [36], in specific fractions of plant biomass (especially oil seeds, oil palm and the likes), and in fractions of animal biomass [37, 38]. *In vivo,* lipids are commonly present as triacylglycerols, ester complexes of glycerol with three fatty acids. These compounds are of considerable economic value themselves, as food additives, and as platform chemicals for the production of renewable fuels. They are easily extracted and refined from biomass via simple mechanical or thermal processes, such as grinding and pressing, or through rendering,

whereafter their hydrophobicity facilitates their extraction by causing them to phase separate from the mass of hydrophilic biomass [39]. The defatted waste products from such processes may then be used as a substrate for further refining, though the majority of organic biomass at this point will likely consist of carbohydrate, and proteins.

The non-organic fractions of the biomass can present further a further consideration. Hydration level can be expressed as the fraction of total solids to fresh weight (TS/FW). As TS is the fraction from which products are derived, a high TS or low water content is typically preferable as it facilitates efficient process logistics. Hydration among feedstocks can vary considerably, from a TS/FW of up to 100% in dry agricultural residues such as wheat straw, to under 1% in low-strength waste waters. The TS fraction may itself contain a considerable inorganic fraction, which must also be considered. As most bioproduction processes aim to produce organic products (consisting mainly of C, O, N, and H), feedstocks with a high organic content will contain a larger fraction of biomass theoretically convertible to the desired end product [40], and therefore be more valuable substrates. The volatile solids (VS) content of the biomass, defined as the fraction of dry biomass (TS) lost through heating at 550 ^{o}C [41], provides a measure of the organic content of the substrate, and is the standard measure applied throughout this document to estimate this parameter. The residual ash content (i.e., TS – VS) represents the inorganic fraction of the biomass. As the processes in this thesis attempt to produce alternatives to fossil hydrocarbons, a high VS/TS ratio is considered a favourable biomass property.

2.1.2 Strategies to reduce biomass heterogeneity and insolubility

The primary obstacle to biorefinery thus becomes to efficiently reduce biomass heterogeneity, and to yield, with minimal additional process cost, a homogeneous or near-homogeneous intermediate for subsequent processing to end product. Any biorefinery process which intends to produce a usable intermediate from heterogeneous feedstocks will need to consider the specific composition of the biomass as introduced in **Section 2.1.1**, and no process will be able to accommodate all feedstocks with equal efficiency. Several process options exist to allow this preliminary degradation of biomass to a usable form, these include thermal/physical methods such as pyrolysis, methods employing chemical and enzymatic hydrolysis, and fermentative approaches which harness the existing biological processes by which biomass is degraded in the environment.

In pyrolysis, biomass is heated in a non-reactive environment, typically in a range of between 200 and 2500 °C depending on the process [42]. It thus undergoes thermo-chemical decomposition to yield biochar, bio-oil, and syngas as the solid, liquid, and gaseous fractions, respectively. The bio-oil fraction arising from pyrolysis of lignocellulosic biomass is a complex mixture of hydrocarbons including alcohols, aldehydes, carboxylic acids, phenolic compounds and sugars [43], and thus provides an ideal substrate for production of fuels and chemicals. Yields of crude bio-oil for various biomass sources have been reported well in excess of 50% of biomass TS, reaching as high as 80% under certain conditions [42].

Anaerobic fermentative approaches instead operate under milder, biological conditions at temperatures typically not exceeding 45 °C in mesophilic reactors (or 70 °C in thermophilic reactors [44]. Anaerobic digestion (AD) is the most widely deployed of such technologies, seeing widespread use at industrial scale in the treatment of municipal food waste [45], of sewage sludge [46], and of agricultural residues [47]. Conventional anaerobic digestion is the controlled degradation of biomass to yield a methane rich biogas which after upgrading can be used as a substitute for natural gas, as a fuel for transport, heating, and electricity generation. The conversion of the input biomass into biogas is performed under anaerobic conditions by a mixed microbial consortium and may be broadly classified into four consecutive processes of hydrolysis, acidogenesis, acetogenesis and methanogenesis, each facilitated by distinct microbial subpopulations as summarised in **Fig. 2.2**. In hydrolysis, organic macromolecules are degraded to their monomeric constituents, these then provide the substrates for acidogenesis (or fermentation), in which these are fermented to yield 2-6 carbon volatile fatty acids (VFA) and acetogenesis, in which these acids are further degraded to acetic acid. This acetic acid then provides the substrate for acetoclastic methanogenesis, in which methanogenic archaea produce methane [48]. Despite these successes, conventional AD produces a low-value product which leaves many AD facilities to operate on slim margins, though this income may be supplemented with additional revenue streams such as gate fees charged for the processing of organic waste [49]. At a process-level, methanogenesis is also highly sensitive to reactor parameters and the need to maintain the stability of methanogenesis in reactors imposes a considerable constraint on operating conditions and throughput rates. Methanogens are sensitive to inhibition by long-chain fatty acids present in many organic waste streams, and to ammonia, released by the anaerobic degradation of protein-rich materials, which limits its ability to treat wastes rich in these materials [38, 50]. Perhaps most importantly however, methanogens are subject to inhibition by the very VFAs upon which they depend as substrates. This substrate inhibition demands that rates of methanogenesis be maintained in excess of hydrolysis in order to prevent

the accumulation of VFA which can lead to reactor 'souring' or a shut down in methanogenesis. Many of these issues may be managed by co-feeding with substrates of different composition to keep inhibitory compounds within appropriate limits, or by dilution of the reactor contents. This latter strategy in particular reduces the energy density of the overall reactor, increasing the working volume and overall footprint required to treat a given quantity of material. These concerns also limit the employment of reactor strategies intended to increase reaction speed, such as the use of thermophilic reaction. Thermophilic reactors, while achieving more rapid degradation and faster throughput than mesophilic reactors, are famously unstable and are accordingly seldom deployed [44].

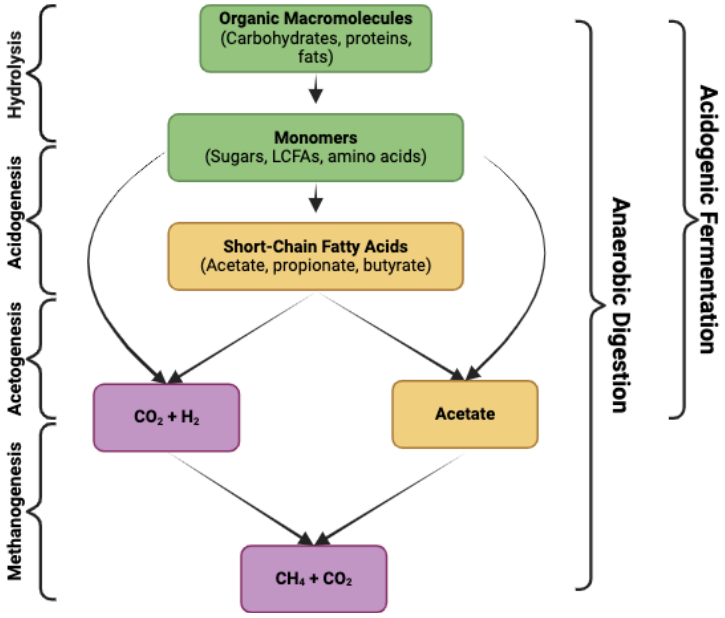


Figure 2.2: Overview of sequence of biomass degradation to end product in anaerobic digestion and acidogenic fermentation. [Original figure created in BioRender.com based on [48, 51]]

Acidogenic fermentation is a variant of this AD process (AF – **Figure. 2.2**) in which methanogenesis is blocked to allow accumulation of VFA, which is then extracted from the fermentation broth. Much like the mixed carbon sources arising from biomass pyrolysis as detailed above, these VFAs can then provide platform chemicals from which high-value products may be produced.

2.1.3 Acidogenic fermentation – Hydrolysis

Hydrolysis is the process by which biological macromolecules within the substrate biomass are monomerised for fermentation to VFA. Accordingly, hydrolysis is often measured as the solubilisation of the input biomass, as measured from the release of soluble organic matter (Soluble Chemical Oxygen Demand - SCOD) from the input total organic matter (Total Chemical Oxygen Demand - TCOD) [52]. Hydrolysis is performed by extracellular enzymes secreted by hydrolytic subpopulations within the reactor microbial community. Hydrolysis of the three major groups of organic macromolecules (carbohydrates, proteins, and lipids) proceeds via distinct enzymes, and often microbial species. Hydrolysis of carbohydrates (cellulose, hemicellulose, and starch) is performed by the broad classes of cellulase, hemicellulase, and amylase enzymes, respectively [53, 54]. Hydrolysis of proteins proceeds through the action of two groups of enzymes, the proteases and the peptidases, in which the former is concerned with the cleavage of proteins into smaller peptides, and the latter with the degradation of these to release amino acid monomers [55]. Lipids are commonly present as triacylglycerides, consisting of a glycerol group bonded via ester bonds to three long chain fatty acids (LCFA). Lipase enzymes cleave these lipids to yield glycerol and three LCFAs [55].

In AD, the hydrolysis step is intentionally maintained as rate-limiting to avoid reactor souring, or a situation in which the accumulation of VFA (or other reaction intermediates) leads to inhibition of methanogens. This is achieved both by limiting the rate of hydrolysis by keeping substrate loadings low, especially where the feedstock is highly degradable, and by employing strategies to avoid excessive accumulation of reaction intermediates which are inhibitory to methanogens. Such strategies include dilution of reactor contents to maintain concentrations below inhibitory levels, co-digestion with substrates of appropriate macronutrient profiles to prevent accumulation of, for example ammonium or long chain fatty acids.

AF is freed of this requirement to appease methanogens, and yet here too, given the great speed of the acidification step, hydrolysis will nonetheless likely represent the rate-limiting step [55, 56]. Thus, for most typical feedstocks and reactor configurations, the efficiency of hydrolysis will determine the efficiency of the overall AF process, as measured both by reaction rate, and by overall VFA yield. As hydrolysis of all three of the broad classes of organic macromolecules: carbohydrates, proteins, and lipids, is performed by extracellular enzymes (amylases, cellulases, hemicellulases, proteases, and lipases) secreted by hydrolytic microbial subpopulations, the rate of degradation of these macromolecules will depend both on the specific nature of the biomass and also on reactor parameters which will affect both the

abundance of relevant microbial subpopulations, and the activity of the relevant extracellular enzymes.

At a bulk level, biomass which is more readily accessible to the solvent (water), will present a larger surface area to enzymatic attack. This is true at the level of substrate particle size; assuming other reactor parameters remain unaffected, finer particulates will generally be more readily hydrolysed than larger materials. This is the justification for using comminution processes (e.g. grinding, milling) to reduce biomass prior to AD, which have been reported as increasing both product yields [57], and reaction rates [58]. This principle applies to the macromolecular organisation of biomass too. Macromolecules with greater aqueous surface area (e.g., globular proteins, starches, amorphous cellulose), present more surface area for hydrolytic enzymes than do their insoluble, often fibrous counterparts (e.g. structural proteins such as keratin, or carbohydrates such cellulose when in a crystalline form). Organisation of these macromolecules into larger assemblies, such as lignocellulose (**Fig. 2.1**), can also impact hydrolysis. In addition to mechanical comminution methods, thermal and chemical techniques also exist to assist the process of biomass hydrolysis. An extensive literature exists on the application of biomass pre-treatments to lignocellulosic biomass for anaerobic degradation. These include alkaline [59, 60], as well heat treatments [61] and mechanical methods such as ultrasound [62], and steam explosion [63]. In the above examples, pre-treatment is broadly understood to have facilitated either increased products yields, or hydrolysis rates due to a disruption of the lignocellulosic biomass which rendered degradable components enzymatically accessible to cellulases and hemicellulases. These benefits however come with the caveat of increased process costs, through reagents, and energy expenditure which must be evaluated against the increased productivities they allow.

Lignin represents a particularly significant obstacle to the efficient hydrolysis of many plant substrates. While a wide variety of microbial species are able to hydrolyse cellulose and hemicellulose, efficient degradation mechanisms for lignin are instead largely confined to the clade of white-rot fungi [64]. The fact that so few degradation mechanisms exist for one of the most abundant biopolymers is a significant biorefinery problem in and of itself. However, even more significantly, through its complex arrangement with cellulose and hemicelluloses *in vivo*, lignin renders even these otherwise degradable polymers resistant to enzymatic hydrolysis. Several hypotheses exist as to the mechanism of inhibition, which include physical occlusion of the degradable material (i.e. by reducing its enzymatic accessibility), and through unproductive and inhibitory binding of cellulases to lignin. Vermaas et al. [65] performed molecular dynamics

simulations of the interaction of a model cellulase from the fungus *Trichoderma reesei* to lignocellulose. They found lignin to bind to chemical motifs within the cellulose, and within the cellulase enzyme itself, which are required to facilitate enzyme binding to the cellulose, thus inhibiting cellulolysis. Lignin content can vary considerably between plant tissues, and between species. Lourenço and Pereira [66] for example quote lignin percentages of 5-12%, 15-30%, and 25-35% of plant cell walls in monocotyledons, hardwoods, and softwoods, respectively. Lignin content is additionally influenced by cultivation conditions and by stresses (both physiological and mechanical) experienced during growth [67]. This suggests that selection of a low-lignin biomass sources could provide an alternative to expensive pre-treatments while still allowing for efficient hydrolysis. A low lignin content is one of several rationales given for research into the use of Crassulacean Acid Metabolism (CAM) plants, such as *Opuntia ficus indica*, as AD and AF substrates [19, 32]. These are discussed in more detail in **Section 2.2**. The reactor microbial community may also be tailored by selecting microbes evolved to the degradation of structurally similar materials. Yue et al. [68] for example, compared AD of bulrush biomass with a reactor sludge inoculum against AD using rumen inoculum taken from a fistulated goat. While gas yields were higher with sludge, hydrolysis rates were maximal with rumen fluid. The rumen is an environment specifically evolved for the microbial degradation of lignocellulosic substrates and has been found to show higher hydrolytic and acidogenic activities with lignocellulose than other anaerobic microbiomes [69]. This is in part thought to be due to a particularly active subpopulation of adhesive, hydrolytic microbes which form cellulolytic biofilms [69]. This suggests that tailoring the reactor microbiome to the specific biomass can allow for higher productivities.

Reactor operating conditions such as pH, temperature, and the presence of degradation products and inhibitory compounds will also affect hydrolysis through their influence on substrate structure, on the abundance of relevant microbial subpopulations, and on the activity of relevant extracellular enzymes [70]. The presence of VFA in the reactor has been suggested to loosen the structure of lignocellulose, and thereby to improve hydrolysis, suggesting co-digestion of highly degradable substrates with more recalcitrant substrates can improve the breakdown of the latter [71]. However, the presence of degradation products (glucose, amino acids, VFA and ammonium) can also inhibit hydrolysis [55]. pH is another major consideration which affects hydrolytic efficiency. VFA and ammonium exhibit a pH-dependent toxicity for microbes which can influence the reactor community. At low pH, VFAs are disproportionately present in their undissociated form [72], which are capable of passive diffusion across the cell membrane and are therefore more toxic to cells. Ammonium nitrogen, conversely has a pK_a of

9.3, and thus is disproportionately present in its toxic free-form (NH_3) at higher pH [73]. It is thus difficult to isolate the effect of pH from the effects of these other compounds, or to make broad statements as to globally preferable reactor parameters as parameters exhibit a high degree of inter-dependence. However, in general, a neutral to mildly alkaline pH could be said to be favourable to hydrolysis, with several studies identifying improved protein digestion in alkaline pH [74, 75]. Duong et al. [34] reported significantly higher proteolysis at neutral pH than at pH 5.

As the likely rate-limiting step of any AF-based biorefinery, maintaining a high hydrolytic efficiency is crucial to an efficient bioconversion process. Where feasible, processes should endeavour to use feedstocks low in recalcitrant constituents such as lignin, or highly insoluble proteins, and of a moderate nitrogen concentration. Where this is not possible, imbalances may be addressed through co-fermentation with feedstocks of different macromolecular composition, or through careful selection of microbial communities with high hydrolytic efficiencies for the feedstock in question.

2.1.4 Acidogenic fermentation – Acidogenesis

Unlike the relatively homogeneous biogas produced by conventional AD, which consists almost entirely of CH_4 and CO_2, the VFA product of AF consists of a mixture of linear C2-C6 fatty acids, and branched isomers thereof. The relative abundances of these will depend on the relative contributions of the multiple pathways through which substrate fermentation may proceed. This will in turn be a product of both the composition of the input biomass, as well as reactor parameters such as pH, microbial community, retention time, and the presence of inhibitory compounds. VFAs may thereafter be subjected to further processing to yield various products (covered in **Section 2.3**).

Taking an economic view, while acetate is commonly the most abundant VFA produced from AF, it is also the least valuable as a bulk chemical. Ramos-Suarez et al. [76] give price estimates of $US 0.89/kg for acetate, $US 2.2-2.75/kg for C3-C4 fatty acids, and as high as $US 4.63/kg for valeric acid (C5). Accordingly, significant economic upside is available for processes biased toward longer VFA products. These VFAs can be used as a carbon source for bioproduction of economically important chemicals, such as oils [77], and polyhydroxyalkanoate (PHA) plastics [78, 79]. Integration of AF reactors with in-line upgrading of VFA to high-value chemicals could allow for more attractive economics, provided process

and extraction costs can be maintained at a minimum. This point is expanded in **Sections 2.3** and **2.4**.

In a typical biorefinery 'cascade', fractions of the input material are isolated in descending order of economic value. This rule will broadly apply for those biomass fractions whose market price exceeds the costs of extraction. Such examples of this are in the extraction of sucrose from sugar cane or beet, or of oils from oilseeds. What remains after this process is a heterogeneous waste product consisting of those fractions for which this price condition is not met. It is to this latter material that biorefinery should look if it intends to substitute petrochemicals at a broader scale. Carbohydrates (including cellulose and hemicellulose) are typically the most abundant macromolecules in such plant biomass. Hydrolysis of these macromolecules yields primarily monomers of cellulose and xylose, which are acidified via pyruvate-dependent pathways to yield acetate, propionate, and butyrate as summarised in **Fig. 2.3**.

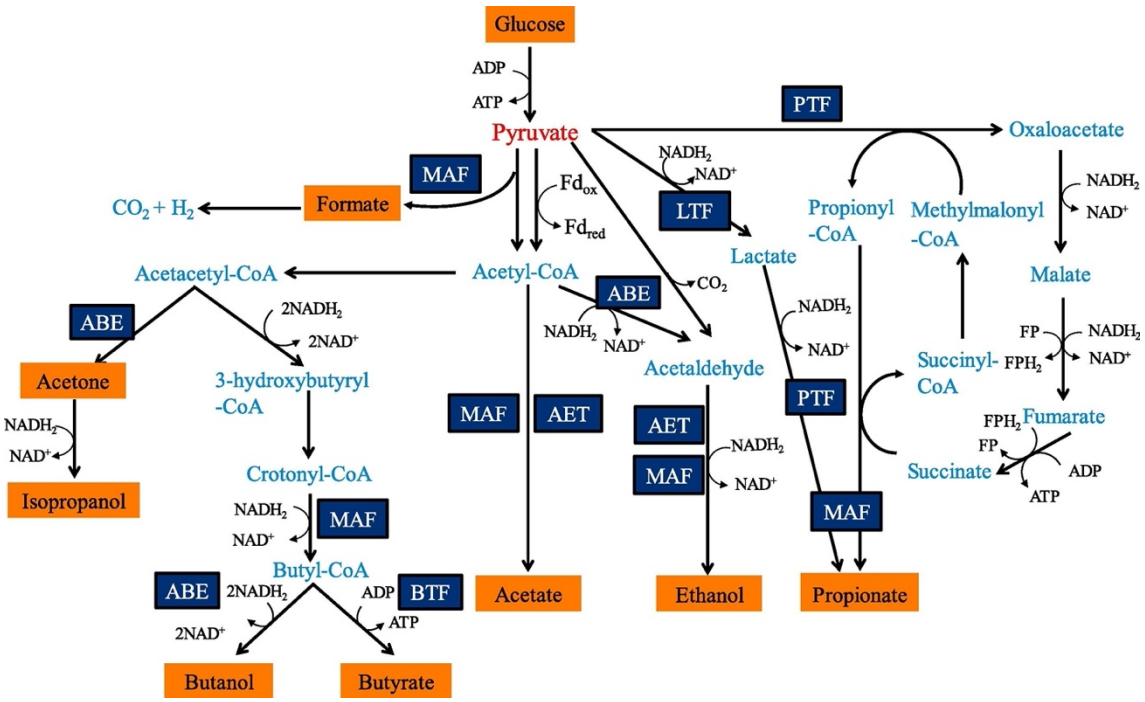


Figure 2.3: Metabolic pathways for anaerobic fermentation of carbohydrates to VFA. Figure reproduced, with explicit permission, from Zhou et al. [80].

Proteins undergo hydrolysis to yield amino acids which are mainly fermented via Stickland reactions, a mechanism specific to a number of common species of *Clostridia* common to AD reactors, such as *C. bifermentans*, *C. sordellii,* and *C. sporogenes* [81]. In such reactions, amino acids are fermented in pairs: one acting as the electron donor, and the other as

acceptor. Under these conditions, amino acid fermentation proceeds with a relatively clear stoichiometry [81], which is summarised in **Table 2.1**. It should be noted that the stoichiometry of Stickland acceptors and donors will not typically balance, leaving a surplus of one or the other to be degraded via non-Stickland mechanisms. Changes in reactor community to favour protein-degraders which utilise non-Stickland mechanisms could also allow for a shift in VFA profile. Such shifts could be brought about through the usual mechanisms of pH, and accumulation of reaction intermediates, to result in a shift in community structure

Table 2.1: Stoichiometries of amino acid fermentation assuming Stickland mechanisms. Data sourced from Ramsay and Pullammanappallil

			Fermentation products									
Stickland Function	**Amino acid**	**Carbon number**	**Acetate**	**Propionate**	**Butyrate**	**Isobutyrate**	**Valerate**	**Isovalerate**	**Aromatic acids**	**CO_2**	**Ammonia**	**H_2**
Electron donors	Alanine	3	1							1	1	2
	Cysteine	3	1							1	1	0.5
	Glutamate	5	1		0.5					1	1	
	Histidine	6	1		0.5					1	2	
	Isoleucine	6						1		1	1	2
	Lysine	6	1		1						2	
	Methionine	5		1						1	1	1
	Serine	3	1							1	1	1
	Threonine	4	1		0.5						1	-1
	Valine	5				1				1	1	2
Electron acceptors	Aspartate	4	1							2	1	2
	Glycine	2	1								1	-1
	Proline	6	0.5	0.5			0.5				1	-1
Either*	Arginine	6	0.5	0.5			0.5			1	4	-1
	Leucine	6						1		1	1	2
	Phenylalani	9							1.103	1	1	2
	Tryptophan	11							1.379	1	1	2
	Tyrosine	9							0.828	1	1	1

**May act as either electron donor or acceptor depending on partner amino acid.*

The LCFA produced from hydrolysis of lipids is anaerobically fermented via ß-oxidation to sequentially yield a C2 product (acetate) and H_2 [82]. One further mechanism exists by which fatty acids may be synthesised, this time through the synthesis of acetate from the gaseous products (CO_2 and H_2) of the above hydrolytic and fermentative processes. This 'homoacetogenesis' proceeds via the Wood-Ljungdahl pathway to reduce CO_2 to acetate using H_2 as electron donor. This recycling of inorganic carbon back into the pool of organic carbon (VFA) serves to increase reactor VFA yields. It should however be noted that homoacetogens may be inhibited by some antimethanogenic agents [83] and thus if homoacetogenesis is to be maximised, reactor processes should be selected which endeavour to avoid the use of chemical agents for methanogenic repression.

2.1.5 VFA post processing – Acetogenesis and chain elongation

The VFA arising from fermentation of biomass hydrolysates may be subjected to further post-processing by the microbial community. This can take the form of acetogenic processes, in which longer VFAs are consumed to yield acetate (C2), or chain-elongation processes by which shorter VFAs are consumed to yield longer VFAs, such as hexanoate (C6). The sum of these first and second order processes will give the overall composition of the VFA produced from a particular reactor configuration. As discussed in **Section 2.1.4**, acetic acid may be produced from fermentation of the hydrolysis products of all three classes of biological macromolecules (carbohydrates, proteins, and fats), and also via homoacetogenesis from CO_2 and H_2. Acetogenesis may additionally occur via oxidation of the longer fatty acids to produce acetate, CO_2, and H_2, which is summarised in **Table 2.2**.

Table 2.2: Pathways of butyrate and propionate oxidation to acetate (Data from Stams and Dong [84])

Substrate	Reaction	ΔG°' [kJ]
Propionate	$Propionate^- + 3\ H_2O \rightarrow Acetate^- + HCO_3^- + 3\ H_2 + H^+$	76.1
	$Propionate^- + 2\ HCO_3^- \rightarrow Acetate^- + 3\ HCOO^- + H^+$	72.0
Butyrate	$Butyrate^- + 2\ H_2O \rightarrow 2\ Acetate^- + H^+ + 2\ H_2$	48.1
	$Butyrate^- + 2\ HCO_3^- \rightarrow 2\ Acetate^- + H^+ + 2\ HCOO^-$	45.5

These reactions are sensitive to the presence of hydrogen and are only energetically favourable where hydrogen partial pressure is kept low. Under methanogenic AD, this is achieved through hydrogenotrophic methanogenesis. However in methanogen-inhibited

environments such as AF, this H_2-scavenging function may also be performed by homoacetogens [85]. The accumulation of formate can also render the above reactions unfavourable, unless kept low by the actions of formate-consuming community members [84].

While these pathways reduce the average chain length of the VFA pool, chain elongation is also possible to produce medium chain fatty acids, especially hexanoate (C6) and octanoate (C8). Some studies have reported anaerobic synthesis of hexanoate via fatty acid biosynthesis (FAB) pathways, however the most widely recognised, and most energetically favourable pathway is via acidogenesis (as in **Section 2.1.4**) followed by chain elongation of these shorter VFA products via reverse ß-oxidation [86]. Common fermentation products which may form the basis of chain elongation to hexanoate include acetate, butyrate, lactate, and ethanol. Propionate is instead elongated to odd chain fatty acids such as valerate (C5) and heptanoate (C7). A variety of factors can influence the efficiency of chain elongation in the reactor, such as the complex competitive interactions between acidogens, acetogens, and chain elongators within the community. Here too H_2 partial pressure can also play a role, with higher pressures tending to favour flux of VFA carbon to chain elongation processes [86].

2.1.6 Methanogenesis and its inhibition

Under conventional AD, methane, produced by methanogenic archaea, represents the primary end product of the fermentation process. Methane is produced either from acetate via acetoclastic methanogens or from H_2 and CO_2 by hydrogenotrophic methanogens (**Fig. 2.2)**. Under AF, in which the VFAs themselves are the desired product, methanogenesis is undesirable as it represents a degradation pathway for these and reduces yields.

At lab scale, small molecule inhibitors, specific to the metabolism of methanogenic archaea are commonly employed to inhibit methanogenic processes where VFA accumulation is desirable. Bromoethane sulfonate (BES) is often used for this purpose, though its high cost (~$41/kg [87]) precludes its use at industrial scale. At large scale, reactors are often run at parameters unfavourable to methanogens, such as an operating pH outside of the neutral range [88]; Dahiya et al [89] argue VFA production to be optimal between 5.25-11.0, but methanogenesis to prefer a neutral pH of 6.8-7.2. Allowing the accumulation of inhibitory concentrations of fermentation products such as VFA and ammonium may also be used to inhibit methanogens, or by reducing HRT to ensure methanogens are flushed out. Alternative large scale reactor designs avoid the issue of methanogenesis through continuous selective membrane filtration of the reactor fluid to remove VFAs while cycling undigested substrate back into the reactor [88].

Multiple studies have identified the methanogenesis-inhibition capacity of red seaweeds (esp. *Asparagopsis taxiformis*) in rumen microbiomes [90-94]. Such seaweeds may offer a scalable and economical alternative to BES as inhibitors for industrial biorefinery. Previous studies have focused narrowly on rumen microbial communities and over short retention times (<4 days). It would be valuable to analyse the efficacy of *Asparagopsis* in an industrial reactor microbiome and at the longer retention times (>14 days), which are relevant to acidogenic fermentation.

2.2 Crassulacean acid metabolism crops as biomass sources for biorefinery

Assuming an efficient biorefinery process can be engineered to derive usable products from biomass, the problem then becomes one of sourcing sufficient biomass to allow the process to be scaled. As introduced above, biorefineries have been designed which use the waste products of existing activities, such as agricultural residues, municipal waste, and sewage sludge, which serves a valuable dual purpose of producing products while also processing waste. However, such systems function as appendages to existing activities and are subject to the vagaries of these activities, such as seasonal gluts and shortages in crop residue availability. To reach the scale required to make a meaningful dent in demand for petrochemical products, dedicated, large-scale cultivation of biorefinery crops is likely necessary. The United States and Brazil have established large scale industries for bioproduction of ethanol, based largely on corn and sugarcane as feedstocks [95]. The production of biodiesel, from oilseeds such as soybean, provides a further major source of biofuel in both countries [95]. These offer real examples of the scale of biorefinery required, with fully 40% of the 2015 US corn crop being dedicated to fermentative ethanol production [95]. Such schemes involving “First Generation Bioenergy Crops” are however controversial for their use of edible crops, as this contributes to price inflation for staple foods, to deforestation, and to soil degradation. “Second Generation” biomass attempts to address these concerns by using either inedible, lignocellulosic fractions of staple crops (e.g., waste biomass) or through dedicated cultivation of inedible lignocellulosic energy crops, such as microalgae or jatropha [96]. However, large scale production of these crops for bioproduction may also have a similar effect on food prices to first-generation crops, to the extent that they occupy arable land otherwise suitable for food production. Their cultivation may similarly contribute to eutrophication, deforestation, and soil degradation.

Several studies have suggested that plants displaying Crassulacean Acid Metabolism (CAM) could provide a solution, as they are cultivable on marginal, semi-arid land poorly suited

to conventional agriculture, and usually poor in native biodiversity [19, 32, 97, 98]. This class of plants which encompasses 16,000 species includes such economically relevant members as *Opuntia ficus indica* (prickly pear), *Agave spp.* – used variously in food, alcohol, and fibre production, and *Ananas comosus* (pineapple), as well as other species proposed as possible biomass crops, such as *Euphorbia tirucalli* (Indian tree spurge) [99]. CAM carbon fixation represents an evolutionary response to arid environments, which permits plants to undertake photosynthesis during the day, but only perform gas exchange at night, which minimises water loss through transpiration. Malic acid, accumulated in the vacuole, provides a temporary store for CO_2 carbon at night, which is then decarboxylated and fixed by RuBisCO during the day cycle (**Figure 2.4**) [100].

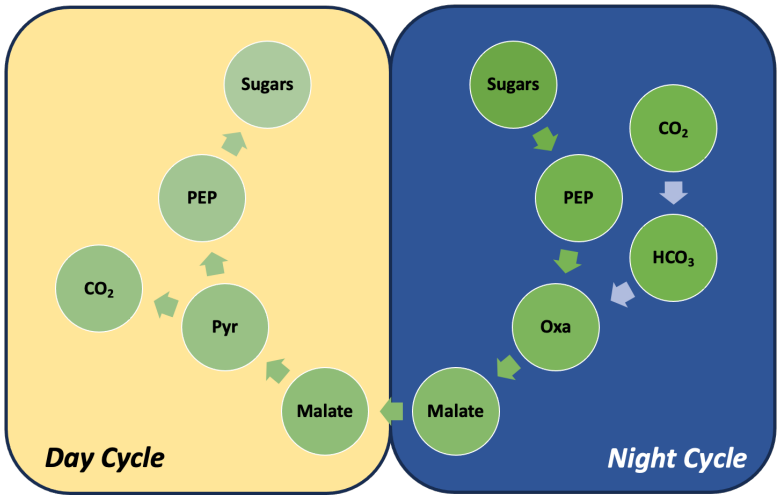


Figure 2.4: Temporal segregation of carbon fixation in Crassulacean Acid Metabolism into day and night cycles: **Night Cycle**: At night PEP carboxylase functions to fix CO_2, via oxaloacetate, as malate, which is stored in the vacuole. **Day Cycle**: Stored malate is decarboxylated and fixed by RuBisCO during the day. Relevant enzymes not shown. **PEP**: Phosphoenolpyruvate, **Oxa**: Oxaloacetate, **Pyr**: Pyruvate. [Figure based on data in Edwards [100]].

By relegating respiration to the night-time CAM plants achieve considerable water use efficiency as compared to their C_3 and C_4 counterparts, assimilating as much as 4-10 mmol CO_2 per mol H_2O, as compared to just 1-2 mmol and 0.5-1.5 mmol for C_4 and C_3 plants, respectively [19]. These plants are capable of similar biomass productivities to conventional C_3 and C_4 crops, with just 20% of the water requirement [101]. As an additional adaptation to water scarcity, CAM plants are succulent and demonstrate considerable water storage capacity in their tissues. Biomass from CAM plants has also been reported as having a low lignin content [19]. The high internal turgor pressure of CAM plants, which arises from their succulence, has been suggested

to provide structural support, which reduces their reliance on lignin for support [102]. An alternative hypothesis to explain the low lignin content of CAM crops is that the low transpiration rates of CAM plants leads to lower xylem pressures, thereby reducing the need for extensive lignocellulosic support [19]. Lignin is commonly cited as being inhibitory in anaerobic fermentation processes though various theories exist as to the specific mechanisms of inhibition. Lignin is itself poorly anaerobically degradable, with the most common mechanisms for its degradation being aerobic processes mediated by white rot fungi [64]. It may also directly inhibit the enzymes required to degrade other biomass components, and otherwise render these materials less amenable to degradation by occluding them from their hydrolytic enzymes [65]. Conversely, it may simply be that fibre content, of which lignin is a part is negatively correlated with lower biomass degradability as compared to biomass sources consisting of more soluble carbohydrate sources [103]. Whatever the origin of this feature, on a process level a low lignin-content typically correlates with improved fermentability.

Multiple authors have thus suggested that CAM crops should prove readily degradable under anaerobic conditions [19, 32, 99]. Interestingly, Lueangwattanapong et al. [32] found CAM crops of several species to perform comparably to maize stover as a substrate for AD production, though the lignin contents of the species used were found to be higher than those in the literature for other CAM plants [104, 105]. Reported lignin contents for a range of CAM and non-CAM species are summarised in **Table 2.3**.

Table 2.3.: Reported lignin content of CAM crop fractions reported across the literature, as compared to several key non-CAM species.

	Species	**Fraction**	**Lignin (%TS)**	**Citation**
CAM	*Agave angustifolia*	Leaf	8.5	[32]
			14	[106]
	Agave americana	Leaf	2.7 - 9.1	[106]
	Agave tequilana	Leaf	9.8 - 16.3	[106]
	Euphorbia tirucalli	Stem	4.1-6.1	[99]
	Euphorbia virosa	Stem	17.6	[32]
	Kalanchoe daigremontiana	Leaf	10.0	[32]
	Opuntia fragilis	Cladode	9.5	[32]
			3.9	[104]
	Ananas comosus	Leaf	17.5	[32]
	Opuntia ficus indica	Cladode	4.7	[19]
		Cladode	1.8-3.9	[99]
		Bagasse	12.3	[105]
Non-CAM	*Zea mays*	Shoots	15.6	[32]
		Straw	17.6	[107]
	Miscanthus spp.	Leaves	13.8 - 31.1	[108]
		Stalks	12.7 - 27.4	
	Pinus spp.	Sawdust	20.5-25.8	[109]
		Needles	26.38	[107]

CAM crops thus resolve two of the primary feedstock-level obstacles to large-scale biorefinery, namely the competition for arable land between feedstock crops and conventional agriculture, and the incompatibility of much lignocellulosic biomass with fermentative processes. Mason et al. [19] cite two species, *O. ficus-indica* and *E. tirucalli,* as particularly promising feedstocks due to their high drought tolerance and ability to achieve high biomass productivities with very low rainfall.

Various CAM species have been assessed as AD substrates for biogas production and have shown comparable yields to standard, non-CAM substrates in both mono- and co-digestion formats, and much of this can be extrapolated to suggest a suitability for mechanistically similar processes such as AF [32, 99, 102, 110]. However, the potential for CAM crops to provide the raw substrate for the mass bioproduction of high-value products remains to be evaluated in detail.

2.3 Microbial production of industrially relevant storage lipids

2.3.1 Microbial storage lipids as substitutes to high-value petroleum products

Section 2.1 introduced the extraction and purification of high-value fractions from biomass, often for use as food or fine chemicals and the refining of the residual mixed biomass from these processes, of organic waste streams, and of dedicated bioenergy crops to produce volatile fatty acids through acidogenic fermentation. VFAs are valuable in their own right if extracted for direct sale. The global fatty acid market stood at US$ 27.22 billion in the year 2022, with some of this demand met through petrochemical synthesis [111]. Thus, biogenic VFA production allows for direct substitution of this existing source of petrochemical use. More significantly however, they can be used as platform chemicals to produce high-value products currently derived from fossil fuels.

Perhaps the most promising such use of VFAs is as the carbon source for microbial production of alternatives to petrochemicals with far more extensive markets, such as oils and plastics. Multiple microbial species of bacteria and yeast accumulate microbial storage lipids (MSL) as energy storage molecules under conditions of physiological stress. Examples of such MSLs include oils [112, 113], wax esters [114], and polyhydroxyalkanoates (PHA) [115]. These compounds often bear close chemical and physical resemblance to common petrochemical products, for which they could provide renewable alternatives, from lubricants, to esters, to plastics. Storage lipid accumulation is spread across diverse kingdoms of life, though those of

most relevance to industry include multiple species of unicellular yeasts and bacteria. Oleaginous yeasts accumulate significant quantities of TAG and sterol esters, such as *Rhodotorula glutinis*, reported as achieving up to 72% oil accumulation by weight [116], or *Yarrowia lipolytica*, reported by Papanikolaou and Aggelis [117] to accumulate 44% of cell weight as oil when grown on glycerol. Choi et al. [118] summarise accumulation of PHA reported across the literature for a variety of microbial species including *Vibrio proteolyticus* (59% of cell dry weight (CDW), 2.7 g/L) *Cupriavidus necator* (83.1% CDW, 93.5 g/L), and *Pseudomonas putida* (67% CDW, 41.5 g/L), on a variety of carbon sources and in various reactor conditions.

2.3.2 Polyhydroxyalkanoates as alternatives to conventional plastics

By 2015 an estimated 8.3 billion metric tonnes of plastic had been produced, of which 6.3 billion tonnes had been disposed of as waste with fully 79% of this latter figure accumulating either in landfills or in the natural environment [17]. None of the most common plastics are biodegradable and they thus represent a permanent source of environmental pollution. Their bioplastic alternatives, such as the PHAs, typically show good environmental degradability [119] and yet despite this, in 2021 the global market for bioplastics stood at just 2.1 million tonnes, or less than 1% of the global plastics market [120]. This demand is limited in part of this due to their cost, which arises itself in part from the use of costly pure carbon sources such as glucose for their production. The poor or limited mechanical properties of many common PHAs further limits their scope in the market. The former problem is largely addressed by use of low-cost substrates, such as VFA produced through AF. The latter problem may be ameliorated through blending of PHAs with additives such as cellulose to improve the thermal and mechanical properties of PHAs. PHA mechanical properties may be improved through co-polymerisation, i.e., selecting blends of monomers which produce a polymer with the desired mechanical properties [120]. The PHAs are a diverse class of thermoplastic polyesters formed from R-hydroxyalkanoic acid monomers [121] and may exist as homopolymers (i.e., containing a single monomer) such as the extensively studied polyhydroxybutyrate (PHB), or as heteropolymers of multiple monomers. PHAs are classed based on the sizes of the individual monomer units incorporated into the polymer. Most common in the literature are the short chain PHAs (scPHA) consisting of mainly 4-5 carbon monomers, and the medium chain PHAs (mcPHA), containing monomer units of 6-16 carbons [122]. This general PHA structure is introduced in **Fig. 2.5**. The specificity of an organism's PHA synthase (PhaC) enzymes is the most important factor defining PHA structure [123], and leads to the broad groupings of short, medium, and even to the less common long chain PHAs. Very few bacteria have broad-

specificity PhaC enzymes capable of synthesising copolymers combining short and medium-chain monomers. Around 150 distinct monomers are known, which include linear, branched, and aromatic sidechain structures [121], the location of these sidechains is indicated "R" in **Fig. 2.5** panel **A**. This chemical diversity allows for customisation of the material properties of the resulting plastic. The short chain homopolymer polyhydroxybutyrate (PHB), for example, contains 4 carbon hydroxybutyrate monomer units and is readily produced by such PHA-hyperaccumulators as *Cupriavidus necator*, which has been reported to accumulate up to ~90% of cell dry weight as PHA [124]. This polyhydroxybutyrate (PHB) homopolymer typically produced by wild-type *C. necator* is however crystalline and brittle - rendering it ill-suited to many industrial and commercial applications [118]. *C. necator* is however also able to incorporate the C5 monomer 3-hydroxyvalerate (3HV) to produce the copolymer poly(3HB-co-3HV) [125]. The 3HV monomer introduces irregularities to the polymer, which reduces its crystallinity and melting temperature to give a plastic both less brittle and more amenable to thermal moulding and processing [126].

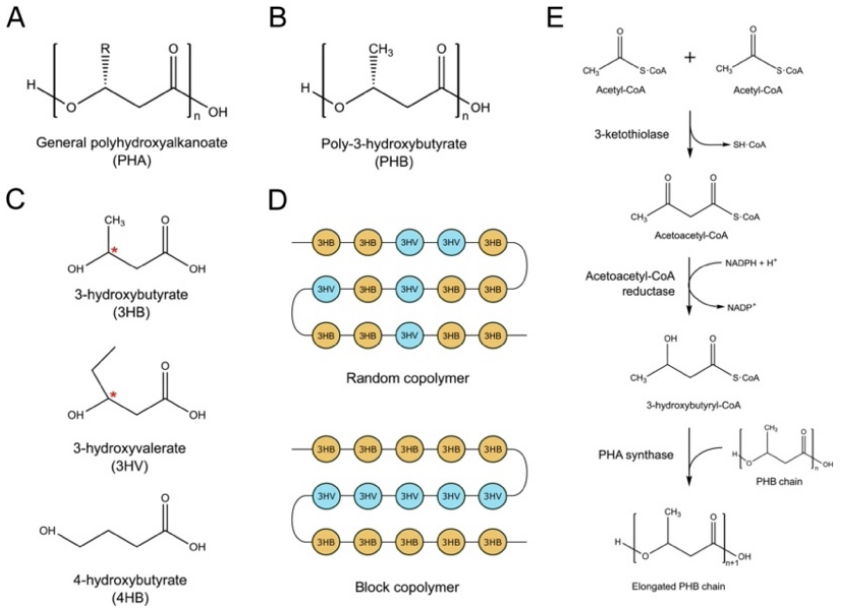


Figure 2.5: Overview of the structure and biosynthesis of the PHA polymer. **A**) General structure of the PHA polymer repeat unit, **B**) General structure of PHB polymer repeat unit, **C)** Chemical structures of common monomers (* shows chiral carbons), **D)** Random vs. block copolymer organisation of PHB-V, **E)** Generic pathway for synthesis of PHB polymer as performed by *C. necator*. Figure reproduced from Morlino et al. [126], licenced under CC-BY-NC-ND 4.0.

Short-chain PHAs such as these are typically hard and highly crystalline thermoplastics, while medium-chain PHAs such as are produced by *P. putida* are more elastic, rubber-like substances. The thermal and mechanical properties of several PHA homo and heteropolymers reported in the literature are presented in **Table 2.4**. Choi et al. [118] draw particular attention to the copolymer of Poly(3HB-3HH), which shows an intermediate characteristic with significantly improved flexibility over a pure Poly(3HB) homopolymer, while retaining good mechanical strength.

Table 2.4: Thermal and mechanical characteristics of selected PHA homo and heteropolymers

	Polymer	Mechanical properties				Citation
		T_m (°C)	Young's modulus (MPa)	Tensile Strength (MPa)	Elongation at break (%)	
Homopolymers	Poly(3HB)	178 -	3500 1100	43 62	5 58	[118]
	Poly(3HV)	104.2-109.7	-	31.2	14	[118]
	Poly(3HD)	72.2	12.0	19.9	312.9	[118]
Copolymers	Poly(3HB-17%3HHx)	120	-	20	850	[118]
	PHH-rich mcPHA	131.1	-	-	-	[79]
	3HD-rich mcPHA	43.2	17.3	1.0	20	[79]

The ability of many PHA-producing species including *P. putida*, and *C. necator* to use VFAs as a carbon source indicates a route by which these plastics could be derived from low-value biomass, via the intermediate acidogenic fermentation to VFA [79, 124]. PHA quality must however also be considered, and production directed towards polymers with favourable thermal and mechanical properties. Taking *C. necator* and *P. putida* as model organisms, it can be seen at the very coarsest level that the type of PHA (short or medium chain) can be chosen through the choice of accumulator species. At a finer level of granularity, Dartiailh et al. [79]

indicated that the monomer composition of PHA produced by *P. putida* could be shifted with changes in feedstock, which may allow creation of polymers with custom mechanical properties, as direct substitutes for existing bulk and specialty plastics. This group found the monomer compositions of mcPHA produced by *P. putida* LS46 to be highly responsive to carbon source (**Fig. 2.6**). *C. necator* will also readily incorporate odd-carbon number VFAs (such as propionate) into 3HV monomers [125, 126], suggesting that the odd-even blend of VFAs in the feed can be used to manipulate the 3HV content of the short-chain Poly(3HB-co-3HV) co-polymer produced by this species, to achieve desired properties.

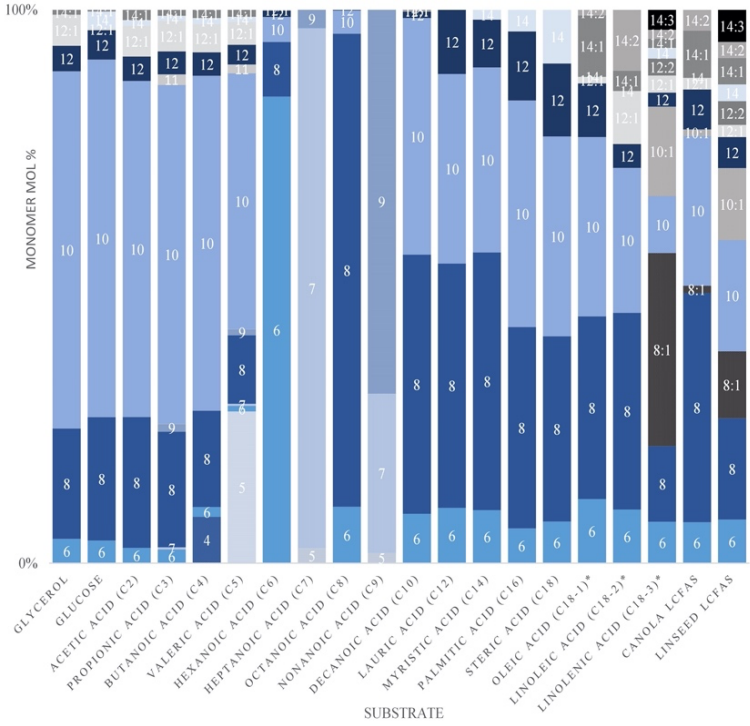


Figure 2.6: Molar monomer compositions of PHAs produced by *P. putida* on various carbon sources as reported by Dartiailh, et al. [79]. Note in particular the C2-C5 VFAs, which can be derived through AF. Figure reproduced from Dartiailh et al. [79] licenced under CC BY 4.0.

The ability of the feedstock used to influence the composition of the PHA produced suggests that custom AF configurations – targeted toward specific VFA profiles, might be used to produce PHAs of a particular monomer composition. In **Fig. 2.6** cultures fed with fatty acids of a given length (especially those with 6, 7, and 8 carbons) showed an increase in PHA monomers of the same length.

This suggests a direct route of incorporation via the fatty acid ß-oxidation pathway [79]. Conversely, PHAs produced from glucose, glycerol and VFAs of fewer than 6 carbons had very similar compositions, suggesting that PHA production from these substrates proceeded through

a common mechanism. This common mechanism was likely substrate oxidation to acetyl-CoA, with subsequent fatty acid synthesis for PHA monomer production as shown in **Fig. 2.5**. This has important implications for PHA production from VFAs derived through AF as the longest VFA typically produced through AF is hexanoate. The majority of the VFA in an acidogenic fermentate will thus be present as C2-C4 acids, which can be expected to be incorporated by *P. putida* via acetyl-CoA into a "typical" C10-rich PHA. The narrow product spectrum of AF appears to leave little room to use custom VFA profiles to generate PHAs of custom or useful properties in *P. putida*, with the exception of manipulation of hexanoate levels, which might be expected to increase the content of the C6 (3-hydroxyhexanoic acid) monomer.

A further requisite for efficient PHA production is nutrient limitation, which is required to shift allocation of substrate carbon from the accumulation of biomass to storage as PHA. Hyperaccumulation is most commonly achieved through nitrogen limitation, though limitation of other nutrients such as phosphate may also produce a similar response [127]. The primary metabolic means through which nitrogen limitation dictates PHA accumulation is by influencing the allocation of acetyl-CoA away from the TCA cycle, to which it is preferentially allocated under nutrient balanced conditions, directing it instead to PHA accumulation [128]. Nitrogen limitation is proposed to induce PHA accumulation by causing an accumulation of reduced cofactors, such as NADPH, for which PHA production provides a sink (specifically in the reduction of acetoacetyl-CoA to 3-hydroxybutyryl-CoA – **Fig. 2.5**). PHAs thus perform a dual function, storing carbon when in excess, and providing a sink for surplus reducing power and acetyl-CoA when these are in excess – thus providing a route to regenerate oxidised cofactors (NADP+) and free CoA [126, 128]. The abundance or limitation of nitrogen in culture conditions is commonly expressed as the carbon to nitrogen ratio (either in molar or mass units), which allows for some standardisation of comparisons across the literature: high C:N ratios are thus typically associated with PHA accumulation. Wen et al. [127] found maximal PHA accumulation (59% of CDW) in a mixed microbial population at a C:N ratio of 125. [129] found maximal PHA production in *C. necator*, both as % CDW and g/L at a C:N of 36 (the highest ratio tested in this particular study). Ahn et al. [130] conversely found maximal PHA production by *C. necator* at a C:N of 360, as measured in g/L. Control of C:N in these studies was established by the controlled dosing of carbon and nitrogen sources. It should also be mentioned that limitation of nutrients other than nitrogen can be used to induce storage lipid accumulation, in particular phosphorus, in which case it is the carbon: phosphorus ratio that is of interest [114, 127, 131]. Wen et al [127] for example compared nitrogen and phosphorus limitation strategies for PHA production in a mixed culture system. They found nitrogen limitation to be more

effective for overall PHA production but found also that PHA composition differed based on the type of inhibition used, with a higher PHB:PHV content identified for PHAs produced under phosphorus limitation. C:P ratio manipulation can also be used to select for microbial subpopulations with a high PHA accumulation capacity prior to inducing accumulation through nutrient limitation [132].

While nitrogen-limitation induces PHA accumulation, nitrogen is also required to allow for proliferation of the very cells which produce this PHA. The relationship between PHA accumulation and nitrogen limitation is thus not monotonic. For example, while Ahn et al. [130] identified an increase in PHB production with nitrogen limitation, they also found nitrogen limited conditions (i.e., 20 g glucose + 0.01 g NH_4Cl) to produce PHA titres almost 10-times higher than when nitrogen was absent (3.1 vs. 0.37 g/L PHB). Maximising PHA production thus becomes a question of identifying the optimum C:N for a given reactor configuration, rather than simply one of minimising nitrogen. PHA accumulation may also be measured in several ways, most commonly as % of CDW, as total concentration (g/L), or as conversion efficiency from input carbon source (%), with the maxima for each metric possibly occurring at different C:N ratios.

PHAs thus offer a promising route for upgrading VFAs to produce thermoplastic polymers with the potential to displace common synthetic plastics. The use of low-cost AF-derived VFAs as the carbon source for this process reduces feedstock costs (as compared to glucose for example) to improve the economics of PHAs against their synthetic alternatives. This process must however be optimised along two axes: quantity (i.e., PHA yield), and quality (i.e., PHA polymer composition). The former must contend with the question of how to induce conditions of nitrogen limitation in AF fermentates in which VFA and nitrogen are combined so as to maximise PHA yields, the latter must consider how the composition of the VFA pool, and the accumulator species, affect the composition and industrial compatibility of the resultant PHA.

2.4 Use of aluminosilicates to remove fermentate nitrogen

While the acidogenic processes detailed in the preceding chapters are capable of processing biomass into a usable VFA intermediate, this must typically be extracted and purified from the reactor broth prior to upgrading to high value chemicals. Straathof [133] gives an overview of such downstream processing (DSP) costs for a variety of fermentative processes. While estimates for VFAs are not given, the estimated DSP cost for citric acid is given as 20-

30% of overall process cost, and as 36% for lactic acid. Several methods exist for VFA purification, including electrodialysis [134], adsorbent-based systems [135], and liquid-liquid extraction into organic solvent. Bekatorou et al. [136] demonstrate recovery of fermentative C2-C4 VFAs into a variety of solvents, in particular alcohols such as 1-butanol and 3-methyl-1-butanol. Extraction of nearly 100% of VFAs is reported with sequential extraction, though the process broadly showed a preference for longer chain fatty acids and was less efficient with acetate. This highlights a common limitation of extraction processes, which, in addition to their cost, may preference specific VFA species and lead to incomplete or biased extractions.

When used as the carbon source for biological fermentations, such as the production of PHA and other microbial storage lipids, a pure VFA source has significant advantages. As established in **Section 2.3**, the limitation of key nutrients, especially nitrogen, is a precondition for the efficient accumulation of PHA by microbial species. The Stickland degradation of amino acids present in the input biomass (as detailed in **Table 2.1**), will liberate ammonium nitrogen into the same broth as the VFA. Control of C:N ratios to maximise PHA accumulation demands that VFA and ammonium levels may be manipulated independently of one another. As PHA is accumulated under conditions of nitrogen limitation (i.e., high C:N), it is likely that the C:N ratio of the VFA broth will be lower than is optimal for PHA production. The simplest solution would be to supplement the broth with an exogenous source of VFA to increase the C:N to within an optimal range, though this presupposes an external source of VFA which presumably would be subject to the high purification costs detailed by Straathof [133].

A simple and elegant solution to this problem could be instead to reduce the nitrogen concentration through controlled stripping, thereby establishing control over C:N ratio of the fermentate to allow for direct, *in situ* bioproduction of PHAs on the reactor effluent. Conveniently, ammonium/ammonia represents the terminal product of acidogenic fermentation of biological nitrogen sources such as protein (**Table 2.1**), meaning nitrogen stripping approaches need only consider this chemical species. Multiple nitrogen stripping techniques have been applied to acidogenic fermentate and to anaerobic digestates, in order to recover nitrogen in a usable form, and to minimise eutrophication of the surrounding environment from discharge of AD effluent. Examples of such techniques include gas stripping [137, 138], electrodialysis [139, 140], precipitation [141], and ion-exchange methods [141-144].

Gas stripping involves the removal of free ammonia from the solution as gas, typically through bubbling, which encourages exchange of ammonia from the liquid into gas phase. Efficient removal of ammonia from digestates has been demonstrated with this method, including by Palakodeti et al. [137], who found both temperature and pH to be highly influential

over process efficiency, and who reported removal efficiencies of over 90%. Efficiency increased with temperature due to reduced solubility of NH_3 at higher temperature and increased with increasing pH due to its effect on the equilibrium of the ammonium/ammonia system, to favour free ammonia. The equilibrium between ionic ammonium (NH_4^+) and free ammonia (NH_3), is dependent on both pH and temperature and is shown in **Fig. 2.7** [145]. This equilibrium will affect the efficiency of the stripping modality employed, as it will typically either target the ionic or free side of the equilibrium.

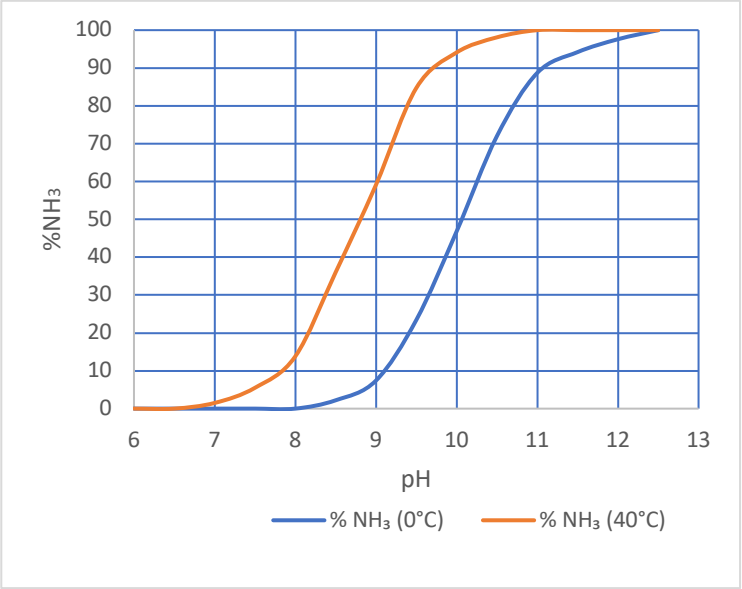


Figure 2.7: Temperature and pH dependence of ammonium/ammonia equilibrium. Figure data sourced from Huang and Shang [145]. Note that the system has a pK_a of 9.25 at 25°C.

While degassing methods benefit from increased temperature and alkaline pH, these both entail increased process costs in energy and alkaline reagents. As most acidogenic fermentation occurs at or near a neutral pH, ionic ammonium (NH_4^+) will overwhelmingly be the dominant species in most AF configurations and many stripping techniques target this species directly. Examples of such include anammox conversion of NH_4^+ to diatomic nitrogen [146], membrane osmosis [147], and precipitation as struvite [148, 149]. An alternative solution is offered by abundant, naturally occurring aluminosilicate minerals, which show an endogenous capacity to bind ammonium ions. Zeolites are a broad group of such minerals and encompass a wide range of microporous frameworks, both naturally occurring and synthetic. Their useful properties (a well-defined porous structure, stability, tunability, and ion-exchange capacity) have led to their extensive use in varied industrial applications [150].

Zeolites have the following general chemical composition:

$$[(SiO_2)(AlO_2)_x]M_{x/n}^{n+} \bullet wH_2O$$

In this structure, M is a cation, with positive charge ‘n’. This is most commonly a proton, or metal ion of group I or II, but this position may also be occupied by other cations such as ammonium (NH_4^+) [151]. Zeolites have been demonstrated to be able to strip ammonium from waste waters [152], and even to successfully recover nitrogen from acidogenic fermentates [153]. Naturally occurring zeolites such as chabazite, clinoptilolite, and heulandite are present in huge quantities in natural deposits, and are accordingly available at very low cost (<$US1 /kg) [154]. They are thus particularly appealing ammonium removal agents for large-volume, low-value applications such as fermentate upgrading in biorefinery. Zeolites differ from one another chemically, most notably in their silicon to aluminium ratio, and in their structure, which can take the form of one of many well characterised microporous structures. Around 40 naturally occurring zeolites are known, and over 200 synthetic zeolite frameworks are theoretically possible. An overview of common zeolite pore frameworks is given in **Fig. 2.8**. Pore structure influences a zeolite’s ability to discriminate between molecules, such as when used as adsorbents or filters in industrial application [150].

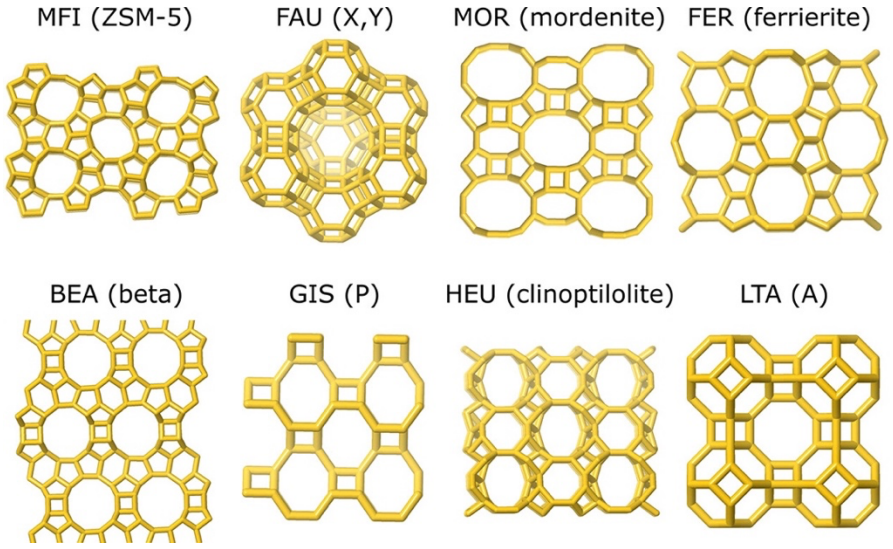


Figure 2.8. Pore structure of selected common zeolites. Each structure is provided with its associated three letter code assigned by the International Zeolite Association. In brackets, the names of common zeolites presenting those frameworks. Figure reproduced from Pérez-Botella et al. [150] licenced under CC BY 4.0.

Natural clinoptilolite zeolite, the pore framework of which can be seen in **Fig. 2.8**, has been extensively applied in the literature as an exchange medium for ammonium removal from water, anaerobic digestate and other complex waste streams [142, 153, 155]. Several studies have tested the ability of this and other zeolites to ameliorate the effect of ammonium toxicity on AD, by directly binding and immobilising the ion as it is produced within the reactor, [156, 157]. Of most relevance to this study, however, are methods which employ zeolites as for post-fermentation processing of fermentates such as those of Kocatürk-Schumacher et al., [144] and Martin-Ryals [142]. These processes suggest the possibility of a simple, in-line process which could allow direct use of fermentate for PHA production, in such a way that bypasses the need for expensive VFA extraction. At time of writing clinoptilolite zeolite could be obtained at a cost of just $US 120/tonne [158], which further suggests the economy of such an approach. Recycling and reuse of the zeolite use in the process, and recovery of the bound ammonium in a usable, saleable form could further improve system economics. VFA extraction techniques tend to extract VFA from the aqueous solution based on hydrophobicity, and so achieve poor results, biased in favour of longer VFAs. Zeolite extraction extracts ammonium ions based on charge and should not affect the VFA in any appreciable way.

The study of Martin-Ryals [142] is perhaps the closest approximation to the system envisaged in this thesis. The authors of this study operated a mixed culture fermentation system to produce VFA from biomass, and then undertook community enrichment to facilitate mixed-culture PHA accumulation. They tested the application of zeolites to minimise ammonium inhibition on PHA production and report a modest increase in PHA from 17 to 23% of VSS, between untreated and zeolite-treated conditions. This study however treated ammonium as a purely inhibitory compound and targeted its removal. It achieved only a modest increase in PHA production and does not attempt to achieve accurate control of C:N ratios to maximise PHA production as the PHA literature (**Section 2.3**) suggests should be possible. In practice, fixed bed zeolite reactor schemes have been demonstrated in which zeolites are added directly to the primary reaction chamber in which biomass digestion occurs, and have demonstrated increased biogas production through reduced ammonium inhibition [159]. Such configurations present logistical challenges, as ammonium-saturated zeolite cannot easily be removed and refreshed without opening the reactor. Wijesinghe et al. [160] instead demonstrated an AD system in which zeolite was held in an external column through which digestate was passed. A zeolite-based chromatography approach such as this also suggests a mechanism for ammonium recovery through elution of ammonium from the column using a competing metal cation (K^+, Na^+). The selection of eluent should take into consideration both economic and technical

considerations, considering both the market for the salt produced, and such considerations as its aqueous solubility and tendency to precipitate, which will influence both system stability and recovery efficiency. The study of Bolan et al [161] found zeolite to be reusable over multiple cycles of binding and refreshing with no detectable degradation over 12 binding cycles, suggesting that chromatography-format systems could be used reliably without need to regularly change the zeolite stationary phase.

Such systems must however also consider that this ammonium binding interaction is not occurring in a 'pure' medium and so must also contend with competing cations, particularly metals, and also protons which will be more abundant at low pH. Several zeolite studies report lower ammonium binding capacities in wastewaters than in pure media of equal ammonium concentration, largely due to the presence of competing ions [155, 161]. Many zeolite studies have largely taken place in lower strength wastewaters than those produced from acidogenic fermentation, hence the influence of ammonium ion strength on this binding interaction should be considered. Presumably though, the high concentration of ammonium ions in AF effluents would improve recovery efficiency over that achievable for lower strength wastewaters.

Combining the zeolite-chromatography approach of Wijesinghe et al. [160] and the PHA production demonstrated by Martin-Ryals [142] suggests a system that could integrate AF and PHA production into a simple two-step biorefinery system to derive bioplastics from biomass, and which could collect the green ammonium in a usable form. Optimising this system to target the C:N maxima identified for various species in the literature (**Section 2.3**), could further increase efficiency.

2.5 Research gap

The literature review presented above provides an overview of a two-step process for the production of PHA bioplastics from biomass via the fermentation to VFAs as an intermediate. Several clear research gaps have been identified across these various process steps. A primary obstacle to the mass production of renewable PHA plastics is the high cost of feedstocks, such as glucose. VFAs provide a low-cost alternative as they can be derived from cheap organic waste streams and energy crops through the process of acidogenic fermentation, and yet common energy crops compete for agricultural land and can show poor anaerobic degradability. This relatively low anaerobic degradability has been attributed to high lignin content by several authors [19, 32]. Working with the energy crop *Miscanthus* x *giganteus*, Schmidt et al. [103] found biomethane potential to differ greatly with harvest time, being particularly low in mature biomass. The authors attribute this observation to both a high content of poorly degradable complex lignocellulosic material, and low concentration of soluble carbohydrates. CAM crops, being cultivable on marginal lands and having a less-recalcitrant biomass structure relatively low in fibre and high in soluble organics, sidestep these major issues and have been demonstrated as effective feedstocks for anaerobic digestion [32, 99, 110, 162]. Their amenability as feedstocks for VFA production through AF has however not been extensively investigated.

Red seaweeds such as *Asparagopsis taxiformis* have been identified as effective methanogenesis-inhibitors in ruminant animals suggesting it may provide a cheap alternative to small-molecules for controlling methanogenesis in AF reactors [90-92, 94, 163], however this potential application has not been experimentally investigated.

The bioproduction of PHAs on VFAs is well established [118, 124], and nitrogen-limitation is known to increase PHA production in various species [118, 129, 130]. This suggests that controlled nitrogen stripping of fermentates could be used as a strategy to maximise PHA accumulation. As most nitrogen in fermentates is present as ammonium, naturally occurring zeolites, which show an inherent ability to bind ammonium could provide a means to optimise fermentate C:N ratios for PHA production [142, 151, 153].

The research presented in this thesis addresses these research gaps in the following ways:

1. The CAM crop *Euphorbia tirucalli* was subjected to acidogenic fermentation at various substrate loadings, and with various ratios of a nitrogen-rich co-substrate (pig blood) to determine the effect of C/N ratio on VFA yield and composition.

2. Several industrially relevant CAM crops were subjected to acidogenic fermentation with distinct microbial communities (AD sludge and rumen fluid), and the kinetics of their degradation then compared with those of common energy crops and agricultural residues.

3. The methanogenic efficiency of *Asparagopsis taxiformis* was compared against that of a common small-molecule inhibitor, bromoethane sulfonate, in two microbial communities (AD sludge and rumen fluid), to evaluate its potential as an abundant and natural alternative for AF reactor control.

4. Two aluminosilicates (bentonite and zeolite) were assessed for their capacity to strip nitrogen (as ammonium) from acidogenic fermentates and to establish control over C:N ratios. These were tested first in batch format and are then incorporated into an ion-exchange chromatography device as the stationary phase.

5. PHA production in two species (*P. putida* and *C. necator*) was observed on AF fermentate treated to various C:N ratios with zeolite, to establish whether zeolite-treatment could enable improved PHA production as an alternative to expensive VFA extraction techniques.

2.6 Aims and Objectives

Overall aim: The overall aim of this project was to optimise a process for PHA production from biomass via acidogenic fermentation to VFA and subsequent upgrading to PHA in pure culture.

This overall aim contains multiple specific aims:

1. To evaluate the effect of both organic loading rate and co-substrate (C:N) ratio on the quantity and quality of VFA produced through acidogenic fermentation of *Euphorbia tirucalli*.

2. To evaluate the performance of several economically relevant CAM substrates against several non-CAM substrates through a comparison of their fermentation kinetics.

3. To evaluate the potential of *Asparagopsis taxiformis* as a methanogenesis inhibitor for AF applications.

4. To evaluate the capacity of zeolite to manipulate C:N ratios in acidogenic fermentate.

5. To evaluate the effect of zeolite-treatment on PHA yields in *C. necator* and *P. putida*.

6. To determine the effect of VFA composition in fermentates on the monomer composition in PHAs produced by *P. putida*.

Chapter 3. Anaerobic co-digestion of *Euphorbia tirucalli* with pig blood for volatile fatty acid production

Disclaimer

The following manuscript was accepted for publication in Volume 21 of the journal Bioresource Technology Reports on 05/01/2023. Several minor edits have been made to it in fulfilment of the suggestions of thesis examiners.

The published article (licenced under CC BY 4.0) may be accessed at:

Tenci, N. A., Ammam, F., Huang, W. E., & Thompson, I. P. (2023). Anaerobic co-digestion of *Euphorbia tirucalli* with pig blood for volatile fatty acid production. *Bioresource Technology Reports*, *21*, 101333.

Anaerobic co-digestion of *Euphorbia tirucalli* with pig blood for volatile fatty acid production

Authors: Nicholas A. Tenci[a], Fariza Ammam[a], Wei E. Huang[a], Ian P. Thompson[a]*

Affiliations: [a]University of Oxford, Department of Engineering Science, Parks Road, Oxford, OX1 3PJ, United Kingdom.

*Corresponding author: ian.thompson@eng.ox.ac.uk. Department of Engineering Science, University of Oxford, Parks Road, Oxford, OX1 3PJ, United Kingdom.

Abstract:

Acidogenic fermentation of biomass to produce volatile fatty acids provides a renewable pathway to industrial chemicals ordinarily derived from petrochemicals. Crassulacean acid metabolism plants such as *Euphorbia tirucalli* are cultivable on marginal land and offer promising feedstocks for this purpose. This study investigated how the refining of *E. tirucalli* biomass to fatty acids could be augmented with a high-protein co-substrate, pig blood. Blood mono-digestions provided the highest titres of total fatty acid (up to 38 ± 2 g/L), while at high substrate concentrations, acetic acid was maximal in co-digestions. 75 % blood with 25 % *E. tirucalli* produced acetic acid titres 40.8 % ($p < 0.001$) and 30.8 % ($p = 0.001$) higher than those in mono-digestions of *E. tirucalli* and blood, respectively. Where acetate is the desired product, inclusion of blood as a co-substrate offers significant benefit for *Euphorbia* biorefining.

3.1 Introduction:

Against a backdrop of accelerating climate change, renewable alternatives to petrochemicals are increasingly being sought. Anaerobic digestion (AD) is commonly employed to produce biomethane but may instead be configured to refine biomass into volatile fatty acid (VFA) from which industrial chemicals can be produced. VFAs generated via acidogenic fermentation (AF), and derivatives thereof, may be used to produce oil/biodiesel (Christophe et al., 2012), polyhydroxyalkanoate bioplastics (Mengmeng et al., 2009) and other bulk chemicals conventionally derived from fossil carbon (Lee et al., 2018; Zhou et al., 2020). This bypasses the need to derive these petrochemically.

While the cultivation of dedicated crops can provide an abundant feedstock for this purpose, this approach is criticised for its use of arable land otherwise needed to feed a still growing population. Feedstocks that do not compete with conventional agriculture, or that derive from the by-products of existing processes, are therefore desirable. Crassulacean acid metabolism (CAM) plants employ a unique form of photosynthesis, distinct from the C3 and C4 pathways of most common food crops, which allows them to readily adapt to restricted water availability. They have thus attracted attention as potential AD substrates, due to their cultivability in semi-arid areas ill-suited to conventional agriculture (Buckland and Thomas, 2021; Mason et al., 2015). CAM biomass is also notable for its relatively low lignin content (Lueangwattanapong et al., 2020). Lignin, a major constituent of lignocellulosic biomass, is highly inhibitory to hydrolytic processes in the AD bioreactor. This naturally lends CAM biomass to refining. While CAM photosynthesis is relatively widespread, occurring in an estimated 16,000 species (Winter and Smith, 2012), two plants in particular, *Euphorbia tirucalli* (Indian tree-spurge) and *Opuntia ficus indica* (Prickly pear), are able to yield considerable biomass under severe water restriction, and thus merit further investigation (Krümpel et al., 2020; Mason et al., 2015).

Despite these advantages as a feedstock, the introduction of a protein rich co-substrate might nonetheless allow for process optimisation. This co-digestion approach was recently shown to improve biomethane yields from AD of Opuntia, with slaughterhouse wastewaters providing the high-protein co-substrate (Panizio et al., 2020). Slaughterhouse by-products, such as blood, offal, and wastewaters have attracted considerable attention as potential AD substrates, with blood having recently been reviewed as a substrate for biomethane production (Nazifa et al., 2021). The low C/N ratios of these substrates makes them ill-suited to methanogenic AD in a mono-digestion mode, with several authors recommending their use as co-substrates with

high-carbon, or low-strength substrates (Hejnfelt and Angelidaki, 2009; Jensen et al., 2014). Successful methanogenic AD of meat wastes in a co-digestion format has been demonstrated with high carbon substrates such as paunch grass (Astals et al., 2014), maize (Cuetos et al., 2013) and Opuntia (Panizio et al., 2020). Slaughterhouse wastes have been shown to greatly improve stability of AD of carbohydrate-rich feedstocks, due to the pH-buffering effect of the ammonium released from their degradation (Miramontes-Martínez et al., 2021).

Substrate concentrations are another key parameter for optimisation in AD. Under conventional methanogenic AD, substrate concentrations must be kept low to prevent an accumulation of degradation products, mainly fatty acids and ammonium, which can inhibit methanogenesis (Abbassi-Guendouz et al., 2012). Under acidogenic AD, however, methanogenesis is undesirable and high VFA concentrations are instead favourable, as they allow for simplified product extraction. This freedom allows acidogenic reactors to be optimised over a wider parameter space of substrate concentrations than when biogas is the desired product. Despite this, a balance must still be struck between the increased titres achievable at higher substrate loadings, and the reduced yields of VFA (per unit of substrate) which have been documented at higher substrate concentrations. This decline in yields at higher loadings has been attributed to factors such as reduced hydrolytic efficiency and product inhibition (Abbassi-Guendouz et al., 2012; Bermúdez-Penabad et al., 2017; Pratt et al., 2012).

The composition of the resultant VFA is a further consideration in acidogenic AD. Unlike the relatively uniform product of methanogenic AD, biogas, acidogenic AD yields a mixture of fatty acids of different carbon chain lengths, typically ranging in size from 2 to 6 carbon compounds. The composition of any VFA produced will be highly responsive to reactor parameters and must be considered in conjunction with total VFA titres and yields when evaluating the suitability of a given reactor configuration (Jiang et al., 2013; Tepari et al., 2020). From an economic perspective, longer chain fatty acids typically command higher market prices as bulk chemicals and are cheaper to extract due to their higher hydrophobicity. These however typically constitute only a minority of the VFA produced. VFA-rich digestates are often applied as carbon sources for biological nitrogen removal from wastewater. As denitrifying bacteria preferentially utilize shorter classes of VFA in this process, here acetate is most desirable (Elefsiniotis and Wareham, 2007). The desired VFA composition will thus depend on the specific needs of the intended downstream applications of the acids being produced.

The objective of this study is thus to understand whether co-feeding with pig blood has any effect on the quantity or quality of VFA produced from *Euphorbia*. Feedstocks were tested at various concentrations and ratios. While co-digestion did not significantly improve overall TVFA titres, VFA composition was changed markedly. Acetate production benefitted significantly from co-feeding with blood.

3.2. Materials and methods

3.2.1 Biomass and inoculum

Euphorbia tirucalli biomass was obtained from the Royal Botanic Garden, Kew, United Kingdom, in dried form. This dry material was ground in a blender (Waring, USA) and passed through a screen (no. 10 mesh - 1 mm) to ensure a maximum particle size of 1 mm. Food-grade, dried pig blood was obtained from Tongmaster Seasonings (Coatbridge, United Kingdom). The inoculum used was anaerobic digestion sludge from a local biogas plant processing food waste and operating under mesophilic conditions (M&M Waste Solutions, Cassington, Oxford, United Kingdom). This was stored at 30 ºC until used. The inoculum was deployed within 4 days of collection.

3.2.2 Anaerobic batch assays

Synthetic basic medium was prepared according to the recommendations of Angelidaki and Sanders (2004), but with the omission of sodium sulphide. Medium was used to provide the requisite balance of micronutrients, trace metals, vitamins, and growth factors for robust microbial growth.

Batch assays were performed in 250 mL serum vials with a 150 mL working volume. The reaction mixture consisted of 20 mL inoculum sludge and 130 mL of microbial growth medium. Bromoethane sulfonate (BES - Sigma Aldrich, USA) was added to a final concentration of 10 mM to inhibit methanogenesis. The pH of the bulk reaction mixture was adjusted to 8.1 ± 0.1 before addition to serum vials into which the appropriate dried substrates had previously been added. Adjustment of initial pH to mildly alkaline was performed to provide a small amount of buffering capacity to allow VFA accumulation to occur. Five initial substrate concentrations were prepared: 100% blood, co-digestions of 25/75%, 50/50%, and 75/25% blood to *Euphorbia* on a volatile solids (VS) basis. Each of these conditions was prepared to three initial substrate concentrations (ISC) of 10, 30, and 60 g-VS/L.
Vials were sealed and capped with rubber septa and aluminium crimp-caps and mixed by inversion. In this experiment, the headspace gas was not purged to remove residual oxygen. A sludge-only control, with no added substrate, was prepared as a blank. As the residual volatiles

were not purged from the inoculum, this blank was subtracted from all treatment conditions to control for the effect of residual volatiles in the inoculum. Note that all substrate concentrations, co-substrate ratios, and VFA yields in this work are calculated on a mass basis considering only the volatile solids (degradable) fraction of the feedstocks. C:N ratios of the individual feedstocks are calculated on a total solids (TS) basis.

A cellulose control (at 10 g-VS/L microcrystalline cellulose - Avicel, Sigma-Aldrich, USA) was used to validate inoculum activity. All sample and control conditions were prepared in triplicate. Vials were incubated under mesophilic (37 °C) conditions, with constant agitation at 125 rpm.

3.2.3 Analytical methods

The inoculum and both substrates were characterised by standard methodologies (APHA, 1998). Determinations of cellulose, hemicellulose, and lignin content were performed according to the methodologies of van Soest et al (1991).

The biogas produced was measured by gas displacement of water in a eudiometer. Gas composition was measured using a gas chromatography device (Shimadzu – 2010, Shimadzu, Japan) equipped with a thermal conductivity (TCD) detector and 2 m x 0.53 mm 'ShinCarbon ST 80/100' (Restek) packed column. Helium provided the carrier gas at a flow rate of 3.39 mL/min. Injector, oven, and detector temperatures were set to 150, 75, and 200 °C, respectively. Biogas volumes were corrected to standard temperatures and pressures (273.15 K, 101.3 kPa) according to the method of Richards et al. (1991).

The pH of liquid samples was determined immediately upon sample collection using a pH probe (ThermoScientific, USA). To analyse VFA concentrations, liquid samples were centrifuged at 30,000 xg for 12 minutes and the supernatant collected into 1.5 mL GC vials. Samples were acidified by 1:1 dilution in 10% formic acid. VFA analysis was performed using a gas chromatography device (Shimadzu-2010) equipped with a flame-ionisation (FID) detector and 30 m x 0.25 mm x 0.25 μm fused silica column (nitroterephthalic acid-modified polyethylene glycol-phase) (ZB-FFAP). Injector and detector temperatures were 250 and 350°C, respectively. The oven was set to 100 °C for 2 minutes, ramped at 8 °C/min to 150 °C, and held

at 150 °C for 2 minutes. Acetic, propionic, isobutyric, butyric, isovaleric, valeric, and hexanoic acids were quantified against standards. Total VFA (TVFA) was calculated as the sum of these[2].

Concentrations of soluble protein were determined using a modified bicinchoninic acid (BCA) assay (Pierce Modified BCA Protein Assay Kit - ThermoScientific). Protein concentrations were provided by measurement of absorbance at 480 nm on a plate reader (Tecan, Switzerland) and quantified against a BSA standard curve.

Ammonium nitrogen was measured spectrophotometrically using a kit-based assay (HACH Lange - LCK303 kit) and DR2800 spectrophotometer.

3.2.4 Statistical analysis

All data herein are presented as means ± standard deviations of triplicate measurements. All statistical analyses were calculated, and all models fitted, in Microsoft Excel and in GraphPad PRISM. All figures presented herein were prepared in GraphPad PRISM.

3.3 Results and Discussion

3.3.1 Characterisation of substrates and inoculum

3.3.1.1 Characterisation of substrates

The compositions of the two substrates used herein are given in **Table 3.1**. As substrates were obtained in dried form, TS/FW (Total Solids/Fresh Weight) values were not biologically relevant and have been omitted. It should be noted that while dried substrates were used, literature values for the total solids content of livestock blood sit in the range of ~10–20 %, or 100–200 gTS/L (Nazifa et al., 2021). Accordingly, the working concentrations used in this study (up to 60 g-VS/L) would all be achievable in practice through simple dilution of fresh substrate.

VS/TS gives the fraction of volatile, or degradable content in the solid fraction. A high VS/TS is a desirable trait in a feedstock as a greater proportion of the solid material is available for conversion to product (Li et al., 2013). The calculated VS/TS of *Euphorbia tirucalli* (82.55

[2] TVFA yields in this study are calculated on a mass basis vs volatile solids (gVFA/gVS). The laboratory lacked the facilities to quantify COD of the insoluble feedstock as would have been required to calculated yields on a COD basis, but nonetheless allowed calculation of conversion of degradable fraction.

± 0.34 %) is close to literature values for other CAM plants – with literature values of 88.32 and 85.75 % for *Euphorbia virosa* stem and *Opuntia fragilis* cladodes, respectively (Lueangwattanapong et al., 2020). Notably in this study, the lignin content of *Euphorbia tirucalli* biomass was found to be just 3.65 %, considerably lower than literature values for other lignocellulosic biomass such as corn stover (18.8 %) (Yang et al., 2016) and wheat straw (18.52%) (Zeng et al., 2013), and of the CAM plants Agave (14.42 %), *Euphorbia virosa* (13.89 %), and pineapple (17.35 %) (Lueangwattanapong et al., 2020).

Total Organic Carbon (TOC) and Total Kjeldahl Nitrogen for *Euphorbia* biomass were calculated as 40.80 and 1.18%, respectively, giving a C:N ratio of 34.60. This is a moderate C:N ratio, falling near the range of 20-30 widely used for conventional anaerobic digestion (Wang et al., 2012).

Pig blood was calculated to have a VS/TS of 96.37 ± 0.03%, in agreement with the value of 95.79% (Kovács et al., 2013). TOC and TKN values of 34.10 and 14.80 %TS, respectively gave a low C:N ratio of just 2.3.

Table 3.1: Biomass characteristics of substrates and inoculum. All values are means ± standard deviations of triplicate measurements.

Characteristic	*Euphorbia*	Blood	AD Sludge
TS/FM (%)	N/A	N/A	4.77 ± 0.13
VS/TS (%)	82.55 ± 0.34	96.37 ± 0.03	64.75 ± 0.10
Cellulose (%TS)	27.94	-	-
Hemicellulose (%TS)	3.81	-	-
Lignin (%TS)	3.65	-	-
Crude Protein (%TS)	7.38	92.63	3.69
Total Organic Carbon (%TS)	40.80	34.10	33.50
Total Kjeldahl Nitrogen (%TS)	1.18	14.82	0.59
Carbon to Nitrogen Ratio (w/w)	34.58	2.30	56.78
Initial pH	-	-	8.02
Acetic acid (g/L)	-	-	0.17 ± 0.02
Propionic -hexanoic acids (g/L)	-	-	0.00 ± 0.00

*TS, FM, and VS, refer to total solids, fresh matter, and volatile solids, respectively

3.3.1.2 Characterisation of inoculum

Characteristics of the AD sludge inoculum are provided in **Table 3.1**. AD sludge was found to have a total solids content of 4.77 ± 0.13 %, of which 64.75 ± 0.10 % was volatile solids. TOC

and TKN values of 33.50 and 0.59 % gave a C:N ratio of 56.78. This high ratio is within expectation for a commercial AD facility processing municipal food waste, which is a homogeneous feedstock, the C/N ratio of which can vary widely depending on its constituent materials (Salangsang et al., 2022). The inoculum was additionally found to have low concentrations of VFA (at 0.17 ± 0.02 g/L acetic with no C3-C6 acids detectable), and an initial pH of 8.02, consistent with the low VFA concentrations sought in methanogenic reactors.

3.3.2 Acidogenic anaerobic digestion of *Euphorbia* and blood by AD sludge

3.3.2.1 Acidification profiles of *Euphorbia*, blood, and co-digestions thereof

Reactor pH and concentrations of VFA and soluble protein over the 16-day time-course are shown in **Fig. 3.1**. Blood-rich and *Euphorbia*-rich digestions generated distinct profiles of VFA accumulation, the former showing more rapid initial VFA production in days 0–5 than the latter, likely due to differences in substrate degradability. Differences in the availability of soluble substrate between sample groups can be seen in the soluble protein concentrations between reactors. Soluble protein concentrations rapidly declined over the first week as substrate was acidified. In conditions where soluble protein accounted for a large proportion of substrate volatiles at day 0, this depletion of soluble substrate accounted for the fast accumulation of VFA observed. Other studies have also reported maximal VFA titres at short retention times (<7 days) when a large proportion of substrate volatiles were present in a soluble form (Zhang et al., 2005). Also of note in **Fig. 3.1** is the de-coupling of VFA concentrations from pH. At each substrate concentration, blood-rich mono-digestions showed both the highest TVFA concentrations and yet also the most alkaline pH. This observation is likely the result of the release of ammonium from protein degradation, with NH_3 and NH_4^+ providing a buffer pair which checks the acidifying effect of VFA release in protein-rich digestions (refer to endpoint ammonium concentrations in **Table 3.2**). This and other ammonium-mediated buffering mechanisms have been implicated in improved AD efficiency at moderate C/N ratios (Miramontes-Martínez et al., 2021).

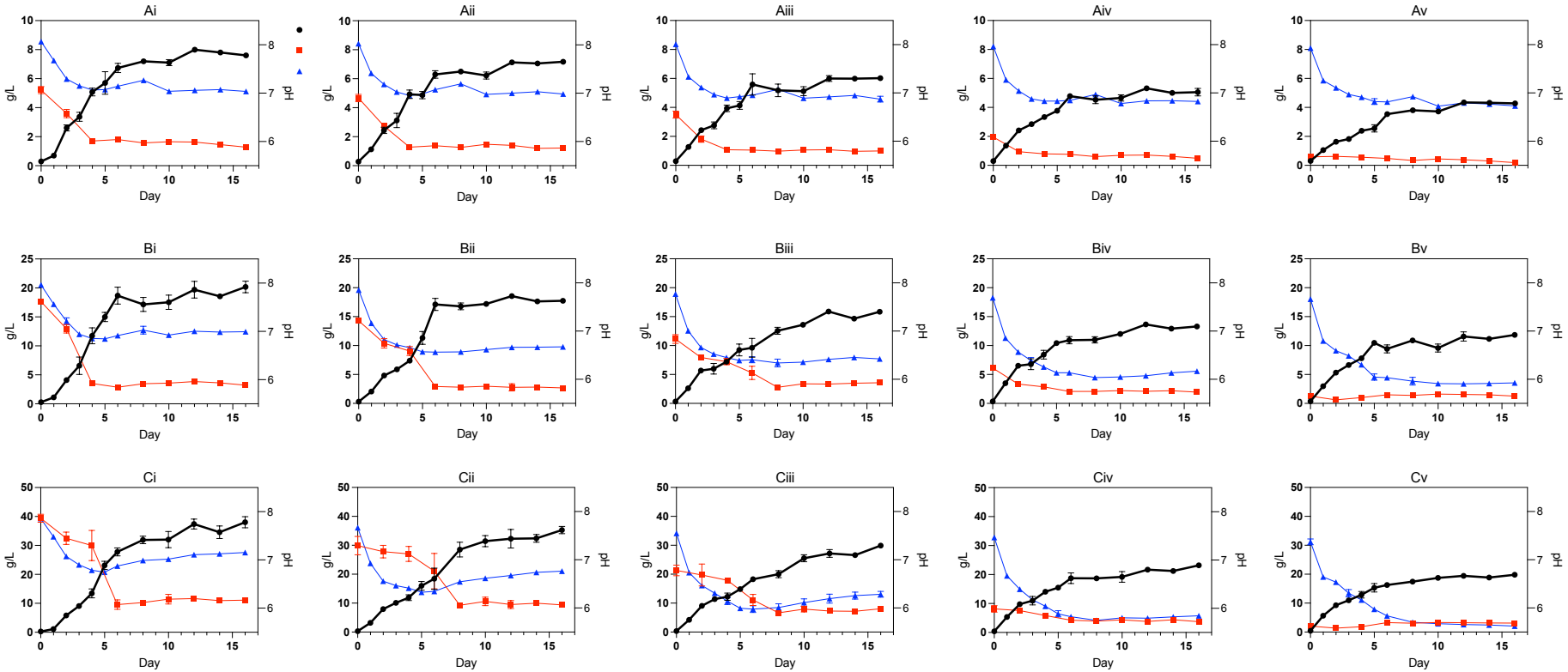


Figure 3.1: Acidification time-courses of *Euphorbia* and blood by AD sludge in mono- and co-digestion formats. Total volatile fatty acid concentrations (g/L), soluble protein concentrations (g/L), and pH are denoted by ●, ■, and ▲, respectively. All values are given as means ± standard deviations of triplicate measurements. A, B, and C denote initial substrate concentrations of 10, 30, and 60 g-VS/L. Substrate ratios (*Euphorbia* to blood of 0:100, 25:75, 50:50, 75:25 and 100:0 (% VS) are indicated by i, ii, iii, iv, and v, respectively.

3.2.2 Total VFA production

Total VFA concentrations (titres) at experiment termination at day 16 are given in **Table 3.2**. Endpoint VFA titres were highest in blood mono-digestions and showed a monotonic decrease with increasing *Euphorbia* fraction. This decreasing trend extended to VFA yields (**Fig. 3.2C**). This monotonic, linear decrease in yields with increasing *Euphorbia* content, visualised in **Fig. 3.2C** indicates an absence of synergistic effects of co-digestion on overall VFA yields.

Declining yields accompanied increased substrate concentrations in all sample groups in this study. Blood mono-digestions gave VFA yields of 0.65 ± 0.01, 0.58 ± 0.03, and 0.54 ± 0.03 g-VFA/g-VS at substrate concentrations of 10, 30, and 60 g/L-VS, respectively, while the corresponding *Euphorbia* digestions yielded 0.38 ± 0.01, 0.35 ± 0.01, and 0.29 ± 0.01 g/L-VS. The above values additionally demonstrate that VFA yields were affected more by substrate composition than by substrate concentration. The discrepancy between the yields of blood and *Euphorbia* is again likely explained by the relative availability of soluble substrate at day 0, rather than a preference of acidification at low C/N ratios. Reactors fed blood at 60 g/L-VS had soluble protein concentrations at day 0 of 39 ± 1 g/L, as compared to just 2.1 ± 0.3 g/L for those fed equivalent amounts of *Euphorbia*. This disparity in soluble substrate likely accounts for a large part of the observed difference in yields.

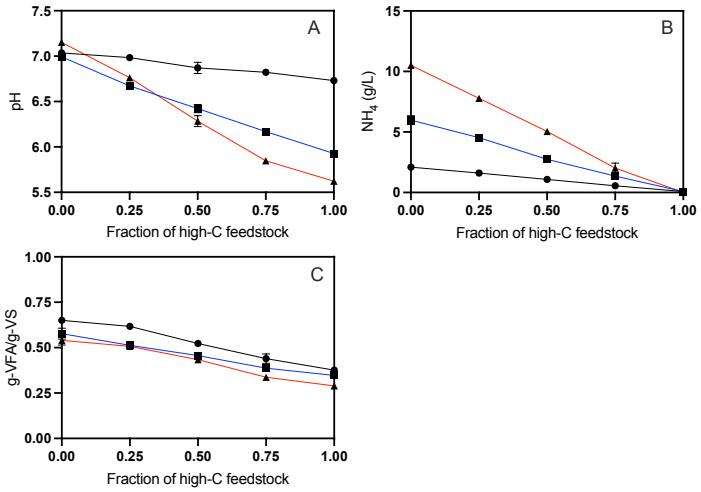


Figure 3.2: Endpoint (day 16) reactor parameters. Panels are as follow: A) Reactor pH, B) ammonium concentrations, C) TVFA yields (volatile solids basis – g-VFA/g-VS). Initial substrate concentrations of 10, 30 and 60 g-VFA/L are denoted by ●, ■, and ▲.

Product-inhibition by VFA may also have influenced observed yields. The acidification of amino acids, whether by Stickland or alternative mechanisms, released ammonium which raised reactor pH. This partially compensated for the acidifying effect of VFA release. At low pH, VFAs are disproportionately present in their undissociated forms and more easily traverse the cell membrane of microbes, inhibiting growth and leading to greater product inhibition than at higher pH (Babel et al., 2004). The higher pH detected in the protein-fed digestions may thus have lessened VFA product-inhibition. In *Euphorbia*-fed conditions, lacking the compensatory effect of ammonium release (see **Table 3.2** and **Fig. 3.2**), higher VFA toxicity may have contributed to lower yields. It should be noted that acidogenic reactors are often run at a mildly acidic pH of ~6 to minimise VFA losses to methanogenesis. In this study, methanogenesis was inhibited by BES (see **Table 3.2** gas data), which masked the yield improvements a mildly-acidic pH might have otherwise provided. Endpoint gas data in **Table 3.2** also show that at each substrate concentration, *Euphorbia*-fed conditions produced more biogas, as CO_2, than did blood-fed conditions. This "mis"-allocation of carbon to biogas may additionally account for the lower VFA yields of *Euphorbia*-fed conditions.

Co-digestion of *Euphorbia* with blood did not produce the increase in total VFA yields expected, which conflicts with some evidence in the literature for its benefits to anaerobic fermentation[3]. Several mechanisms have been proposed to explain synergistic interactions between co-substrates, which may explain this observation. VFA and ammonium produced from protein degradation may loosen the structure of lignocellulosic biomass, increasing its degradability (Saritpongteeraka et al., 2014), with "Ammonia Fibre Expansion" (AFEX) having been elsewhere demonstrated as a biomass pre-treatment in its own right (Lau et al., 2010). Similarly, digestion of protein-rich meat waste has benefitted from the addition of high-C biomass, as it dilutes the long chain fatty acids (LCFA) and ammonium, often present in these wastes, both of which can inhibit reactor processes (Astals et al., 2014; Jensen et al., 2014). The relatively low concentration of lignin in the *Euphorbia* (3.65 %) and of LCFA in the blood used in this experiment may explain the observed lack of cooperativity between these substrates as these compounds are integral to the above mechanisms of cooperativity.

[3] This statement also holds when yields are calculated on a carbon molar yield basis. Please see the appendix to this chapter which provides these data for comparison.

Table 3.2: Batch reactor endpoint parameters at day 16. All values are given means ± standard deviations of triplicate measurements.

Initial substrate concentration (g-VS/L)	*Euphorbia*: blood (%VS)	pH	TVFA (g/L)	Acetic acid (g/L)	TVFA yield (g-VFA/g-VS)	Ammonium (g/L)	Cumulative biogas produced (mL)	Headspace gas composition (CH_4, CO_2 %v/v)
10	0:100	7.04 ± 0.02	7.6 ± 0.1	4.07 ± 0.06	0.65 ± 0.01	2.1 ± 0.1	66 ± 2	4.6 ± 0.6, 57.7 ± 0.6
	25:75	6.98 ± 0.02	7.2 ± 0.2	3.9 ± 0.1	0.62 ± 0.02	1.6 ± 0.1	88.9 ± 0.8	5.6 ± 0.6, 66 ± 5
	50:50	6.87 ± 0.06	6.0 ± 0.1	3.5 ± 0.1	0.52 ± 0.01	1.08 ± 0.08	103 ± 3	3.7 ± 0.6, 73 ± 1
	75:25	6.82 ± 0.04	5.1 ± 0.3	3.1 ± 0.2	0.44 ± 0.02	0.6 ± 0.1	115.5 ± 0.8	1.3 ± 0.6, 79.9 ± 0.5
	100:0	6.73 ± 0.03	4.28 ± 0.04	2.50 ± 0.05	0.38 ± 0.01	0.08 ± 0.04	127 ± 2	- 82 ± 3
30	0:100	6.99 ± 0.01	20 ± 1	8.4 ± 0.3	0.58 ± 0.03	6.0 ± 0.4	248 ± 3	- 96.4 ± 0.6
	25:75	6.67 ± 0.04	17.7 ± 0.4	9.5 ± 0.3	0.51 ± 0.01	4.5 ± 0.1	302 ± 3	- 95 ± 3
	50:50	6.42 ± 0.05	15.9 ± 0.4	9.0 ± 0.5	0.46 ± 0.01	2.7 ± 0.1	347 ± 3	- 99 ± 2
	75:25	6.17 ± 0.03	13.3 ± 0.4	8.1 ± 0.2	0.39 ± 0.01	1.4 ± 0.1	407 ± 4	- 99 ± 7
	100:0	5.93 ± 0.03	11.8 ± 0.2	7.0 ± 0.4	0.35 ± 0.01	0.08 ± 0.03	412 ± 5	- 90 ± 10
60	0:100	7.15 ± 0.01	38 ± 2	11.8 ± 0.4	0.54 ± 0.03	10.5 ± 0.2	502 ± 8	- 91 ± 5
	25:75	6.76 ± 0.02	35 ± 1	15.4 ± 0.8	0.51 ± 0.02	7.8 ± 0.3	640 ± 4	- 87.5 ± 0.4
	50:50	6.28 ± 0.06	29.9 ± 0.6	15.2 ± 0.4	0.43 ± 0.01	5.1 ± 0.3	670 ± 20	- 95 ± 5
	75:25	5.85 ± 0.02	23.2 ± 0.5	13.2 ± 0.2	0.34 ± 0.01	2.0 ± 0.4	680 ± 7	- 99 ± 9
	100:0	5.62 ± 0.03	19.8 ± 0.2	10.9 ± 0.7	0.29 ± 0.01	-	760 ± 50	- 93 ± 7

* VS and TVFA refer to volatile solids and total volatile fatty acid, respectively

In a similar experiment to this, Zhang et al. (2016) digested excess sludge (high-N) with tall fescue biomass (high-C). VFA yields in co-digestions were significantly higher than for mono-digestions, indicating a strong, synergistic relationship between feedstocks. Saritpongteeraka et al. (2014) digested pig manure (high-N) with palm oil residues (high-C) and found a more muted effect, with an overall trend of declining yields with increased fraction of the lignocellulosic (high-C) feedstock, which provide a closer parallel to this study.

Co-digestion is also held to aid AD by keeping C:N ratios within the 'ideal' range of 20–30 (Parkin and Owen, 1986). This provides sufficient nitrogen for microbial growth, while avoiding potentially toxic accumulation of ammonium from excessive protein degradation. In the context of acidogenic co-digestion, Smith et al. (2011) found acid productivity to be maximal at a C:N ratio (g/g) of 30. In this study, *Euphorbia* was found to have a TKN of 1.18 % and moderate C/N ratio of 34.58 (**Table 3.1**). There may thus have been sufficient endogenous nitrogen in the *Euphorbia* to allow robust microbial growth. With a non-limiting amount of nitrogen already present, the growth benefits of protein supplementation would have been limited.

It is notable that *Euphorbia* addition was not seen to increase VFA yields from blood by relieving ammonium toxicity, given the high ammonium concentrations seen (**Table 3.2**) in blood-rich digestions. At neutral to mildly acidic pH, ammonium nitrogen is primarily present in its less-toxic, ionic (NH_4^+) form, rather than as ammonia (NH_3). Had these digestions been instead carried out under alkaline conditions, the need to moderate ammonia toxicity may have seen co-digestions out-perform blood mono-digestions.

3.2.3 Responses of individual VFA titres over the co-digestion parameter space

The time dependent composition of VFA produced is given in **Fig. 3.3**. Acidification was primarily acetogenic at earlier timepoints (<5 days), with a shift to mixed-acid fermentation at later timepoints, with greater proportions of C3, 4, and 5 acids seen in all conditions. Acetic acid represented a majority of the produced VFA in nearly all conditions tested at day 5 and remained the most abundant individual species in all conditions by day 16. Higher protein (blood) content, longer retention time, and higher substrate concentrations were all associated with an increased fraction of longer-chain fatty acids. In just one condition, blood mono-digestion at a substrate concentration of 60 g/L-VS, C4 compounds (isobutyric and butyric acids) represented a greater fraction of TVFA by day 16 than did C2 (**Fig. 3.3**).

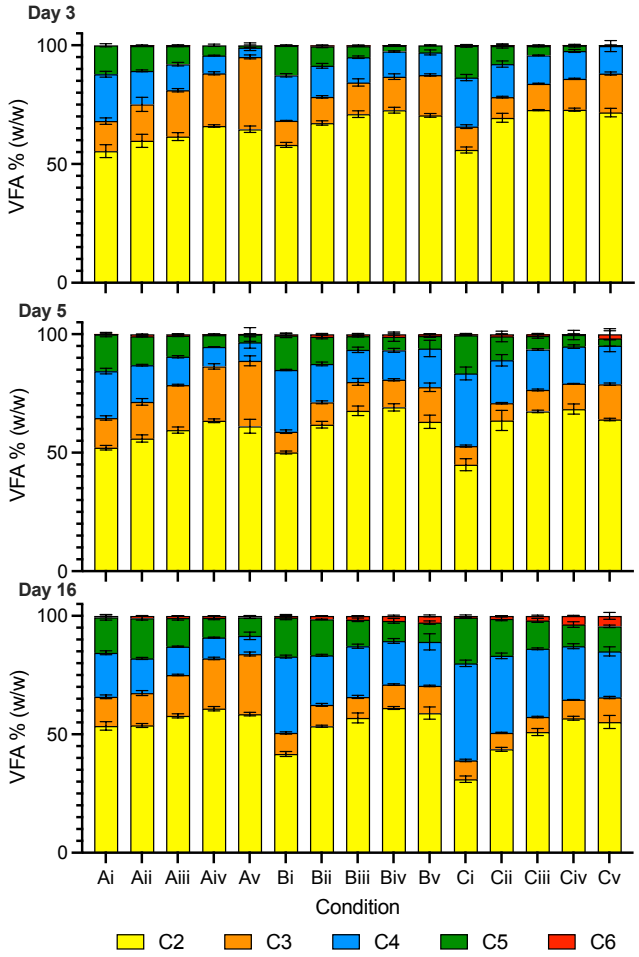


Figure 3.3: Time dependence of VFA product spectra. VFA profiles are shown at day 3, 5, and 16 (endpoint). Initial substrate concentrations of 10, 30 and 60 g-VS/L are denoted by A, B, and C, respectively. Substrate ratios (*Euphorbia* to blood of 0:100, 25:75, 50:50, 75:25 and 100:0 (% VS) are indicated by i, ii, iii, iv, and v.

The response of endpoint fatty acid titres to substrate composition and concentration is summarised in **Fig. 3.4**. For all fatty acids, higher substrate concentrations gave higher titres. Titres of C4 and C5 compounds (isobutyric, butyric, isovaleric, and valeric acids) assumed the same monotonic, linear response shown by total VFA with the highest titres seen in blood, and lowest in *Euphorbia* mono-digestions. Valeric and hexanoic acids demonstrated the inverse of this trend, with highest titres seen in *Euphorbia* mono-digestions, though the biological or economic importance of this observation is limited by the low concentrations of these species.

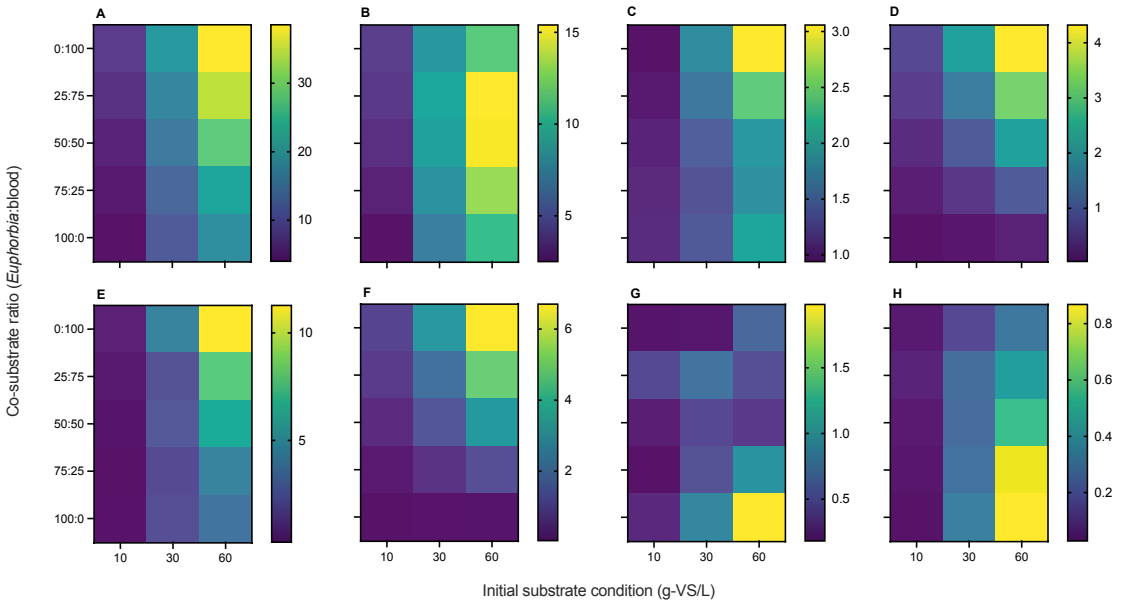
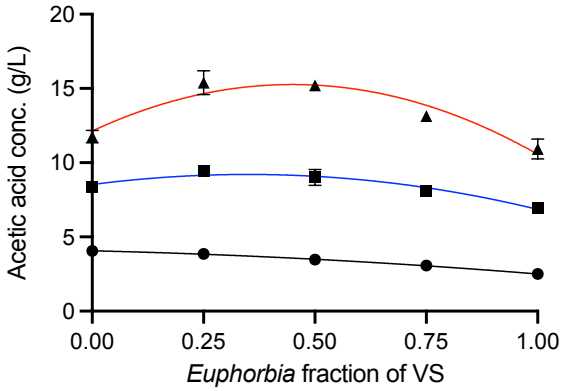


Figure 3.4: Total endpoint (day 16) VFA titres. VFA shown are A) Total VFA, B) Acetic, C) Propionic, D) Isobutyric, E) Butyric, F) Isovaleric, G) Valeric, and H) Hexanoic acid. Heatmap shows mean of triplicate measurements, all VFA concentrations are given in g/L.

Acetic acid was the most abundant individual VFA in all conditions. Importantly, it was also the only fatty acid whose generation was found to benefit from co-digestion, (**Fig. 3.4B**). The strength of this synergistic effect was found to be dependent on substrate concentration, with a more pronounced effect at higher concentrations. At the highest substrate concentrations (60 g/L substrate VS), all three co-digestion ratios significantly outperformed the mono-digestions, with the highest acetic acid titres found in digestions of 75 % blood with 25 % *Euphorbia* (15.4 ± 0.8 g/L acetic acid). This synergistic relationship is further examined in **Fig. 3.5** in which a quadratic model was fit to acetic acid titres. As substrate concentration increased, so too did the absolute magnitude of the coefficient ß2, defining an increasingly pronounced relationship between co-digestion and acetic acid titre. Conversely, reducing substrate concentration towards 10 g/L caused this quadratic relationship to decay, ß2 to reduce, and the relationship to approach linearity. Co-substrate benefits thus increase with increased substrate concentration, perhaps due to dilution of toxic degradation products (e.g. ammonium) or due to the pH buffering effect of ammonium on acid release, both of which become more pronounced at higher substrate concentrations.



	Initial substrate concentration (g-VS/L)		
	10	30	60
$ß_0$	4.07 [3.94, 4.20]	8.53 [8.09, 8.98]	12.13 [11.24, 13.03]
$ß_1$	-0.72 [-1.34, -0.10]	3.89 [1.78, 5.99]	13.95 [9.70, 18.20]
$ß_2$	-0.84 [-1.43, -0.25]	-5.56 [-7.58, -.3.54]	-15.51 [-19.59, -11.44]
Model R^2	0.9698	0.8594	0.8649

Figure 3.5: Quadratic model of endpoint acetic acid titre responses to substrate composition. Initial substrate concentrations of 10, 30 and 60 g-VS/L are denoted by ●, ■, and ▲. Model parameters are given below with their respective 95% confidence intervals.

When attempting to understand these findings mechanistically, it is important to recognise that the major constituents of *Euphorbia* and blood i.e., carbohydrate and protein, respectively, are acidified for the most part via independent pathways. In *Euphorbia*, structural carbohydrates (cellulose and hemicellulose) represented 31.75 % of total solids (**Table 3.1**). AF of carbohydrate proceeds mainly via pyruvate, which represents a central node from which acetate, propionate, and butyrate may all be derived (Zhou et al., 2018). Protein accounted for 92.63 % of total solids in blood, but just 7.38 % in *Euphorbia* (**Table 3.1**). Acidification of protein occurs primarily via Stickland (redox) mechanisms, in which pairs of amino acids (AAs) act as electron donors and acceptors. Fixed stoichiometries for protein conversion to VFA have been proposed (Ramsay and Pullammanappallil, 2001), which assume VFA profile to be a product mainly of protein composition, independent of reactor parameters. Imbalances in Stickland redox pairs, the availability of alternative Stickland pathways for some AAs, and non-Stickland degradation reactions add nuance to this picture. Several studies, including that of (Tepari et al., 2020), have shown VFA product spectra from protein to be responsive to reactor parameters such as pH.

In this study, the early fermentation was primarily acetic acid-rich, which has precedent in the literature (Saritpongteeraka et al., 2014). This shifted to a more mixed-acid fermentation at later timepoints, after which significant differences in VFA composition became apparent. In **Fig. 3.3**, **Fig. 3.4**, VFA composition can be seen to change as co-feedstock ratios change. This is partially a result of the different metabolic pathways used, from mostly Stickland reactions for blood, to pyruvate-mediated mechanisms for *Euphorbia*. A higher abundance of longer chain fatty acids has been reported with increased protein content (Saritpongteeraka et al., 2014) and in mono-digestions of high-protein substrates (Yu et al., 2018). This mirrors results seen in Fig. 3, showing abundant C4 and C5 compounds in digestions of 75 % and 100 % blood.

This observation will also have been influenced by the relative sensitivities of these pathways to shifting reactor parameters such as pH and ammonium. Several studies have shown pH to be the dominant parameter in defining VFA composition (Bermúdez-Penabad et al., 2017; Horiuchi et al., 2002). The relative pH stability of blood digestions due to ammonium release thus likely also contributed to the divergence of blood and *Euphorbia*-derived VFA profiles. However a detailed, mechanistic exploration of the underlying pathways is beyond the scope of this study.

Yet another consideration is the C:N contribution of the inoculum, which in this study had a high C:N of 56.78. This means that the effective C:N ratio of 10, 30, and 60 g/L substrate loadings at each substrate ratio will have been higher at lower loadings than at higher. This does not appear to have significantly affected substrate acidogenesis, with yields across substrate loadings being relatively consistent despite this effect (**Table 3.2**). From these data TVFA yields appear significantly more responsive to substrate solubility considerations than to C:N ratio. This is not to say however that inoculum C:N would not have an effect under different conditions, for example with digestion of a nitrogen-limited substrate.

Having demonstrated that co-digestion of *Euphorbia* with blood can provide increased yields of acetic acid, future investigation should aim to explore the underlying mechanisms of this synergy. Disentangling the relative contributions of pH, ammonium, and substrate composition through active buffering and controlled ammonium dosing would allow for greater control of product spectra. It would also do to test whether these results generalise to other CAM feedstocks, such as *Opuntia*, and other protein-rich co-substrates. Of particular interest for future investigation would be to test co-substrates whose sources might geographically co-localise with existing or potential areas of CAM cultivation.

3.4. Conclusion

The co-substrates *Euphorbia tirucalli* and pig blood were subjected to acidogenic fermentation in batch format at various mixing ratios and substrate concentrations. Higher fractions of pig blood gave greater overall titres of VFA, likely due to a higher fraction of the substrate being present in suspension. Greater fractions of blood, higher substrate concentrations, and longer retention times were all associated with an increased fraction of C4 and C5 fatty acids. Maximal titres of acetic acid were detected in co-digestions of 75:25 and 50:50 blood: *Euphorbia*, exceeding mono-digestions by over 40%. Co-digestion thus offers great benefit where acetic acid is the desired product.

3.5 Acknowledgements

Funding: This work was supported by East Alpha and Rotary International (Grant number: GG2128217).

3.6 References

Abbassi-Guendouz, A., Brockmann, D., Trably, E., Dumas, C., Delgenès, J.-P., Steyer, J.-P., Escudié, R. 2012. Total solids content drives high solid anaerobic digestion via mass transfer limitation. Bioresour. Technol. 111, 55-61.

Angelidaki, I., Sanders, W. 2004. Assessment of the anaerobic biodegradability of macropollutants. Rev. Environ. Sci. Biotechnol. 3, 117-129.

APHA. 1998. Standard methods for the examination of water and wastewater. American Water Works Association and Water Environment Federation.

Astals, S., Batstone, D.J., Mata-Alvarez, J., Jensen, P.D. 2014. Identification of synergistic impacts during anaerobic co-digestion of organic wastes. Bioresour. Technol. 169, 421-427.

Babel, S., Fukushi, K., Bunpot, S. 2004. Effect of acid speciation on solid waste liquefaction in an anaerobic acid digester. Water Res. 38, 2417-2423.

Bermúdez-Penabad, N., Kennes, C., Veiga, M.C. 2017. Anaerobic digestion of tuna waste for the production of volatile fatty acids. Waste Manage. 68, 96-102.

Buckland, C.E., Thomas, D.S.G. 2021. Analysing the potential for CAM-fed bio-economic uses in sub-Saharan Africa. Appl. Geogr. 132, 102463.

Christophe, G., Lara Deo, J., Kumar, V., Nouaille, R., Fontanille, P., Larroche, C. 2012. Production of oils from acetic acid by the oleaginous yeast Cryptococcus curvatus. Appl. Biochem. Biotechnol. 167, 1270-1279.

Cuetos, M.J., Gómez, X., Martínez, E.J., Fierro, J., Otero, M. 2013. Feasibility of anaerobic co-digestion of poultry blood with maize residues. Bioresour. Technol. 144, 513-520.

Elefsiniotis, P., Wareham, D.G. 2007. Utilization patterns of volatile fatty acids in the denitrification reaction. Enzyme Microb. Technol. 41, 92-97.

Hejnfelt, A., Angelidaki, I. 2009. Anaerobic digestion of slaughterhouse by-products. Biomass Bioenerg. 33, 1046-1054.

Horiuchi, J.-I., Shimizu, T., Tada, K., Kanno, T., Kobayashi, M. 2002. Selective production of organic acids in anaerobic acid reactor by pH control. Bioresour. Technol. 82, 209-213.

Jensen, P.D., Sullivan, T., Carney, C., Batstone, D.J. 2014. Analysis of the potential to recover energy and nutrient resources from cattle slaughterhouses in Australia by employing anaerobic digestion. Appl. Energy 136, 23-31.

Jiang, J., Zhang, Y., Li, K., Wang, Q., Gong, C., Li, M. 2013. Volatile fatty acids production from food waste: Effects of pH, temperature, and organic loading rate. Bioresour. Technol. 143, 525-530.

Kovács, E., Wirth, R., Maróti, G., Bagi, Z., Rákhely, G., Kovács, K.L. 2013. Biogas production from protein-rich biomass: Fed-batch anaerobic fermentation of casein and pig blood and associated changes in microbial community composition. PLoS One 8, e77265.

Krümpel, J., George, T., Gasston, B., Francis, G., Lemmer, A. 2020. Suitability of *Opuntia* ficus-indica (L) Mill. and Euphorbia tirucalli L. as energy crops for anaerobic digestion. J. Arid Environ. 174, 104047.

Lau, M.J., Lau, M.W., Gunawan, C., Dale, B.E. 2010. Ammonia fiber expansion (AFEX) pretreatment, enzymatic hydrolysis, and fermentation on empty palm fruit bunch fiber (EPFBF) for cellulosic ethanol production. Appl. Biochem. Biotechnol. 162, 1847-1857.

Lee, J.H., Cha, S., Kang, C.W., Lee, G.M., Lim, H.G., Jung, G.Y. 2018. Efficient Conversion of Acetate to 3-Hydroxypropionic Acid by Engineered Escherichia coli. Catalysts 8, 525.

Li, Y., Zhang, R., Liu, G., Chen, C., He, Y., Liu, X. 2013. Comparison of methane production potential, biodegradability, and kinetics of different organic substrates. Bioresour. Technol. 149, 565-569.

Lueangwattanapong, K., Ammam, F., Mason, P.M., Whitehead, C., McQueen-Mason, S.J., Gomez, L.D., Smith, A.C., Thompson, I.P. 2020. Anaerobic digestion of Crassulacean Acid Metabolism plants: Exploring alternative feedstocks for semi-arid lands. Bioresour. Technol. 297, 122262.

Mason, P.M., Glover, K., Smith, J.A.C., Willis, K.J., Woods, J., Thompson, I.P. 2015. The potential of CAM crops as a globally significant bioenergy resource: moving from 'fuel or food' to 'fuel and more food'. Energy Environ. Sci. 8, 2320-2329.

Mengmeng, C., Hong, C., Qingliang, Z., Shirley, S.N., Jie, R. 2009. Optimal production of polyhydroxyalkanoates (PHA) in activated sludge fed by volatile fatty acids (VFAs) generated from alkaline excess sludge fermentation. Bioresour. Technol. 100, 1399-1405.

Miramontes-Martínez, L.R., Rivas-García, P., Albalate Ramírez, A., Escamilla-Alvarado, C., Gomez-Gonzalez, R., Alcalá-Rodríguez, M.M., Valencia-Vázquez, R., Santos-López, I.A. 2021. Anaerobic co-digestion of fruit and vegetable waste: Synergy and process stability analysis. J. Air Waste Manag. Assoc. 71, 620-632.

Nazifa, T.H., Cata Saadi, N.M., Bazan, C., Zendehboudi, S., Aftab, A., Albayati, T.M. 2021. Anaerobic digestion of blood from slaughtered livestock: A review. Energies 14, 5666.

Panizio, R.M., Calado, L.F.d.C., Lourinho, G., de Brito, P.S.D., Mees, J.B. 2020. Potential of biogas production in anaerobic co-digestion of *Opuntia* ficus-indica and slaughterhouse wastes. Waste Biomass Valorization 11, 4639-4647.

Parkin, G.F., Owen, W.F. 1986. Fundamentals of anaerobic digestion of wastewater sludges. J. Environ. Eng. (New York) 112, 867-920.

Pratt, S., Liew, D., Batstone, D.J., Werker, A.G., Morgan-Sagastume, F., Lant, P.A. 2012. Inhibition by fatty acids during fermentation of pre-treated waste activated sludge. J. Biotechnol. 159, 38-43.

Ramsay, I.R., Pullammanappallil, P.C. 2001. Protein degradation during anaerobic wastewater treatment: derivation of stoichiometry. Biodegradation 12, 247-257.

Richards, B.K., Cummings, R.J., White, T.E., Jewell, W.J. 1991. Methods for kinetic analysis of methane fermentation in high solids biomass digesters. Biomass Bioenerg. 1, 65-73.

Salangsang, M.C.D., Sekine, M., Akizuki, S., Sakai, H.D., Kurosawa, N., Toda, T. 2022. Effect of carbon to nitrogen ratio of food waste and short resting period on microbial accumulation during anaerobic digestion. Biomass Bioenerg. 162, 106481.

Saritpongteeraka, K., Boonsawang, P., Sung, S., Chaiprapat, S. 2014. Co-fermentation of oil palm lignocellulosic residue with pig manure in anaerobic leach bed reactor for fatty acid production. Energy Convers. Manag. 84, 354-362.

Smith, A. D., Lockman, N. A., & Holtzapple, M. T. 2011. Investigation of nutrient feeding strategies in a countercurrent mixed-acid multi-staged fermentation: experimental data. Applied biochemistry and biotechnology, 164, 426-442.

Tepari, E.A., Nakhla, G., Idris, M., Haroun, B.M., Hafez, H. 2020. Stoichiometry of Anaerobic Protein Fermentation. Biochem. Eng. J. 158, 107564.

Van Soest P., Robertson J.B, Lewis B.A. Methods for dietary fiber, neutral detergent fiber, and nonstarch polysaccharides in relation to animal nutrition. Journal of dairy science. 1991;74(10):3583-97.

Wang, X., Yang, G., Feng, Y., Ren, G., Han, X. 2012. Optimizing feeding composition and carbon-nitrogen ratios for improved methane yield during anaerobic co-digestion of dairy, chicken manure and wheat straw. Bioresour. Technol. 120, 78-83.

Winter, K., Smith, A.C. 2012. Crassulacean acid metabolism: biochemistry, ecophysiology and evolution. Springer Science & Business Media.

Yang, S., Zhang, Y., Yue, W., Wang, W., Wang, Y.-Y., Yuan, T.-Q., Sun, R.-C. 2016. Valorization of lignin and cellulose in acid-steam-exploded corn stover by a moderate alkaline ethanol post-treatment based on an integrated biorefinery concept. Biotechnol. Biofuels 9, 1-14.

Yu, X., Yin, J., Shen, D., Shentu, J., Long, Y., Chen, T. 2018. Improvement of acidogenic fermentation for volatile fatty acid production from protein-rich substrate in food waste. Waste Manage. 74, 177-184.

Zeng, J., Helms, G.L., Gao, X., Chen, S. 2013. Quantification of wheat straw lignin structure by comprehensive NMR analysis. J. Agric. Food Chem. 61, 10848-10857.

Zhang, B., Zhang, L.-L., Zhang, S.-C., Shi, H.-Z., Cai, W.-M. 2005. The influence of pH on hydrolysis and acidogenesis of kitchen wastes in two-phase anaerobic digestion. Environ. Technol. 26, 329-339.

Zhang, D., Fu, X., Jia, S., Dai, L., Wu, B., Dai, X. 2016. Excess sludge and herbaceous plant co-digestion for volatile fatty acids generation improved by protein and cellulose conversion enhancement. Environ. Sci. Pollut. Res. 23, 1492-1504.

Zhou, M., Yan, B., Wong, J.W.C., Zhang, Y. 2018. Enhanced volatile fatty acids production from anaerobic fermentation of food waste: A mini-review focusing on acidogenic metabolic pathways. Bioresour. Technol. 248, 68-78.

Zhou, S., Lama, S., Jiang, J., Sankaranarayanan, M., Park, S. 2020. Use of acetate for the production of 3-hydroxypropionic acid by metabolically-engineered Pseudomonas denitrificans. Bioresour. Technol. 307, 123194.

Statement of Authorship for joint/multi-authored papers for PGR thesis

To appear at the end of each thesis chapter submitted as an article/paper

The statement shall describe the candidate's and co-authors' independent research contributions in the thesis publications. For each publication there should exist a complete statement that is to be filled out and signed by the candidate and supervisor **(only required where there isn't already a statement of contribution within the paper itself).**

Title of Paper	Anaerobic co-digestion of *Euphorbia tirucalli* with pig blood for volatile fatty acid production
Publication Status:	☒ Published ☐ Accepted for publication ☐ Submitted for publication ☐ Unpublished and unsubmitted work written in manuscript style
Publication Details:	Tenci, N. A., Ammam, F., Huang, W. E., & Thompson, I. P. (2023). Anaerobic co-digestion of *Euphorbia tirucalli* with pig blood for volatile fatty acid production. *Bioresource Technology Reports*, *21*, 101333.

Student Confirmation

Student Name:	*Nicholas A. Tenci*	
Contribution to the paper:	*Designed the study, performed the experiments, analysed the data, wrote the manuscript.*	
Signature: 	Date:	*11/09/2024*

Supervisor Confirmation

By signing the Statement of Authorship, you are certifying that the candidate made a substantial contribution to the publication, and that the description described above is accurate.

Supervisor name and title: *Prof. Ian P. Thompson*		
Supervisor comments: I agree with this summary.		
Signature: 	Date:	*17/09/2024*

This completed form should be included in the thesis, at the end of the relevant chapter

Chapter 4. Biorefinery for a circular carbon economy: process benefits to the use of dryland CAM crops for anaerobic volatile fatty acid production

Disclaimer

Having in the previous chapter analysed the co-digestion characteristics of a single CAM crop, the following study, presented in manuscript form, was undertaken to identify whether CAM feedstocks more broadly might act as suitable feedstocks for renewable fatty acid production.

The following manuscript was under review for publication in the journal Bioresources for Biotechnology and Biofuels at the time of acceptance of this thesis. Several minor edits have been made to it in fulfilment of the suggestions of the thesis examiners.

Following acceptance of this thesis, a subsequent version of the manuscript was published in the above journal (licenced under CC BY-NC-ND 4.0) which may be accessed at:

Tenci, N. A., Austen, N., Martin, L. K., Smith, J. A. C., & Thompson, I. P. (2025). Biorefinery for a circular carbon paradigm: process benefits to the use of dryland CAM crops for anaerobic volatile fatty acid production. *Biotechnology for Biofuels and Bioproducts*, *18*(1), 85.

Biorefinery for a circular carbon economy: process benefits to the use of dryland (CAM) crops for anaerobic volatile fatty acid production

Authors: Nicholas A. Tenci[1]‡, Nichola Austen [2,1]‡, Laura K. Martin[1], J. Andrew C. Smith[2], Ian P. Thompson[1]*

Affiliations:

1 Department of Engineering Science, University of Oxford, Parks Road, Oxford, OX1 3PJ, UK.

2 Department of Biology, University of Oxford, South Parks Road, OX1 3RB, UK.

I Now at Department of Engineering Science, University of Oxford, Parks Road, Oxford, OX1 3PJ, UK.

*Corresponding author: ian.thompson@eng.ox.ac.uk. Department of Engineering Science, University of Oxford, Parks Road, Oxford, OX1 3PJ, UK.

‡ NAT and NA contributed equally to the study.

Abstract

Anaerobic digestion (AD) of biomass can generate either biogas fuel, or C2 - C8 volatile fatty acids (VFAs), as feedstocks for synthesis of other petrochemical products. Typical AD feedstocks such as maize require large amounts of land that could otherwise be used for food production. Unlike these traditional bioenergy crops, plants using Crassulacean Acid Metabolism pathway (CAM), such as cacti and succulents, may be cultivated on degraded and semi-arid land which cannot support conventional agriculture. Several economically important CAM crops (pineapple, agave, prickly pear) are cultivated globally, with waste biomass that could be valorised as a biorefinery feedstock.

Here, we investigate the fermentation kinetics of this novel feedstock class (CAM plants) against traditional bioenergy crops with two contrasting inocula: AD sludge and rumen fluid. CAM and non-CAM substrates in this study demonstrated distinct degradation kinetics (yields and degradation rates). We demonstrate that regardless of the inoculum type, CAM crops show higher hydrolysis rates for VFA production. Moreover, yields of VFAs from CAM crops (0.41 ±0.01 - 0.48 ±0.02 g/gvs) were higher than for the three non-CAM crops (0.213 ±0.009 - 0.38 ±0.01 g/gvs) where AD sludge was used as the inoculum. At industrial scale, these CAM-

specific kinetic advantages could translate to process enhancements which would greatly improve the cost-competitiveness of anaerobic biorefinery.

4.1. Background

Urgent decarbonisation of the energy and petrochemical sectors is required to mitigate the increasingly extreme effects of anthropogenic climate change. While the reliance on crude oil for energy and transportation is predicted to stabilise and then decline over the coming decades its exploitation in the petrochemical sector looks set to buck this trend, with robust growth expected to at least 2040 (IEA, 2022;bp Energy, 2020). Full transition to a renewable economy would demand that these petrochemical needs also be met with carbon from other sources. The current low cost of crude oil, and its established place in industrial chemistry, renders this sector relatively resistant to decarbonisation. Acidogenic fermentation (AF), a variant form of anaerobic digestion (AD), is one means by which part of this demand may be met sustainably. AF is the controlled anaerobic fermentation of biomass to produce a suite of volatile fatty acids (VFA) from which high value products including chemicals and plastics can be synthesised. In 2020, the global annual market for VFAs (acetic, propionic, and butyric acids), was estimated to be 18.5 Mt (Vázquez-Fernández et al., 2022). Currently, 90% of the market demand for VFA is met through petrochemical synthesis, with the remainder produced via biological methods (Agnihotri et al., 2022). Increased deployment of AF offers an opportunity to directly substitute this existing source of petrochemical demand. Moreover, VFA can be used as a feedstock for synthesis of multiple other products currently produced via petrochemical routes, including polyhydroxyalkanoate bioplastics (PHAs), food additives, and pharmaceuticals (Strazzera et al., 2018). The availability of a price-competitive source of renewable VFA is a major factor in determining whether these alternative synthesis methods might be a viable alternative to petrochemical synthesis of these products.

The availability of adequate input feedstock is a major constraint to AF, along with other biomass-dependent processes, as any large-scale cultivation of biomass crops would typically compete for arable land currently dedicated to food production (Mason et al., 2015; Pols, 2015). Currently, ~ 40% of the global land area is characterized as drylands (Arba, 2020; UNDP/UNSO, 1997). This figure looks likely to increase due to changing climate and land degradation, leading to uncertainty for future crop production (Sarr, 2012). Much like traditional C3 and C4 agricultural crops, plants that utilise the Crassulacean Acid Metabolism (CAM) pathway for carbon fixation may also be used as a bioenergy crop for AD. Because CAM plants can conduct most of their gas exchange with the atmosphere at night, rather than during the

daytime, and can store large amounts of water in their succulent tissues, they show a higher efficiency of water-use and greater resilience to drought than C3 or C4 plants (Borland et al., 2009). Thus, unlike traditional crops, CAM species can survive on marginal, degraded, and semi-arid land (Buckland & Thomas, 2021; Mason et al., 2015) that cannot be reliably used for food production. CAM plants require as little as ~20% of the water needed to cultivate C3 and C4 crops (Borland et al., 2009), while still yielding comparable biomass (Lueangwattanapong et al., 2020; Mason et al., 2015; Nobel, 1991). CAM plants also offer process-level benefits. The rate-limiting step in AD and AF is often hydrolysis, and the lignin content of plant biomass can impede hydrolysis through occlusion of digestible carbohydrates (cellulose and hemicellulose) and by adsorption of hydrolytic enzymes (Börjesson et al., 2007; Mason et al., 2015; Shrestha et al., 2017). Many CAM species are notable for their low lignin content: ~1% - ~16% for *Opuntia ficus indica* (Castellano et al., 2021; Chen et al., 2008; Mannai et al., 2016; Quiroz et al., 2021), compared with 11% - 26% for wheat straw (C3) (Zhang et al., 2022) literature values for maize residue lignin vary widely, from as low as 3.4 (%VS) (He et al., 2018), or 3.1 and 8.0 (%TS) for leaves and stalks (Menardo et al., 2015) to as high as 21.7 %TS for maize stalk (C4) (Liu et al., 2014). CAM biomass has been demonstrated as a suitable substrate for biomethane production via AD (Krümpel et al., 2020; Lueangwattanapong et al., 2020), with yields comparable to widely used feedstocks such as *Miscanthus* (Mangold et al., 2019), and agricultural residues such as maize stover and wheat straw (Ge et al., 2016) (Mancini et al., 2018).

To characterize their potential for anaerobic VFA production, three globally economically important CAM species were included in this study: *Ananas comosus* (hereafter referred to as pineapple), *Opuntia ficus indica* (*Opuntia*) and *Agave angustifolia* (Agave). 28.6 million tons of pineapples were harvested globally in 2021 (FAO, 2021). Apipatpapha et al. (2022) estimate annual production of pineapples and associated leaf-waste in Thailand to be 1.7 million tonnes, and 2.7 million tonnes respectively, a ratio of leaves to fruit of ~1.6 suggesting pineapple residues could represent a significant opportunity if properly valorised. *Opuntia* produces edible fruits and cladodes, and though less widely cultivated than pineapple, is nonetheless an important crop in its native Mexico, and in Mediterranean regions of Africa and Europe (Andreu-Coll et al., 2020). *Opuntia* is one of the most widely investigated CAM crops for biorefinery and biogas production (Comparetti et al., 2017; do Nascimento Santos et al., 2016; Krümpel et al., 2020; Quiroz et al., 2021; Ramadan et al., 2021). As for other CAM plants, its water-use efficiency (WUE) is greater than that of C4 and C3 plants (Nobel, 1991; Park S Nobel, 2002), and its low percentage of lignocellulosic material as a proportion of total

biomass (Castellano et al., 2021; Mannai et al., 2016; Quiroz et al., 2021) makes it a favourable candidate feedstock. Various agaves are cultivated for production of food and fibre. *Agave angustifolia* is grown to produce mezcal liquor (Davis et al., 2019) and is the wild progenitor of both the tequila agave, *Agave tequilana* (Cabrera-Toledo et al., 2022), and of Agave fourcroydes, whose leaves are used to produce henequen fibre, to make rope, twine, and paper (Davis et al., 2019). *Agave sisalana* (a hybrid of *A. angustifolia* and *A. kewensis*) is also a major commercial fibre Agave. *A. angustifolia* was thus selected as a representative of commercial agaves used in both fibre and liquor industries.

This study aimed to draw conclusions as to the suitability of CAM feedstocks as AF substrates. Given the hypothesis that any performance advantage of CAM would be due to its lower lignin content, fermentations were performed both with a standard AD sludge inoculum, and a rumen community (Ihoeghian et al., 2022; Lueangwattanapong et al., 2020), which could be expected to be more adapted to degradation of lignocellulose. CAM crops (pineapple, Agave and *Opuntia*) were tested against a widely used energy crop, *Miscanthus sinensis* (hereafter *Miscanthus*) and two common agricultural residues (wheat straw (*Triticum aestivum* L.) and maize stover (*Zea mays* L.)), to assess both their maximum yield of VFA, and their initial rates of hydrolysis. This study also examined the composition of the microbial communities present in the two inocula to identify key taxa responsible for the various bioconversion steps in the reactor.

This research is timely due to the increased demand for renewable sources of carbon to produce high-value products, and to replace the need for petrochemical synthesis without adding to the “food vs. fuel” debate. It has the added benefit of offering a path for economic improvement of degraded lands.

4.2. Methods

4.2.1 Biomass and inoculum

Plants of pineapple (*Ananas comosus* (L.) Merr.), Agave (*Agave angustifolia* Haw.), maize (*Zea mays* L.), and wheat (*Triticum aestivum* L.) were grown in glasshouses at the Department of Biology, University of Oxford. Plants were cultivated under natural solar irradiation with supplementary heating to maintain minimum temperatures of 10°C (night) and 25°C (day). Live, mature cladodes of *Opuntia ficus-indica* (L.) Mill. were obtained from Pepe Aromas (Azaruja, Portugal). These were subsequently propagated and grown under the same conditions as above; the new, young cladodes produced were harvested at two months of age

from the same plant as the mature cladode. Agave fibre was extracted through mechanical decortication of *Agave angustifolia* leaves, and the resultant pulp was collected and analysed as a distinct feedstock. Mature *Miscanthus sinensis* (Andersson) was obtained from Jackson's Nurseries (Stoke-on-Trent, UK).

All harvested plant biomass material was dried in an oven at 80°C to constant biomass (Table 1). The dry biomass was ground using a blender (Waring Pro® Stainless Steel Blender, 550 W) and passed through a 1 mm sieve to ensure a consistent particle size prior to fermentation.

Two distinct inocula were used for the experiment (Table 2). AD sludge was obtained from a local biogas facility (Severn Trent Green Power, Cassington, UK) and stored under anaerobic conditions at 30°C before use. Rumen fluid was collected from a fistulated cow (The Centre for Dairy Research, University of Reading, UK). To properly incorporate large particulates, the rumen fluid was homogenised by blending and passed through a 1 mm sieve before use.

4.2.2 Anaerobic batch assays

The AF experiment was conducted as a batch assay in 125 ml vials with a working volume of 75 mL. The culture medium was prepared according to Angelidaki and Sanders (2004), with the exclusion of sodium sulphide. A master-mix of media, deionised water, and inoculum was prepared to a final concentration of 5 g/L inoculum (on a volatile solids (VS) basis). Methanogenesis was inhibited through the addition of bromoethane sulfonate (10 mM) (BES - Sigma Aldrich, USA). The bulk pH of the media mixture was adjusted to 8.1 ± 0.1 and 75 mL of the master-mix was added to vials containing the dried substrate. Vials were sealed with rubber septa and aluminium crimp caps and mixed by inversion. The headspace was not purged to remove residual oxygen (Tenci et al., 2023).

The substrate to inoculum ratio was set to 1.6:1 (w/w) on a VS-basis, with a low ratio being selected to allow isolation of the degradation kinetics with minimal product inhibition[4]. The experiment was performed with each biological substrate in triplicate. A blank control consisting of the inocula and media solution was run in triplicate for each inoculum and was

[4] This ratio is lower than those used in subsequent chapters due to the limited availability of certain feedstocks used in this experiment.

subtracted from treatment conditions to account for any residual volatiles present in the inocula. A positive control with microcrystalline cellulose (Avicel®, Sigma-Aldrich, USA) was used to monitor inoculum activity. All samples were incubated at 37°C (mesophilic) under constant agitation at 125 rpm. The experiment was terminated on day 16.

4.2.3 Analytical methods

Determination of total solids (TS) and volatile solids (VS) of biomass material and the inocula was conducted according to standard methodologies (APHA, 1998), though using an oven temperature of 80°C for total solids determinations. Analysis of lignin, cellulose, and hemicellulose were performed as described previously (Van Soest et al., 1991). At each time point, liquid samples of 600 µL were extracted using a syringe and the pH of the liquid samples measured immediately after sample collection (Thermo Scientific, USA). Samples were frozen at -20°C ready for VFA, soluble chemical oxygen demand (SCOD), and metagenomic analyses. For VFA analysis, samples were centrifuged at 15,500 x g for 10 min, and 300 µL of the supernatant was transferred to 1.5 mL GC vials. The supernatant was acidified by 1:1 dilution in 20% (v/v) formic acid. VFA concentrations were measured using a GC device (GC-2010, Shimadzu) with a 30 m × 0.25 mm × 0.25 µm fused-silica column (nitroterephthalic acid-modified polyethylene glycol-phase) (ZB-FFAP) and flame ionisation detector (FID). Injector and detector temperatures were 250 and 350°C, respectively. The initial oven temperature was set to 100°C for 2 min, ramped at 8°C/min to 150°C, and then held at 150 °C for 2 min. Total VFA (TVFA) was calculated as the sum of acetic, propionic, isobutyric, butyric, isovaleric, valeric, and hexanoic acids, which were quantified against standards.

For determination of initial substrate SCOD, dried substrate samples were resuspended in deionised water and allowed to fully rehydrate; these were then centrifuged at 15,500 xg. The supernatant was then analysed using an LCI400 COD Cuvette Test and DR2800 spectrophotometer (Hach Lange).

4.2.4 Metagenomic analyses

Metagenomic analyses were conducted by an external provider (Genewiz UK Ltd.) according to the following protocol, which has been reproduced with their express permission. DNA was extracted using NucleoMag DNA Microbiome Kit following manufacturer's instructions (Takara, San Jose, CA, USA). 16S-EZ rDNA next generation sequencing library preparations and Illumina MiSeq sequencing were conducted at Azenta, Inc. (South Plainfield, NJ, USA). Sequencing library was prepared using a MetaVx™ 16S rDNA Library Preparation kit (Azenta, Inc.). Briefly, the DNA was used to generate amplicons that cover V3 and V4

hypervariable regions of bacteria and archaea16S rDNA. Indexed adapters were added to the ends of the 16S rDNA amplicons by limited cycle PCR. DNA libraries were validated and quantified before loading. The pooled DNA libraries were loaded on an Illumina MiSeq instrument according to manufacturer's instructions (Illumina, San Diego, CA, USA). The samples were sequenced using a 2 x 250 paired-end (PE) configuration. Image analysis and base calling were conducted by the Illumina Control Software on the Illumina instrument. Raw sequence data (.bcl files) generated from Illumina MiSeq was converted into FASTQ files and de-multiplexed using Illumina's bcl2fastq 2.17 software.

4.2.5 Statistical analysis and modelling

All experimental data are presented as means ± standard deviation of triplicate biological samples, unless otherwise specified. Errors of model parameters are given as standard errors. Data were processed in Microsoft Excel and Graphpad Prism 9.5.0 (GraphPad, 2023). VFA yield curves were fitted with the following first-order kinetic model, as previously used with VFA and biogas data (Mancini et al., 2018; Wang et al., 2019):

$$\mathbf{Y = Y_{max}\ [1\text{-}exp\ (\text{-}kt)]}$$

in which **Y** = VFA yield at time '**t**,' $\mathbf{Y_{max}}$ = maximum theoretical VFA yield, **t** = time, and **k** = first-order rate constant. This model was fitted to the mean VFA yield data for each substrate to determine estimates of the potential maximum yield (Ymax) and specific rate constant (k) for each substrate.

4.3 Results

4.3.1 Characterisation of feedstock and inocula for VFA production

The data in **Table 1** detail the biomass characteristics of both CAM and non-CAM plants investigated as feedstock in this experiment. Agave fibre, though not used as a feedstock, was also characterised to allow a direct comparison between the whole Agave leaf and decorticated pulp which results as the waste product of commercial Agave fibre extraction. The total solids (TS) (%) content of the biomass as a percentage of fresh weight (TS/FW) ranged from 7.7 % ± 0.3 (young *Opuntia* cladode) to 93 % ± 4 (wheat straw). Due to their high moisture content, all the CAM feedstocks exhibited a lower proportion of TS than the C3 and C4 plants, except for the Agave fibre, which had a TS of 39% ± 0.9. Both young and old *Opuntia* cladodes had a TS % of under 10 % (7.7% ± 0.3 and 8.5 % ± 0.5, respectively). Agave pulp and whole leaf had a TS% of 11.9% ± 0.3 and 18.9% ± 0.7, respectively, and pineapple had

a TS % of 13.7% ± 0.6. Maize had the lowest TS % of the non-CAM feedstock, at 29.4 % ± 4, as compared to *Miscanthus* (55% ± 4) and wheat straw (93% ± 4).

Table 4.1: Characterisation of CAM, C_3 and C_4 plant biomass used in this study. All measurements provided as means ± standard deviations of technical triplicates of bulk biomass.

Characteristic	**CAM Biomass**						**Non-CAM Biomass**		
Species	Pineapple	Agave	Agave	Agave	*Opuntia*	*Opuntia*	*Miscanthus*	Maize	Wheat
Fraction	Whole leaf	Whole leaf	Pulp	Fibre	Cladode - old	Cladode - young	Whole leaf	Stover	Straw
TS/FW (%)	13.7 ±0.6	18.9 ±0.7	11.9 ±0.3	39.0 ±0.9	8.5 ±0.5	7.7 ±0.3	55 ±4	29 ±4	93 ±4
VS/TS (%)	89.71 ±0.05	90.87 ±0.01	88.9 ±0.4	98.3 ±0.1	79.7 ±0.5	76.60 ±0.07	93.56 ±0.06	94.73 ±0.07	85.45 ±0.03
Cellulose (%TS)	10.1	18.0	9.0	50.6	12.6	8.6	22.8	28.0	17.2
Hemicellulose (%TS)	21.1	5.1	N.D.	17.4	5.5	6.4	37.6	21.0	26.5
Lignin (%TS)	15.1	7.7	9.2	3.1	8.7	6.6	12.2	3.2	11.6

The volatile (degradable) fraction of these biomass solids is shown in **Table 4.1** by the fraction of volatile to total solids (VS/TS). Maize and *Miscanthus* showed the highest VS/TS ratios at 94.73 % ± 0.07 and 93.56% ± 0.06. Whole agave and pineapple had the highest VS/TS ratios of the CAM feedstocks, at 90.87% ± 0.01 and 89.71% ± 0.05, while the decorticated agave pulp had a higher VS/TS% than wheat straw (88.87% ± 0.36 and 85.45% ± 0.03, respectively). Both old and young *Opuntia* had the lowest VS/TS ratios of all the feedstocks, with % VS of 79.74% ± 0.49 and 76.60% ± 0.07, respectively. The agave fibre had a higher VS/TS than all the feedstocks, at 98.25% ± 0.01.

There was a high degree of variability in the structural composition (lignin, cellulose, hemicellulose) of the plant species investigated. Maize had the lowest lignin content at just 3.18 % of TS. In contrast, both *Miscanthus* and wheat straw had a lignin content of almost four times that of maize, at 12.22 % w/w and 11.6 %, respectively. However, maize had the highest cellulose content (28 %TS) of all the feedstocks investigated. Pineapple had the highest lignin content of all the feedstock investigated (15.1 %). In contrast to the C3 and C4 plants, pineapple had a low cellulose content of 10.1 %. Overall, the C3 and C4 plants had a higher lignin, cellulose, and hemicellulose content than the CAM plants (except for the lignin content of maize). Agave pulp had a higher lignin content than the whole agave leaf (9.17 % and 7.69 %, respectively). Removal of the agave fibre, (consisting of 50.6, 17.4, and 3.09 % TS cellulose, hemicellulose, and lignin, respectively) appears to account for the compositional differences

seen between whole agave leaf and the decorticated pulp, the latter of which shows a depletion of cellulose and hemicellulose and slight enrichment of lignin relative to whole leaf, which seems to arise from the disproportionate depletion of hemicellulose and cellulose from the fibre extraction process. As expected, the old *Opuntia* cladode had a higher proportion of lignin and cellulose (8.7 % and 12.6 %) than the young cladodes (6.6 % and 8.6 %).

The initial compositions of the two inocula investigated are given in **Table 4.2**. The TS fraction of the AD sludge (6.7 ± 0.4%) was over twice that of rumen fluid (3.0 ± 0.1%), though the proportions of VS to TS for the two were comparable at 62.60 ± 0.02% and 67.4 ± 0.6%, respectively. The AD sludge exhibited an alkaline pH (8.00 ± 0.01) and low total VFA concentration of 0.66 ± 0.04 g/L, consistent with conditions of biogas production. Rumen fluid had a lower pH (6.3 ± 0.3) and a higher total VFA concentration of 11.0 ± 0.1 g/L VFA. Rumen fluid was particularly rich in acetic (5.22 ± 0.08 g/L), propionic (3.17 ± 0.07 g/L), and butyric acids (1.65 ±0.03 g/L). In the AD sludge, C4–C6 acids were not detected by Gas Chromatography Flame Ionisation Detection (GC-FID) analysis.

Table 4.2: Characterisation of AD sludge and rumen inocula compositions and microbial community structures. TS/FW = total solid of fresh weight (%), VS/TS = volatile solid of total solid (%), n.d. = Not detected. Compositional data are presented as mean ± standard deviation of triplicate measurements.

Characteristic	Inoculum Source		Putative community function
	AD Sludge	Rumen Fluid	
TS/FW (% w/v)	6.7 ±0.4	3.0 ± 0.1	
VS/TS (% w/w)	62.60 ±0.02	67.4 ±0.6	
pH	8.00 ±0.01	6.3 ±0.3	
Total VFA (g/L)	0.66 ±0.04	11.0 ±0.2	
of which:			
• Acetic acid (g/L)	0.13 ±0.01	5.22 ±0.08	
• Propionic acid (g/L)	0.45 ±0.03	3.17 ±0.07	
• Isobutyric acid (g/L)	n.d.	0.10 ±0.01	
• Butyric acid (g/L)	n.d.	1.65 ±0.03	
• Isovaleric acid (g/L)	n.d.	0.20 ±0.01	
• Valeric acid (g/L)	n.d.	0.39 ±0.01	
• Hexanoic acid (g/L)	n.d.	0.24 ±0.01	
Relative community abundance (Key genera)			
• Clostridium (%)	19.26	1.57	Hydrolysis, Fermentation, Acetogenesis (Harirchi et al., 2022)
• Sedimentibacter (%)	7.31	n.d.	Fermentation* (Whitman et al., 2015)
• Gallicola (%)	5.99	n.d.	Fermentation* (Whitman et al., 2015)
• Prevotella (%)	n.d.	15.84	Hydrolysis, Fermentation (Betancur-Murillo et al., 2022; Dao et al., 202)
• Succiniclasticum (%)	n.d.	10.45	Fermentation (Van Gylswyk, 1995)
• Butyrivibrio (%)	n.d.	6.92	Hydrolysis, Fermentation (Harirchi et al., 2022)

*Sedimentibacter and Gallicola known to participate in fermentation of amino acids but not of carbohydrates.

Metagenomic characterisation of the two anaerobic inocula revealed considerable, differences between their respective microbial communities. *Clostridium* was the most abundant genus in sludge and *Prevotella* the most abundant in rumen, while each only represented a small fraction of the other community. **Table 4.2** provides an approximate assignment of function to these genera based on previous literature. Key AF functions of hydrolysis and fermentation (acidogenesis) are performed by distinct communities in the two inocula. *Clostridia* and *Prevotella* represent the most abundant hydrolytic and fermentative communities identified in sludge and rumen, respectively.

4.3.2 VFA yield comparison of two inocula with novel feedstocks

The results of the time series of VFA accumulation from acidogenic fermentation are shown in **Fig. 4.1**. Panels A–H represent the VFA yield of each CAM and non-CAM feedstock

with each inoculum, and their associated pH values over the study time course. CAM feedstocks (**Fig. 4.1 A–E**) exhibited more logarithmic VFA production, with maximal rates of production near time zero. Non-CAM feedstocks, in particular *Miscanthus* and wheat (**Fig. 4.1 F, H**), showed an initial lag phase followed by a period of rapid acidification before plateauing. Maize (**Fig. 4.1G**) showed logarithmic VFA production with AD sludge but exhibited a lag phase with rumen fluid. All CAM feedstocks (**Fig. 4.1 A–E**) and maize (**Fig. 4.1G**) exhibited higher VFA production with AD sludge than with rumen fluid. Acidification curves for *Miscanthus* (**Fig. 4.1F**) and wheat (**Fig. 4.1H**) were comparable in both inocula.

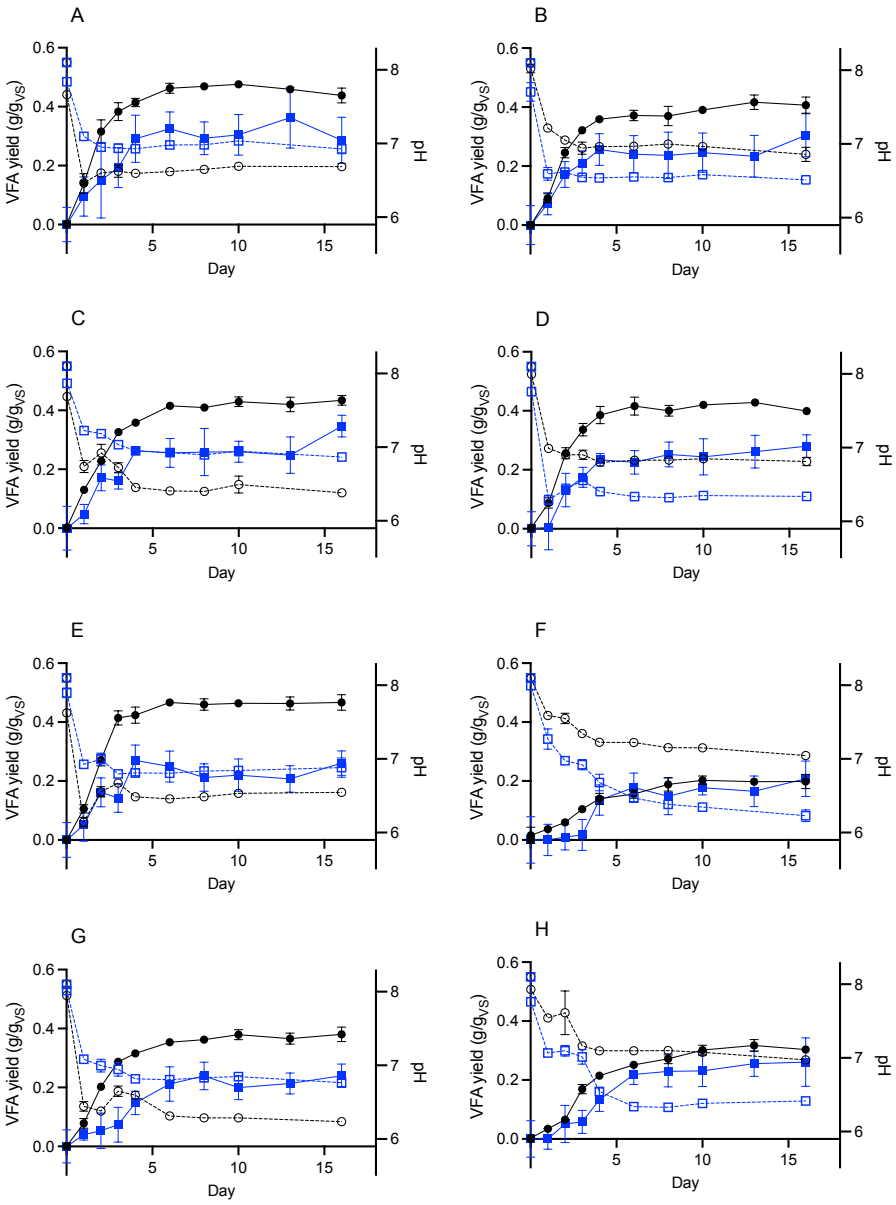


Figure 4.1: Total VFA yield and pH time-courses for CAM and non-CAM feedstocks with AD sludge (black circles) and rumen fluid (blue squares) inocula. VFA and pH are indicated by closed

and open symbols, respectively. Feedstocks shown are **A**, young *Opuntia*; **B**, old *Opuntia*; **C**, pineapple; **D**, whole Agave; **E**, decorticated Agave pulp; **F**, *Miscanthus*; **G**, maize stover; and **H**, wheat straw. Yields are given on a VS basis (g/g_{vs}), VFA and pH data presented as means ± standard deviation of triplicate fermentations.

Despite yielding less VFA from the feedstocks, rumen-driven conditions demonstrated a greater drop in pH. The VFA data in **Fig. 4.1** are shown net of the underlying inoculum. Undiluted rumen fluid contained 11.0 ± 0.1 g/L VFA as compared to just 0.66 ± 0.04 g/L VFA in AD sludge (**Table 2**). While all conditions were started at an initial pH of 8.1, the progression of pH seen in Fig. 1 is a product of both VFA production from biomass, as seen in **Fig. 4.1** yield curves, and the underlying behaviours of these distinct inocula. First-order models (**Fig. 4.2**) fitted to the VFA yield data in **Fig. 4.1** further emphasised the above observations. First-order models of best fit broadly converged to higher maxima for AD sludge (**Fig. 4.2A**) than for rumen fluid (**Fig. 4.2B**), indicating maximal theoretical yields were higher with AD sludge.

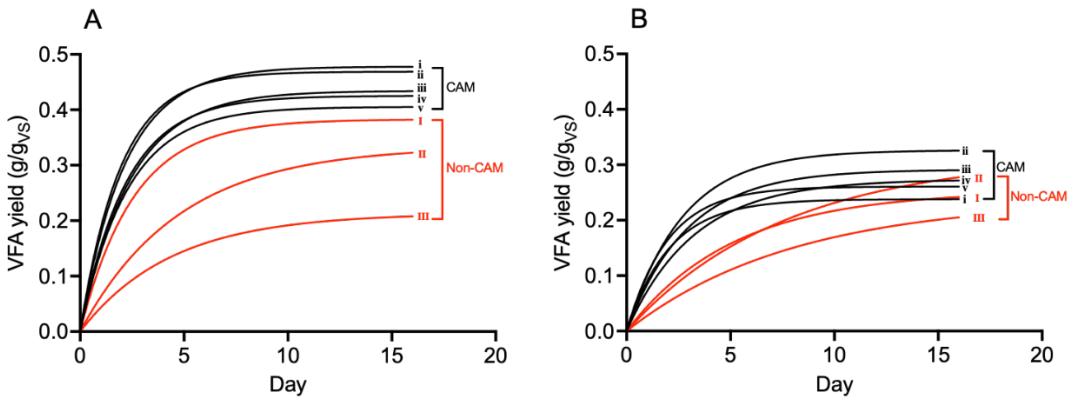


Figure 4.2: First-order models of VFA yields. Data shown represent first order models of best fit for raw data depicted in Fig. 1. VFA yield (g/g_{vs}) curves produced with AD sludge are given in panel **A**, and with rumen fluid in panel **B**. CAM feedstocks are shown in black with lower-case symbols, and non-CAM in red, uppercase. Feedstocks are as follows: **i** - Agave pulp, **ii** - Young *Opuntia*, **iii** - Pineapple, **iv** - Whole agave, **v** - Old *Opuntia*, **I** - Maize, **II** - Wheat, **III** - *Miscanthus.*

CAM and non-CAM feedstocks also clustered into distinct groupings, with CAM feedstocks converging to higher yield maxima than non-CAM, especially with AD sludge inoculum. CAM feedstocks showed a more biphasic VFA production, with a rapid initial phase followed by a plateau, while non-CAM exhibited a gradual convergence to maximum yield.

4.3.3 Relationship between substrate solubility and acidification rate

The first-order rate constant 'k,' derived from the first-order models in **Fig. 4.2**, provides a measure of the rate of acidification of each substrate (**Table 4.3**). It was hypothesised that the highest rates would be observed in feedstocks containing larger amounts of soluble organic matter, which would hydrolyse rapidly. Soluble Chemical Oxygen Demand (SCOD) at time point zero provided an experimental proxy for substrate solubility. First-order rate constants (**Fig. 4.3A**) for each feedstock were found to demonstrate a linear trend (**Fig. 4.3C**) when regressed against SCOD (**Fig. 4.3B**). With both AD sludge and rumen fluid, linear regression of k against SCOD revealed a positive relationship. R^2 values of 0.608 and 0.518 for AD sludge and rumen fluid, respectively, indicated that approximately half of the observed variability in k values could be explained by the SCOD content of the feedstock. As CAM feedstocks demonstrated higher SCOD (p-value <0.01, by Mann-Whitney test) (**Fig. 4.3B**), this solubility argument partially accounts for the higher 'k' values seen in CAM-fed fermentations (Fig. 3A).

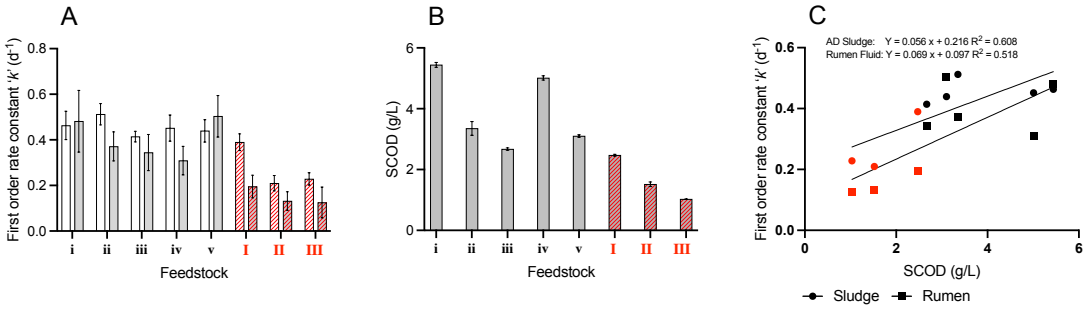


Figure 4.3: Comparison of the first-order rate constants of acidification and substrate soluble organics to test the hypothesis that reaction rate is defined by substrate solubility. Non-CAM feedstocks are indicated in red. **A:** First order rate constants ('*k*') for each substrate with AD sludge (white) and rumen fluid (grey), **B**: Soluble chemical oxygen demand (SCOD) of each substrate (g/L). Feedstocks are as follows: **i** - Agave pulp, **ii** - Young *Opuntia*, **iii** - Pineapple, **iv** - Whole Agave, **v** - Old *Opuntia*, **I** - Maize, **II** - Wheat, **III** - *Miscanthus.* **C**: Regression of SCOD (g/L) against rate constant '*k*'(d^{-1}). Black circles = sludge, black squares = rumen. First order rate constants in panel A are determined from models of best fit and are shown with their associated standard errors. SCOD data in panel B are shown as means ± standard deviation of triplicate measurements. Models in panel C: R^2 of sludge = 0.608, R^2 of rumen = 0.518. Gradients of both models are non-zero at 5% significance level ($p < 0.05$).

4.3.4 Relationship between substrate structural characteristics and total VFA yield

Theoretical maximum yields (Y_{max}), as calculated from the first-order models, varied between feedstocks and inoculum sources (**Fig. 4.4A, Table 4.3**). With AD sludge, Y_{max} was highest for Agave pulp (0.48 ± 0.02 gVFA/gVS) and lowest for *Miscanthus* (0.21 ± 0.009 gVFA/gVS). Highest and lowest yields for rumen fluid were observed in young *Opuntia* biomass (0.33 ± 0.02 gVFA/gVS) and *Miscanthus* (0.24 ± 0.07 gVFA/gVS), respectively.

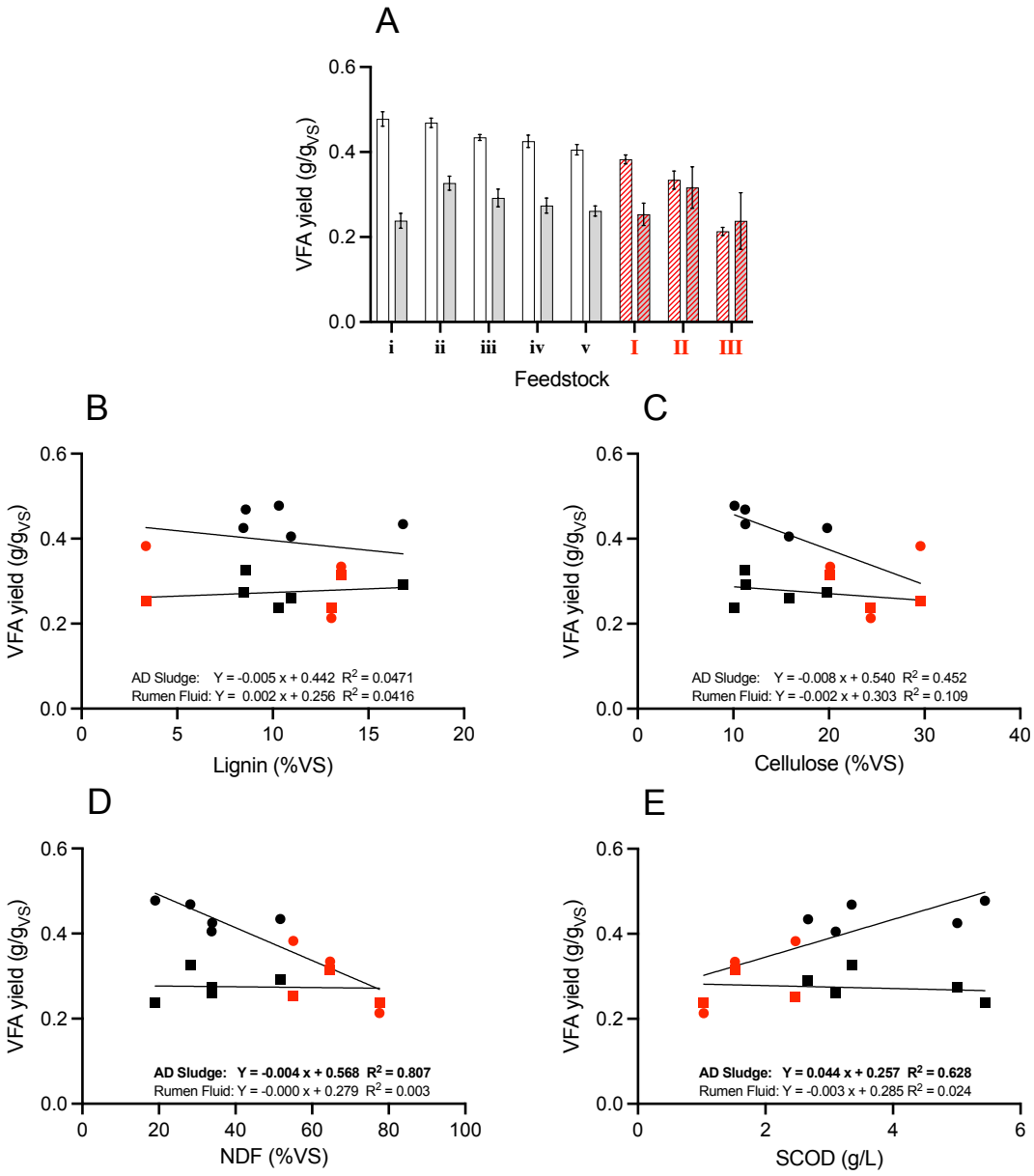


Figure 4.4: VFA yields as calculated by first-order models and their linear least squares regressions against substrate structural characteristics and soluble chemical oxygen demand (SCOD) indicating relationships between biomass parameters and fermentation characteristics. **A:** Theoretical maximum yield (Y_{max}) of VFA yields (g/g_{vs}) ± standard errors. CAM biomass:

white = sludge, grey = rumen; non-CAM: light red = sludge, dark red = rumen. **B:** Regression of VFA yield (g/g_{vs}) vs lignin (%VS), **C:** VFA yield (g/g_{vs}) vs. cellulose (%VS), **D:** VFA yield (g/g_{vs}) vs. neutral-detergent fibre (%VS), **E:** VFA yield (g/g_{vs}) vs. soluble chemical oxygen demand (SCOD, g/L) yield. R^2 of regression given in each panel. Only AD sludge regressions against NDF and SCOD were significant at 5% level with p-values of 0.019 and 0.002, respectively. CAM = black, non-CAM = red. Circles = sludge, squares = rumen.

Table 4.3. Kinetic parameters from first order model of VFA yield over time. All model parameter estimates are quoted ± standard errors. Experimentally observed yields at experiment termination at day 16 (Y_{End}) are given for comparison, as means ± standard deviation. Table ordered in descending order of Y_{Max} with AD sludge.

Inoculum source	Feedstock	First order model parameters			Observed endpoint yields
		Model R^2	k (d^{-1})	Y_{max} (gVFA/gVS)	Y_{End} (gVFA/gVS)
AD Sludge	Agave pulp	0.974	0.46 ±0.06	0.48 ±0.02	0.47 ±0.03
	Young *Opuntia*	0.988	0.51 ±0.05	0.47 ±0.01	0.44 ±0.03
	Pineapple	0.995	0.41 ±0.02	0.434 ±0.007	0.43 ±0.02
	Whole Agave	0.976	0.45 ±0.06	0.43 ±0.01	0.40 ±0.01
	Old *Opuntia*	0.982	0.44 ±0.05	0.41 ±0.01	0.41 ±0.03
	Maize	0.987	0.39 ±0.04	0.38 ±0.01	0.38 ±0.02
	Wheat	0.971	0.21 ±0.03	0.33 ±0.02	0.303 ±0.003
	Miscanthus	0.982	0.23 ±0.03	0.213 ±0.009	0.20 ±0.02
Rumen Fluid	Agave pulp	0.897	0.5 ±0.1	0.24 ±0.02	0.26 ±0.04
	Young *Opuntia*	0.957	0.37 ±0.06	0.33 ±0.02	0.29 ±0.08
	Pineapple	0.926	0.34 ±0.08	0.29 ±0.02	0.35 ±0.04
	Whole Agave	0.947	0.31 ±0.06	0.27 ±0.02	0.28 +0.04
	Old *Opuntia*	0.954	0.50 ±0.09	0.26 ±0.01	0.30 ±0.07
	Maize	0.935	0.20 ±0.05	0.25 ±0.03	0.24 ±0.04
	Wheat	0.943	0.13 ±0.04	0.32 ±0.05	0.26 ±0.08
	Miscanthus	0.854	0.13 ±0.07	0.24 ±0.07	0.21 ±0.06

Interestingly, while VFA yields tended to be higher from AD sludge than those of rumen fluid, VFA yields from wheat and *Miscanthus* were comparable with both inocula. It was originally hypothesised that the overall degradability of the biomass, and therefore VFA yields,

would be determined by lignin content of the biomass. However, linear regressions of Ymax against lignin (%VS) did not find a strong relationship between these variables (**Fig. 4.4B**) (Model R^2 values for rumen and sludge were 0.0471 and 0.0416). A stronger trend was also found for regression of Y_{max} against cellulose content, especially in the samples with AD sludge (Model $R^2 = 0.452$) (**Fig. 4.4C**).

Single linear regressions of AD sludge Y_{max} values against neutral detergent fibre (NDF) (i.e., the sum of cellulose, hemicellulose, and lignin in sample biomass) and SCOD accounted for much of the variability in feedstock yields with AD sludge (with R^2 of 0.809 and 0.628, respectively), though no significant relationship was found between NDF and rumen fluid yields. This suggests that the greater the 'structural' content of the biomass (here the NDF) the lower its degradability by AD sludge. The relative overperformance of CAM feedstocks thus appears to be because of their low structural content, rather than from the increased degradability of these structural components due to lower lignin content. Multiple linear regression of sludge Y_{max} against both NDF and SCOD produced no appreciable increase in model R^2, suggesting no improvement in the explanatory power of the model from inclusion of both variables. This suggests that the two variables (NDF and SCOD) are not independent. This makes sense when considering that SCOD measures soluble material, which will derive from the non-structural components of the biomass: it is thus strongly, but inversely, correlated with 'structural' components, and thereby acts as a negative proxy of NDF, leading to the result observed in **Fig. 4.4E**.

4.4. Discussion

4.4.1 Characterisation of VFA yield

This study found higher VFA yields with AD sludge than with rumen fluid as inoculum. A similar difference in inoculum performance has been previously reported by Yue et al. (2012), which found reactor sludge to produce higher biomethane yields than rumen fluid in AD of bulrush biomass. One explanation for these divergent yields could be the high endogenous concentrations of VFA in rumen fluid relative to those in AD sludge (**Table 4.2**). At t=0 this initial VFA concentration amounted to 2.9 ± 0.1 g/L in rumen conditions, but just 0.36 ± 0.01 g/L in AD sludge conditions. This VFA was present throughout the fermentation process and could have led to inhibition of hydrolytic, fermentative, or methanogenic processes (Siegert & Banks, 2005). Future investigations could control for this possibility by purging residual VFA and volatiles from rumen fluid prior to inoculation.

With AD sludge, CAM feedstocks showed a clear advantage over non-CAM feedstocks, with yields of 0.48 ± 0.02 to 0.41 ± 0.01 gVFA/gVS for CAM compared to 0.38 ±0.01 to 0.213 ± 0.009 for non-CAM feedstocks. Lueangwattanapong et al. (2020) made a similar comparison between CAM crops and maize as feedstocks for biomethane production by AD but did not find CAM crops to have a higher biomethane potential than maize. In this study, maize was the non-CAM crop which performed most comparably to CAM, with both wheat and *Miscanthus* showing poorer yields than either CAM or maize. With rumen fluid, a less dramatic bifurcation in yields was seen between biomass classes (**Table 4.3**). From a yield-perspective, CAM crops clearly outperform non-CAM when AD sludge provides the inoculum community. When rumen fluid provides the inoculum, the results are inconclusive.

4.4.2 Hydrolysis rates are faster when CAM biomass is used as a substrate in methanogenesis-inhibited AD sludge

Apart from agave pulp and old *Opuntia* cladodes (**Fig. 4.2, Table 4.3**), the first-order rate constant 'k' was higher for the AD sludge than for the rumen inoculum. Hydrolysis rates are typically defined by the structural complexity and insolubility of the feedstock. This is the rationale behind substrate pre-treatment techniques, which aim to address this process bottleneck by increasing substrate solubility and thereby accessibility to hydrolytic enzymes. Lee et al. (2014) for example, demonstrated that ultrasound pre-treatment of algal biomass led to an increase in SCOD, which improved both yields and hydrolysis rates during fermentation. **Fig. 4.3C** shows that approximately half of the observed variability in fermentation rates between feedstocks could be accounted for by differences in SCOD.
In CAM plants, due to the high-water content and succulence of their shoot tissues, structural support is provided by turgor pressure and quantity of structural carbohydrate is relatively low (**Table 4.1**). A greater amount of the biomass volatiles could therefore be expected to be present as soluble sugars and organic acids, which are readily hydrolysed (do Nascimento Santos et al., 2016; Mertens, 2010). Consistent with this expectation, CAM feedstocks exhibited higher amounts of SCOD at t = 0 than did non-CAM feedstocks (**Fig 4.3B**).

While initial hydrolysis rates were lower when non-CAM biomass was used as a feedstock, hydrolysis rates in AD sludge were still broadly faster than those in rumen fluid (**Fig. 4.2, Fig. 4.3A**). Interestingly, in two studies in which sludge and rumen fluid inocula were compared, both of which found higher product yields with sludge, the authors diverged on the question of reaction rate. (Lueangwattanapong et al., 2020) found AD sludge to have a higher gas production rate than rumen fluid, whilst (Yue et al., 2012) reported faster production with

rumen fluid. It is important to note, however, that both studies were investigating biogas production, and therefore the experiments were run for longer, without a methanogenesis inhibitor added, and kinetics were determined via modelling of biomethane potential rather than VFA accumulation.

For both inocula, first-order rate constants were higher for CAM than non-CAM feedstocks. A faster 'k' indicates a more rapid convergence to maximum yield, allowing biomass degradation over shorter hydraulic retention times (HRT). At an industrial scale, a shorter HRT allows a smaller reactor footprint and construction cost, improving reactor economics. While for rumen fluid the yields for CAM and non-CAM feedstocks were similar, the rates at which they converged to these maxima were different, indicating that even under a rumen fluid-driven system, CAM biomass can offer considerable benefit.

4.4.3 Yield performance of AD sludge is inhibited by high Neutral Detergent Fibre (NDF) from traditional biofuel feedstock

It has been argued that the low lignin content of CAM biomass renders it more readily degradable and therefore more amenable as a feedstock for biorefinery (Mason et al., 2015). This was one initial hypothesis of this study. While our data do support this argument for the superiority of CAM biomass as biorefinery feedstocks over the conventional non-CAM feedstocks tested, our results could not attribute this performance advantage to lignin alone. Regression of VFA yields against key substrate parameters detected no significant relationship between lignin content and VFA yield. Pineapple was found to have the highest lignin content at 15.1 %TS, and yet consistently outperformed maize, which contained just 3.2%. In fact, as the regressions in **Fig. 4.4** show, the superior performance of CAM feedstocks, when inoculated with AD sludge, could be best explained by variation in NDF content. While pineapple had a high lignin content, it also had a very low content of structural carbohydrates (cellulose and hemicellulose) and therefore a lower NDF, which in this study appears to have better predicted the overall degradability of a substrate than lignin. This interpretation is intuitive when considering that the most common application of the NDF measure is in the analysis of the energy density of agricultural feed, a higher NDF will typically correlate negatively with feed digestibility and energy density (Mertens, 2010). In contrast, the non-CAM biomass had an overall higher NDF content, leading to an underperformance when fermented with AD sludge. This can be seen in **Fig. 4.1**, where the AD sludge performed worst with *Miscanthus* and wheat straw feedstocks. In contrast, maize performed better, possibly due to its low lignin content, or higher SCOD content (Del Río et al., 2018; Menardo et al., 2015). Though it had a high

cellulose content, maize had a lower overall percentage content of NDF than the other two non-CAM crops, which it broadly outperformed.

Interestingly, these relationships between yield and NDF seen in AD sludge were not evident when rumen fluid was used as the inoculum (**Fig. 4.4D**). As the rumen is one of the few animal digestive organs capable of digesting structural carbohydrate, it would follow that its microbiome would be well attuned to NDF digestion. While AD sludge broadly outperformed rumen fluid in this study, for the two feedstocks with the highest NDF percentages, wheat and *Miscanthus*, the performance of the two inocula converged (**Fig. 4.1F, H, Fig. 4.4D**).

4.4.4 Implications for biorefinery

The results demonstrate that VFA production under the conditions tested was faster from CAM than non-CAM biomass. This is significant since it potentially enables CAM-fed reactors to be run at shorter hydraulic retention times (HRT) for equivalent yields. Smaller CAM-fed reactors could thus digest the biomass and produce the VFA of a larger non-CAM reactor. Similar VFA productivities could thus be achieved for a smaller initial capital outlay, improving the cost-competitiveness of 'green' VFA with alternatives to fossil fuels. The greater yields seen with sludge also mean greater productivity of desired end products for a given quantity of substrate organics. This comes with the caveat that CAM biomass did show a higher inorganic content than non-CAM (as seen by the lower VS/TS values in **Table 4.1**), suggesting this observed yield outperformance would be slightly less pronounced on a TS basis.

The global market for petrochemicals stands at US$ 585 billion (Grand View Research, 2022), while global markets for renewable chemicals remain in the mere tens of billions (Patel & Shah, 2021). The global pineapple market alone, including fresh and processed fruit, stood at ~US$10.3 billion in 2021, generated from an annual global harvest of 28.6 million tonnes of fruit (FAO, 2021). Assuming the ratio of 1.6 for leaf to fruit biomass calculated earlier, this suggests a possible resource of ~45.8 million tonnes of leaf residue available annually for potential biorefinery application. Applying the biomass composition (13.7% TS, 89.71% VS/TS) and yields (0.43 gVFA/gVS) calculated herein, this could represent a source of an additional 2.4 million tonnes of renewable VFA production annually. At a VFA price of $400 per tonne (Alibaba.com, 2023), this waste biomass source alone could represent US$0.97 billion in annual renewable petrochemicals. While this would represent a considerable increase to existing biorefinery activity, if the sector is to reach a scale commensurate with the market demand it seeks to meet, a shift is required. Currently, the residues of existing agricultural industries provide the bulk of feedstock for any local biorefinery activity, but this forces the biorefinery sector to deal with seasonal fluctuations in substrate availability. Second-generation energy

crops such as (e.g. *Miscanthus* and switchgrass) (Sims et al., 2010) may be used to supplement seasonal variability, but these compete directly for finite arable land. In contrast, the dedicated, widespread cultivation of stress-tolerant CAM plants on marginal lands could allow this transition to large scale biorefinery.

4.5 Conclusion

The acidogenic fermentation kinetics of a variety of CAM crops were found to compare favourably against three conventional biorefinery feedstocks in two different anaerobic inocula. CAM-plant biomass broadly produced higher yields of volatile fatty acids when fermented with AD sludge and showed more rapid degradation in both AD sludge and rumen fluid than did non-CAM feedstocks. These results endorse the suitability of CAM crops as biorefinery substrates and support their more widespread cultivation on marginal lands, which could thereby facilitate a shift to large scale biorefinery production of renewable chemicals.

Acknowledgements

The authors would like to thank Severn Trent Green Power Cassington AD facility, Oxfordshire for providing the AD sludge and Prof. Chris K. Reynolds and David Humphries from the University of Reading for providing the rumen fluid. The authors would also like to thank Dr. Andrew Lilley for his advice on the manuscript's statistical analyses.
Funding declaration

The project was supported by funding from the Oxford Martin School Dryland Bioenergy Project, University of Oxford. Funding was additionally provided by East X LLP and by Rotary International (Grant number: GG2128217).

Competing interest statement

The authors declare that the research was conducted in the absence of any commercial or financial relationships that could be construed as a potential conflict of interest.

Author contributions

NAT NA IPT & JACS designed the study. NAT & NA conducted the experimental work with assistance from LKM. NAT & NA analysed the data & wrote the first draft of the manuscript. All authors contributed to and edited the final manuscript.
Availability of data and materials

The datasets used and/or analysed during the current study are available from the corresponding author on reasonable request.

References

International Energy Agency. World Energy Outlook 2022 2022 [Available from: https://www.iea.org/reports/world-energy-outlook-2022.

bp Energy. bp Statistical Review of World Energy 2020 2020 [Available from: https://www.bp.com/en/global/corporate/energy-economics/statistical-review-of-world-energy.html

Vázquez-Fernández A, Suárez-Ojeda ME, Carrera J. Review about bioproduction of Volatile Fatty Acids from wastes and wastewaters: Influence of operating conditions and organic composition of the substrate. Journal of Environmental Chemical Engineering. 2022;10(3):107917.

Agnihotri S, Yin D-M, Mahboubi A, Sapmaz T, Varjani S, Qiao W, et al. A glimpse of the world of volatile fatty acids production and application: A review. Bioengineered. 2022;13(1):1249-75.

Strazzera G, Battista F, Garcia NH, Frison N, Bolzonella D. Volatile fatty acids production from food wastes for biorefinery platforms: A review. Journal of environmental management. 2018;226:278-88.

Mason PM, Glover K, Smith JAC, Willis KJ, Woods J, Thompson IP. The potential of CAM crops as a globally significant bioenergy resource: Moving from 'fuel or food'to 'fuel and more food'. Energy & Environmental Science. 2015;8(8):2320-9.

Pols A. The rationality of biofuel certification: A critical examination of EU biofuel policy. Journal of Agricultural and Environmental Ethics. 2015;28:667-81.

Arba M. The potential of cactus pear (*Opuntia* ficus-indica (L.) Mill.) as food and forage crop. Emerging research in alternative crops. 2020:335-57.

UNDP/UNSO. Aridity zones and dryland populations: An assessment of population levels in the world's drylands with particular reference to Africa. New York; 1997.

Sarr B. Present and future climate change in the semi-arid region of West Africa: a crucial input for practical adaptation in agriculture. Atmospheric Science Letters. 2012;13(2):108-12.

Borland AM, Griffiths H, Hartwell J, Smith AC. Exploiting the potential of plants with crassulacean acid metabolism for bioenergy production on marginal lands. Journal of Experimental Botany. 2009;60:2879-96.

Buckland CE, Thomas DSG. Analysing the potential for CAM-fed bio-economic uses in sub-Saharan Africa. Appl Geogr. 2021;132:102463.

Nobel PS. Achievable productivities of certain CAM plants: basis for high values compared with C3 and C4 plants. New phytologist. 1991;119(2):183-205.

Lueangwattanapong K, Ammam F, Mason PM, Whitehead C, McQueen-Mason SJ, Gomez LD, et al. Anaerobic digestion of Crassulacean Acid Metabolism plants: Exploring alternative feedstocks for semi-arid lands. Bioresource Technology. 2020;297:122262.

Shrestha S, Fonoll X, Khanal SK, Raskin L. Biological strategies for enhanced hydrolysis of lignocellulosic biomass during anaerobic digestion: Current status and future perspectives. Bioresource Technology. 2017;245:1245-57.

Börjesson J, Engqvist M, Sipos B, Tjerneld F. Effect of poly (ethylene glycol) on enzymatic hydrolysis and adsorption of cellulase enzymes to pretreated lignocellulose. Enzyme and Microbial Technology. 2007;41(1-2):186-95.

Castellano J, Marrero MD, Ortega Z, Romero F, Benitez AN, Ventura MR. *Opuntia* spp. fibre characterisation to obtain sustainable materials in the composites field. Polymers. 2021;13(13):2085.

Chen Y, Cheng JJ, Creamer KS. Inhibition of anaerobic digestion process: a review. Bioresource technology. 2008;99(10):4044-64.

Mannai F, Ammar M, Yanez JG, Elaloui E, Moussaoui Y. Cellulose fiber from Tunisian Barbary Fig "*Opuntia* ficus-indica" for papermaking. Cellulose. 2016;23:2061-72.

Quiroz M, Varnero MT, Cuevas JG, Sierra H. Cactus pear (*Opuntia* ficus-indica) in areas with limited rainfall for the production of biogas and biofertilizer. Journal of Cleaner Production. 2021;289:125839.

Zhang L, Larsson A, Moldin A, Edlund U. Comparison of lignin distribution, structure, and morphology in wheat straw and wood. Industrial Crops and Products. 2022;187:115432.

He Y, Mouthier TM, Kabel MA, Dijkstra J, Hendriks WH, Struik PC, et al. Lignin composition is more important than content for maize stem cell wall degradation. Journal of the Science of Food and Agriculture. 2018;98(1):384-90.

Menardo S, Airoldi G, Cacciatore V, Balsari P. Potential biogas and methane yield of maize stover fractions and evaluation of some possible stover harvest chains. Biosystems engineering. 2015;129:352-9.

Liu X, Zhang Y, Li Z, Feng R, Zhang Y. Characterization of corncob-derived biochar and pyrolysis kinetics in comparison with corn stalk and sawdust. Bioresource technology. 2014;170:76-82.

Krümpel J, George T, Gasston B, Francis G, Lemmer A. Suitability of *Opuntia* ficus-indica (L) Mill. and Euphorbia tirucalli L. as energy crops for anaerobic digestion. Journal of Arid Environments. 2020;174:104047.

Mangold A, Lewandowski I, Hartung J, Kiesel A. Miscanthus for biogas production: Influence of harvest date and ensiling on digestibility and methane hectare yield. Gcb Bioenergy. 2019;11(1):50-62.

Ge X, Xu F, Li Y. Solid-state anaerobic digestion of lignocellulosic biomass: Recent progress and perspectives. Bioresource Technology. 2016;205:239-49.

Mancini G, Papirio S, Lens PN, Esposito G. Increased biogas production from wheat straw by chemical pretreatments. Renewable energy. 2018;119:608-14.

FAO. Crops and livestock products https://www.fao.org/faostat/en/#data/QCL2021 [Available from: https://www.fao.org/faostat/en/#data/QCL.

Apipatpapha T, Ongkunaruk P, Chollakup R, editors. Pineapple leaf fiber supply chain analysis for the sustainability of community enterprise: A case study in Thailand. IOP Conference Series: Earth and Environmental Science; 2022: IOP Publishing.

Andreu-Coll L, Cano-Lamadrid M, Noguera-Artiaga L, Lipan L, Carbonell-Barrachina ÁA, Rocamora-Montiel B, et al. Economic estimation of cactus pear production and its feasibility in Spain. Trends in Food Science & Technology. 2020;103:379-85.

do Nascimento Santos T, Dutra ED, do Prado AG, Leite FCB, de Souza RdFR, dos Santos DC, et al. Potential for biofuels from the biomass of prickly pear cladodes: Challenges for bioethanol and biogas production in dry areas. Biomass and Bioenergy. 2016;85:215-22.

Comparetti A, Febo P, Greco C, Mammano MM, Orlando S. Potential production of biogas from prickly pear (*Opuntia* ficus-indica L.) in Sicilian uncultivated areas. Chem Eng. 2017;58:559-64.

Ramadan MF, Ayoub TEM, Rohn S. *Opuntia* spp.: chemistry, bioactivity and industrial applications: Springer; 2021.

Park S Nobel EGB. Environmental Biology. In: Nobel P, editor. Cacti: Biology and uses. Los Angeles: University of California Press; 2002. p. 57-74.

Davis SC, Simpson J, Gil-Vega KdC, Niechayev NA, Tongerlo Ev, Castano NH, et al. Undervalued potential of crassulacean acid metabolism for current and future agricultural production. Journal of Experimental Botany. 2019;70(22):6521-37.

Cabrera-Toledo D, Mendoza-Galindo E, Larranaga N, Herrera-Estrella A, Vásquez-Cruz M, Hernández-Hernández T. Genomic and morphological differentiation of spirit producing Agave angustifolia traditional landraces cultivated in Jalisco, Mexico. Plants. 2022;11(17):2274.

Ihoeghian NA, Amenaghawon AN, Ajieh MU, Oshoma CE, Ogofure A, Erhunmwunse NO, et al. Anaerobic co-digestion of cattle rumen content and food waste for biogas production: Establishment of co-digestion ratios and kinetic studies. Bioresource Technology Reports. 2022;18:101033.

Angelidaki I, Sanders W. Assessment of the anaerobic biodegradability of macropollutants. Rev Environ Sci Biotechnol. 2004;3:117-29.

Tenci NA, Ammam F, Huang WE, Thompson IP. Anaerobic co-digestion of Euphorbia tirucalli with pig blood for volatile fatty acid production. Bioresource Technology Reports. 2023;21:101333.

APHA. Standard Methods for the Examination of Water and Wastewater. Washington DC: American Water Works Association and Water Environment Federation; 1998.

Van Soest Pv, Robertson JB, Lewis BA. Methods for dietary fiber, neutral detergent fiber, and nonstarch polysaccharides in relation to animal nutrition. Journal of dairy science. 1991;74(10):3583-97.

GraphPad. GraphPad Prism version 9.5.0 for Windows 2023 [Available from: www.graphpad.com.

Wang S, Tao X, Zhang G, Zhang P, Wang H, Ye J, et al. Benefit of solid-liquid separation on volatile fatty acid production from grass clipping with ultrasound-calcium hydroxide pretreatment. Bioresource technology. 2019;274:97-104.

Harirchi S, Wainaina S, Sar T, Nojoumi SA, Parchami M, Parchami M, et al. Microbiological insights into anaerobic digestion for biogas, hydrogen or volatile fatty acids (VFAs): a review. Bioengineered. 2022;13(3):6521-57.

Whitman WB, Rainey F, Kämpfer P, Trujillo M, Chun J, DeVos P, et al. Bergey's manual of systematics of Archaea and Bacteria: Wiley Online Library; 2015.

Betancur-Murillo CL, Aguilar-Marín SB, Jovel J. Prevotella: A key player in ruminal metabolism. Microorganisms. 2022;11(1):1.

Dao T-K, Do T-H, Le N-G, Nguyen H-D, Nguyen T-Q, Le T-T-H, et al. Understanding the role of Prevotella genus in the digestion of lignocellulose and other substrates in Vietnamese native goats' rumen by metagenomic deep sequencing. Animals. 2021;11(11):3257.

Van Gylswyk N. Succiniclasticum ruminis gen. nov., sp. nov., a ruminal bacterium converting succinate to propionate as the sole energy-yielding mechanism. International Journal of Systematic and Evolutionary Microbiology. 1995;45(2):297-300.

Yue Z-B, Wang J, Liu X-M, Yu H-Q. Comparison of rumen microorganism and digester sludge dominated anaerobic digestion processes for aquatic plants. Renewable energy. 2012;46:255-8.

Siegert I, Banks C. The effect of volatile fatty acid additions on the anaerobic digestion of cellulose and glucose in batch reactors. Process Biochemistry. 2005;40(11):3412-8.

Lee K, Chantrasakdakul P, Kim D, Kong M, Park KY. Ultrasound pretreatment of filamentous algal biomass for enhanced biogas production. Waste management. 2014;34(6):1035-40.

Mertens D, editor NDF and DMI-Has anything changed. Proc Cornell Nutr Conf, Syracuse, NY Pp; 2010.

Del Río JC, Rencoret J, Gutiérrez A, Kim H, Ralph J. Structural characterization of lignin from maize (Zea mays L.) fibers: Evidence for diferuloylputrescine incorporated into the lignin polymer in maize kernels. Journal of agricultural and food chemistry. 2018;66(17):4402-13.

Research GV. Petrochemicals Market Size, Share & Trends Analysis Report By Product (Ethylene, Propylene, Butadiene), By Region (North America, Europe, Asia Pacific, Latin America, Middle East, Africa), And Segment Forecasts, 2023 - 2030 2022 [Available from: https://www.grandviewresearch.com/industry-analysis/petrochemical-market.

Patel A, Shah AR. Integrated lignocellulosic biorefinery: Gateway for production of second generation ethanol and value added products. Journal of Bioresources and Bioproducts. 2021;6(2):108-28.

Alibaba.com. MSDS glacial acetic acid 99.85% 2023 [Available from: https://detail/MSDSglacialaceticacid998560544854004.html?spm=a27aq.rank_detail.6404617500.1.557c54d7EPYrHU&cardType=101001155&cardId=10001241624.

Sims RE, Mabee W, Saddler JN, Taylor M. An overview of second generation biofuel technologies. Bioresource technology. 2010;101(6):1570-80.

Statement of Authorship for joint/multi-authored papers for PGR thesis

To appear at the end of each thesis chapter submitted as an article/paper

The statement shall describe the candidate's and co-authors' independent research contributions in the thesis publications. For each publication there should exist a complete statement that is to be filled out and signed by the candidate and supervisor **(only required where there isn't already a statement of contribution within the paper itself).**

Title of Paper	Biorefinery for a circular carbon economy: process benefits to the use of dryland (CAM) crops for anaerobic volatile fatty acid production
Publication Status:	☐ Published ☒ Accepted for publication ☐ Submitted for publication ☐ Unpublished and unsubmitted work written in manuscript style
Publication Details:	Provisionally accepted for publication in the journal 'Biotechnology for Biofuels and Bioproducts' pending author revisions.

Student Confirmation

Student Name:	*Nicholas A. Tenci*	
Contribution to the paper:	*Designed the study, performed the experiments, analysed the data, and wrote the manuscript in collaboration with Dr. Nichola Austen.*	
Signature: 	Date:	*11/09/2024*

Supervisor Confirmation

By signing the Statement of Authorship, you are certifying that the candidate made a substantial contribution to the publication, and that the description described above is accurate.

Supervisor name and title: *Prof. Ian P. Thompson*		
Supervisor comments: I agree with this summary.		
Signature: 	Date:	*17/09/2024*

This completed form should be included in the thesis, at the end of the relevant chapter.

Chapter 5. Red seaweed as an abundant, natural methanogenesis inhibitor for industrial biorefinery

Disclaimer

The following manuscript was accepted for publication in Volume 454 of the Journal of Cleaner Production on 07/04/2024. Several minor edits have been made to it in fulfilment of the suggestions of thesis examiners.

The published article (licenced under CC BY 4.0) may be accessed at:

Tenci, N. A., Ammam, F., Austen, N., Huang, W. E., & Thompson, I. P. (2024). Red seaweed as an abundant, natural methanogenesis inhibitor for industrial biorefinery. *Journal of Cleaner Production*, *454*, 142166.

Red seaweed as an abundant, natural methanogenesis inhibitor for industrial biorefinery

Authors: Nicholas A. Tenci[a], Fariza Ammam[a], Nichola Austen[a,b], Wei E. Huang[a], Ian P. Thompson[a]

Affiliations:

[a]University of Oxford, Department of Engineering Science, Parks Road, Oxford, OX1 3PJ, UK

[b]University of Oxford, Department of Biology, South Parks Road, OX1 3RB, UK

Abstract

Acidogenic fermentation offers a means to renewably refine biomass to volatile fatty acids from which industrial chemicals can be sustainably derived. Small molecules (bromoethane sulfonate) are used in the literature to inhibit methanogenesis and improve fatty acid yields but are impractical at industrial scale due to cost. The red seaweed *Asparagopsis taxiformis* has been shown to provide methanogenesis inhibition in the microbiome of the ruminant gut over short retention times (up to 72 h), but its suitability for bioreactor control has not been previously characterised. This study investigated the responses of both rumen fluid and anaerobic digester sludge to various *Asparagopsis* doses. In rumen fluid, doses of ≥5% *Asparagopsis* showed equivalent inhibition to bromoethane sulfonate at retention times under 30 days, producing VFA of both similar yields and qualities to this standard inhibitor. Digester sludge was not found to respond to *Asparagopsis* treatment at the levels tested, suggesting a specificity of treatment to microbial community. These data support the application of *Asparagopsis* as a scalable reactor control agent for rumen-driven fermenter configurations.

5.1. Introduction

Volatile fatty acids (VFA) produced from the acidogenic fermentation (AF) of biomass offer a sustainable alternative to petrochemicals as substrates for the chemical industry. VFAs have been demonstrated as substrates for bioproduction of polyhydroxyalkanoate bioplastics (PHA) (Mengmeng et al., 2009; Shen et al., 2014), oils (Christophe et al., 2012), waxes (Martin et al., 2023), and other chemicals. They are additionally used as additives in food, pharmaceuticals, and cosmetics, and as a carbon source for biological nutrient removal from wastewater (Agnihotri et al., 2022). AF is a modified form of anaerobic digestion (AD), where methanogenesis is inhibited to allow VFA to accumulate.

Methanogenesis can be inhibited by several means. Acidogenic and acetogenic bacteria exhibit a wider pH tolerance than do methanogenic archaea, which can be inhibited by reducing reactor pH to <6 (Wang et al., 2014). Inhibition can also be achieved through accumulation of degradation products such as VFA or ammonium (Shi et al., 2017; Siegert and Banks, 2005). Another common strategy for inhibiting methanogens is the use of dedicated methanogenesis inhibitor chemicals (Yin et al., 2016). The use of the 2-bromoethanesulfonate (BES) is particularly widespread in the literature (Tenci et al., 2023;Yin et al., 2016). BES is a structural analogue of Coenzyme M (CoM), a methanogen-specific cofactor. BES is typically understood to inhibit methanogenesis through competitive inhibition of this essential cofactor (Liu et al., 2011), which is required for the enzyme methyl-coenzyme M reductase (MCR) to catalyse the terminal step in all forms of methanogenesis (Liu and Whitman, 2008). BES accordingly demonstrates efficacy in a broad spectrum of methanogenic cultures, including anaerobic soils (Chidthaisong and Conrad, 2000), rumen fluid (Lazuka et al., 2015), and AD sludge (Tenci et al., 2023) and at low (typically millimolar) concentrations. Its broad efficacy, relatively low effective dose, and relative specificity for methanogenic archaea have contributed to the favoured status of BES as a laboratory scale methanogenesis inhibitor. Despite these considerable benefits, the high cost of BES (US$41/kg) (Baleeiro et al., 2022) precludes its wider use at industrial scale.

The red seaweed *Asparagopsis taxiformis* has recently gained attention as a potential feed additive to reduce carbon emissions from livestock. *Asparagopsis* has demonstrated an ability to inhibit methanogenesis in rumen fluid both *in vitro* (Kinley et al., 2016a; Machado et al., 2014), and *in vivo* (Li et al., 2016; Roque et al., 2021). The proposed active ingredient in this process is bromoform ($CHBr_3$), a halogenated methane analogue (Machado et al., 2016b). While the preliminary efficacy of *Asparagopsis* has been

demonstrated, key questions remain unanswered. Current literature on the subject is mainly focused on agricultural applications and the timescales studied are based on the retention times of the ruminant digestive tract (<4 days) (Kinley et al., 2016a; Machado et al., 2018), with little known about its efficacy over the longer timescales relevant to AF. Studies have also worked exclusively in rumen fluid, which contains a microbiome distinct from those typically found in commercial acidogenic fermenters. While a 2015 analysis by Meat and Livestock Australia (Cotter et al., 2015) placed the cost of wild-harvested *Asparagopsis taxiformis* at $AU 200/kg, this same report claims that prices below $AU 5/kg may be feasible with commercial cultivation and further mentions that imported, commercially grown algae (of other species) can retail for as little as $AU 1.50/kg. Recent data show bulk quantities of various species of seaweed of several species may be obtained for just $US 0.5–0.8/kg (Alibaba.com, 2023a; Alibaba.com, 2023b). Assuming these lower price bands to be feasible with large scale cultivation, farmed *Asparagopsis* could prove a cheap and renewable future alternative to BES for reactor control, if its efficacy can be demonstrated.

This study presents, to the best of our knowledge, the first systematic evaluation of *Asparagopsis* as a potential bioreactor control agent for VFA production. Its inhibitory effect on methane production and related kinetics was quantified in both rumen fluid and in commercial AD sludge over a 70-day time course, using biomass from *Euphorbia tirucalli* as a substrate. These effects were evaluated against a standard, small-molecule inhibitor – BES. VFA production was quantified, and its temporal variation mapped to the corresponding biomethane data, to understand how carbon allocation shifted as inhibition waned and methanogenesis resumed. A mechanistic explanation for these results was sought through a metagenomic characterisation of the two microbial communities, both prior to treatment, and at key timepoints throughout the fermentation time course.

5.2. Materials and methods

5.2.1. Biomass and inoculum

AD sludge was obtained from an anaerobic digestion facility processing municipal food waste (Severn Trent Green Power, Cassington, UK). Rumen fluid was collected from a fistulated cow (The Centre for Dairy Research, University of Reading, UK). Both sludge and rumen fluid were passed through a 1 mm sieve to remove any large particulates before characterisation and use.

Euphorbia tirucalli biomass provided the substrate for anaerobic digestion. This was field grown in Kenya and dried at 80 °C for storage. Prior to use, the dried biomass was ground in a blender (Waring Pro® Stainless Steel Blender, 550 W) to ensure homogeneity. *Asparagopsis taxiformis* biomass was obtained in dried form (seaExpert, Horta, Faial, Azores, Portugal). This was sourced from wild *Asparagopsis* grown in the coastal waters of the Azores, Portugal. Dried *Asparagopsis* was ground in a blender and passed through a 1 mm sieve to ensure consistent particle size.

5.2.2. Anaerobic batch assays

Anaerobic digestion experiments were performed in batch format in 250 mL vials with a 150 mL working volume. A standard culture medium was prepared as per Angelidaki and Sanders (2004), with the exclusion of sodium sulphide. This medium ensured an adequate supply of nutrients, vitamins, and trace minerals to promote robust microbial growth. A digestion master mix of medium, deionised water and the appropriate inoculum was prepared to a final inoculum concentration of 5 gVS/L, and the pH adjusted to 8.1. This bulk reaction mixture was aliquoted into vials containing the dried substrate. Adjustment to a mildly alkaline pH was both to allow for methanogenesis, and to allow for accumulation of VFA. Vials were sealed with rubber septa and aluminium crimp caps and inverted to mix their contents. The headspace gas was not purged to remove residual oxygen.

Each vial contained dried *E. tirucalli* biomass to give a 2:1 substrate to inoculum ratio (VS-basis). To test the efficacy of *Asparagopsis* as a methanogenesis inhibitor, *Asparagopsis* biomass was added to vials in five concentrations of 0.5, 1, 2, 5, and 10% (VS) of the *E. tirucalli* substrate. Three further positive control conditions were prepared with bromoethane sulfonate at concentrations of 5, 10, and 20 mM. A further condition containing *E. tirucalli,* but no inhibitor provided the negative (uninhibited) control. An 'inoculum blank' containing the digestion master mix but no substrate, was also prepared to account for the behaviour of the underlying inoculum. All conditions were prepared in triplicate. All conditions were incubated under mesophilic (37 °C) conditions, with constant agitation at 125 rpm. The experiment was terminated on day 70. This entire experimental setup was replicated for each of the two inocula tested. Neither inoculum source was purged of residual volatiles prior to the experiment.

5.2.3. Analytical methods

Determination of bulk biomass and inoculum parameters (total and volatile solids) was conducted as per standard methods (APHA, 1998), but with oven temperatures for determination of total solids (TS) set to 80 °C. Analysis of lignin, cellulose, and hemicellulose for *Euphorbia* and *Asparagopsis* were performed as described by van Soest et al. (1991).
The production of biogas was monitored by water displacement in a eudiometer. Gas volume data were corrected to standard temperature (273.15 K) and pressure (101.3 kPa) as previously described (Richards et al., 1991). The composition of biogas produced was analysed by Gas Chromatography with Thermal Conductivity Detection (GC-TCD) (Shimadzu GC-2010, Japan) with a ShinCarbon capillary column. Injector, oven, and detector temperatures were 150, 75, and 200 °C, respectively, with helium providing the carrier gas.

At each timepoint, liquid samples of 1.5 mL were withdrawn using a syringe. The pH of liquid samples was measured upon sample collection with a pH probe (Thermoscientific, USA). Samples were frozen at −20 °C for later analysis of VFA, and for metagenomic analysis.
For analysis of VFA, samples were centrifuged at 15,500×*g* for 10 min to obtain a clarified supernatant. Supernatant samples were transferred to 1.5 mL GC vials and acidified by 1:1 dilution with 20% formic acid. VFA concentrations were quantified by Gas Chromatography-Flame Ionisation Detection (GC-FID) using a 30 m × 0.25 mm x 0.25 μm fused-silica column (ZB-FFAP). Temperatures of the injector and detector were set at 250 and 350 °C, respectively. The oven temperature was held for 2 min at 100 °C and then ramped at 8 ºC/min to 150 °C, where it was held for a further 2 min. Acetic, propionic, isobutyric, butyric, isovaleric, valeric, and hexanoic acids were detected and quantified against standards. Total volatile fatty acid (TVFA) was calculated as the sum of these fatty acids.

Metagenomic analyses of inocula and reactor microbial communities were outsourced to an external provider (Genewiz Ltd., United Kingdom). The following protocol detailing the analytical procedures followed has been reproduced with their express permission:
DNA was extracted using NucleoMag DNA Microbiome Kit following manufacturer's instructions (Takara, San Jose, CA, USA). 16S-EZ rDNA next generation sequencing library preparations and Illumina MiSeq sequencing were conducted at Azenta, Inc. (South Plainfield, NJ, USA). Sequencing library was prepared using a MetaVx™ 16s rDNA Library Preparation kit (Azenta, Inc., South Plainfield, NJ, USA). Briefly, the DNA was used to generate amplicons that cover V3 and V4 hypervariable regions of bacteria and archaea16S rDNA. Indexed adapters were added to the ends of the 16S rDNA amplicons by limited cycle

PCR. DNA libraries were validated and quantified before loading. The pooled DNA libraries were loaded on an Illumina MiSeq instrument according to manufacturer's instructions (Illumina, San Diego, CA, USA). The samples were sequenced using a 2x 250 paired-end (PE) configuration. Image analysis and base calling were conducted by the Illumina Control Software on the Illumina instrument. Raw sequence data (.bcl files) generated from Illumina MiSeq was converted into FASTQ files and de-multiplexed using Illumina's bcl2fastq 2.17 software.

5.2.4. Statistical analysis and modelling

All experimental data herein are presented as the mean ± standard deviation of triplicate samples, unless otherwise stated. Model parameters are quoted with their associated standard errors. Data processing was performed in Microsoft Excel and GraphPad Prism 9.5.0 (GraphPad Prism version 9.5.0 for Windows, 2023). Biomethane yields were calculated based on total reactor volatiles (calculated as the sum of substrate, inoculum, and inhibitor volatile solids). Biomethane yield data were fitted using the following Modified Gompertz kinetic model, as previously demonstrated by Lueangwattanapong et al. (2020):

Modified Gompertz Model: $Y = A \exp[-\exp[(\mu_m e/A)(\lambda - t) + 1]]$

In which, Y = cumulative methane yield at time 't', A = maximum theoretical methane yield, t = time, λ = lag phase, μ_m = maximum methane production rate. This model was fitted in GraphPad Prism 9.5.0 to the methane yield data for each substrate to extract the above kinetic parameters for each condition. These parameters provided a standardised measure of the defining features of methane production: lag, rate, and yield. They were thus used as the basis by which the inhibition phenomenon was compared across treatment conditions.

5.3. Results

5.3.1. Characterisation of feedstock and inocula

Table 5.1 details the bulk characteristics of feedstocks and inocula in this experiment.

Table 5.1: Bulk characteristics of substrates and inocula used in this experiment. All data are given as means ± standard deviations of triplicate measurements.

	Substrates		**Inocula**	
Characteristic	***Euphorbia***	***Asparagopsis***	**AD sludge**	**Rumen Fluid**
TS/FM (%)	N/A	N/A	4.81 ±0.08	2.48 ±0.03
VS/TS (%)	83.3 ±0.3	52.94 ±0.03	60.3 ±0.2	61.3 ±0.2
Ash/TS (%)	16.7 ±0.3	47.06 ±0.03	39.7 ±0.2	38.7 ±0.2
Cellulose (%TS)	27.50	5.8	-	-
Hemicellulose (% TS)	2.78	12.1	-	-
Lignin (% TS)	5.32	1.25	-	-
TVFA (g/L)	-	-	0.28 ±0.05	8.80 ±0.03

*TS – Total solids, FM – Fresh matter, VS – Volatile solids, TVFA – Total volatile fatty acids

5.3.2. Response of biomethane production to *Asparagopsis* and BES treatment

Methane yields are given in **Fig. 5.1**. Uninhibited conditions (shown in red) showed characteristic, sigmoidal methane production curves for both rumen fluid (**Fig. 5.1 A, C1**) and AD sludge (**Fig. 5.1 B, D1**).All three concentrations of BES tested showed near complete inhibition of methane production in both inocula (**Fig. 5.1 A, B**), with only trace amounts of methane registered, and only at later timepoints.

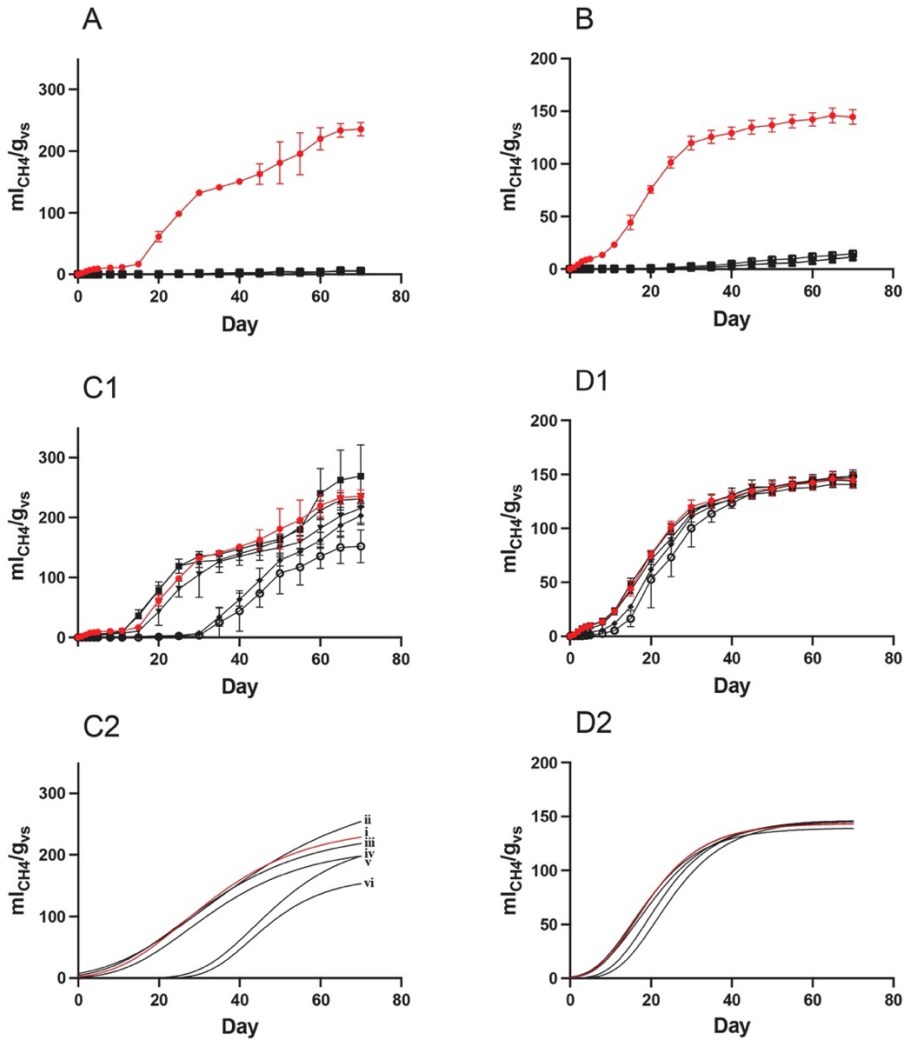


Fig. 5.1. Biomethane yields from *Euphorbia* biomass under inhibition with *Asparagopsis* and bromoethane sulfonate indicating partial and complete inhibition, respectively.
Panels **A** and **B** show biomethane production from rumen fluid and AD sludge, respectively, under BES inhibition. **C1** and **D1** show biomethane production from rumen fluid and AD sludge, respectively, under *Asparagopsis* inhibition. **C2**, and **D2** show Modified Gompertz models of best fit obtained from the data in **C1** and **D1**. The uninhibited control and *Asparagopsis* treatments of 0.5, 1, 2, 5, and 10% are indicated by ●, ■, ▲, ▼, ◆ and, ○ respectively, or by i, ii, iii, iv, v, and vi in **C2**. BES concentrations of 5, 10, and 20 mM are indicated by □, △, and ▽.

For *Asparagopsis*-inhibited conditions, biomethane production was sigmoidal at all treatment levels, and a Modified Gompertz model (**Fig. 5.1 C2, D2**) was accordingly fit to facilitate comparison of dose-response. With rumen fluid, methanogenesis appeared to respond in a dose-dependent fashion to *Asparagopsis* treatment. Negligible inhibition was observed at

doses of 0.5–2% (of substrate VS) *Asparagopsis*, with these curves broadly corresponding to the negative control. At the 10% inhibition level, theoretical maximum methane yields were notably reduced relative to the negative control (170 ± 10 vs. 250 ± 10 ml/gVS). However, it was in the lag phase that the inhibition phenomenon manifested itself most clearly; conditions treated with 5 and 10% *Asparagopsis* demonstrated a considerably extended lag phase, while also ultimately resuming a sigmoidal pattern of methane production. The Modified Gompertz parameter lambda (λ -Table 2) measures the lag phase prior to initiation of methane production and allows a standardised comparison of this observed inhibitory effect. In rumen-fed conditions fed 0–2% *Asparagopsis*, λ ranged from 7 to 11 days, while 5% and 10% doses saw lag phases of 30.3 and 32 days, respectively. Such a dramatic shift in lag phase was not registered in conditions inoculated with AD sludge, with lag increasing from 6.4 to just 11.6 days between the uninhibited control and 10% *Asparagopsis* treatment with this inoculum.

Table 5.2: Kinetic parameters derived from Modified Gompertz Models of methane production by AD sludge and rumen fluid at varying levels of *Asparagopsis* inhibition.

Inoculum	***A. taxiformis* dose**	**Model parameters**			**Model R^2**
		A (ml/gVS)	μ_m (ml/gVS/d)	λ (d)	
AD Sludge	Control	143 ±1	5.6 ±0.2	6.4 ±0.4	0.993
	0.5%	139.3 ±0.9	5.4 ±0.1	5.8 ±0.3	0.997
	1%	147 ±1	5.1 ±0.1	6.4 ±0.4	0.996
	2%	143.5 ±0.6	5.67 ±0.09	6.7 ±0.2	0.999
	5%	145 ±1	5.7 ±0.2	9.76 ±0.4	0.997
	10%	146 ±2	5.5 ±0.3	11.6 ±0.8	0.986
Rumen fluid	Control	250 ±10	5.4 ±0.3	9 ±1	0.974
	0.5%	310 ±30	4.8 ±0.3	8 ±2	0.934
	1%	240 ±10	4.8 ±0.3	7 ±1	0.965
	2%	210 ±10	4.7 ±0.4	11 ±2	0.949
	5%	230 ±10	6.2 ±0.3	**30.3 ±0.8**	0.987
	10%	170 ±10	5.7 ±0.7	**32 ±2**	0.938

A*- methane production potential, μ_m – maximum production rate, λ – lag phase.** BES-inhibited conditions were omitted as these failed to produce sigmoidal response data.

5.3.3. Response of VFA production to *Asparagopsis* and BES treatment

Fig. 5.2 details production of total volatile fatty acids (TVFA). Uninhibited conditions for both rumen fluid and AD sludge showed an initial spike in VFA concentrations, which then dropped as methanogenesis rose, ultimately converging to near zero. BES treated conditions in

both rumen fluid and AD sludge (**Fig. 5.2 A, B**) also saw a rapid initial acidification, with titres remaining at or near maximum concentrations for the duration of the experiment.

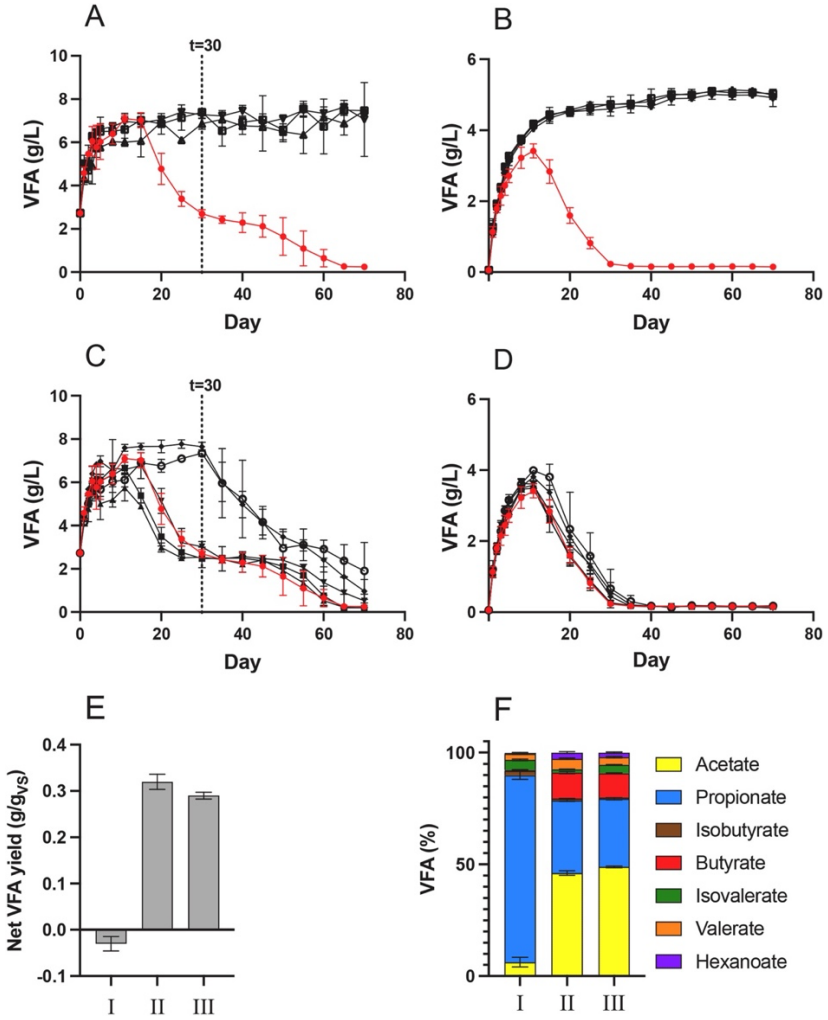


Fig. 5.2. Volatile fatty acid production from *Euphorbia* under treatment with *Asparagopsis* and bromoethane sulfonate to test the equivalence of these methanogenesis-inhibition strategies. Panels **A** and **B** show observed VFA titres in rumen fluid and AD sludge, respectively, treated with BES. **C** and **D** show VFA titres in rumen fluid and AD sludge, respectively, when treated with *Asparagopsis*. Panel **E** shows the VFA yield between days 0 and 30 in rumen fluid with no treatment (I), and treatments of 5% *Asparagopsis* (II) and 5 mM BES (III). Panel **F** gives the composition of VFA in these same treatment conditions at day 30. Uninhibited controls and *Asparagopsis* treatments of 0.5, 1, 2, 5, and 10% are indicated by ●, ■, ▲, ▼, ◆ and, ○ respectively. BES concentrations of 5, 10, and 20 mM are indicated by □, ◭, and ▽.

Rumen conditions treated with 0.5–2% *Asparagopsis* clustered with the uninhibited control (**Fig. 5.2C**). 5 and 10% *Asparagopsis*-inhibited rumen conditions maintained high concentrations to day 30 – corresponding to the lag phase (λ) seen in Gompertz models for these

conditions (**Table 5.2**). Beyond this point, VFA concentrations fell consistently for the remainder of the experiment. All *Asparagopsis*-treated AD sludge conditions (**Fig. 5.2D**) clustered with the uninhibited control.

As day 30 was the longest retention time at which *Asparagopsis*-treated rumen conditions behaved like those of BES, an analysis of both VFA yields and compositions is provided for this timepoint (**Fig. 5.2E and F**). VFA yields with 5% Asparagopsis and 5 mM BES were found to be equal, and both significantly higher than the uninhibited control. The composition of the VFA produced at this timepoint (**Fig. 5.2F**) is also similar, showing an acetic acid and propionic acid-rich fermentation, with smaller amounts of C4–C6 compounds. In the uninhibited control, a substantial reduction in C2 and C4 compounds can be seen - corresponding to the resumption of methanogenesis.

5.3.4 Microbial communities of initial inocula and community response to *Asparagopsis* treatment

The relative abundance of microbial communities (at phylum level) in the fresh inoculum sources is provided in **Table 5.3**.

Table 3: Phylum-level community structure of initial inocula and of rumen-fed conditions at day 25 (relative abundance - %). Selected microbial families seen to respond to *Asparagopsis* treatment are included under their respective phyla.

Phylum - Family	Sludge (t=0)	Rumen (t=0)	Rumen (t=25)	Rumen (t=25) +*Asparagopsis*
Firmicutes	69.58	60.56	59.53	45.53
- Lachnospiraceae	1.56	11.41	14.72	5.5
- Ruminococcaceae	0.34	13.82	15.01	5.02
- Veillonellaceae	N.D.	11.35	10.31	6.52
- Streptococcaceae	0.3	N.D.	0.52	13.67
Bacteroidetes	15.31	25.67	11.81	17.83
- Prevotellaceae	N.D.	13.65	0.15	0.77
Actinobacteria	0.53	7.23	5.27	4.91
Thermotogae	6.2	N.D.	N.D.	N.D.
Synergistetes	4.09	0.13	5.98	5.6
Proteobacteria	0.57	1.57	12.6	21.7
- Enterobacteriaceae	N.D.	0.06	10.58	16.79
Euryarchaeota	0.02	1.04	2.4	0.17
- Methanosarcinaceae	N.D.	N.D.	1.78	0.02
- Methanobacteriaceae	N.D.	1.04	0.61	0.06

Rumen reactor communities were also characterised at day 25 with and without *Asparagopsis* treatment at the maximum treatment level (10%). Among the firmicutes, the families *Lachnospiraceae, Ruminococcaceae*, and *Veillonellaceae* were depleted in treated conditions relative to the control, while *Streptococcaceae* were enriched. As expected, the methanogenic phylum *Euryarchaeota* was substantially depleted at day 25 between untreated and *Asparagopsis*-treated conditions.

5.4. Discussion

5.4.1. Efficacy of Asparagopsis as a methanogenesis inhibitor in rumen and AD sludge inocula

Asparagopsis was found to provide effective inhibition of methanogenesis at levels of 5% and 10% VS in rumen fluid up to day 30 but was not found to effectively inhibit methanogenesis in AD sludge at any of the concentrations tested (**Fig. 5.1, Table 5.2**). It should be noted that all conditions, whether inhibited or not demonstrated an initial lag phase in methane production of several days suggesting that early intervention to create antimethanogenic conditions could be an effective strategy for methanogenic control without explicit use of inhibitors. Reducing HRT may also be a feasible strategy to maintain low methanogen activity by exploiting their lower growth rates by flushing them from the reactor while still in lag phase. This may nonetheless periodically need to be stabilised, for which an exogenous inhibitor would be required. BES was included in this study as a positive control against which the inhibitory efficacy of *Asparagopsis* could be tested and was found to provide effective inhibition of methanogenesis at all concentrations tested, and in both inocula, to experiment termination on day 70 (**Fig. 5.1**). BES is a pure compound typically understood to inhibit the terminal step of methanogenesis through competitive inhibition of CoM (Liu et al., 2011). *Asparagopsis* conversely contains many known antimethanogenic compounds, though its antimethanogenic activity is generally attributed to its bromoform content (Machado et al., 2016b). Halomethanes, such as bromoform, have been reported to inhibit methanogenesis by reacting with key cofactors, such as vitamin B_{12} which is required for CoM-methyltransferase to catalyse methyl group transfer onto CoM (Glasson et al., 2022; Wood et al., 1968; Romero et al., 2023). They have also been shown to directly inhibit the terminal reduction step, in which this methyl group is then reductively released from CoM as CH_4, by binding the cofactor F430 (nickel tetrapyrrole) of MCR (Glasson et al., 2022; Romero et al., 2023).

The efficacy of *Asparagopsis* was clear in rumen fluid, but only a very slight shift in Gompertz lag phase was seen for biomethane production in AD sludge when treated with

10% *Asparagopsis* (from 6.4 to 11.6 days – **Table 5.2**). This suggests the minimum effective inhibitory dose of *Asparagopsis* to be much higher in AD sludge than rumen fluid – beyond the concentrations tested in this study. This observation has important practical ramifications for biorefinery application of *Asparagopsis*. It suggests that any use of *Asparagopsis* in sludge-driven systems would require a very large fraction of the substrate volatiles to be provided by *Asparagopsis* – shifting its role from inhibitor to co-substrate. Aside from the practical issues of needing to cultivate such large quantities of seaweed, on a process level too, its high ash content (**Table 5.1**) would also mean VFA yields would suffer on a TS basis, reducing reactor efficiency. Sludge-driven systems could circumvent this ash limitation by extracting bromoform for direct application, but this would entail additional process costs.

The minimum effective inhibitory concentration of *Asparagopsis* in rumen fluid this study was 5% of substrate VS. Machado et al. (2016a) and Kinley et al. (2016b) found *Asparagopsis* at 2% of substrate VS to be effective at inhibiting methanogenesis over short timescales in rumen fluid. This reduced potency might have arisen from differences in processing and storage. In this study, *Asparagopsis* was dried in the dark at ambient temperature. The dried, ground biomass was stored in the dark in a sealed container at ambient temperature (~21 °C). The biomass in Kinley et al. (2016b) was instead freeze-dried, and then stored at −20 °C. Tan et al. (2023) found the bromoform content of freeze-dried *Asparagopsis* powder to be temperature sensitive, finding bromoform levels to show good stability over 24 weeks at −20 °C and 4 °C, but that they depleted by approximately half at over this same timeframe, when stored at 25 °C.

In rumen fluid, the effect of *Asparagopsis* treatment began to abate after day 30. (**Fig. 5.2C**). Halomethanes, such as chloroform, are known to be anaerobically degradable (Cappelletti et al., 2012; Nijenhuis and Kuntze, 2016; van Beelen and van Keulen, 1990) and methanogens of the genus *Methanosarcina* have been demonstrated to effectively dehalogenate both chloroform and bromoform (Mikesell and Boyd, 1990). Metagenomic analyses (Table 3) confirmed the presence of the family *Methanosarcinaceae* in rumen-driven reactors. The existence of anaerobic mechanisms to degrade bromoform is relevant if *Asparagopsis* is to be considered for biorefinery applications requiring continuous dosing, as chronically exposed anaerobic microbiomes may acclimate to its presence. Under these conditions, enrichment of bromoform-degrading subpopulations, or of methanogenic species less susceptible to bromoform inhibition could effectively restore stable methanogenesis despite the presence of *Asparagopsis*.

5.4.2. Effect of Asparagopsis treatment on volatile fatty acid production and biorefinery

Volatile fatty acid titres in rumen conditions with *Asparagopsis* treatment showed a clear divergence between uninhibited controls and treatments of 5 and 10% *Asparagopsis* at retention times beyond 15 days (**Fig. 5.2C**). From t = 0 to t = 30 days, 5 and 10% *Asparagopsis*-treated rumen conditions demonstrated acidification profiles largely analogous to BES-treated rumen conditions (**Fig. 5.2A**), suggesting the appropriateness of *Asparagopsis* as an alternative to BES at retention times of ≤30 days. 5% *Asparagopsis* treatment and 5 mM BES treatment produced comparable VFA yields at day 30 (**Fig. 5.2E**). Moreover, the compositions of the VFA at t = 30 was found to be near identical between these conditions (**Fig. 5.2F**), further supporting the use of *Asparagopsis* as a BES-substitute.

Rumen fluid-driven AF is not commonly employed at industrial scale, though it has been successfully demonstrated at laboratory scale (Lazuka et al., 2015; Liang et al., 2022). Particular attention has been paid to the potential of rumen microbes to improve hydrolysis of recalcitrant lignocellulosic biomass (Meyer et al., 2022; Wang et al., 2018). While these lab-scale systems used BES as the antimethanogenic agent, given the above results, *Asparagopsis,* could conceivably be used in its place. At an industrial scale, the transient, ≤30-day inhibition provided by *Asparagopsis* could be used to establish initial control of the bioreactor, allowing for VFA accumulation, which can then provide sustained product-inhibition of methanogenesis. An alternative system could be envisioned based on the findings of Karekar and Ahring (2023). This paper suggested that a methanogenic (rumen) consortium could be supplemented with homoacetogens to compete for the hydrogen-scavenging function typically played by methanogens. One-time BES inhibition of the methanogens allowed homoacetogens to become established, whereafter they appeared to prevent the reestablishment of methanogenesis. Such a system could be envisioned at industrial scale but with *Asparagopsis* playing the role of transient inhibitor: establishing the system initially, and if required, periodically returning it to equilibrium if methanogens reappear. Halogenated hydrocarbons, such as bromoform, may however also modify the activity of microbial species other than methanogens, including homoacetogens (Liu et al., 2011), and this system would need to be experimentally validated to ensure that *Asparagopsis* does not also inhibit this key community member.

5.4.3. Interplay of Asparagopsis and rumen microbial community

It is necessary to acknowledge that the microbiome of any given bioreactor will depend not just on the initial inoculum, but also on the parameters under which the reactor is run.

Substrate composition, loading rates, pH, and the concentrations of degradation products such as VFA and ammonium will all affect community structure. Despite these caveats, AD sludge inoculum is taken here to provide a reasonable approximation of the microbiome of an industrial-scale AD plant. In this study, *Asparagopsis* was not found to provide significant methanogenesis inhibition in sludge-fed reactors. The most likely explanation is that the concentrations tested (up to 10% *Asparagopsis*), were below the minimum inhibitory concentration (MIC) for sludge. A slight shift in lag phase was registered at the 5 and 10% dose levels (**Table 5.2**), suggesting the MIC could lie just beyond this point.

Only methanogens of the family *Methanobacteriaceae* were detected in the initial rumen inoculum. At day 25, the untreated reactor was found to contain both both *Methanobacteriaceae* and *Methanosarcinaceae* and both methanogenic families were detected at low levels in *Asparagopsis*-treated samples. Treatment was found to significantly perturb other community members (**Table 5.3**).Perhaps the most noteworthy community level changes were among the firmicutes, where the families *Lachnospiraceae*, *Ruminococcaceae*, and *Veillonellaceae* were depleted in treated conditions, while *Streptococcaceae* were greatly enriched. *Lachnospiraceae* and *Ruminococcaceae* are hydrolytic, specialising in fibrolysis, or the degradation of the recalcitrant, structural components of lignocellulosic biomass (Biddle et al., 2013). These communities are also fermentative, producing VFAs - butyrate in particular (Vacca et al., 2020). Depletion of key fibrolytic/fermentative community members did not produce a reduced VFA yield as might be expected. However, the low lignin content of the *Euphorbia* substrate used in this study may have masked this effect. Testing with a higher-lignin biomass source should be done to determine whether *Asparagopsis* treatment interferes with the fibrolytic capacity of rumen fluid.

Veillonellaceae, which were slightly depleted, are known propionate producers (Kishimoto et al., 2006). Interestingly, Machado et al. (2016a) found *Asparagopsis* to increase the ratio of propionate to acetate over short timescales. Despite quite considerable shifts in community structure in *Asparagopsis* treated samples, VFA composition was nearly identical to that produced through BES inhibition, suggesting from an industrial perspective that these community level shifts are not of concern as VFA quality is equal to that produced through standard inhibitory processes. While the depletion of methanogens can most likely be attributed to bromoform, it is unknown whether this, or other compounds present in *Asparagopsis*, is responsible for these broader community-level perturbations. Further investigation would be required to determine this. Despite these considerable shifts in reactor community, at day

30 *Asparagopsis* produced inhibition in rumen fluid that was quantitatively and qualitatively equivalent to BES.

5.5. Conclusion

Asparagopsis was found to provide effective methanogenesis inhibition in rumen fluid at concentrations at or above 5% of substrate (VS-basis). Complete inhibition persisted to day 30, suggesting the suitability of *Asparagopsis* over timescales relevant for acidogenic fermentation. *Asparagopsis* was not found to provide effective inhibition of methanogenesis in AD sludge inoculum at the treatment levels tested. In rumen fluid, *Asparagopsis* produced VFA both of equal quantity and quality to reactors inhibited with bromoethane sulfonate. These results suggest *Asparagopsis* could find use as an alternative control agent in rumen-driven acidogenic reactor systems.

CRediT authorship contribution statement

Nicholas A. Tenci: Conceptualization, Data curation, Formal analysis, Investigation, Methodology, Validation, Visualization, Writing – original draft, Writing – review & editing.
Fariza Ammam: Conceptualization, Methodology, Writing – review & editing.
Nichola Austen: Data curation, Formal analysis, Writing – review & editing.
Wei E. Huang: Supervision.
Ian P. Thompson: Conceptualization, Project administration, Resources, Supervision, Writing – review & editing.

Declaration of competing interest

The authors declare the following financial interests/personal relationships which may be considered as potential competing interests:

Nicholas A. Tenci reports financial support was provided by Rotary International and East X LLP.

Acknowledgements

The authors would like to thank Prof. Chris K Reynolds and David Humphries (University of Reading) and Severn Trent Green Power (Cassington, Oxfordshire, UK) for providing the rumen fluid and AD sludge inocula, respectively. Nicholas A. Tenci would like to thank East X LLP. and Rotary International (Grant number: GG2128217) for their financial support of this research.

Data availability

Data will be made available on request.

References

Agnihotri, S., Yin, D.-M., Mahboubi, A., Sapmaz, T., Varjani, S., Qiao, W., KoseogluImer, D.Y., Taherzadeh, M.J., 2022. A glimpse of the world of volatile fatty acids production and application: a review. Bioengineered 13, 1249–1275.

Alibaba.com, 2023a. Eucheuma Cottonii Dried Seaweed from Vietnam Sea. (Accessed 11 October 2023).

Alibaba.com, 2023b. Wholesale High Quality Dried Sargassum Seaweed. (Accessed 11 October 2023).

Angelidaki, I., Sanders, W., 2004. Assessment of the anaerobic biodegradability of macropollutants. Rev. Environ. Sci. Biotechnol. 3, 117–129.

APHA, 1998. Standard Methods for the Examination of Water and Wastewater. American Water Works Association and Water Environment Federation.

Baleeiro, F.C.F., Kleinsteuber, S., Strauber, ¨ H., 2022. Recirculation of H2, CO2, and ethylene improves carbon fixation and carboxylate yields in anaerobic fermentation. ACS Sustain. Chem. Eng. 10, 4073–4081.

Biddle, A., Stewart, L., Blanchard, J., Leschine, S., 2013. Untangling the genetic basis of fibrolytic specialization by Lachnospiraceae and Ruminococcaceae in diverse gut communities. Diversity 5, 627–640.

Cappelletti, M., Frascari, D., Zannoni, D., Fedi, S., 2012. Microbial degradation of chloroform. Appl. Microbiol. Biotechnol. 96, 1395–1409.

Chidthaisong, A., Conrad, R., 2000. Specificity of chloroform, 2-bromoethanesulfonate and fluoroacetate to inhibit methanogenesis and other anaerobic processes in anoxic rice field soil. Soil Biol. Biochem. 32, 977–988.

Christophe, G., Lara Deo, J., Kumar, V., Nouaille, R., Fontanille, P., Larroche, C., 2012. Production of oils from acetic acid by the oleaginous yeast Cryptococcus curvatus. Appl. Biochem. Biotechnol. 167, 1270–1279.

Cotter, J., Glass, R., Black, J., Madden, P., Davidson, T., 2015. A marginal abatement cost analysis of practice options related to the NLMP program. Meat & Livestock Australia Limited.

Glasson, C.R.K., Kinley, R.D., de Nys, R., King, N., Adams, S.L., Packer, M.A., Svenson, J., Eason, C.T., Magnusson, M., 2022. Benefits and risks of including the bromoform containing

seaweed Asparagopsis in feed for the reduction of methane production from ruminants. Algal Res. 64, 102673.

Karekar, S.C., Ahring, B.K., 2023. Reducing methane production from rumen cultures by bioaugmentation with homoacetogenic bacteria. Biocatal. Agric. Biotechnol. 47, 102526.

Kinley, R.D., de Nys, R., Vucko, M.J., Machado, L., Tomkins, N.W., 2016a. The red macroalgae Asparagopsis taxiformis is a potent natural antimethanogenic that reduces methane production during in vitro fermentation with rumen fluid. Anim. Prod. Sci. 56, 282–289.

Kinley, R.D., Vucko, M.J., Machado, L., Tomkins, N.W., 2016b. In vitro evaluation of the antimethanogenic potency and effects on fermentation of individual and combinations of marine macroalgae. Am. J. Plant Sci. 7, 2038–2054.

Kishimoto, A., Ushida, K., Phillips, G.O., Ogasawara, T., Sasaki, Y., 2006. Identification of intestinal bacteria responsible for fermentation of gum Arabic in a pig model. Curr. Microbiol. 53, 173–177.

Krümpel, J., George, T., Gasston, B., Francis, G., Lemmer, A., 2020. Suitability of *Opuntia* ficus-indica (L) Mill. and Euphorbia tirucalli L. as energy crops for anaerobic digestion. J. Arid Environ. 174, 104047.

Lazuka, A., Auer, L., Bozonnet, S., Morgavi, D.P., O'Donohue, M., Hernandez-Raquet, G., 2015. Efficient anaerobic transformation of raw wheat straw by a robust cow rumenderived microbial consortium. Bioresour. Technol. 196, 241–249.

Li, X., Norman, H.C., Kinley, R.D., Laurence, M., Wilmot, M., Bender, H., de Nys, R., Tomkins, N., 2016. Asparagopsis taxiformis decreases enteric methane production from sheep. Anim. Prod. Sci. (58), 681–688.

Liang, J., Fang, W., Chang, J., Zhang, G., Ma, W., Nabi, M., Zubair, M., Zhang, R., Chen, L., Huang, J., Zhang, P., 2022. Long-term rumen microorganism fermentation of corn stover in vitro for volatile fatty acid prodution. Bioresour. Technol. 358, 127447.

Liu, H., Wang, J., Wang, A., Chen, J., 2011. Chemical inhibitors of methanogenesis and putative applications. Appl. Microbiol. Biotechnol. 89, 1333–1340.

Liu, Y., Whitman, W.B., 2008. Metabolic, phylogenetic, and ecological diversity of the methanogenic archaea. Ann. N. Y. Acad. Sci. 1125 (1), 171–189.

Lueangwattanapong, K., Ammam, F., Mason, P.M., Whitehead, C., McQueen-Mason, S.J., Gomez, L.D., Smith, A.C., Thompson, I.P., 2020. Anaerobic digestion of Crassulacean Acid Metabolism plants: exploring alternative feedstocks for semi-arid lands. Bioresour. Technol. 297, 122262.

Machado, L., Magnusson, M., Paul, N.A., de Nys, R., Tomkins, N., 2014. Effects of marine and freshwater macroalgae on in vitro total gas and methane production. PLoS One 9, e85289.

Machado, L., Magnusson, M., Paul, N.A., Kinley, R., de Nys, R., Tomkins, N., 2016a. Dose-response effects of Asparagopsis taxiformis and Oedogonium sp. on in vitro fermentation and methane production. J. Appl. Phycol. 28, 1443–1452.

Machado, L., Magnusson, M., Paul, N.A., Kinley, R., de Nys, R., Tomkins, N., 2016b. Identification of bioactives from the red seaweed Asparagopsis taxiformis that promote antimethanogenic activity in vitro. J. Appl. Phycol. 28, 3117–3126.

Machado, L., Tomkins, N., Magnusson, M., Midgley, D.J., de Nys, R., Rosewarne, C.P., 2018. In vitro response of rumen microbiota to the antimethanogenic red macroalga Asparagopsis taxiformis. Microb. Ecol. 75, 811–818.

Martin, L.K., Huang, W.E., Thompson, I.P., 2023. The effect of nutrient limitation on bacterial wax ester production. Bioresour. Technol. Rep. 22, 101423.

Mengmeng, C., Hong, C., Qingliang, Z., Shirley, S.N., Jie, R., 2009. Optimal production of polyhydroxyalkanoates (PHA) in activated sludge fed by volatile fatty acids (VFAs) generated from alkaline excess sludge fermentation. Bioresour. Technol. 100, 1399–1405.

Meyer, G., Okudoh, V., van Rensburg, E., 2022. A rumen based anaerobic digestion approach for lignocellulosic biomass using barley straw as feedstock. S. Afr. J. Chem. Eng. 41, 98–104.

Mikesell, M.D., Boyd, S.A., 1990. Dechlorination of chloroform by Methanosarcina strains. Appl. Environ. Microbiol. 56, 1198–1201. Nijenhuis, I., Kuntze, K., 2016. Anaerobic microbial dehalogenation of organohalides - state of the art and remediation strategies. Curr. Opin. Biotechnol. 38, 33–38.

Regal, A.L., Alves, V., Gomes, R., Matos, J., Bandarra, N.M., Afonso, C., Cardoso, C., 2020. Drying process, storage conditions, and time alter the biochemical composition and bioactivity of the anti-greenhouse seaweed Asparagopsis taxiformis. Eur. Food Res. Technol. 246, 781–793.

Richards, B.K., Cummings, R.J., White, T.E., Jewell, W.J., 1991. Methods for kinetic analysis of methane fermentation in high solids biomass digesters. Biomass Bioenergy 1, 65–73.

Romero, P., Belanche, A., Jim´enez, E., Hueso, R., Ramos-Morales, E., Salwen, J.K., Kebreab, E., Y´ anez-Ruiz, ˜ D.R., 2023. Rumen microbial degradation of bromoform from red seaweed (Asparagopsis taxiformis) and the impact on rumen fermentation and methanogenic archaea. J. Animal Sci. Biotechnol. 14, 133.

Roque, B.M., Venegas, M., Kinley, R.D., de Nys, R., Duarte, T.L., Yiang, X., Kebreab, E., 2021. Red seaweed (Asparagopsis taxiformis) supplementation reduces enteric methane by over 80 percent in beef steers. PLoS One 16, e0247820.

Shen, L., Hu, H., Ji, H., Cai, J., He, N., Li, Q., Wang, Y., 2014. Production of poly (hydroxybutyrate-hydroxyvalerate) from waste organics by the two-stage process: focus on the intermediate volatile fatty acids. Bioresour. Technol. 166, 194–200.

Shi, X., Lin, J., Zuo, J., Li, P., Li, X., Guo, X., 2017. Effects of free ammonia on volatile fatty acid accumulation and process performance in the anaerobic digestion of two typical bio-wastes. J. Environ. Sci. 55, 49–57.

Siegert, I., Banks, C., 2005. The effect of volatile fatty acid additions on the anaerobic digestion of cellulose and glucose in batch reactors. Process Biochem. 40, 3412–3418.

Tan, S., Harris, J., Roque, B.M., Askew, S., Kinley, R.D., 2023. Shelf-life stability of Asparagopsis bromoform in oil and freeze-dried powder. J. Appl. Phycol. 35, 291–299.

Tenci, N.A., Ammam, F., Huang, W.E., Thompson, I.P., 2023. Anaerobic co-digestion of Euphorbia tirucalli with pig blood for volatile fatty acid production. Bioresour. Technol. Rep. 21, 101333.

Vacca, M., Celano, G., Calabrese, F.M., Portincasa, P., Gobbetti, M., De Angelis, M., 2020. The controversial role of human gut Lachnospiraceae. Microorganisms 8, 573.

van Beelen, P., van Keulen, F., 1990. The kinetics of the degradation of chloroform and benzene in anaerobic sediment from the river Rhine. Hydrobiol. Bull. 24, 13–21.

van Soest, P.J., Robertson, J.B., Lewis, B.A., 1991. Methods for dietary fiber, neutral detergent fiber, and nonstarch polysaccharides in relation to animal nutrition. J. Dairy Sci. 74, 3583–3597.

Wang, K., Yin, J., Shen, D., Li, N., 2014. Anaerobic digestion of food waste for volatile fatty acids (VFAs) production with different types of inoculum: effect of pH. Bioresour. Technol. 161, 395–401.

Wang, S., Zhang, G., Zhang, P., Ma, X., Li, F., Zhang, H., Tao, X., Ye, J., Nabi, M., 2018. Rumen fluid fermentation for enhancement of hydrolysis and acidification of grass clipping. J. Environ. Manag. 220, 142–148.

Wood, J.M., Scott Kennedy, F., Wolfe, R.S., 1968. The reaction of multihalogenated hydrocarbons with free and bound reduced vitamin B12. Biochemistry 7, 1707–1713.

Yin, J., Yu, X., Zhang, Y., Shen, D., Wang, M., Long, Y., Chen, T., 2016. Enhancement of acidogenic fermentation for volatile fatty acid production from food waste: effect of redox potential and inoculum. Bioresour. Technol. 216, 996–1003.

Statement of Authorship for joint/multi-authored papers for PGR thesis

To appear at the end of each thesis chapter submitted as an article/paper

The statement shall describe the candidate's and co-authors' independent research contributions in the thesis publications. For each publication there should exist a complete statement that is to be filled out and signed by the candidate and supervisor **(only required where there isn't already a statement of contribution within the paper itself).**

Title of Paper	Red seaweed as an abundant, natural methanogenesis inhibitor for industrial biorefinery
Publication Status:	☒ Published ☐ Accepted for publication ☐ Submitted for publication ☐ Unpublished and unsubmitted work written in manuscript style
Publication Details:	Tenci, N. A., Ammam, F., Austen, N., Huang, W. E., & Thompson, I. P. (2024). Red seaweed as an abundant, natural methanogenesis inhibitor for industrial biorefinery. *Journal of Cleaner Production*, *454*, 142166.

Student Confirmation

Student Name:	*Nicholas A. Tenci*		
Contribution to the paper:	*Designed the study, performed the experiments, analysed the data, wrote the manuscript.*		
Signature: 		Date:	*11/09/2024*

Supervisor Confirmation

By signing the Statement of Authorship, you are certifying that the candidate made a substantial contribution to the publication, and that the description described above is accurate.

Supervisor name and title: *Prof. Ian P. Thompson*		
Supervisor comments: I agree with this summary.		
Signature: 	Date:	*17/09/2024*

This completed form should be included in the thesis, at the end of the relevant chapter.

Chapter 6. Zeolite treatment of acidogenic fermentates for accurate control of C:N ratio

Disclaimer

The following chapter presents unpublished data detailing the optimisation of a novel process for manipulating the C:N ratio of acidogenic fermentates. This chapter has accordingly been formatted as a conventional thesis chapter.

6.1 Introduction

As reviewed in **Section 2.3**, microbial storage lipids offer a promising path to produce high value industrially- relevant chemicals from low value, carbon-rich substrates. This section also reviewed the role of limitation of key nutrients, particularly nitrogen, in diverting carbon flux away from growth (biomass production) and toward the accumulation of intracellular lipid stores. The ability to induce nutrient limitation will thus heavily influence the efficiency of any industrial process targeting the production of storage lipids such as PHA. As covered in **Section 2.4**, many aluminosilicate minerals demonstrated an innate ability to reversibly bind cations, including the ammonium (NH_4^+) ion which represents the terminal form of nitrogen in most anaerobic fermentative processes and therefore the primary form of nitrogen in most acidogenic fermentates. Aluminosilicates thus offer a potentially low-cost route to induce nitrogen limitation in fermentates to allow for efficient microbial upgrading of the VFA therein to high-value industrial chemicals.

This chapter details the development of this digestate ammonium depletion method. The paper of Seruga et al. [152] was taken as the starting point for these experiments. This paper identified both bentonites and zeolites as effective sorbents for ammonium removal from wastewater, and as such these materials were selected for initial tests detailed in **Section 6.3.1**. The aims of this section are as follow:

Overall aim: To evaluate the capacity of zeolite to manipulate C:N ratios in acidogenic fermentate.

Specific aims:

1. To determine the efficacy of various aluminosilicates in removing ammonium from fermentates.
2. To determine the specificity of this binding interaction for ammonium nitrogen – i.e., to test whether zeolite also depleted the VFA carbon source.
3. To test the dose-response relationship between zeolite and ammonium concentration over time.
4. To identify whether this may be reconfigured into an in-line, chromatographic method for rapid ammonium depletion – that would be compatible with large-scale industrial processes.
5. To recover bound ammonium in a usable form.

6.2 Materials and Methods

6.2.1 Materials

Bentonite clay was obtained from Fisher Scientific, and zeolite (of natural origin) was purchased from Finest Aquatics Ltd. (United Kingdom). The zeolite was analysed by x-ray powder diffraction and found to consist mainly of clinoptilolite, with trace amounts of other phases (tridymite, stilbite). This analysis is detailed in the appendix to this chapter.

The acidogenic fermentate used as a test substrate was obtained from Dr. Fariza Ammam and was produced from acidogenic fermentation of Agave biomass, under conditions of methanogenesis inhibition using BES.

Artificial digestate used in chromatography experiments was produced by dissolving sodium acetate and ammonium chloride in deionized water to approximate the composition of a representative fermentate that might be produced from fermentation of biomass. Zeolites could then be tested for their ability to separate out these components.

Bentonite ceramic was made from hydrating, oven-drying and then firing bentonite clay at 1200^{o}C for 2 hours.

For binding experiments shown in **Fig. 6.1** alone, the bentonite ceramic and zeolite samples were ground in a pestle and mortar and passed through a 1 mm sieve to ensure consistent particle sizes (**Fig. 6.1 A-C**).

6.2.2 Methods

In all of the following methods for the quantification of soluble metabolites, samples were subjected to centrifugation at 15,500 xg for 10 minutes prior to analysis to obtain a clarified supernatant which was subsequently analysed.

Ammonium nitrogen (NH_4^+-N) was quantified using two different spectrophotometric methods. Initial experiments were performed with a kit-based assay, however the cost of these kits, combined with the number of samples produced in the following experiments rapidly rendered this method unsuitable. As such a separate method was obtained from publicly available protocols and used thereafter.

6.2.2.1 Quantification of ammonium nitrogen – Hach Lange LCK303

Samples were diluted in deionised water to a concentration of between 2 and 47 mg/L of ammonium nitrogen and the absolute concentration determined by analysis with Hach-Lange LCK 303 test cuvettes analysed using a DR2800 spectrophotometer.

6.2.2.2 Quantification of ammonium nitrogen – Salicylate method

Without detailing the specific reaction mechanisms, the following method quantifies ammonium through measurement of the absorbance (at 650 nm) of indophenol blue, produced by the reaction of ammonium with hypochlorite and salicylate. This method was based on the methods of [164, 165]. Sample processing and analysis were thereby miniaturised to be compatible with 96-well plate to facilitate high-throughput analysis of samples, using analytical reagents prepared as follows (per 100 mL):

Sodium hydroxide solution: 6 g sodium hydroxide
Salicylate solution: 6 g sodium salicylate, 5.6 sodium citrate dihydrate, 5 g sodium potassium tartrate tetrahydrate, 0.025 g sodium nitroprusside

A **Bleach solution** was prepared fresh before each analysis by combining 9.8 mL of sodium hydroxide solution with 0.2 mL 5% sodium hypochlorite solution.

For 96-well plate analysis, 20 µL of dilute sample, 90 µL of bleach solution, and 90 µL of salicylate solution were added to each well and pipetted to mix. Due to the light sensitivity of this reaction, samples were incubated in the dark for 50 minutes at ambient temperature before measurement of absorbance (650 nm) using a Tecan Spark plate reader (Tecan Group Ltd., Männedorf, Switzerland). Samples were quantified against an ammonium chloride standard curve.

6.2.2.3 Quantification of VFA and determination of carbon to nitrogen ratios

VFA concentrations were determined according to the standard GC-FID analysis method detailed in Chapters 3-5, and were quantified against standards.

Carbon to nitrogen ratios are given herein as mass ratios calculated from the ratio of TOC to TN as experimentally determined by the Hach-Lange analysis kits. TOC was quantified using the LCK 386 cuvette kit, and TN using the LCK 238 kit. In both cases analysis was

performed with a Hach Lange DR 2800 spectrophotometer. C:N mass ratios quoted in this chapter are calculated as TOC/TN.

6.2.2.4 Ammonium stripping experiments – Batch format

Experiments in **Figures 6.1 – 6.3** detail the depletion of ammonium in both digestate and an ammonium chloride solution by direct incubation with zeolite. These experiments were performed at 30 ºC with constant agitation at 125 rpm. Samples were either taken at t=0 and at endpoint as for 5.1, or over a time-course as in 5.2, and 5.3.

6.2.2.5 Statistical analyses

All data are presented as means ± standard deviations of triplicate measurements. All data analysis was performed in Microsoft Excel and GraphPad PRISM.

6.3 Results and discussion

6.3.1 Ammonium depletion with bentonite and zeolite

The following investigations took the paper of Seruga et al. [152] as a starting point. This study had identified both bentonite clay and zeolite as effective ammonium removal agents, and these provided the starting material for initial experiments into ammonium depletion. Bentonite is used extensively in ceramics, which suggested the possibility, if bentonite-based ceramics retained the ammonium-binding characteristics of bentonite clay, that ceramic components could be used in acidogenic reactors to strip ammonium. Examples of such might include ion exchange resins consisting of bentonite ceramic beads, or chromatography columns made from a porous bentonite ceramic stationary phase. To test this possibility, three materials were used in initial tests: raw bentonite clay, a bentonite ceramic and zeolite. These materials were incubated with each of an ammonium chloride solution, and an Agave fermentate according to method **6.2.2.4**, at a concentration of 10% w/v, and endpoint ammonium concentrations calculated, the results of which can be seen in **Fig. 6.1 D-I**. This figure details the endpoint concentrations achieved after three different incubation conditions. In these experiments, the solutions were incubated with 10% aluminosilicate either for 1 hour, 2 hours, or were subjected to 2x 1-hour treatments with 10 % aluminosilicate.

Both the bentonite clay and zeolite treatments exhibited ammonium depletion, while none of the treatments with bentonite ceramic showed effective depletion of ammonium. This suggests that firing the bentonite may result in a reduction of dimensionality or structure that

renders the end product unable to participate in ion-exchange reactions. It is possible that a lower firing temperature may allow ceramics to be produced which retain their binding capacity, but the efficacy of the other two materials suggest these offer simpler routes to deplete fermentate ammonium. In both bentonite clay and zeolite samples, ammonium depletion in ammonium solution was greater than in agave fermentate. As starting ammonium concentrations were equal, this may suggest the presence of either competitive binding interactions among ions present in the fermentate, or the effect of biofouling in which particulates within the fermentate may have clogged the microporous structure of the aluminosilicate, reducing its effective surface area. Determining the source of this interference – ionic or particulate, may be relevant for future systems in which the zeolite is to be reused, as biofouling may be cumulative and would need to be overcome lest it degrade the binding capacity of the zeolite over time.

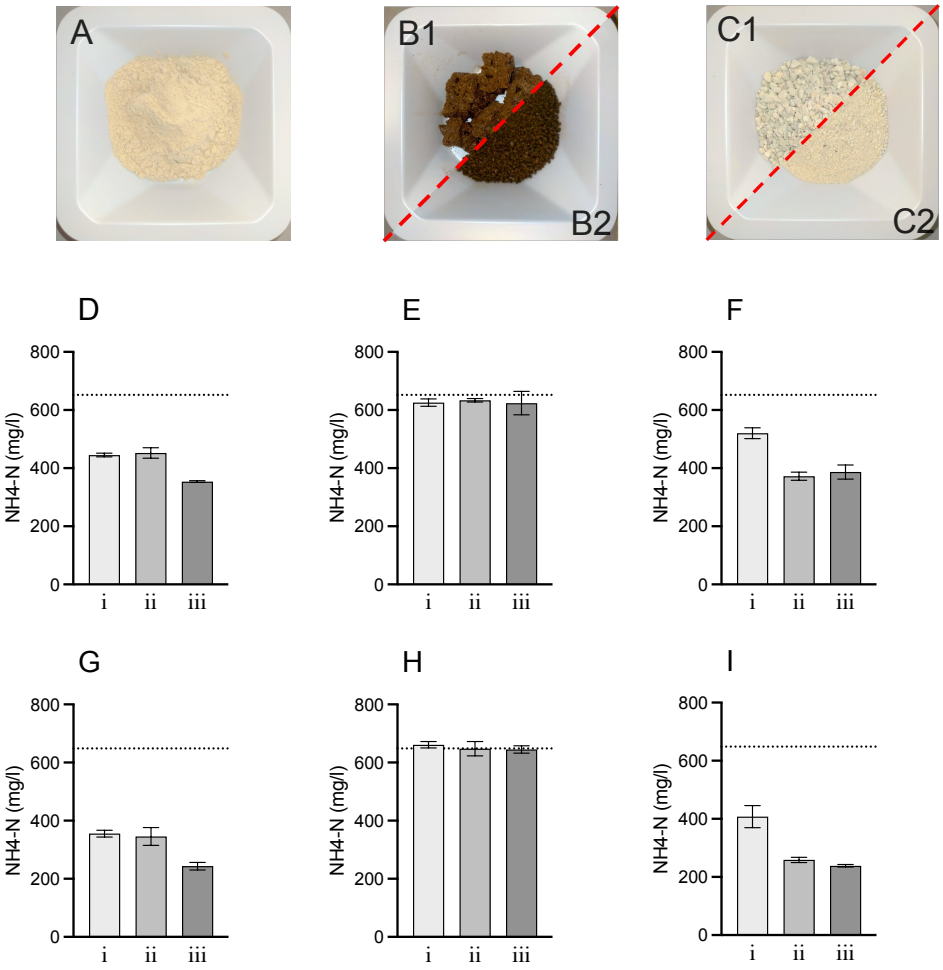


Figure 6.1: Testing of ammonium depletion by various aluminosilicates. The aluminosilicates tested, bentonite, a bentonite ceramic, and zeolite, are shown in Panels **A**, **B**, and **C**, respectively. Subpanels of **B** and **C** show the material before (**1**) and after (**2**) grinding and

homogenisation to the <1 mm particle size used in ammonium depletion experiments. An *Opuntia* digestate (**D**-**F**) and ammonium chloride solution (**G**-**I**) were treated with 10% (w/v) of each material for either 1 hour (**i**), 2 hours (**ii**), or were subjected twice to 1 hour treatment (**iii**). Post-treatment NH_4^+-N concentrations are shown as mean values of triplicate experiments with their corresponding standard deviations. The initial NH_4^+-N concentration (650 mg/L) is indicated by a dotted line.

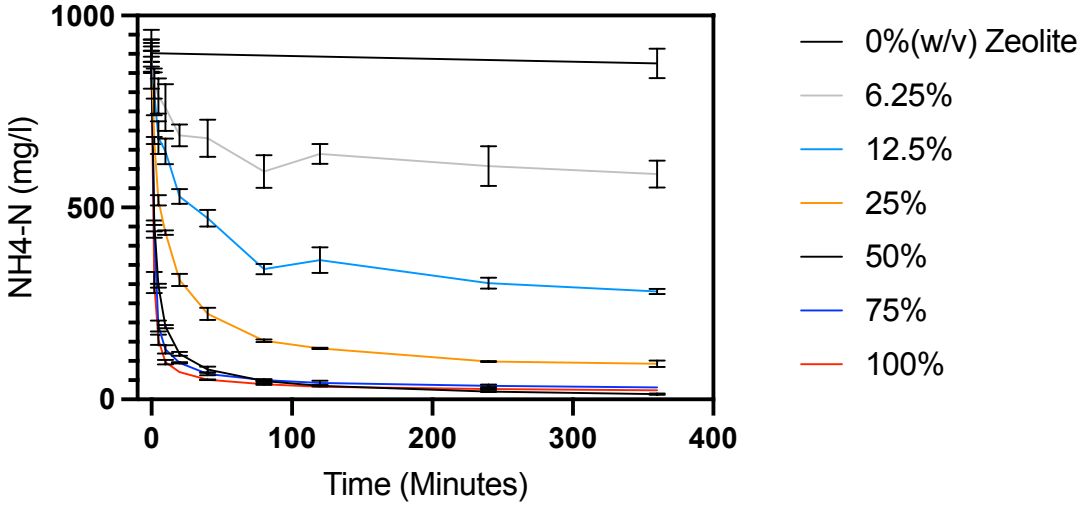
Ammonium levels showed little change when treated with bentonite clay for 2 hours, as opposed to 1 hour, though these did reduce with sequential 1-hour treatments with fresh bentonite. This indicates that the binding had run to completion within 1 hour, and that further reduction of ammonium required provision of fresh binding sites. This was not the case for zeolite, where longer incubation showed lower ammonium levels, apparently due to binding site saturation taking longer. This is possibly the result of the larger particle size of the zeolite requiring a longer time for diffusion of ammonium to saturate internal binding sites. Despite these differences, both materials showed comparable ammonium depletion capacities, with zeolite having the notable advantage over bentonite that its large, particulate nature makes it easy to separate from solution. This advantage made it the material of choice for further experiments.

6.3.2 Establishing the zeolite dose-response relationship and binding kinetics

While the capacity of zeolites to reduce fermentate ammonium concentrations was validated in **Fig. 6.1** a more detailed understanding of this binding interaction was needed to allow process calibration. Specifically, it was important to identify both the zeolite doses and timescales required to achieve levels of ammonium depletion sufficient to induce nutrient limitation responses in storage lipid accumulating microbes. To this end, a series of batch-format ammonium stripping test were run in agave digestate, for a period of 6 hours, with initial zeolite doses of 6.25, 12.5, 25, 50, 75 and 100% (w/v) zeolite. These were sampled at regular intervals and ammonium depletion monitored[5]. **Fig 6.2** shows the evolution of free ammonium concentrations in fermentates treated with each of the above zeolite doses. NH_4-N concentration curves at all concentrations show a rapid initial drop in concentration, and subsequent asymptotic convergence to an equilibrium concentration. At doses of 50, 75, and 100% (w/v) zeolite, curves approach zero, suggesting a surplus of zeolite binding sites relative to the ammonium substrate. This also indicates that zeolites can be used to achieve near complete

[5] By salicylate method (**6.2.2.2**)

depletion of ammonium in digestates, such as might be required if a very high C:N ratio were desired for a particular reactor configuration. At lower doses, this equilibrium point is reached at a non-zero concentration, indicating an excess of substrate. **Figure 6.2** calculates bound ammonium per gram of zeolite. Notably, at both 6.25 and 12.5 % treatments, approximately 4.9 mg of NH_4-N was calculated to have been immobilised per gram of zeolite. This suggests 4.9 mg/g to represent the upper limit of the binding capacity of this zeolite for ammonium under conditions of surplus substrate.



Treatment (% w/v zeolite)	(Δ mg/L)	Bound NH_4-N (mg/g $_{zeolite}$)
0	-	-
6.25	310 ± 40	4.9 ± 0.6
12.5	614 ± 7	4.91 ± 0.06
25	803 ± 9	3.21 ± 0.04
50	881 ± 2	1.76 ± 0.01
75	864.57 ± 0.06	1.15 ± 0.01
100	871.4 ± 0.3	0.87 ± 0.01

Figure 6.2: Zeolite-ammonium dose-response curves obtained from treatment of Agave digestates with various initial doses of zeolite over a six-hour time course.

6.3.3 Determining zeolite binding specificity and ability to manipulate C:N ratios

While zeolites were able to achieve considerable depletion of ammonium in Agave fermentates, the desired parameter is not an absolute reduction in ammonium nitrogen, but rather a depletion of nitrogen relative to the carbon present. It was thus important to test the

specificity of this binding interaction for the ion of interest, ammonium, and whether it had any adverse effect on VFA levels. **Figure 6.3A** depicts the treatment of Agave digestate for two hours with 25% zeolite, in which both ammonium and VFA concentrations are plotted at each timepoint. VFA concentrations were found to be unaffected by zeolite treatment, with no measurable shift in concentration over the two-hour treatment window, indicating the appropriateness of zeolite treatment for nitrogen depletion in media in which VFA is the carbon source. When considering the binding mechanism of zeolite, in which small, positively charged (typically metal) cations are reversibly exchanged, it is understandable that a fatty acid, being both physically large and carrying a negative charge, would not be bound and depleted.

The net effect of this zeolite specificity for the nitrogen source is an increase in C:N ratio, as was hypothesised. In **Fig. 6.3 B**, the samples of the 0, 25% and 50% zeolite treatments in **Fig. 6.2** were reanalysed for their total carbon and total nitrogen concentrations, and the C:N ratio of the medium at each timepoint accordingly calculated.

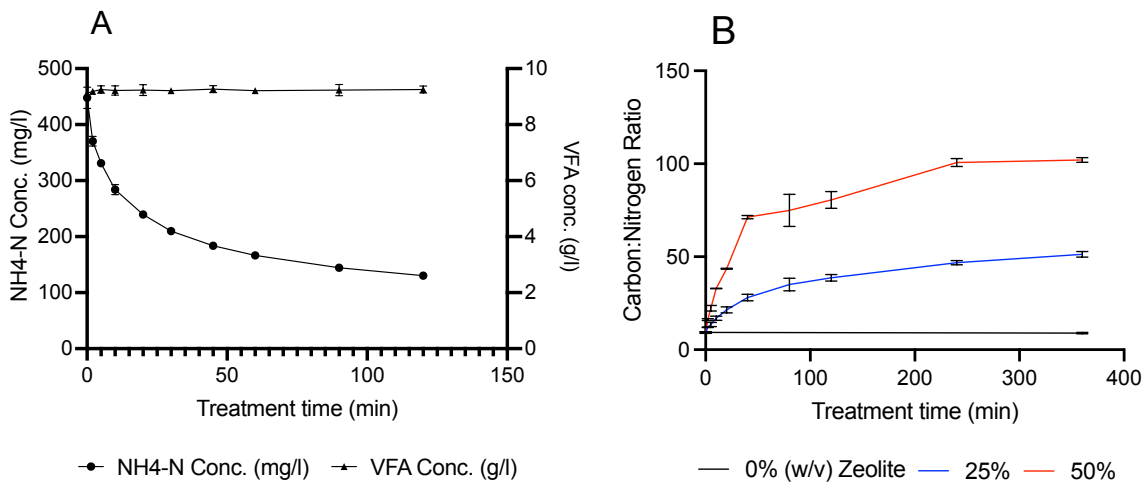


Figure 6.3: The specificity of zeolite for ammonium nitrogen and its ability to manipulate C:N ratios in digestates. Panel **A** gives the responses in NH_4^+-N and VFA concentrations in an Agave digestate treated for two hours with 25% (w/v) zeolite[6]. Panel **B** gives the responses of Agave digestate treated for six hours with various doses of 0, 25, and 50% (w/v) zeolite, in units of C:N mass ratios.

[6] By HACH method (5.2.2.1).

The C:N ratio of the untreated fermentate was 9.3 ±0.3, while the maximum C:N ratios achieved in 25% and 50% zeolite treatment conditions were 51 ±2 and 102 ±1, respectively. For context, Zhou et al. [166] found maximal PHB production on VFA by a mixed microbial culture at a C:N (molar) of 40 (i.e. a mass ratio of ~34), and Martin et al. [167] found optimal wax ester production by *Acinetobacter baylyi* ADP1 on acetic acid at a molar ratio of 80 (mass ratio of ~69). Thus, the 'optimal' C:N ratios identified by these authors are comfortably within the capacity of zeolite to deliver, with the even stronger treatments still available should a yet higher C:N be desirable (see **Fig. 6.2**).

6.4 Development and optimisation of a zeolite-chromatography process for in-line digestate treatment

Fig. 6.3 shows the remarkable capacity of zeolites to modify medium C:N ratios, however the batch format of the process is somewhat limited in its scalability for several reasons. Firstly, the process offers no simple way by which the ammonium bound to the zeolite can be removed and the medium refreshed to treat subsequent batches. Moreover, the high internal volume of the zeolite means that removal of the hydrated medium from the fermentate causes a loss of fermentate held within the zeolite's internal porous structure. The natural progression of this technology is to a zeolite-based chromatography system, in which the zeolite forms the stationary phase within an ion-exchange column, which will resolve the above issues. As seen through the biphasic binding curves in **Fig. 6.2**, the majority of the ammonium bound in each treatment was bound in the initial phase when both substrate and free binding sites were abundant. Accordingly, even with the short residence times of fermentate passing through a chromatography column, the majority of this binding efficiency should be achievable. To this end, such a system was constructed and is shown in **Fig. 6.4**.

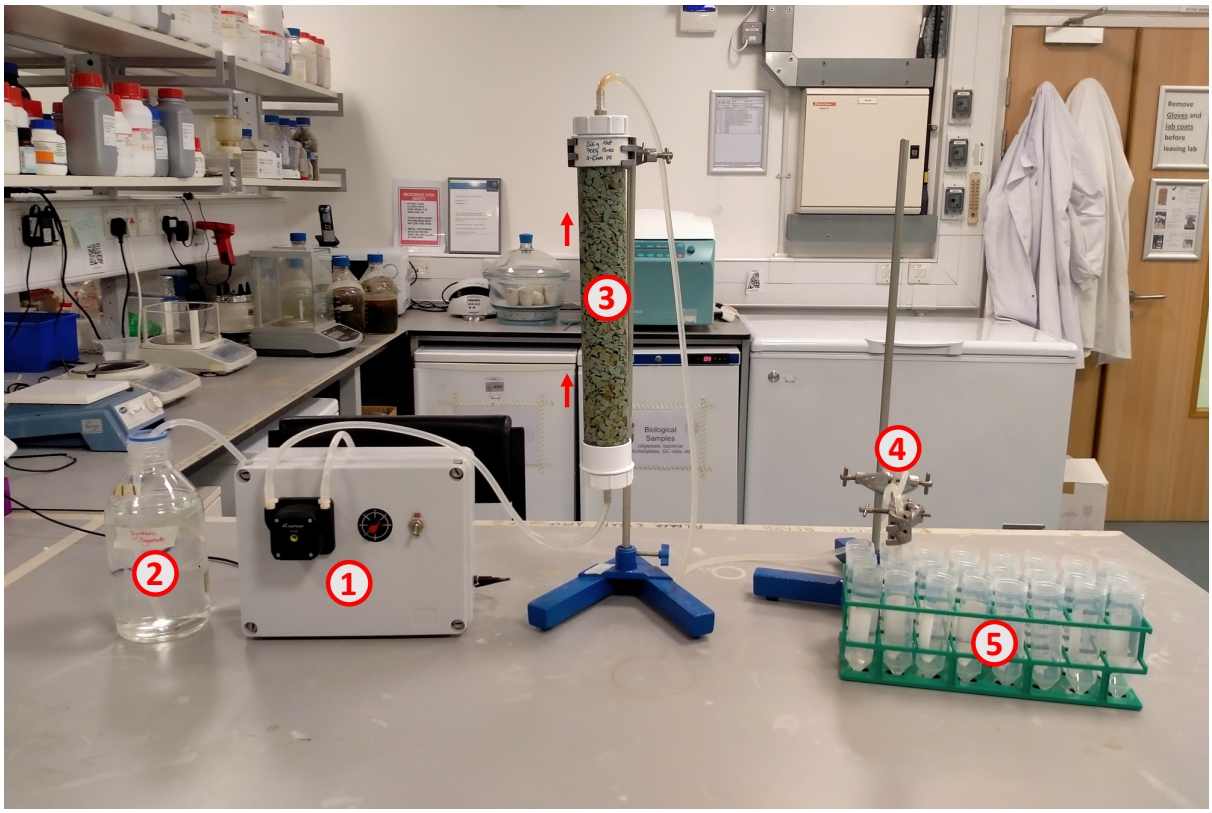


Figure 6.4: Layout of chromatography device constructed to test in-line zeolite separation of fatty acids from ammonium. This device was built around a 12V DC variable flow-rate peristaltic pump unit (1), which collected the mobile phase (2), and loaded it onto a zeolite-stationary phase chromatography column (3). The mobile phase eluted from the column at point (4) and was collected as 50 mL eluate fractions. Note that red arrows indicate direction of buffer flow through the column.

Given the large volumes required to test this system, a synthetic fermentate was used for analysis of this system to avoid consuming large quantities of CAM fermentate. The mobile phases used are as follow:

Synthetic fermentate (1L): Sodium acetate trihydrate 23.07 g, ammonium chloride 2.97 g

- This equates to a final concentration of 10 g/L acetate and 1 g/L ammonium.

Wash buffer: Deionised water

Elution buffer (1L): 58.44 (or 292.2)[7] g sodium chloride

[7] Corresponding to 1 M and 5 M NaCl solutions, as used in **Fig. 5.4.2**.

The chromatography system was run by feeding 1 L of synthetic digestate, followed by 1 L of wash buffer to flush residual fermentate from the system without introducing contaminating ions. An elution buffer of 1M NaCl was then flushed through the system to elute bound ammonium from the zeolite stationary phase. Subsequent flushing with wash buffer serves to remove residual NaCl from the system prior to repetition of the binding phase. **Fig. 6.5** shows the results of two sequential binding and elution runs from the system. VFA (blue) can be seen to pass through the system without any notable interaction with the stationary phase, while ammonium is retained on the stationary phase and eluted during the elution step. Note that the influent ammonium concentration was 1 g/L (or 780 mg/L NH_4-N), while digestate ammonium concentrations in the effluent did not exceed 500 mg/L, suggesting effective nitrogen depletion.

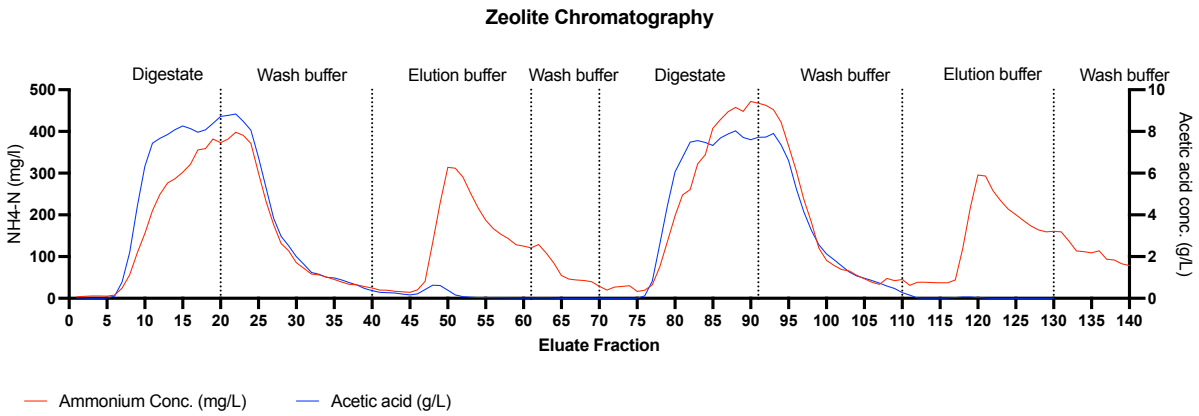


Figure 6.5: Proof of concept - Zeolite chromatograms indicating efficacy of in-line zeolite treatment. Note that elution step 1 was performed with an eluent of 1M (58.44 g/L) NaCl, while elution step 2 was performed with 5M (292.20 g/L) NaCl.

The ammonium elution peak can be seen to exhibit a ‘tail’, indicative of inefficient dissociation. An attempt to sharpen this elution peak was made by increasing the strength of the elution buffer by 5x, (elution peak 2), but this did not resolve the issue. The observation however that concentration was not the limiting factor suggest that efficient elution could be achieved at eluent concentrations below 1M. It is possible that the tailing phenomenon observed is a result of the large particle size of the zeolite medium, as it may take time for eluent to diffuse in, and ammonium to diffuse out of the interior of the zeolite particles. Optimisation of these elution dynamics lies somewhat beyond the core focus of this work, and as such this process was not investigated further.

6.5 Recovery of bound ammonium as fertiliser

One further area of the elution dynamics which was briefly investigated was the possibility of recovering the bound ammonium in a usable form. The use of sodium chloride as the eluent salt has the obvious benefit in that seawater may be used and this cheap eluent proved effective at recharging the binding capacity of the zeolite stationary phase, however the ammonium was eluted as a mixture of ammonium chloride contaminated with sodium chloride brine.

Fully realising the 'biorefinery concept' means recovering, as much as possible, every usable fraction of the biomass, and the ammonium here is no exception. Ammonium sees considerable use as a fertiliser (as ammonium nitrate, ammonium sulphate, ammonium phosphate and others). Recovery of the zeolite-bound ammonium in one of these forms could allow for its direct use as a fertiliser. By changing the anion of the eluent salt from chloride to phosphate, bound ammonium would be eluted as ammonium phosphate – a fertiliser. This however still leaves the issue of sodium contamination from surplus eluent cation. The use of potassium phosphate in place of sodium chloride as the eluent would elute a mixture of nitrogen, phosphorus, and potassium (N-P-K) that might be usable, and marketable as a fertiliser. The non-coincidental etymological origin of the word potassium from 'potash' (or biomass ash) raises one more possibility to recover a fraction of the biomass heretofore unused – the undigested, inorganic, solid fraction of the biomass not consumed in fermentation. Incinerating the non-digested fraction of the biomass could liberate its potassium-rich inorganics, which when acidified with phosphoric acid could produce potassium phosphate. This would not provide a pure source of potassium and it might be expected that considerable quantity of other ions would also be present, including Ca^{2+}, and Na^{+} [168]. Caution would also need to be exercised to avoid the precipitation of struvite-type compounds such as magnesium potassium phosphate and magnesium ammonium phosphate, given the likely presence of Mg^{2+} ions in solution [169]. When used to elute the bound ammonium from the zeolite column these cations would then be recovered as fertiliser. A flow-diagram showing this full proposed biorefinery cycle is given in **Fig. 6.6**.

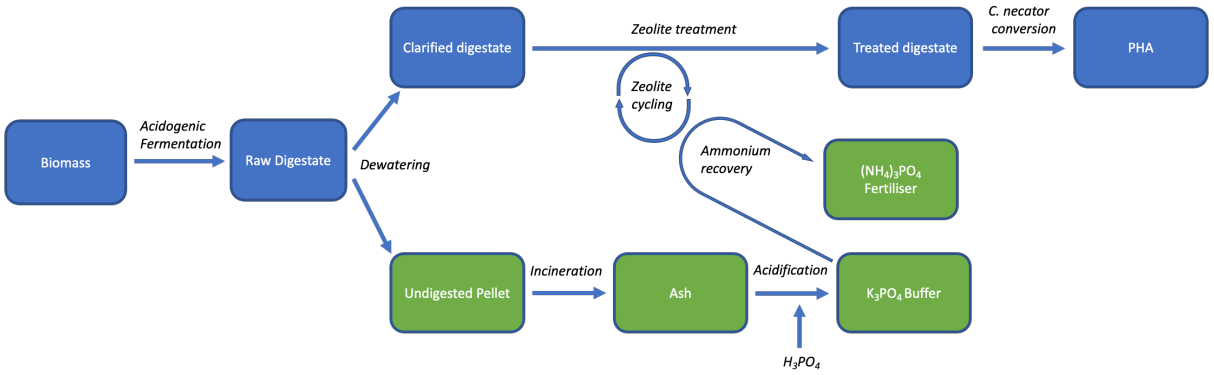
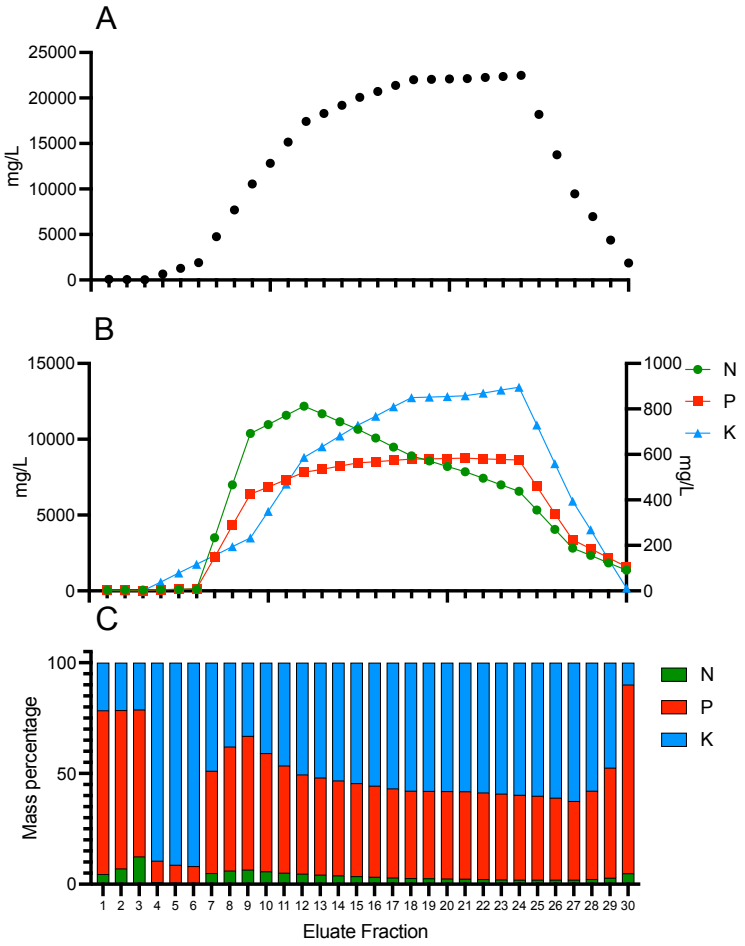


Figure 6.6: Process schematic including potential recovery of zeolite-bound ammonium as N-P-K fertiliser

An attempt was made to demonstrate this concept by eluting bound ammonium using potassium phosphate. The zeolite column was equilibrated with 1L of synthetic fermentate to bind ammonium to the column and washed with 1L of deionised water to flush residual fermentate from the system. The elution step was subsequently performed using 0.25 M of pH 7.0 potassium phosphate (providing 0.5 M of K^+) ions and the results of this elution are shown in **Fig. 6.7**. This figure shows the absolute concentrations of the key nutrients in panels **A** and **B** (nitrogen, phosphorus, and potassium), while panel **C** gives the mass percentage nutrient composition (N-P-K %) of each eluate fraction. Among the eluate fractions within the main elution peak (from fraction 7 onwards), nitrogen concentrations peak in fraction 9 at a mass percentage of just 6.6% of total nutrients (N-P-K of 6.6 - 70.4 - 33.1). This fraction also shows the lowest potassium concentration among these key fractions, demonstrating the exchange of potassium onto the column as nitrogen is released. The nutrient content, and therefore N-P-K of all eluent fractions, is dominated by the phosphorus and potassium of the eluent salt, resulting in a low nitrogen concentration. This is due to two factors, first of these is the excessively high concentration of eluent cation, which despite being halved from the 1M concentration tested in **Fig 6.7**, appears still to be well in excess of what is necessary. The poor resolution of the ammonium elution peak is also a major issue (visible in the nitrogen curve in **Fig. 6.7 B**), as this results in the ammonium being eluted gradually over many eluate fractions, resulting in a large volume of eluate dominated by the elution salt. While the results in **Fig. 6.7** provide an interesting initial proof of concept, these two issues need to be resolved before ammonium fertiliser recovery from a zeolite column would be feasible. Again, as these optimisations lay somewhat beyond the key focus of this thesis, they were not explored further, but are discussed in more detail in the future work section of this chapter.



Eluate fraction	Total Nutrient conc. (mg/L)	N:P:K (% g/g)
1	72	4.5: 73.9: 21.5
4	651	0.8: 9.7: 89.5
7	4762	4.9: 46.2: 48.9
10	12827	5.7: 53.4: 40.9
13	18298	4.3: 43.8: 51.9
16	20715	3.2: 41.1: 55.6
19	22058	2.6: 39.5: 57.9
22	22252	2.2: 39.1: 58.6
25	18192	2.0: 37.9: 60.2
28	6961	2.2: 39.9: 57.8

Figure 6.7: Elution of zeolite-bound ammonium using potassium phosphate. **A**) Elution peak indicating total eluted nutrients (calculated as sum of nitrogen, potassium, and phosphate), **B**) Elution profiles of individual key nutrients (NH_4^+-N, $PO4^{-3}$-P, K^+), with nitrogen shown on the right axis, **C**) Mass percentages of each key nutrient giving the nutrient profiles of each eluate fraction. These composition of these eluate fractions is summarised in the attached table.

6.6 Conclusion and future directions

Clinoptilolite zeolite was found in this chapter to provide effective depletion of ammonium nitrogen in acidogenic fermentates at levels theoretically sufficient to induce storage lipid accumulation. It was shown moreover, to not negatively affect the levels of VFA, thus nitrogen depletion corresponded with an increase in C:N ratio. Under the conditions tested, zeolite showed a maximum binding efficiency of 4.91 ±0.06 mg of NH_4-N per gram of zeolite in fermentate, several fold lower than literature values such as in Ji et al. [170] for clinoptilolite-zeolite in wastewater, which report capacities over 25 mg/g (NH_4^+). A discrepancy in binding affinity was also observed in **Fig. 6.1** in which zeolite showed a higher binding capacity in an ammonium chloride solution than in fermentate. The basis of these two discrepancies should be investigated as it may arise from the specific structure of the zeolite used, from interference of competing ions in the fermentate, or from blockage of the microporous structure of the zeolites by particulates within the fermentate. Optimising conditions to increase the binding capacity of the zeolite would yield considerable advantages in terms of smaller column sizes, lower system volumes, and tighter elution kinetics. The reusability of the zeolite also needs to be determined, i.e., whether binding capacity degrades over repeated use and whether, if such a degradation is observed, treatments can be devised to revive it.

Zeolite chromatography was demonstrated in principle but requires considerable optimisation before it can be used either to effectively strip nitrogen from fermentates, or to recover ammonium efficiently. The elution of NPK fertiliser was demonstrated as a possible exemplar of ammonium recovery from this process configuration, but the elution dynamics need to be optimised before this can be considered an efficient process. It is possible that reducing the particle size of the zeolite medium could allow for cleaner association/ dissociation of ammonium to the medium by minimising diffusion times required for the mobile phase to access the interior of zeolite particles. Various zeolites with different microporous structures may also show different elution dynamics and allow rapid elution of ammonium as a concentrated solution, rather than gradual dissociation and elution seen in **Fig. 6.5** and **6.7B** Having optimised this, it would then be valuable to identify the lowest concentration of eluent ion, whether potassium or another ion, required to achieve clean elution and medium regeneration.

As suggested, the undigested solid fraction removed from the AF process, enriched as it is in inorganics, may itself offer a source of cations that could be used to produce this eluent.

This would require a series of experiments to determine the composition of ashes generated from incineration at various temperatures, and of the salt solutions generated when resuspended according to different protocols. Whether this could offer an economic source of potassium or other ions for use in this role remains to be seen but is perhaps worth consideration, as the inorganic fraction of biomass subjected to AF/AD is rarely valorised.

Chapter 7. A two-stage biorefinery for renewable industrial chemical production

Disclaimer

The following chapter presents a range of experiments to test the effect of zeolite treatment of acidogenic fermentates on the microbial production of polyhydroxyalkanoates in microbial pure cultures. It contains both a draft manuscript, intended for future publication, and the results of several other supporting experiments, which are presented in standard thesis format.

The chapter is divided into **Section 7.1**, containing the draft manuscript and **Section 7.2**, containing experimental results not intended for publication, but pertaining to the same experimental question of PHA production on zeolite-treated fermentates.

The bioproduction process detailed herein, and supported by the evidence in this chapter is the subject of a patent filed on 09/04/2024, under application number 2405054.4 (Patent application provided in the appendix to this chapter).

Section 7.1 – Manuscript "A two-stage bioreactor for renewable industrial chemical production"

Authors: Nicholas A. Tenci, Laura K. Martin, Wei E. Huang, Ian P. Thompson

Abstract

A novel process is proposed allowing for the direct bioproduction of polyhydroxyalkanoate (PHA) bioplastics on VFA-rich acidogenic fermentates. A low-cost, zeolite-based treatment of fermentate provided controlled depletion of ammonium, producing the high carbon to nitrogen (C:N) ratios known to be optimal for efficient microbial PHA production. *Pseudomonas putida* KT2440 was grown on fermentates treated to various C:N ratios, and a ratio of 43 was found to increase PHA titres over threefold from 80 ±10 to 270 ±20 mg/L ($p<0.0001$) and to increase yields four-fold from 10.0 ±0.8 to 40 ±7 % of cell dry weight ($p<0.0001$). This novel two-step process, which links acidogenic fermentation to PHA accumulation through controlled zeolite-treatment, could potentially render a wide range of low-cost, heterogeneous waste feedstocks suitable for highly optimized PHA production, significantly reducing the cost of renewable plastics. The universality of the underlying principle of nitrogen limitation to many hundreds of species of PHA and microbial storage lipid accumulators suggests it might have wide applicability beyond the scope of PHA production in *P. putida*.

7.1.2 Introduction

Microbial storage lipids (MSLs) are a broad class of energy storage molecules accumulated by microbes when the limitation of essential nutrients, especially nitrogen, precludes the growth of biomass. MSLs may take various forms, including wax esters and triacylglycerides (Martin et al., 2023), oils (Christophe et al., 2012) and polyhydroxyalkanoates (Mengmeng et al., 2009). They are of great economic relevance due to their similarity to many products conventionally derived from petrochemicals, for which they may provide renewable alternatives (Martin et al., 2023; Sabapathy et al., 2020). The substitution of conventional petrochemicals and petrochemical-derived products with MSL alternatives offers myriad benefits. MSL can be produced through microbial synthesis from biological carbon sources, meaning they have the potential to be carbon neutral. They are also typically biodegradable,

such that they do not accumulate in the environment as do their conventional fossil fuel-derived alternatives.

One particularly industrially important class of MSLs is the polyhydroxyalkanoates: polyesters of hydroxyalkanoic acid monomers which are accumulated by various microbial species as hydrophobic, intracellular granules (Alves et al., 2023). These are of interest for their similarity to many of the most widely used plastics, including low-density polyethylene, polypropylene (Dartiailh et al., 2021), and polystyrene. PHA polymers may be constituted from a range of around 150 monomers, yielding plastics with various and customizable chemical, thermal, and mechanical properties. The specific PHA composition will depend on the microbial species in question, the carbon sources available, and on the pathways through which these are metabolized (Dartiailh et al., 2021). Much work to date has focused on polyhydroxybutyrate (PHB), a short-chain PHA polymer consisting of four-carbon (3-hydroxybutyric acid) monomers, and to its accumulation by *Cupriavidus necator*, a metabolically flexible bacterium capable of accumulating over 80% of its cell weight as PHB (Zhang et al., 2022; Passanha et al., 2013). PHB is highly crystalline and brittle, however, rendering it poorly suited for many industrial applications. The medium chain PHAs produced by species such as *Pseudomonas putida*, which occur mainly as copolymers of 6-14 carbon monomers, provide plastics far more amenable to industrial use (Dartiailh et al., 2021).

Despite the many benefits offered by PHAs over their conventional plastic counterparts, their deployment is hampered by their high cost. Substrates constitute a large fraction of this cost (Choi & Lee, 1997), and considerable effort has gone into identifying cheaper carbon sources, such as from the waste streams and byproducts of existing industrial processes (Dalsasso et al., 2019; Passanha et al., 2013; Penkhrue et al., 2020). Among these alternative feedstocks, volatile fatty acids (VFAs) stand out for their extremely low cost, and *P. putida* has demonstrated an ability to accumulate PHA using VFA as a substrate (Dartiailh et al., 2021), as have other species (Jia et al., 2013; Passanha et al., 2013). The attractiveness of VFAs is due to their ability to be derived from essentially any biomass source, including dedicated agricultural crops (Tenci et al., 2023), food and agricultural waste (Eryildiz et al., 2020; Wang et al., 2014), meat industry waste (Tenci et al., 2023), or sewage sludge (Yuan et al., 2011), through the process of acidogenic fermentation. Acidogenic fermentation is the anaerobic decomposition of biomass to produce fatty acids. However, this process also degrades proteins present in the biomass, which releases the nitrogen therein as ammonium. Without separation of the VFA from the ammonium, the essential conditions for PHA accumulation - namely the condition of

nutrient limitation – are not present, and microbes will prioritize growth over PHA production. This concept can be expressed as the carbon to nitrogen (C:N) ratio of the medium. At low C:N, microbes will favour growth, whereas at higher C:N PHA production will be favoured. Separation of carbon and nitrogen sources could be achieved through extraction of the VFAs from the fermentate, but this would impose additional process costs, negating the cost benefits offered by VFA (Pinto et al., 2023). This study therefore validated a low-cost alternative process using zeolite sorbents.

Zeolites are a broad class of microporous aluminosilicate minerals with an inherent ability to participate in ion-exchange reactions (Hedström, 2001). While the ions in question are usually metal cations, zeolites may also reversibly bind ammonium (NH_4^+) ions. This work demonstrates that zeolites may be used to deplete ammonium in acidogenic fermentate and thereby increase the C:N ratio in a controlled fashion. *P. putida* grown on variously zeolite-treated fermentate media showed a marked increase in PHA production (>3-fold) between untreated and zeolite treated media, suggesting that this novel zeolite process could represent a low-cost solution to allow for direct bioproduction of PHA bioplastics in acidogenic fermentates. Given the wide range of carbon sources available for acidogenic fermentation, and the hundreds of known species able to accumulate PHA and other MSLs on fatty acids, this process could have wide-ranging implications for the deployment of cheap and renewable MSL alternatives to conventional industrial and commercial products.

7.1.3 Methods

7.1.3.1 Materials

Fresh *Opuntia ficus indica* (OFI) cladodes were obtained from Pepe Aromas Lda. (Azaruja, Portugal). These were oven dried at 80 ºC, ground in a blender (Waring, USA) and screened through a 1 mm sieve to ensure consistent particle size.

Anaerobic digestion sludge was obtained from an industrial AD facility processing municipal food waste (Severn Trent Green Energy, Cassington, UK).

All experimental reagents were purchased from Sigma-Aldrich (Merck Life Science, United Kingdom). The 3-hydroxyalkanoic acid standards used for quantification of PHA monomers were obtained from Sigma-Aldrich, Manchester Organics Ltd. (Runcorn, United Kingdom), and Tokyo Chemical Industry Europe N.V. (Zwijndrecht, Belgium).

Natural clinoptilolite zeolite was purchased from Finest Filters (Finest Aquatics Ltd., United Kingdom).

7.1.3.2 Preparation of sodium-zeolite

Zeolite was equilibrated 1:1 (w:v) in 1M NaCl solution overnight to saturate binding sites with Na^+ and then serially washed in excess deionized water (4x) to remove excess NaCl.

Zeolite was oven dried at 80 ºC before use in subsequent experiments.

7.1.3.3 Preparation of VFA-rich fermentate

VFA-rich fermentate was prepared by acidogenic fermentation of OFI biomass substrate with AD sludge inoculum. Fermentations were performed with 2 L working volumes and concentration of 30 gVS/L OFI and 5 gVS/L AD sludge. The liquid phase consisted of a medium solution prepared as per the recommendations of Angelidaki and Sanders (2004), with the omission of sodium sulphide. Methanogenesis was inhibited by addition of 10 mM 2-bromoethane sulfonate. The headspace gas was not purged to remove excess oxygen. The headspace was kept anaerobic by means of a fermentation airlock, which permitted egress of surplus biogas, while isolating the system from ambient oxygen. Fermentations were incubated at 37 ºC with agitation at 125 rpm for 12 days, whereupon fermentation was arrested by freezing the cultures at -20 ºC.

7.1.3.4 Preparation of fermentate growth medium

The OFI fermentate was initially clarified by centrifugation at 2000 xg for 10 minutes and the supernatant collected. This was divided into two separate batches, of which one underwent zeolite treatment. The 'treated' fermentate was treated by incubation with 60% (w/v) of sodium-zeolite for two hours at 30 ºC, with agitation at 125 rpm.

The pH of both treated and untreated fermentates was then adjusted to 7.0, and the two batches were autoclaved to induce precipitation. These batches were clarified by centrifugation at 15,500 xg for 15 minutes, the supernatant collected, and the pH again adjusted to 7.0. These were again clarified by centrifugation (15,500 xg for 15 minutes) to remove precipitates arising from pH adjustment. These batches (treated and untreated) were then chemically characterized for their organic acid, total carbon, and total nitrogen composition (see: Analytical methods), and the C:N ratio of the two media was thereby determined.

Microbial growth medium was prepared by diluting the clarified digestates 1:3 with deionized water. For subsequent bioproduction experiments, the untreated fermentate provided the negative control. Various C:N ratios (i.e., the treatment groups) were obtained by blending the untreated and treated batches at different ratios, the highest C/N treatment group was provided by pure treated medium. Given a VFA concentration of ~11.5 g/L in the fermentate (as per Hach Lange organic acid kits in **Section 7.1.3.5**), this dilution method gave a medium

concentration of <3 g/L. This quantification method was preferred over GC-FID quantification during media preparation, as its speed permitted rapid quantification and standardisation of VFA concentrations between treatment conditions. 50 mL volumes of these media were aliquoted into 250 ml Erlenmeyer flasks, sealed with foil and autoclaved to achieve sterility.

7.1.3.4 *Pseudomonas putida* growth time-courses

Cultures of *Pseudomonas putida* KT2440 were prepared in triplicate, with individual colonies taken to represent independent biological replicates. These colonies were used to inoculate initial precultures of 5 mL lysogeny broth, which were incubated overnight. Secondary and tertiary 50 mL precultures were prepared in 250 mL Erlenmeyer flasks, the former consisting of 50% lysogeny broth, 25% OFI fermentate and 25% deionized water, and the latter of 25% OFI fermentate in 75% deionized water. All precultures were incubated at 37 ^{o}C, 125 rpm for ~12 hours. The pellets from these final precultures were obtained by centrifugation at 15,500 xg for 10 minutes, flushed with sterile PBS and used to inoculate the experimental flasks to an initial OD_{600} of 0.1. This additional PBS resuspension step was deemed to provide more precise control of initial OD_{600}. These cultures were incubated at 37 ^{o}C and 125 rpm.

P. putida cultures were sampled at 6-hour intervals and the OD_{600} determined. Once the culture OD_{600} reached 0.5, additional 5 mL samples were taken to measure PHA production. The pellet from these was obtained by centrifugation at 12,000 xg for 10 minutes, was resuspended in deionized water and again pelleted by centrifugation at 15,500 xg. Pellets were frozen at 80 ^{o}C and lyophilized to allow determination of cell dry weights and to obtain a dry pellet from which PHA could be extracted and quantified.

7.1.3.5 Analytical methods

The bulk characteristics of the OFI substrate and AD sludge inoculum were determined by standard methods (APHA, 1998), deviating from these only in that the oven temperature for total solids determination was set to 80 ^{o}C. Determination of the cellulose, hemicellulose, and lignin content of the OFI substrate was performed by van Soest analysis (van Soest et al., 1991).

Liquid samples of both bulk fermentates and *P. putida* growth media were clarified by centrifugation at 15,500 xg and the supernatant collected prior to analysis. For VFA analysis clarified liquid samples were acidified by 1:1 dilution with 20% formic acid in 1.5 mL GC vials. VFA was quantified by gas chromatography with flame-ionization detection (GC-FID) using a

ZB-FFAP column, with helium providing the carrier gas. Acetic, propionic, isobutyric, butyric, isovaleric, valeric, and hexanoic acids were detected and quantified against standards, these values were summed to calculate total VFA (TVFA).

Characterisation of bulk fermentate parameters for preparation of growth media was done using kit-based spectrophotometric assays from Hach Lange Ltd. (Manchester, United Kingdom) as follows: Organic acids were quantified using the LCK365 kit, total organic carbon with the LCK386 kit, and total nitrogen with the LCK238 kit. C:N ratios of media were calculated as the ratio of TOC:TN as determined from these measures and are quoted on a mass basis.

7.1.3.6 Extraction and quantification of PHA

Quantification of PHA from lyophilized cell pellets was performed according to the protocol of Jia et al. (2013), with some minor alterations, wherein PHA undergoes methanolysis to obtain methylated monomers which are then quantified by GC-FID detection. Lyophilized cell pellets were resuspended in 1 mL acidified methanol (9:1 methanol: sulfuric acid v/v) and 2 mL of chloroform containing 10 mg/mL benzoic acid as an internal standard. These were incubated in sealed vials at 105 ºC for 2 hours and then cooled by incubation on ice. Once cool, 1 mL of ice-cold deionized water was added, and the vial sealed and vortexed for 1 minute to mix. The vials were sat at ambient temperature to allow phase separation (~1 hour). The organic (chloroform) phase was collected and pipetted into 1.5 mL GC vials to which sodium sulphate had been added (as a desiccant). The methylated monomers were detected by GC-FID using a 30 m x 0.25 mm x 0.25 μm fused-silica ZB-FFAP capillary column with helium providing the carrier gas and quantified against standards which had been subjected to the same methanolysis protocol. Total PHA was determined as the sum of the monomers (these being 3-hydroxybutyrate, 3-hydroxyvalerate, 3-hydroxyhexanoate, 3-hydroxyheptanoate, 3-hydroxyoctanoate, 3-hydroxynonanoate, 3-hydroxydecanoate, 3-hydroxyundecanoate, 3hydroxydodecanoate, 3-hydroxytetradecanoate). Unsaturated PHA monomers were not quantified. The chromatograms and standard curves for these standards are shown in the appendix to this chapter.

7.1.3 Results

7.1.3.1 Characterisation of AF substrate and feedstock

Opuntia ficus indica biomass was found to have a volatile solids content of 83.51% of total solids (VS/TS), consistent with literature values for other related species such as *Opuntia*

fragilis, *Kalanchoe daigremontiana*, and *Ananas comosus* (pineapple) (Lueangwattanapong et al., 2020). Lignin values were relatively low, at just 8.73 %, consistent with values for *Opuntia fragilis* and *Kalanchoe daigremontiana* (Lueangwattanapong et al., 2020). AD sludge had a VS/TS of 60.30 %, which is also in close agreement with literature values (Lueangwattanapong et al., 2020; Tenci et al., 2023) Sludge was found to have a low initial VFA concentration (0.66 g/L), consistent with expectation for sludge from a methanogenic AD facility in which VFA is rapidly converted to methane. These bulk characteristics are summarised in **Table 7.1**.

Table 7.1: Characterisation of initial biomass and AD sludge inoculum

Characteristic	*Opuntia ficus indica*	AD Sludge
TS/FW (%)	9.66 ± 0.41	4.81 ± 0.08
VS/TS (%)	83.51 ± 0.06	60.30 ±0.21
Cellulose (% TS)	12.6	-
Hemicellulose (%TS)	5.5	-
Lignin (%TS)	8.73	-
pH	-	8.00 ± 0.01
TVFA (g/L)	-	0.66 ±0.04

7.1.3.2 Characterisation of bulk VFA-rich fermentates, with and without zeolite treatment

The bulk fermentate had a TVFA concentration of 13.31 ±0.05 g/L. Given an initial concentration of 35 gVS/L of volatile solids (30 gVS of *Opuntia*, and 5 g/L AD sludge), this indicates a yield of 38.03 ±0.15 % VFA on a VS basis. The produced VFA was primarily acetate (C2) (50.1%) and butyrate (C4) (28.9%), with smaller, but still significant fractions of C3, 5, and 6 fatty acids detected (**Fig. 7.1A**).

The effect of zeolite treatment on both carbon and nitrogen sources in the fermentate is shown in **Fig. 7.1B-D**. Zeolite treatment was not found to affect the abundance of either total organic carbon or of total organic acids in the fermentate, as confirmed by Student's t-test (**Fig. 7.1B**). Conversely both total nitrogen and total ammonium nitrogen were found to be heavily depleted (**Fig. 7.1C**). The cumulative effect of this specific depletion of nitrogen in the fermentate can be seen in **Fig. 7.1D**, in which the C:N ratio of the fermentate shifts from 12.5 to 93.5 (mass basis).

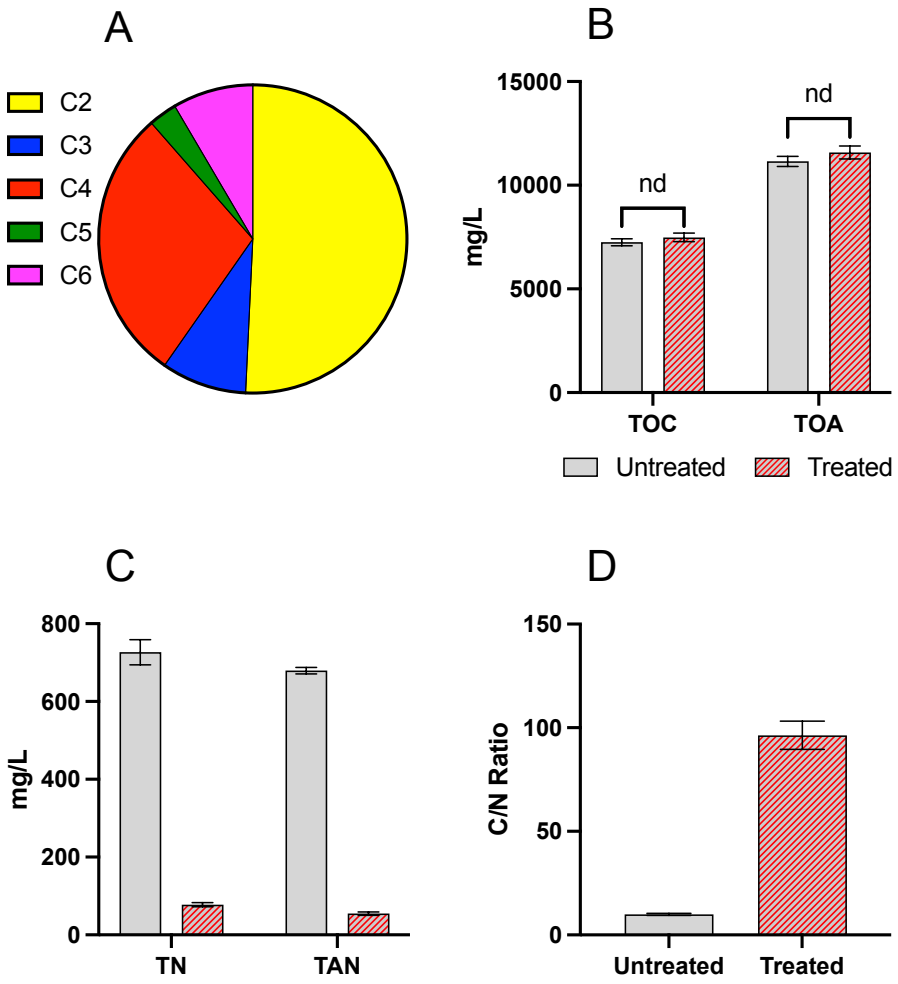


Figure 7.1: Analysis of carbon and nitrogen composition of untreated and treated *Opuntia* fermentates. **A**: Fatty acid composition of total VFA C2 = Acetate, C3 = Propionate, C4 = Butyrate + Isobutyrate +, C5 = Valerate + Isovalerate, C6 = Hexanoate, **B**: Total organic carbon (TOC) and Total organic acids (TOA), **C**: Total nitrogen (TN) and Total ammonium nitrogen (TAN), **D**: Carbon to nitrogen ratio (mass basis).

7.1.3.3 Growth characteristics of *P. putida* on fermentates

P. putida demonstrated robust growth on the diluted fermentate medium at all C:N ratios tested (i.e., from 12.5 to 93.5) – summarised in **Fig. 7.2**. A reduced lag phase was observed in zeolite-treated media (in which nitrogen was reduced) in a dose dependent manner: the longest lag phases were seen in untreated media (C:N of 12.5) and the shortest were seen in the most heavily treated media (C:N of 93.5). The inverse of this effect was seen in growth rates, with the highest maximal growth rates seen at C:N 10 and the slowest growth rates in C:N 93.5, which likely represents the increased capacity for biomass accumulation afforded by the ammonium present in these samples.

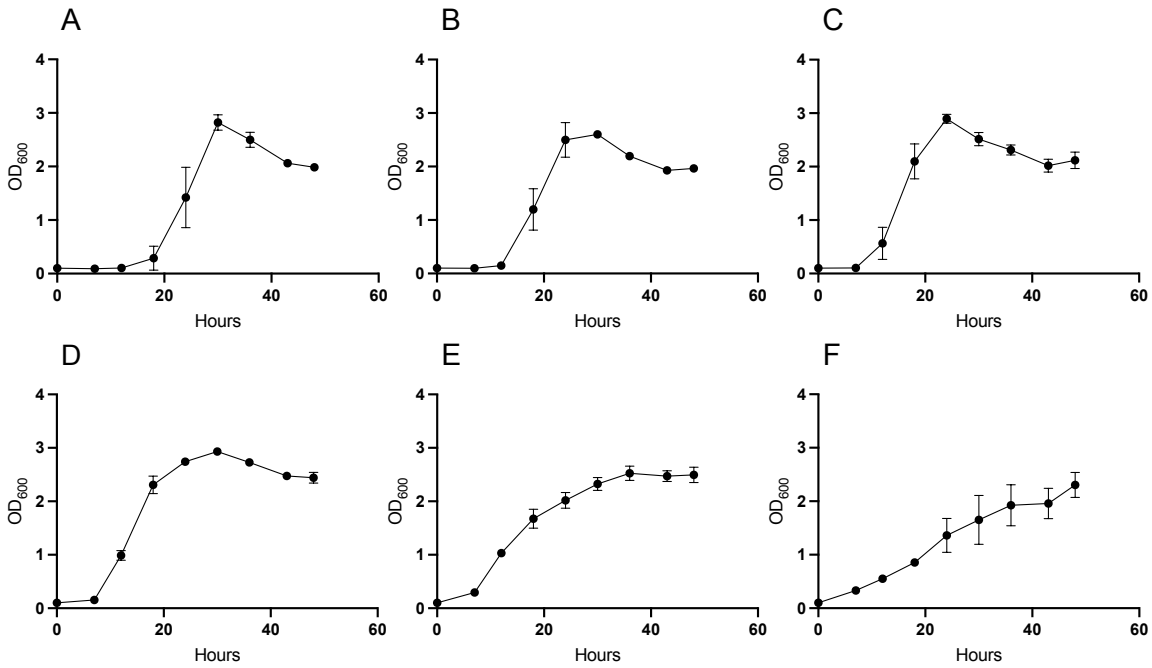


Figure 7.2: Growth characteristics (OD_{600}) of *P. putida* grown on acidogenic fermentates of varying C:N ratio. **A, B, C, D, E**, and **F**, correspond to ratios of 12.5, 13.5, 17.5, 26, 43 and 93.5, respectively.

7.1.3.4 Effect of zeolite treatment on *P. putida* polyhydroxyalkanoate production on fermentate

Polyhydroxyalkanoate production, is shown in **Fig. 7.3**. PHA titres (**7.3A**) and yields (**7.3B**) were found to be highly responsive to both C:N ratio and to incubation time.

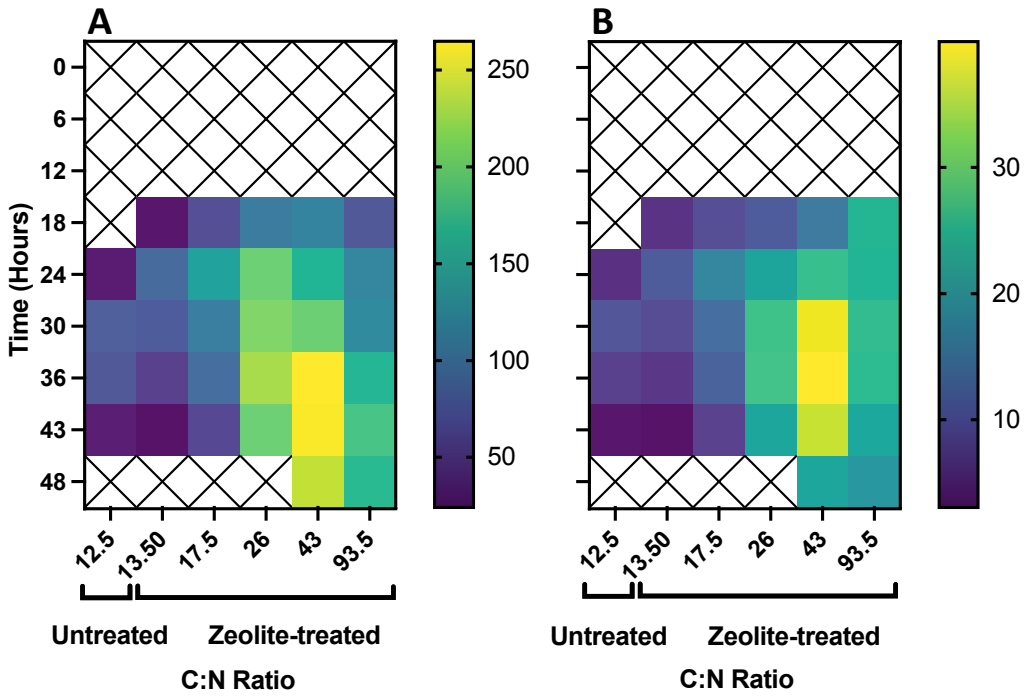


Figure 7.3: PHA production over a parameter space of zeolite treatment vs. time. **A**: Titres of PHA (milligrams per liter of culture medium), **B**: Yields of PHA (% of cell dry weight).

Maximal PHA titres (270 ±20 mg/L) were seen at a C:N ratio of 43 at 36 hours (**Fig. 7.3A**), which corresponds to the maximal OD_{600} seen for this culture in **Fig. 7.2E**. This treatment and timepoint was also found to produce the maximal observed titres of PHA when measured as a percentage of cell dry weight (40 ±7%) suggesting this point represents a global optimum for PHA production under these conditions (**Fig. 7.3B**). Across conditions, PHA yields and titres were seen to decrease after achieving their respective maxima, which likely represents the consumption of PHA as a carbon source by *P. putida*, once free carbon in the medium was exhausted, beyond which point biomass also began to decrease as seen in **Fig. 7.2**.

The various conditions achieved their maximal VFA titres and yields at different timepoints. For C/N ratios of 12.5, 13.5, 17.5, 26, 43 and 93.5 maximal titres were seen at 30, 24, 24, 36, 36, and 43 hours, respectively, while maximal yields were seen at 30, 24, 24, 36, 36, and 30 hours. These titre and yield maxima are shown in **Fig. 7.4A**, and **7.4B**. Mean yield and titre maxima for each of the treatment groups were analysed for the statistical significance of their deviation from the untreated control group by Dunnett's Multiple Comparisons Test. Both yields and titres deviated significantly from the control at C:N ratios of 26 and above. The data in **Fig. 7.4**, including the p-values of pairwise comparisons between zeolite treated conditions and the negative control are summarised in **Table 7.2**.

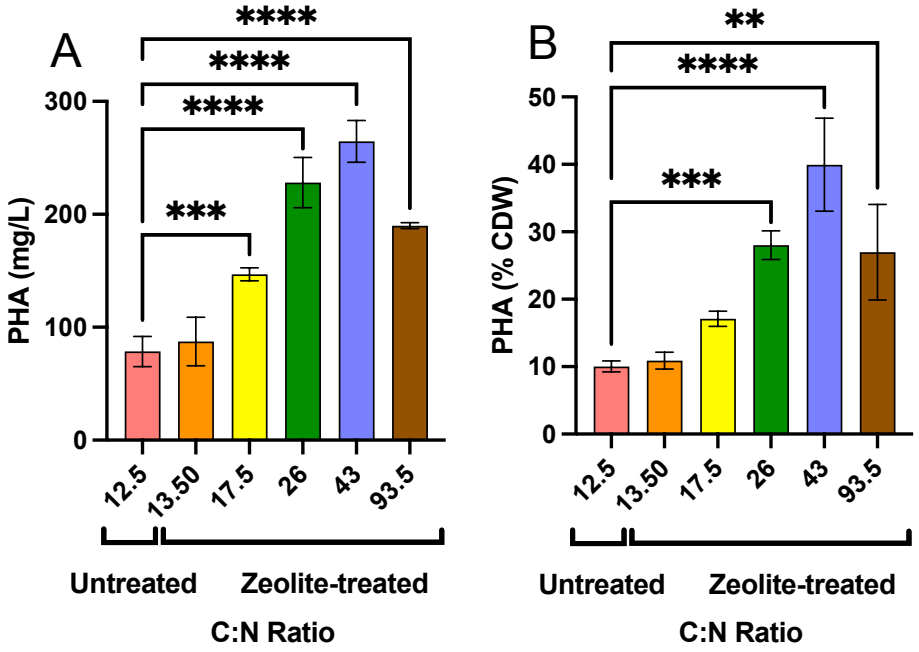


Figure 7.4: Statistical comparison of PHA titre and yield maxima across timepoints. Panels **A**, and **B** show maximum titres and yields respectively. Comparisons of statistical significance of deviation of treatment groups from the untreated control performed using Dunnett's Multiple Comparisons Test. Non-significant comparisons have been omitted.

Table 7.2: Summary of observed PHA titre and yield maxima at various C:N ratios. p-values of pairwise comparisons between treatment groups and the negative control are provided. n.s. = non-significant.

C/N ratio	PHA Titre (mg/L)	p-value	PHA Yield (% CDW)	p-value
12.5	80 ±10	-	10.0 ±0.8	-
13.5	90 ±20	0.9227 (n.s.)	11 ±1	0.9991 (n.s.)
17.5	147 ±6	0.0006	17 ±1	0.2040 (n.s.)
26.0	230 ±20	<0.0001	28 ±2	0.0009
43.0	270 ±20	<0.0001	40 ±7	<0.0001
93.5	190 ±3	<0.0001	27 ±7	0.0014

7.1.3.4 Composition of *P. putida* PHAs across the time / C:N parameter space

The compositions of PHAs produced at each timepoint are provided in **Fig. 7.5**. Note that conditions in **Fig. 7.5** for which data are not given had either not yet reached the requisite OD_{600} of 0.5 (**7.5A**) or had demonstrated several timepoints of negative growth (**5F**). In most conditions and timepoints PHAs were found to be rich in the C10 monomer 3-hydroxydecanoic

acid, which represented a majority of the polymer (by mass) in many conditions. Considerable quantities of the C6 monomer 3-hydroxyhexanoic acid were also observed. This monomer was particularly abundant in early timepoints, and in the C:N 93.5 condition, though PHAs broadly showed a trend of reducing C6 content with increased incubation time in all conditions.

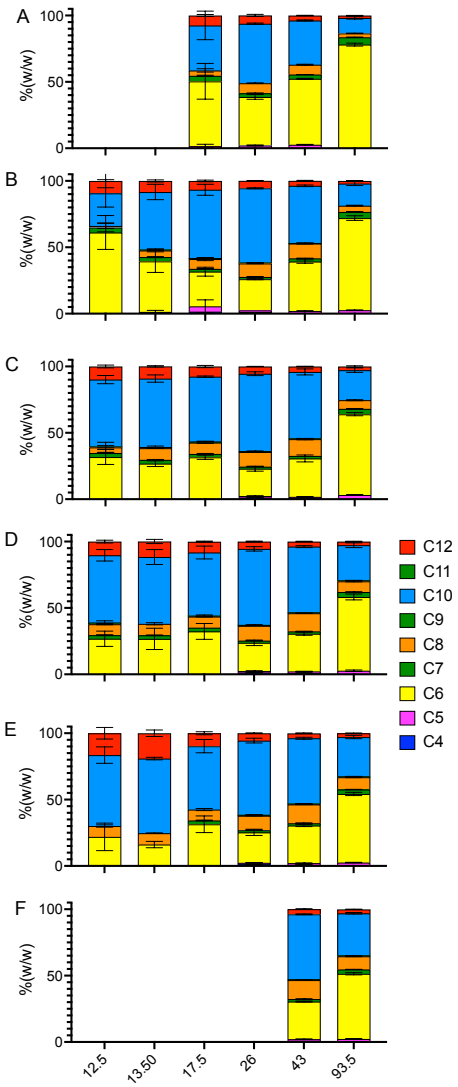


Fig. 7.5: Compositional analysis of PHAs produced by *P. putida* on *Opuntia* fermentates of various C:N ratios at different timepoints. All data are shown as mean ± standard deviation of biological triplicates. Timepoints of 18, 24, 30, 36, 43, and 48 hours are shown in panels A, B, C, D, E, and F, respectively.

7.1.4 Discussion:

7.1.4.1 Zeolite treatment of *Opuntia* fermentate

Zeolite treatment of the *Opuntia* fermentate produced a considerable decrease in total and ammonium nitrogen concentrations (**Fig. 7.1C**). Zeolite demonstrated specificity for ammonium as concentrations of VFA were equal between treated and untreated conditions (**Fig. 7.1B**). This non-retention of VFAs by zeolite has also been reported by Wan et al. (2017) and is relevant as it shows zeolite imposes no measurable loss in VFA yields which would otherwise need to be accounted for.

7.1.4.2 Response of *P. putida* PHA production to zeolite-induced nitrogen limitation

The phenomenon of increased PHA production with increased C:N ratios is reported throughout the literature for multiple species. Examples include PHB production in a mixed microbial consortium grown on acetate (Zhou et al., 2022), PHB production in *Bacillus megaterium* grown on sucrose (Faccin et al., 2009), and production of PHB-co-PHV (a PHA copolymer) by *Nostoc muscorum* on a mixture of acetate, valerate and glucose (Angra et al., 2023). In all these cases, nitrogen limitation was found to increase production of PHA. This is consistent with the findings of this study, which identified maximal PHA titres and yields in *P. putida* at a C:N ratio of 43. However, in stark contrast to this study, in these previous studies, control of C:N ratios was achieved using independent carbon and nitrogen sources whose precise dosing allowed for control of this parameter. This use of pure compounds increases cost and is a major obstacle to the commercialization of PHAs. Bulk prices for acetate for example, the cheapest of the VFAs, stand around US $400-800/tonne (Zacharof & Lovitt, 2013), and are over US $2000/tonne for the longer C4 and C5 fatty acids.

The use of an abundant, heterogeneous waste feedstock, such as agricultural biomass, sewage sludge, or municipal food waste circumvents this cost limitation, as many of these may be obtained at little, no, or negative cost. However, these are variable in both their chemistry and structure and cannot be directly used, or perhaps only partially used, as carbon sources by PHA accumulating species. Dalsasso et al. (2019) for example, produced PHB in *Cupriavidus necator* grown on vinasse and molasses, abundant waste products of sugar processing. Acid and enzymatic hydrolysis of the biomass served to yield free sugars which could be used by *C. necator* for growth and PHB production. The nitrogen content of this hydrolysate however could not be easily controlled as it was chemically heterogeneous. Penkhrue et al. (2020) provide a similar example, in which the juices extracted from waste fruit peels provided a growth medium for PHA accumulation. Here too, given the heterogeneous nature of the

feedstock only a fraction of the soluble carbon sources present could be used by the PHA accumulator, and no means is provided to easily induce nitrogen limitation, as we have demonstrated here. This juicing method also disregards the considerable amount of solid and insoluble biomass present which could not be used for PHA production.

The synergy proposed in our study, that of acidogenic fermentation augmented with zeolite purification combines the cost benefits of heterogeneous feedstocks with the substrate homogeneity and exquisite control of reactor parameters afforded by pure-substrate systems. Acidogenic fermentation allows production of VFA from both the soluble and insoluble fractions of the biomass. It homogenizes all available carbon sources to a pool of VFA which is widely utilizable by many PHA accumulating species. Moreover, the heterogeneous nitrogen sources in biomass, which may take the form of proteins, free amino acids, urea, nitrates, or other chemicals, are hydrolysed to ammonium ions. This is evident in **Fig. 7.1C**, where nearly all the total nitrogen detected in *Opuntia* digestate could be accounted for as ammonium. This homogeneous nitrogen source is then in a form amenable to removal by zeolite, as per the requirements of the downstream bioproduction process.

Zeolites have been widely used for ammonium removal from anaerobic digesters, however this has largely been in the context of alleviating ammonium toxicity to biomethane production (Montalvo et al., 2012; Tada et al., 2005), or on the recovery of ammonium nitrogen from fermentates (Wan et al., 2017). To our knowledge, just one previous author has tested a system analogous to that proposed here (Martin-Ryals, 2017). In this study, zeolites were used to reduce ammonium inhibition of PHA accumulation by a mixed microbial consortium in fermentates from organic waste. This system differs from the one presented herein in two key respects. It uses a mixed-culture system as opposed to the pure-culture system shown here, and it does not identify optimal C:N ratios for PHA accumulation. The authors identified that a 29% increase in PHA yields could be achieved by using zeolites to reduce ammonium inhibition, however only one zeolite-treated condition was tested, and a detailed survey of the zeolite treatment – C:N parameter space was not performed as was done in **Fig. 7.3**. Martin-Ryals (2017) correctly note the inhibitory effect of ammonium and the potential of zeolites in mitigating this. However, the relationship between C:N ratio and PHA production is not monotonic and while nitrogen limitation improves PHA accumulation, its complete absence impedes growth to such an extent that production suffers. Zhou et al (2022) found a C:N ratio of 40 to be optimal for PHA production in a mixed microbial culture, while in our study 43 was optimal (**Fig. 7.4, Table 7.2**), above this ratio (i.e., at a C:N of 93.5), both yields and titres

suffered. While optimal C:N ratios are species and context specific, the ability to modify the fermentate to the needs of any specific downstream process, whether a pure or mixed culture, is granted exclusively by this novel zeolite process. Without it, the C:N ratio of the fermentate can only be increased through supplementation with a pure carbon source, which increases cost.

Somewhat contrary to expectation, considerable variation in PHA composition was observed between treatment conditions and timepoints (**Fig. 7.5**), though this variation was mainly limited to the relative abundance of the C6 and C10 monomers. The hypothesized PHA composition was a C10-rich polymer with smaller percentages of other monomers, as was reported by Dartiailh et al. (2021) for PHA produced on short chain VFAs by *P. putida*. In many conditions this was observed, however at early timepoints and in the C:N 93.5 condition, the C6 monomer was found to dominate (**Fig. 7.5A**). A possible explanation could be a preferential consumption of hexanoate at early timepoints by *P. putida*. Dartiailh et al. (2021) argue that substrates longer than valerate are incorporated into PHA monomers of equivalent length via the fatty acid β-oxidation pathway. The preferential consumption of hexanoate over other VFAs by *P. putida* would explain the disproportionate presence of C6 monomers in the PHA polymer at early timepoints. In C:N 93.5 conditions, in which the absence of nitrogen limits growth, it is possible that the hexanoate was depleted more slowly than in other conditions, allowing a C6-rich PHA polymer to dominate even at later timepoints. Individual VFA consumption data would be required to substantiate this hypothesis.

Future work should aim to verify this zeolite process in pure cultures of other known PHA accumulating species and identify the degree to which the treatments and principles determined herein generalize across the space. A C:N ratio of 80 has been reported as optimal in the PHB hyperaccumulator *C. necator* (Zhang et al., 2022), though this value would need to be independently verified for acidogenic fermentate systems through a systematic analysis of C:N ratios. Other species of interest might include *Bacillus megaterium* and the cyanobacterium *Nostoc muscorum*, the latter of which produces short-chain PHA copolymers. Inclusion of fast-growing species such as *Vibrio natriegens* may allow for a non-sterile PHA accumulation process to be developed from which additional process cost savings could be gleaned. This is to say nothing of the many known species which accumulate MSLs other than PHA, such as waxes and oils, and for which the zeolite process demonstrated here could also be expected to offer considerable benefits.

7.5 Conclusion

This study investigated the potential of natural zeolites to allow for precise control of carbon to nitrogen ratios in acidogenic fermentate. This allowed for its direct use as media for microbial storage lipid production as was demonstrated here through production of PHA in *Pseudomonas putida*. Various strengths of zeolite treatment were tested and a C:N ratio of 43 was identified as optimal for this species, allowing PHA titres >3-fold those achievable in untreated fermentates. Given the wide range of potential feedstocks for acidogenic fermentation, and the hundreds of MSL accumulating species for which nitrogen limitation is a prerequisite, this process could offer considerable promise for the future production of renewable petrochemicals.

References

Alves, A.A., Siqueira, E.C., Barros, M.P.S., Silva, P.E.C., Houllou, L.M. 2023. Polyhydroxyalkanoates: a review of microbial production and technology application. International Journal of Environmental Science and Technology 20, 3409-3420.

Angelidaki, I., Sanders, W. 2004. Assessment of the anaerobic biodegradability of macropollutants. Rev. Environ. Sci. Biotechnol. 3, 117-129.

Angra, V., Sehgal, R., Gupta, R. 2023. Trends in PHA production by microbially diverse and functionally distinct communities. Microbial ecology 85, 572-585.

APHA. 1998. Standard Methods for the Examination of Water and Wastewater. American Water Works Association and Water Environment Federation.

Choi, J.-i., Lee, S.Y. 1997. Process analysis and economic evaluation for poly (3-hydroxybutyrate) production by fermentation. Bioprocess engineering 17, 335-342.

Christophe, G., Lara Deo, J., Kumar, V., Nouaille, R., Fontanille, P., Larroche, C. 2012. Production of oils from acetic acid by the oleaginous yeast *Cryptococcus curvatus*. Appl. Biochem. Biotechnol. 167, 1270-1279.

Dalsasso, R.R., Pavan, F.A., Bordignon, S.E., de Aragão, G.M.F., Poletto, P. 2019. Polyhydroxybutyrate (PHB) production by *Cupriavidus necator* from sugarcane vinasse and molasses as mixed substrate. Process Biochemistry 85, 12-18.

Dartiailh, C., Blunt, W., Sharma, P.K., Liu, S., Cicek, N., Levin, D.B. 2021. The thermal and mechanical properties of medium chain-length polyhydroxyalkanoates produced by *Pseudomonas putida* LS46 on various substrates. Frontiers in Bioengineering and Biotechnology 8, 617489.

Eryildiz, B., Lukitawesa, Taherzadeh, M.J. 2020. Effect of pH, substrate loading, oxygen, and methanogens inhibitors on volatile fatty acid (VFA) production from citrus waste by anaerobic digestion. Bioresource Technology 302, 122800.

Faccin, D.J.L., Martins, I., Cardozo, N.S.M., Rech, R., Ayub, M.A.Z., Alves, T.L.M., Gambetta, R., Resende Secchi, A. 2009. Optimization of C: N ratio and minimal initial carbon source for poly (3-hydroxybutyrate) production by *Bacillus megaterium*. Journal of Chemical Technology & Biotechnology 84, 1756-1761.

Hedström, A. 2001. Ion exchange of ammonium in zeolites: a literature review. Journal of environmental engineering 127, 673-681.

Jia, Q., Wang, H., Wang, X. 2013. Dynamic synthesis of polyhydroxyalkanoates by bacterial consortium from simulated excess sludge fermentation liquid. Bioresource Technology 140, 328-336.

Lueangwattanapong, K., Ammam, F., Mason, P.M., Whitehead, C., McQueen-Mason, S.J., Gomez, L.D., Smith, A.C., Thompson, I.P. 2020. Anaerobic digestion of Crassulacean Acid Metabolism plants: Exploring alternative feedstocks for semi-arid lands. Bioresour. Technol. 297, 122262.

Martin, L.K., Huang, W.E., Thompson, I.P. 2023. The effect of nutrient limitation on bacterial wax ester production. Bioresour. Technol. Rep. 22, 101423.

Martin-Ryals, A.D. 2017. Advancing wastewater valorization using anaerobic membrane bioreactors with bioaugmentation and ion-exchange, and bio-plastic production, University of Illinois at Urbana-Champaign.

Mengmeng, C., Hong, C., Qingliang, Z., Shirley, S.N., Jie, R. 2009. Optimal production of polyhydroxyalkanoates (PHA) in activated sludge fed by volatile fatty acids (VFAs) generated from alkaline excess sludge fermentation. Bioresour. Technol. 100, 1399-1405.

Montalvo, S., Guerrero, L., Borja, R., Sánchez, E., Milán, Z., Cortés, I., De La La Rubia, M.A. 2012. Application of natural zeolites in anaerobic digestion processes: A review. Applied Clay Science 58, 125-133.

Passanha, P., Esteves, S.R., Kedia, G., Dinsdale, R.M., Guwy, A.J. 2013. Increasing polyhydroxyalkanoate (PHA) yields from *Cupriavidus necator* by using filtered digestate liquors. Bioresour. Technol. 147, 345-352.

Penkhrue, W., Jendrossek, D., Khanongnuch, C., Pathom-Aree, W., Aizawa, T., Behrens, R.L., Lumyong, S. 2020. Response surface method for polyhydroxybutyrate (PHB) bioplastic accumulation in *Bacillus drentensis* BP17 using pineapple peel. PloS one 15, e0230443.

Pinto, A.S.S., McDonald, L.J., Jones, R.J., Massanet-Nicolau, J., Guwy, A., McManus, M. 2023. Production of volatile fatty acids by anaerobic digestion of biowastes: Techno-economic and life cycle assessments. Bioresour. Technol. 388, 129726.

Sabapathy, P.C., Devaraj, S., Meixner, K., Anburajan, P., Kathirvel, P., Ravikumar, Y., Zabed, H.M., Qi, X. 2020. Recent developments in Polyhydroxyalkanoates (PHAs) production–A review. Bioresource technology 306, 123132.

Tada, C., Yang, Y., Hanaoka, T., Sonoda, A., Ooi, K., Sawayama, S. 2005. Effect of natural zeolite on methane production for anaerobic digestion of ammonium rich organic sludge. Bioresource technology 96, 459-464.

Tenci, N.A., Ammam, F., Huang, W.E., Thompson, I.P. 2023. Anaerobic co-digestion of Euphorbia tirucalli with pig blood for volatile fatty acid production. Bioresource Technology Reports 21, 101333.

van Soest, P.J., Robertson, J.B., Lewis, B.A. 1991. Methods for dietary fiber, neutral detergent fiber, and nonstarch polysaccharides in relation to animal nutrition. J. Dairy Science 74, 3583-3597.

Wan, C., Ding, S., Zhang, C., Tan, X., Zou, W., Liu, X., Yang, X. 2017. Simultaneous recovery of nitrogen and phosphorus from sludge fermentation liquid by zeolite adsorption: Mechanism and application. Separation and Purification Technology 180, 1-12.

Wang, K., Yin, J., Shen, D., Li, N. 2014. Anaerobic digestion of food waste for volatile fatty acids (VFAs) production with different types of inoculum: Effect of pH. Bioresource Technology 161, 395-401.

Yuan, Q., Sparling, R., Oleszkiewicz, J.A. 2011. VFA generation from waste activated sludge: Effect of temperature and mixing. Chemosphere 82, 603-607.

Zacharof, M.-P., Lovitt, R.W. 2013. Complex effluent streams as a potential source of volatile fatty acids. Waste and Biomass Valorization 4, 557-581.

Zhang, L., Jiang, Z., Tsui, T.-H., Loh, K.-C., Dai, Y., Tong, Y.W. 2022. A review on enhancing *Cupriavidus necator* fermentation for poly (3-hydroxybutyrate)(PHB) production from low-cost carbon sources. Frontiers in Bioengineering and Biotechnology 10, 946085.

Zhou, W., Colpa, D.I., Geurkink, B., Euverink, G.-J.W., Krooneman, J. 2022. The impact of carbon to nitrogen ratios and pH on the microbial prevalence and polyhydroxybutyrate production levels using a mixed microbial starter culture. Science of the Total Environment 811, 152341.

Statement of Authorship for joint/multi-authored papers for PGR thesis

To appear at the end of each thesis chapter submitted as an article/paper

The statement shall describe the candidate's and co-authors' independent research contributions in the thesis publications. For each publication there should exist a complete statement that is to be filled out and signed by the candidate and supervisor **(only required where there isn't already a statement of contribution within the paper itself).**

Title of Paper	Red seaweed as an abundant, natural methanogenesis inhibitor for industrial biorefinery
Publication Status:	☐ Published ☐ Accepted for publication ☐ Submitted for publication ☒ Unpublished and unsubmitted work written in manuscript style
Publication Details:	First draft of manuscript requiring additional experimental work before submission for publication.

Student Confirmation

Student Name:	*Nicholas A. Tenci*	
Contribution to the paper:	*Designed the study, performed the experiments, analysed the data, wrote the manuscript.*	
Signature: 	Date:	*11/09/2024*

Supervisor Confirmation

By signing the Statement of Authorship, you are certifying that the candidate made a substantial contribution to the publication, and that the description described above is accurate.

Supervisor name and title: *Prof. Ian P. Thompson*		
Supervisor comments: I agree with this summary.		
Signature: 	Date:	*17/09/2024*

This completed form should be included in the thesis, at the end of the relevant chapter.

7.2 – Additional Bioproduction Experiments

7.2.1 Introduction

In **Section 7.1** it was found that zeolite treatment of acidogenic fermentates could produce a significant increase in PHA production in *P. putida* KT2440. Very importantly, this indicates that zeolite treatment of acidogenic fermentates could provide a quick, cheap, and likely scalable protocol for production of mcPHA, yet it also raised further questions.

Several studies have successfully demonstrated microbial growth and PHA production on liquid extracts taken from fruit and vegetable wastes, with no intervening hydrolysis or fermentation step [171, 172]. The study of Costa et al. [171] identified soluble residues from apple and melon processing to be particularly effective substrates for PHA production in *C. necator.* Lueangwattanapong [102] demonstrated PHA production on juices taken from *Opuntia ficus indica*, a fraction the author refers to as "*Opuntia* Liquid Extract" or OLE, though provides scant details regarding production yields. The demonstration of effective growth or PHA accumulation on OLE might suggest that the acidogenic fermentation may be surplus to requirement. In **Chapter 4** of this thesis, the suitability of CAM crops as substrates for AF was in part attributed to their higher content of soluble organics, though if *P. putida* is able to use these organics directly, this same feature may also provide the strongest argument against their fermentation prior to PHA production. Acidogenic fermentate was hypothesised to offer two advantages over OLE as a growth and PHA-production medium. The first was that soluble carbon within fermentate is present almost exclusively as VFA, which is readily used as a carbon source by *P. putida*. OLE could be expected to contain a heterogeneous mixture of soluble organic acids, sugars, and other metabolites, which may or may not be accessible to *P. putida* as carbon sources. *Opuntia* cladodes have a high content of complex soluble and insoluble polysaccharides [173]. It might be expected that the soluble polysaccharides, while contributing to the SCOD of OLE, might not be accessible as carbon sources to *P. putida*. *Opuntia* cladodes have however been found to be relatively high in several small molecules such as citric, malic, and oxalic acids, though low in soluble sugars [174]. *P. putida* might thus be expected to be able to use some, but not all of the organics in *Opuntia* extracts. Fermentates offer an additional advantage over liquid extracts due to the chemical homogeneity of their nitrogen content, which is primarily present as ammonium. Zeolite might be expected to be relatively ineffective at removing nitrogen from OLE as the undigested nitrogen would be present in heterogeneous forms, from proteins to free amino acids to other nitrogen compounds which would elude its simple ion-exchange binding mechanism. It was thus deemed important

to test the ability of *P. putida* to utilise *Opuntia* liquid extract as growth medium, to see whether the AF step may be skipped entirely.

The findings of **Section 7.1** raise two further possibilities for novel bioproduction approaches. In **Chapter 3**, acidogenic fermentations were conducted with both high-carbon (*E. tirucalli*) and high-nitrogen (pig blood) feedstocks [20]. Conventional wisdom would dictate that protein fermentates would be poor substrates for PHA production due to their high nitrogen content. Zeolite treatment of these fermentates could allow a route to the valorisation of fermented waste proteins as PHAs, a task previously unthinkable without the addition of an exogenous carbon source.

A second possibility is raised by the extension of PHA production into protein fermentates, which arises from the findings of Dartiailh et al. [79]. This paper demonstrated the monomer profile of PHAs produced by *P. putida* to depend heavily on the carbon source used. Given that fermentations of carbohydrates and proteins may result in vastly different VFA profiles, this suggests that unique PHA formulations could be achieved in *P. putida* through tailoring the initial acidogenic fermentation through selection of co-substrate feeding ratios. This possibility is again only made possible through the intervention of zeolite, which allows removal of surplus nitrogen introduced by protein-rich feedstocks.

Lastly and perhaps the most important question arising from the results of **Section 7.1** was the investigation of zeolite's effect on PHA bioproduction in other species. The underlying mechanism, of nitrogen limitation driving PHA accumulation, is not specific to *Pseudomonas*, and it seemed likely that this would generalise to other PHA-accumulating microbial species. The more PHA-accumulating species can be shown to respond favourably to zeolite-treatment, the greater the potential impact of this innovation and scope for its future implementation at scale. Various species of PHA-accumulating microbes exist and production of VFAs have been demonstrated for production of PHAs in both mixed cultures, and in pure cultures of such species as *B. megaterium* [175], and *C. necator* [124]. As a PHA "hyperaccumulator" *C. necator* is widely reported to accumulate up to and even above 80% of its CDW as PHA [124, 176-178], making it the natural candidate for this investigation. *C. necator* produces short chain PHAs, containing mostly the 3-hydroxybutyrate monomer, and has primarily been investigated as a producer of the homopolymer PHB. Confirming that it responds to zeolite treatment would thus demonstrate zeolite treatment as a strategy to increase short-chain PHA production, to complement the medium-chain PHA production demonstrated in *P. putida*.

Several follow-up experiments were thus conducted in response to the findings of **Section 7.1** to investigate a diverse, but related set of aims. These were as follow:

1. To determine the capacity of *P. putida* to utilise both *Opuntia* juice and *Opuntia* fermentates as growth media.
2. To demonstrate that zeolite treatment permits PHA production in *P. putida* on otherwise unusable fermentates from high-protein substrates.
3. To investigate whether the unique VFA profiles achieved by AF of protein allow customisation of PHA compositions in *P. putida*.
4. To test the efficacy of zeolite treatment on another PHA-producing species, namely *C. necator* H16.

7.2.2 Materials and methods

7.2.2.1 Materials

Three substrates were used to prepare the acidogenic fermentates used in these experiment. These were *Opuntia ficus indica* cladodes, obtained from Pepe Aromas (Azaruja, Portugal). Upon receipt, cladodes were oven dried (<80 ºC), ground to a powder and graded to ensure a particle size of <1 mm. Food grade pig blood was purchased from Tongmaster Seasonings (Coatbridge, United Kingdom), and sugarcane molasses was purchased from Harvest Foods (Alexandria, Egypt).

AD sludge, which provided the inoculum for acidogenic fermentations, was obtained from Severn Trent Green Power (Cassington, UK) and stored anaerobically before use.

7.2.2.3 Preparation of zeolites

Zeolites used in these experiments were graded through a riddle to ensure a particle size of 1-3 mm and equilibrated by overnight incubation with 1 M NaCl at ambient temperature (21ºC). Equilibrated zeolites were flushed of surplus NaCl by washing in excess deionised water and oven dried at 80 ºC before use.

7.2.2.4 Preparation of fermentate

Bulk acidogenic fermentations were performed in triplicate with a 1.5 L working volume. The respective substrate and inocula were added to final concentrations of approximately 30 and 5 gVS/L, respectively. Where molasses provided the substrate, this was added on a COD basis to a concentration of 43 gCOD/L.

Trace elements and micronutrients were provided by a medium solution, prepared according to Angelidaki and Sanders [56], with the exclusion of sodium sulphide. The methanogenesis inhibitor bromoethane sulfonate was added to a final concentration of 10 mM and the medium pH adjusted to 8.0. Fermentations were incubated under anaerobic conditions at 37°C for 12 days with constant agitation at 125 rpm. Use of a fermentation airlock allowed relief of biogas pressure while maintaining fermentations under anaerobic conditions.



Figure 7.6: Exemplar of a triplicate batch fermentation setup for preparation of *Opuntia* fermentate.

7.2.2.5 Zeolite treatment of acidogenic fermentates

Fermentates were zeolite treated with 50-60% (w/v) sodium-equilibrated zeolite for two hours, with shaking incubation at 125 rpm at 30 °C to obtain a treated (high C:N) fermentate.

Blood-based fermentates were subjected to a double treatment due to their significantly higher initial nitrogen concentrations.

7.2.2.6 Preparation of fermentate-based microbial growth media for *P. putida* and *C. necator*

All bulk fermentates underwent the clarification, pH-adjustment, and autoclaving protocol detailed in the methods of **Section 7.1**.

All batches were subjected to chemical characterisation for their organic acid, total carbon, SCOD, total ammonium nitrogen, and total nitrogen compositions via Hach methods and their

C:N ratios determined. Treated (high C:N) and untreated (low C:N) fermentates were back blended to achieve intermediate C:N ratios.

Microbial growth medium was prepared by diluting clarified fermentates with deionised water to achieve VFA concentrations consistent with the VFA tolerances of *P. putida* and *C. necator* determined by initial growth experiments (given in the appendices to this chapter). These concentrations equated to ~3 g/L VFA for *P. putida* and <1 g/L VFA for *C. necator*.

For *P. putida* experiments, 50 mL volumes were aliquoted into 250 mL Erlenmeyer flasks, sealed with foil and autoclave sterilized. A higher culture volume was used for *C. necator* experiments to compensate for the low culture density: 200 mL of media was added to 1 L flasks and these were similarly sealed and autoclaved.

7.2.2.7 Preparation of *Opuntia* Liquid Extract and media thereof

Opuntia liquid extract (OLE) was prepared by resuspending dried *Opuntia* cladode powder (30 g/L) in deionized water overnight with shaking incubation at 30 ºC and 125 rpm. This was then subjected to the same pH adjustment and clarification protocol as per the *Opuntia* fermentate to obtain a clarified soluble fraction at pH 7.0. To prepare a *P. putida* growth medium, OLE was diluted in deionized water to achieve a medium of equal concentration, calculated on a SCOD/L basis, as the corresponding fermentate-based *P. putida* medium. 50 mL aliquots of dilute OLE were added to 250 mL Erlenmeyer flasks, sealed with foil and autoclaved to achieve sterility.

7.2.2.8 Culture conditions *P. putida* and *C. necator*

Cultures of *Pseudomonas putida* KT2440 and *C. necator* H16 were prepared in triplicate, with individual colonies, grown on LBA, taken to represent independent biological replicates. These colonies were used to inoculate initial precultures of 5 mL lysogeny broth, which were incubated overnight. Secondary and tertiary 50 mL precultures were prepared in 250 mL Erlenmeyer flasks. For *P. putida* experiments the first of these precultures consisted of 50% lysogeny broth, 25% OFI fermentate, and 25% deionized water, and the second consisting of 25% fermentate with 75% deionized water. For *C. necator*, fermentate concentrations in each were reduced to 5%, with the difference made up by deionized water. The volume of the final preculture was also increased to 200 mL.

All *P. putida* precultures were incubated at 37 ºC, 125 rpm for ~12 hours. *C. necator* cultures were incubated at 30 ºC, 125 rpm for ~12 hours. The pellets from the final preculture

condition were obtained by centrifugation at 12,000 xg for 10 minutes, flushed with sterile, pH 7.0 PBS and used to inoculate the experimental flasks to an initial OD_{600} of 0.1.

Experimental cultures of *P. putida* and *C. necator* were incubated at 37 and 30 °C, respectively, with agitation at 125 rpm, sampled at regular intervals and the OD_{600} determined. For *P. putida* (*C. necator*) cultures, once the culture OD_{600} reached 0.5 (0.25), additional samples of 5 mL (10 mL) were taken to measure PHA production. The pellet from these cultures was obtained by centrifugation at 12,000 xg for 10 minutes, resuspension in deionized water and re-centrifugation at 15,500 xg. Pellets were frozen at 80 °C and lyophilized to allow determination of cell dry weights and to provide a dry pellet from which PHA could be extracted and quantified.

7.2.2.9 Growth experiments

Growth experiments were conducted broadly along the lines of those with *Pseudomonas* in **Section 7.1**. However, as previous growth optimisation experiments with both *P. putida* and *C. necator* had found *C. necator* to be far less tolerant of high fermentate concentrations than *P. putida* (see **Appendix to Chapter 7**), a 20x dilution of fermentate in deionised water was used rather than the 4x dilution that had been used for *Pseudomonas*. To compensate for this change, the working volume was increased, and experiments performed in a 200 mL working volume in 1L conical flasks, and the sample volume taken at each timepoint for analysis increased to 10 mL of culture.

7.2.2.10 Analytical methods

Bulk media parameters: TOC, TOA, TN, NH_4^+-N, were determined by Hach Lange analysis kits as detailed in the methods of **Section 7.1**. SCOD was determined by Hach Lange LC1400 COD analysis kits, using a DR 2800 Hach-Lange spectrophotometer.

Analysis of VFA concentrations was performed by the standard GC-FID protocol used in **Chapters 3-6** of this thesis and determined against standards.

Quantification of PHA from lyophilized cell pellets was performed according to the protocol detailed in **Section 7.1**, according to Jia et al. [179], with some minor alterations. Quantification of PHA was performed against standards, subjected to the same methanolysis and extraction protocol as the cell pellets. Total PHA levels were determined by quantification of the individual monomers, with total PHA taken as the sum of these numbers. As in **Section**

7.1, the 3-hydroxyalkanoic acid standards used for quantification of PHA monomers were obtained from Sigma-Aldrich, Manchester Organics Ltd., and Tokyo Chemical Industry Europe N.V. The chromatograms and standard curves for these standards are shown in the appendix to this chapter.

7.2.3 Results

7.2.3.1 Utilisation of fermented and non-fermented *Opuntia* media by *P. putida*

The growth of *P. putida* on both *Opuntia* and OLE-based media containing 6 g/L SCOD is shown in **Fig. 7.7 A**. Note that the results of this section are provided on a SCOD basis as this allowed for experimental standardisation of the organic loading of both the heterogeneous OLE medium and fermentate media in a way that accounted for all oxidisable organic material present. The *Opuntia* fermentate used was identical to that in Section 7.1, the VFA profile of which can be seen in **Fig. 7.1A**. Growth curves followed distinct trajectories with an approximately linear increase in OD_{600} in OLE media. Sigmoidal growth was seen in fermentate media, largely consistent with the growth curves seen in **Section 7.1**, which found a considerable lag phase in untreated *Opuntia* fermentates. Maximum OD_{600} values of 2.7 and 1.5 were achieved in fermentate and OLE media, respectively. It should be noted that while a stable maximum OD_{600} value was not achieved in OLE media over the time course covered, by the later timepoints, issues with media precipitation began to reduce the confidence of OD_{600} values, and so the experiment was terminated.

Fig. 7.7 B plots the removal of SCOD by *P. putida* in both OLE and *Opuntia* fermentate media. These graphs are unsurprisingly approximately the inverse of the growth curves, with a relatively linear, monotonic decrease in SCOD in OLE, and a more biphasic reduction in fermentate. Over the time course covered, SCOD removal in OLE proceeded from an initial concentration of 6.2 ±0.2 g/L to a final concentration of 4.30 ±0.06 g/L, or a mean removal efficiency of 31 ±2%. SCOD removal in *Opuntia* fermentates proceeded from an initial concentration of 5.9 ±0.2 to a final concentration of 1.49 ±0.04 g/L, or a mean removal efficiency of 74.8 ±0.9%.

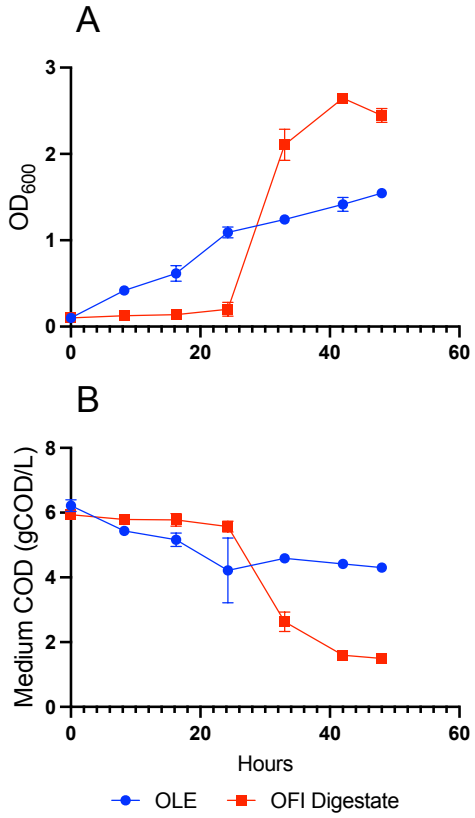


Figure 7.7: Growth on and utilisation of unfermented and fermented *Opuntia*-media by *P. putida*. **A)** Growth curves of P. putida on OLE and *Opuntia* fermentate. **B)** Removal of media SCOD by P. putida in both OLE and *Opuntia* fermentate. All data are presented as means ± standard deviations of biological triplicates.

7.2.3.2 Utilisation of *Opuntia* and blood-based fermentates by *P. putida* and associated PHA accumulation

The C:N ratios of untreated *Opuntia* and blood fermentates were calculated as 10.21 and 2.9, respectively. The C:N ratios of zeolite-treated fermentates were calculated as 87.5 and 56.0, for *Opuntia* and blood respectively. Based on the results of **Section 7.3**, the C:N of the *Opuntia* fermentate was deemed too high for reliable PHA production and this was back blended with untreated *Opuntia* fermentate to a C:N of 22, within the optimum range calculated for PHA production on *Opuntia* fermentate calculated in **Section 7.1**. The more moderate C:N 56 of the treated blood fermentate was deemed acceptable and this fermentate was used without further adulteration.

VFA compositions of the *Opuntia* and blood-derived fermentates are shown in **Fig. 7.8** and are largely consistent with the findings of **Chapter 3** for pure fermentations of *E. tirucalli*

and blood, in which carbohydrate fermentations produced an acetate-majority VFA profile, while protein-based fermentations showed a more mixed-acid fermentation profile, rich in C4 and C5 fatty acids. Also of note is the relative abundance of hexanoic acid in the *Opuntia* fermentation, calculated as 8.5% of the VFA produced by mass. No C6 VFA was detected in the blood fermentate.

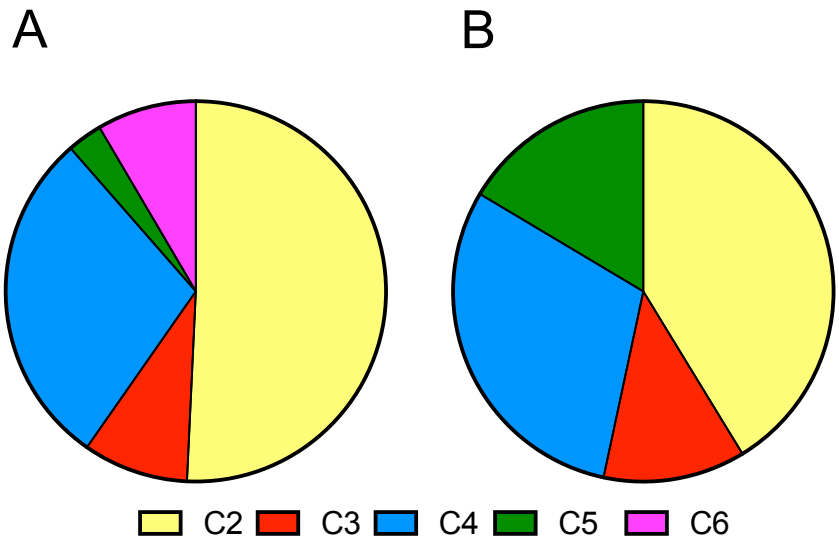


Figure 7.8: VFA composition of bulk *Opuntia* and blood fermentates. **A)** Composition of *Opuntia* fermentate, **B)** Composition of blood fermentate. C2 = Acetic acid, C3 = Propionic acid, C4 = Butyric + Isobutyric acid, C5 = Valeric + Isovaleric acid, C6 = Hexanoic acid.

The results of both growth and fatty acid consumption of these media by *P. putida* are summarised in **Fig. 7.9**. *P. putida* growth on untreated *Opuntia* media followed a familiar sigmoidal growth pattern with an approximately 24-hour lag phase. VFA depletion was inversely correlated with growth, with rapid initial depletion of even carbon-number fatty acids and ultimately of all VFA. *P. putida* showed a shorter lag phase on zeolite-treated *Opuntia* fermentates than on untreated media, but again showed a preference for consumption of even carbon number VFAs with a particularly rapid initial decline in hexanoate concentrations.

P. putida was not found to grow on untreated blood fermentate with both a flat growth curve and no evidence of VFA depletion. Unlike in the untreated media, *P. putida* was able to grow on zeolite-treated blood fermentate, showing a broadly linear growth curve. Again, the experiment was terminated at 48 hours, despite growth curves not achieving a stable OD_{600}. VFA consumption patterns in blood-fermentate showed a preference for acetate, which was

depleted by 24 hours post-inoculation. While growth in this final condition did not run to completion, *P. putida* did not appear to consume isovaleric acid as a carbon source, and initial and final concentrations in the media were similar (0.421 ±0.008 g/L initial, vs 0.387 ±0.005 g/L final).

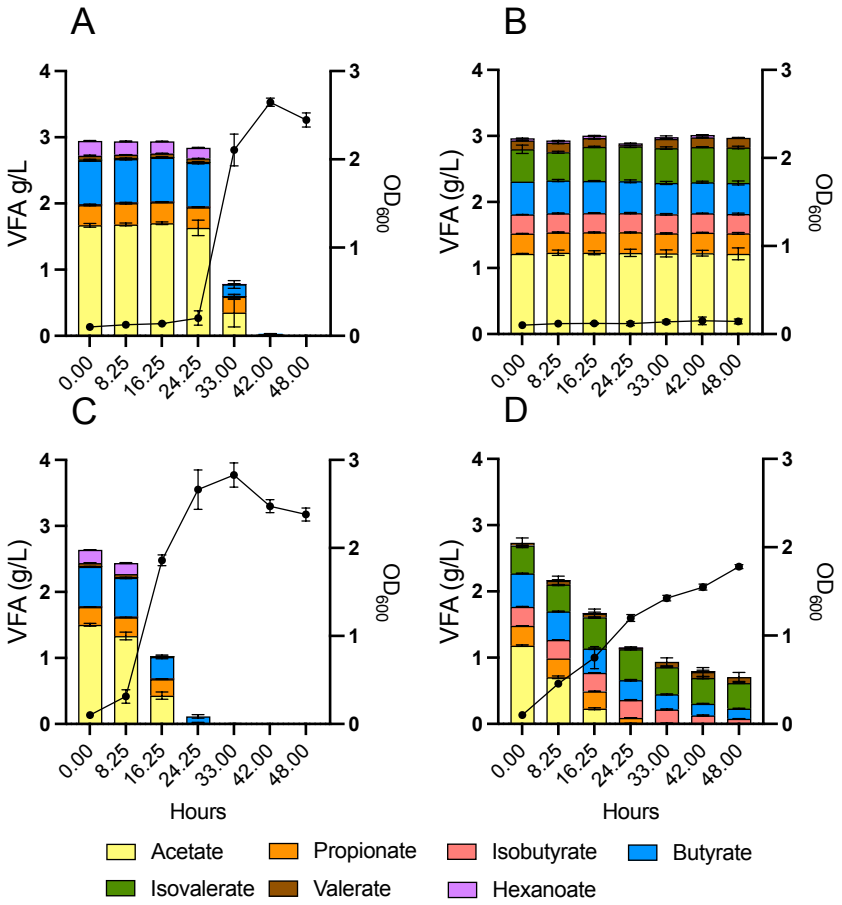


Figure 7.9: Growth and VFA consumption of *P. putida* on *Opuntia* and blood-derived fermentates with and without zeolite treatment. **A)** Untreated *Opuntia* fermentate, **B)** Untreated blood fermentate, **C)** Zeolite-treated *Opuntia* fermentate, **D)** Zeolite-treated blood fermentate. All data are given as means ± standard deviations of biological triplicates.

The compositions of PHA produced on each of the two zeolite-treated media at t=33 hours are given in **Fig. 7.10**. PHAs produced on each medium show a largely similar, C10 (3-hydroxydecanoic acid) dominant polymer composition, with significant contributions of both the C8 (3-hydroxyoctanoic acid) and C6 (3-hydroxhexanoic acid) monomers. The larger C11 and C12 monomers (3-hydroxyundecanoic acid and 3-hydroxydodecanoic acid, respectively) were also present in the range of 5-8% of the polymer mass.

The most significant shift between the two polymers is in the abundance of the C6 monomer, which was largely absent from PHAs produced from blood (<5%) but constituted 20.6 ±0.7% (w/w) of PHAs produced from *Opuntia* fermentate.

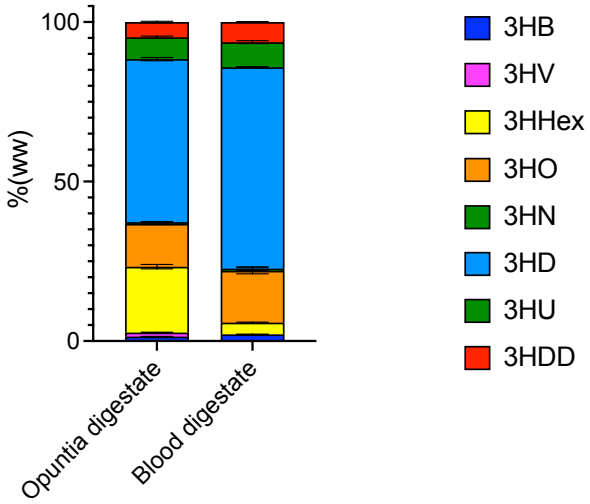


Figure 7.10: Monomer composition (mass basis) of PHAs produced by *P. putida* on *Opuntia* and blood-based fermentates treated with zeolite. All data are given as means ± standard deviations of biological triplicates.

7.2.3.3 Growth and PHA accumulation of C. necator on *Opuntia* fermentates subjected to various zeolite treatments

PHA production was also tested in *C. necator*, using the same *Opuntia* media as in **Section 1**, but with an appropriate degree of dilution to accommodate the lower VFA tolerance of *C. necator*. As will become clear, this experiment was unsuccessful for reasons which will be discussed. As such, the key results of this particular experiment are given below in a reduced form.

Figure 7.11 demonstrates the growth characteristics of *C. necator* on *Opuntia* fermentate media of various C:N ratios. The initial OD_{600} of these cultures was reduced from the intended 0.1 to just 0.03 due to inconsistent growth in preculture conditions, accordingly the time-zero OD_{600} values in this experiment are 0.03. Growth characteristics were nonetheless good across most conditions tested, with growth characteristics largely corresponding to those seen for *P. putida* in the same media. These features include a more biphasic growth seen in conditions with lower C:N, and a more linear growth profile seen in high C:N conditions. High C:N conditions also achieved lower maximum OD_{600} values than lower C:N media. The standard deviations of growth curves were however large, particularly in media of

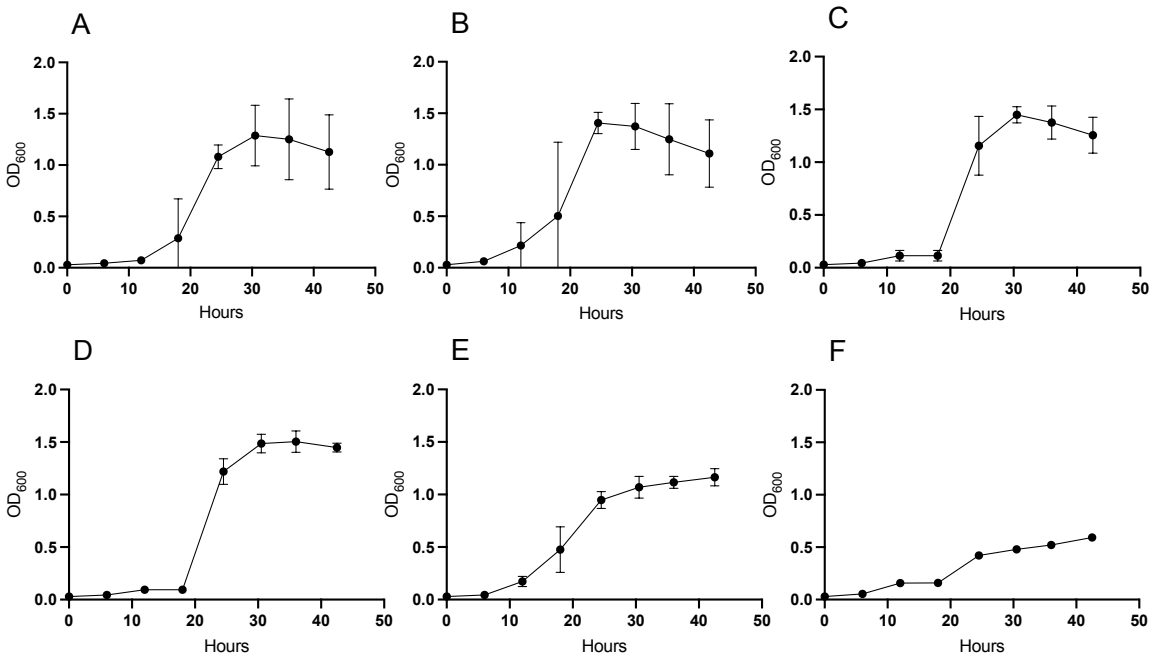


Figure 7.11: Growth characteristics (OD_{600}) of *C. necator* grown on acidogenic fermentates of varying C:N ratio. **A, B, C, D, E**, and **F**, correspond to ratios of 12.5, 13.5, 17.5, 26, 43 and 93.5 respectively. All data are given as means ± standard deviations of biological triplicates.

An initial analysis of PHA production across timepoints t=30 and t=36 hours was performed, the results of which are presented in **Fig. 7.12**. Interestingly, the same general trend in titres seen in *P. putida* was also identified in these figures, with maxima observed at a C:N ratio of 43. Unlike in *P. putida* however, yield maxima appeared to show a monotonic response to increasing C:N with the highest yields seen in C:N 93.5 conditions, though growth at this condition was poor (**Fig. 7.12 F**).

Significant noise was seen in both yield and titre data and at both timepoints. Unfortunately, the most severely affected sample appears to be the negative control (C:N 12.5). As a result of this, pairwise tests between treatment groups and the negative control were mostly insignificant, with the only a significant treatment effect on titre being observed at C:N 93.5 – a decrease. Yield data faired somewhat better, with significant improvements in PHA yield being registered in conditions of C:N 43 and 93.5, at both timepoints.

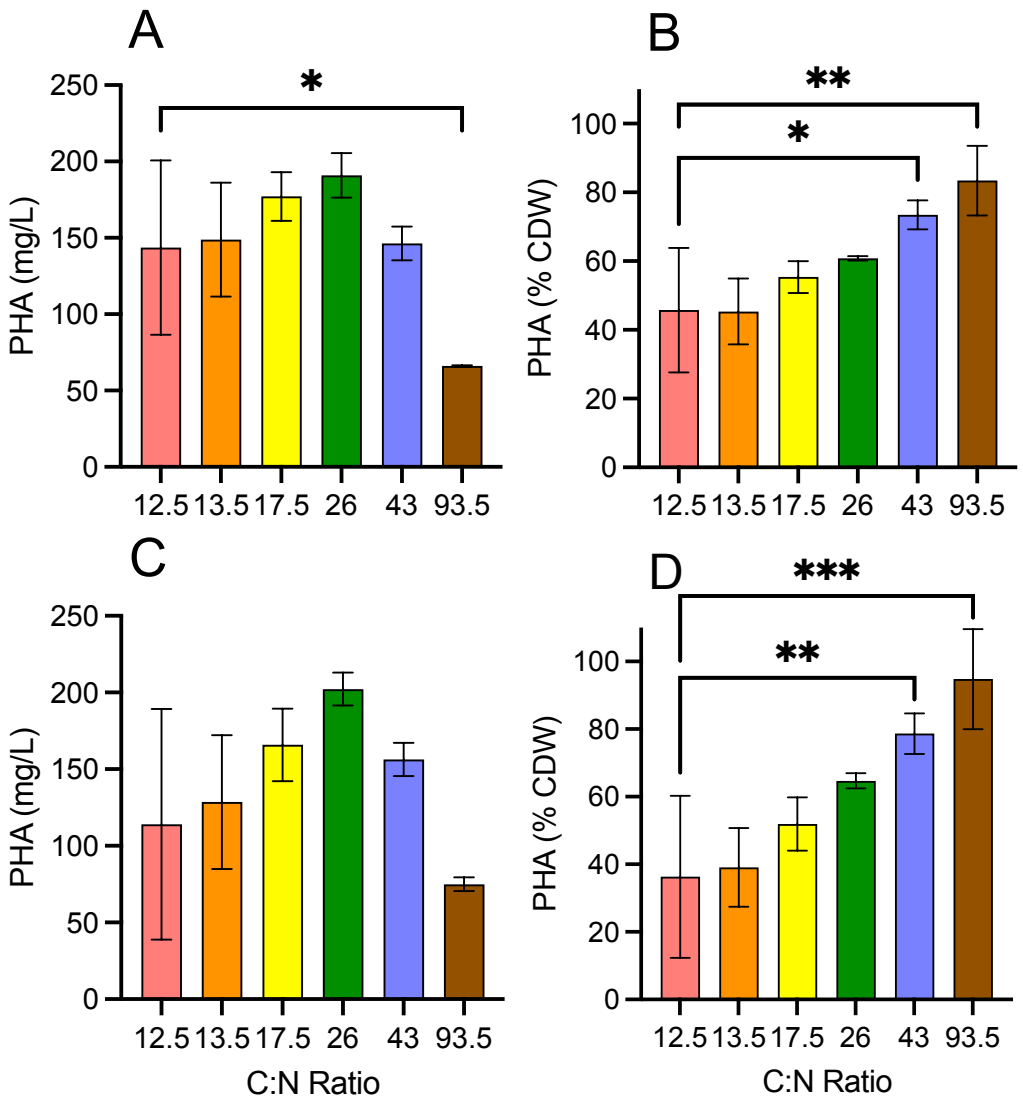


Figure 7.12: Statistical comparison of PHA titres and yields at timepoints t= 30 and t=36 hours. Panels **A**, and **B** show maximum titres and yields respectively for timepoint 30 (hours), with **C** and **D** showing titres and yields for timepoint 36. Comparisons of statistical significance of deviation of treatment groups from the untreated control performed using Dunnett's Multiple Comparisons Test. Non-significant comparisons have been omitted. All data are given as means ± standard deviations of biological triplicates

The data in **Fig. 7.12,** despite their noise, suggest a divergence in optimal C:N ratio between titre and yield measures, with maximum yields occurring at higher C:N than maximum titres. It is likely that the impaired growth of very high C:N ratios causes these conditions to exhibit lower titres, despite a higher PHA content as a percentage of CDW. This suggests that

the higher yields available at higher C:N need to be reconciled with the need for sufficient nitrogen to allow robust microbial growth.

Due to the noise issues identified with the above experiment, it was decided that a repeat experiment should be performed to be able to properly identify whether zeolite treatment has an effect on PHA production in *C. necator*. Due to time and material constraints, this was prepared in a reduced form, using a molasses-derived digestate. The results of this experiment are presented below in **Section 7.2.3.4**.

7.2.3.4 Growth and PHA accumulation of *C. necator* on molasses fermentates subjected to various zeolite treatments

Molasses fermentate was treated with zeolite as per the standard protocol performed in **Part 1**. The bulk parameters of the untreated and treated fermentates are shown in **Figure 7.13**. On a gram-per-gram basis, total organic carbon and total organic acid concentrations were found to be roughly equivalent. This deviates from the results in **Section 7.1**, in which organic acid concentrations (in g/L) exceeded those of total organic carbon. The absolute concentration of organic acids was approximately equal to that in the *Opuntia* fermentate, and the final growth medium was accordingly prepared to the same (20x) dilution as was used for *C. necator* growth on *Opuntia* fermentate.

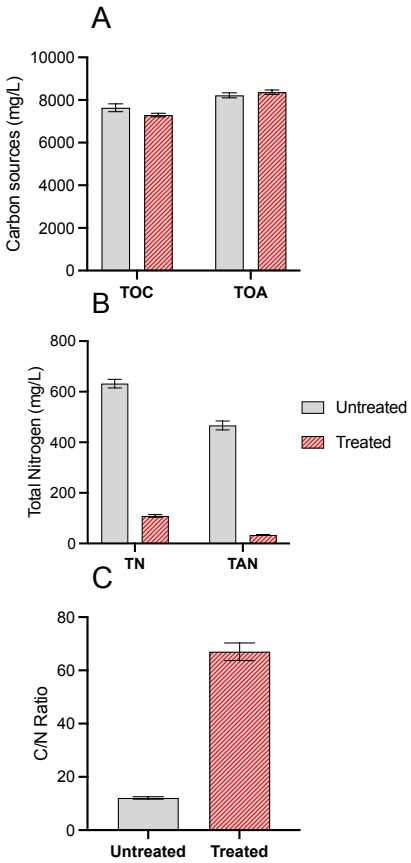


Figure 7.13: Bulk analysis of carbon and nitrogen composition of untreated and zeolite treated molasses fermentates. **A**: Concentrations of Total organic carbon (TOC) and Total organic acids (TOA), **B**: Total nitrogen (TN) and Total ammonium nitrogen (TAN), **D**: Carbon to nitrogen ratio (mass basis).

C. necator appears to have grown well on the diluted fermentate medium, showing rapid growth upon inoculation, with little lag phase. Growth and PHA production in both the untreated control and low-zeolite treated conditions (C:N 12 and 31) peaked at an OD_{600} of approximately 1.25, at 20 hours – corresponding to the point at which medium VFA was depleted (**Fig. 7.14B**), beyond which point they gradually declined. The maximum mean PHA titres observed in each condition in **7.14C** are again shown in **Fig. 7.15A**. In addition, **Fig. 7.15B** presents the maximum observed PHA yields in each of the three conditions in which PHA yield is calculated on a percentage basis against CDW.

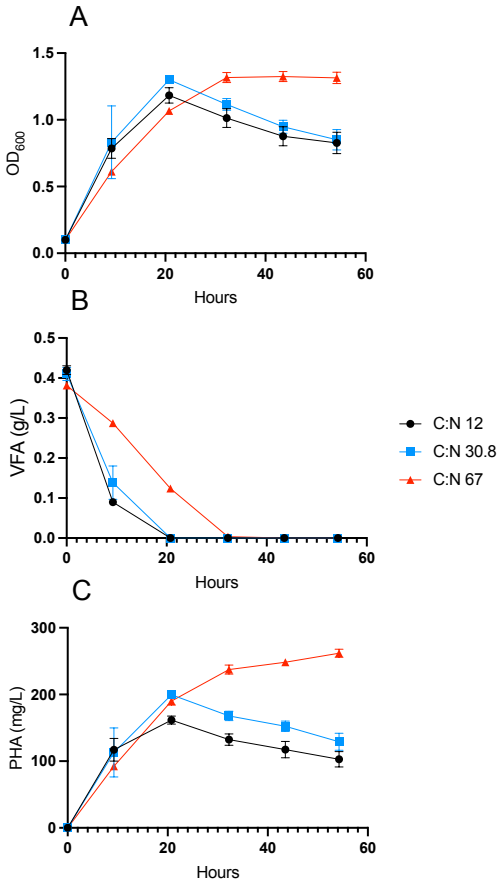


Figure 7.14: *C. necator* growth, fatty acid consumption, and PHA accumulation on molasses digestates of various C:N ratios. **A:** *C. necator* growth as measured by OD_{600} measurement from an initial OD_{600} of 0.1, **B:** Consumption of VFA by *C. necator* at various medium C:N ratios, **C:** Titres of PHA accumulation by *C. necator* across time at various medium C:N ratios. All data are given as means ± standard deviations as calculated from biological triplicates.

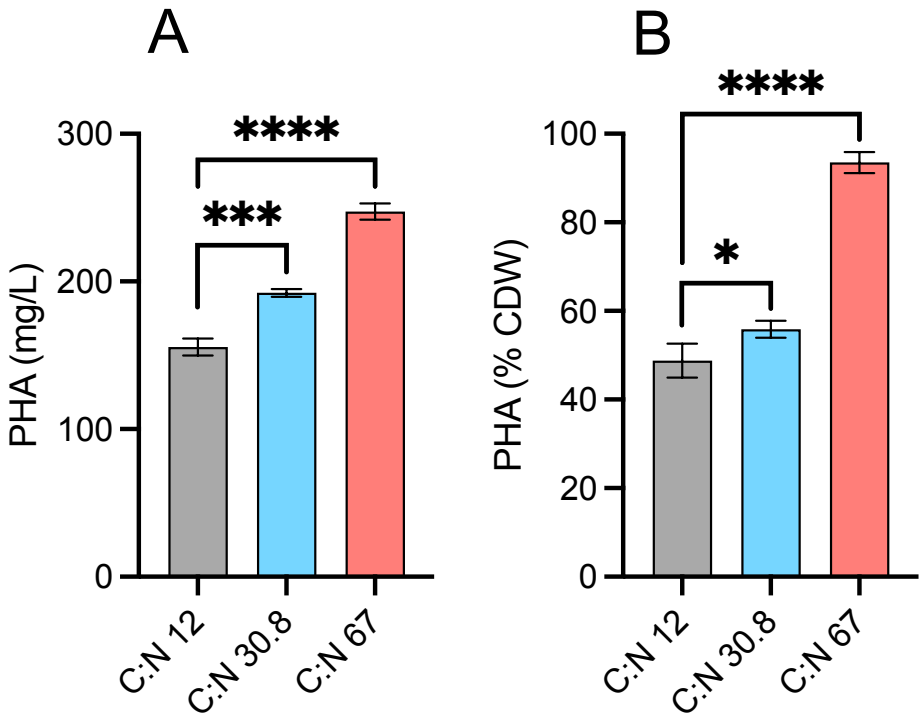


Figure 7.15: Statistical comparison of mean PHA titre and yield maxima across timepoints. Panels **A**, and **B** show maximum titres (g/L) and yields (g_{PHA}/g_{CDW}) observed, respectively. All data are given as the means ± standard deviations of biological triplicates. Pairwise tests of statistical difference between control (C:N 12) and treatment groups shown in figures were determined by Dunnett's Multiple Comparisons Test.

PHA titres and yields in the control achieved maxima of 156 ±6 mg/L and 49 ±0.04 % CDW, respectively. Pairwise significance tests between means of treatment groups and the negative control found all comparisons to be statistically significant at at least the 5% level. Maxima in the lightly-treated condition (C:N 30.8) were 192 ±3 mg/L ($p = 0.0002$), and 56 ±0.02 % CDW ($p = 0.0379$), while in the heavily zeolite-treated condition (C:N 67) they were calculated as being as high as 247 ± 5 mg/L ($p < 0.0001$) and 94 ±0.02 % CDW ($p < 0.0001$), indicative of a significant increase in both titre and concentration of PHA in both treated conditions.

7.2.4 Discussion

7.2.4.1 *P. putida* growth on OLE and *Opuntia* fermentate

While the growth of *P. putida* on OLE was demonstrated, it also showed a much-reduced ability to clear SCOD from the OLE media as compared to *Opuntia* fermentate,

clearing just 31 ±2% of SCOD from OLE as compared to 74.8 ±0.9% of SCOD removed from fermentate media. This is consistent with predictions made in the introduction to this section which suggested that the heterogeneity of carbon sources in the OLE media would likely render a large fraction of these unusable by *P. putida*. This effect provides a strong argument for the fermentation of *Opuntia* biomass prior to its use in PHA production. This is before even considering the insoluble fraction of the *Opuntia* biomass which is completely unavailable to *P. putida* without some kind of hydrolytic or fermentative pre-treatment.

These admittedly limited results were taken to fall sufficiently in favour of the fermentative approach that the investigation of OLE as a medium for PHA production was not investigated further. This should not be taken as a conclusive argument against its future investigation, as various scenarios could be envisaged in which it might be made to work. It was just not deemed an urgent enough concern to warrant further investigation within the course of this thesis.

7.2.4.2 *P. putida* PHA production on *Opuntia* and blood-derived fermentates

Growth of *P. putida* on blood fermentate was unsuccessful in the absence of zeolite treatment, likely due to ammonium toxicity. With zeolite treatment, *P. putida* was able to achieve comparable growth on blood fermentate (up to nearly OD_{600} of 2) as to on *Opuntia* fermentate. This is significant as it opens the possibility that fermentates derived from protein-rich wastes such as from the dairy, meat, fish, and tofu industries, or from sewage sludge [180, 181] could be valorised as media for PHA production.

The compositions of PHAs produced on both *Opuntia* and blood fermentates were largely comparable, with a C10-rich polymer being produced in both conditions. This is consistent with the findings of Dartiailh et al. [79] which found *P. putida* to process C2-C5 fatty acids into a largely generic PHA monomer via a central metabolic route. This paper argued that fatty acids of 6 or more carbons could be incorporated directly into PHA monomers of equivalent length. This is the likely explanation for the biggest observed difference between the PHAs produced from *Opuntia* and blood fermentates, which was the high abundance of the C6 monomer in *Opuntia*-fermentate conditions, as compared to blood-fermentate conditions. As can be seen in **Fig. 7.8**, hexanoate was largely absent from blood fermentate but constituted nearly 10% of *Opuntia* fermentate VFA and appears to have been incorporated directly into the PHA polymer without undergoing a change in carbon number. Aside from modulation of the abundance of the C6 monomer, manipulation of the VFA profile of the acidogenic fermentate

appears to have had little effect on PHA polymer composition. The (C2-C6) product spectrum achievable through AF appears too narrow to allow for an appreciable customisation of PHA polymer structure.

In the manuscript in **Section 7.1**, it was observed that PHAs produced at earlier timepoints contained higher fractions of (C6) 3-hydroxyhexanoic acid monomers than polymers produced at later timepoints. It was proposed that the reason for this could be that hexanoic acid was preferentially consumed among VFAs, meaning it provided the majority of carbon at early timepoints, and was therefore directly incorporated into the PHA polymer as 3HH monomers. This appears to be supported by the results of this subsequent experiment in which the consumption patterns of individual VFAs by *P. putida* were observed. In **Fig. 7.9** hexanoate can be seen to deplete rapidly at early timepoints in both *Opuntia* conditions, suggesting it is preferentially consumed by *P. putida* ahead of other, especially C3 and C4 VFAs.

In blood fermentates, isovaleric acid was not seen to be effectively cleared at any significant rate by *P. putida*, though *P. putida* is documented as being able to utilise isovalerate as a carbon source [182]. Isovalerate is a common fermentation product arising from Stickland degradation of amino acids [81], and thus strategies to valorise protein-derived fermentates need to be able to accommodate it. An extension of this growth curve may have allowed isovalerate consumption to be observed, though as discussed earlier, issues with fermentate precipitation became pronounced at later timepoints, making determinations of OD_{600} and CDW less reliable.

7.2.4.3 *C. necator* PHA production on zeolite treated *Opuntia* fermentates

The attempt to replicate the successes of the *P. putida* experiments of **Section 7.1** with *C. necator* were largely unsuccessful due to the high noise of the negative control. It is possible that the noise in these samples derives from issues with the preculturing step, which in this experiment saw highly inconsistent growth across biological triplicates. In order to maintain a true biological triplicate, the initial OD_{600} of experimental cultures was reduced to 0.03 to accommodate the least grown of the three precultures. This may have introduced error, as while cultures were all inoculated to equivalent OD_{600} values, the respective precultures may have been at different growth phases upon inoculation.

While not statistically significant, the general trends observed from *C. necator* grown on zeolite treated *Opuntia* fermentates were largely corroborated by the far more robust data

achieved from later bioproduction experiments in molasses fermentates. These observations were those of an increase in both titres and yields in zeolite treated fermentates and of a monotonic increase in yields with increasing C:N in the 10-100 range.

7.2.4.4 *C. necator* PHA production on zeolite-treated molasses fermentates

The experiments examining PHA production in *C. necator* in *Opuntia* fermentate produced results suggestive of an improvement in PHB yield through application of zeolite treatment to the fermentate. Mean PHA titres were higher in moderately zeolite-treated fermentates than in the negative control, or in the most heavily zeolite-treated conditions – which mirrors the results seen in *P. putida*. However, noise in the negative control, and to a lesser extent in the zeolite treatments, combined with what appears to be a more muted treatment effect than was observed in *P. putida* experiments prevented these results reaching a level of statistical significance that would allow any solid conclusions to be drawn. Further experimentation was thus required to draw conclusions as to the effect of zeolite-treatment of acidogenic fermentates on PHB production in *C. necator*.

Bioproduction of PHA was attempted in *C. necator*, using a molasses fermentate as the carbon and nitrogen source. The fermentate was treated with zeolite to induce nitrogen limitation and several C/N ratios, corresponding to differing degrees of zeolite treatment were analysed. The molasses digestate used in this experiment was prepared using the standard protocol used in **Section 7.1** for the preparation of an *Opuntia* fermentate. Molasses was selected as the substrate for this digestion in part because of its high solubility which was expected to lend it a high degree of anaerobic degradability. Despite this, the bulk parameters of the molasses fermentate as seen in **Fig. 7.13** show features suggestive of an incomplete digestion process. First among these is the organic acid concentration, which despite an initial substrate loading comparable to that of the *Opuntia* fermentate in **Section 7.1** and the more soluble nature of the molasses feedstock, was found to be lower a lower than in the *Opuntia* fermentate (~8.2 g/L as compared to ~11 g/L of acetate equivalent).

The approximate equivalence of TOC and organic acid concentrations on a gram-to-gram basis tends also to suggest an incomplete digestion (**Fig. 7.13A**). In a ‘complete’ acidogenic fermentation process, to the extent that such a thing exists, nearly all soluble carbon could be expected to be present as VFA. As a significant fraction of the mass of VFA consists of elements other than carbon (oxygen and hydrogen), it could be expected that the concentration of organic

acids (mg/L) should thus exceed that of total organic carbon, as was seen in the parameters of the bulk *Opuntia* digestate in **Section 7.1**. This was not the case for molasses digestate, in which the two values were similar. Indicating a lower fraction of carbon present as VFA than might have been expected.

Further evidence of an incomplete digestion can be seen in analysis of the nitrogen sources in **Fig. 7.13B**. In molasses digestate, total nitrogen exceeded total ammonium nitrogen quite significantly, indicating a notable fraction of soluble nitrogen was present in a non-degraded form (possibly as soluble protein, amino acids, or other nitrogen compounds). This contrasts with the *Opuntia* fermentate in **Section 7.1.**, in which total nitrogen and total ammonium nitrogen concentrations in untreated fermentate were approximately equal, suggesting almost all soluble nitrogen present was in the form of ammonium – the terminal form of nitrogen in anaerobic degradation processes for most nitrogen compounds.

The cumulative effect of this apparently incomplete fermentation and the associated lower ammonium concentration seems to have been to mute the treatment effect of zeolite. In this molasses experiment, despite treatment with an equivalent dose of zeolite to the fermentate in **Section 7.1**, a maximum C:N ratio of just 67 was achieved, as compared to the C:N of 93.5 achieved in **Section 7.1**. This limited the range of C:N ratios that could be tested as increasing the C:N significantly beyond 67 could only have been achieved through supplementation with additional carbon, which was antithetical to the rationale behind zeolite use. Two possible hypotheses could explain this lower VFA yield. One lies in the AD sludge inoculum community used for this particular fermentation, which unlike those used in earlier chapters, and in **Section 7.1**, was not sourced fresh immediately prior to commencing the fermentation, and was instead stored for several weeks prior to use. This extended storage may have led to lower activity and to incomplete fermentation. Another, in the opinion of the author, far more likely explanation lies in the rapid acidification of the fermentation, which despite starting at an initial pH of 8.0 could have dropped to a low pH (<5.0) during fermentation which would have terminated fermentation prior to depletion of the available feedstock.

These issues however do not seem to have significantly impeded either the growth or production of PHA by *C. necator* on medium produced from this digestate. In fact, *C. necator* showed rapid growth in all zeolite treatment conditions with growth curves even lacking the lag phase seen in P. putida experiments, which may have been facilitated by the presence of unfermented sugars, which could have supplemented the VFA as an additional carbon source.

While a detailed metabolomic characterisation of the media might have been excessive for the purposes of this experiment, it might have been valuable to experimentally quantify the SCOD of the medium to estimate the abundance of non-VFA feedstocks. The presence of such additional carbon sources would nonetheless have been accounted for in the C:N ratio calculations performed in **Fig. 7.13C**, as TOC was determined experimentally.

The most important results of this experiment become evident from **Fig. 7.14C**, in which titres in both zeolite-treated conditions exceed those in the negative control at all timepoints from t=21. An even greater bifurcation in titres occurs from t=32 after which point PHA titres are highest in the most heavily treated, C:N 67 condition. The improvement in PHA titres with zeolite treatment is most clearly shown in **Fig. 15A**, which compares the PHA titre maxima observed for each treatment across all timepoints. Titre maxima of 156 ±6, 192 ±3, and 247 ±5, mg/L PHA were observed for the negative control, and the two zeolite-treatments of C:N 31 and C:N 67, respectively.

PHA yields (%CDW) are similarly higher in zeolite-treated conditions than in the negative control, with the C:N 67 condition in particular showing nearly double the yield of the negative control. Noise levels around these means were low, as indicated by their standard deviations, indicating very good agreement between the biological triplicates. This allowed pairwise tests to confirm the statistical significance of the differences between all treatment means and that of the control. Even where the absolute difference in means was low such as between the mean yields in control and C:N 30.8 treatment, this difference was resolvable and found to be significant at the 5% level ($p<0.0379$).

It must be said however, that the yield values calculated for the C:N 67 condition, which find PHA to constitute 93.5% of CDW, somewhat defy credibility. That being said, precedent does exist in the literature for values of this magnitude, such as in Passanha et al. [124], which reported PHA yields of 84 and 90% of CDW in *C. necator* grown on two different blends of VFA-supplemented AD digestates. In this case, the anaerobic digestate used was sourced from a methanogenic AD reactor and so contained no endogenous VFA, which was added as a 1:1 blend of acetic and butyric acids. The end result, however, was a culture condition largely analogous to that used in this experiment, and from which similar results were obtained.

If the 93.5% yield figure in the C:N 67 condition is not to be believed, it is worth considering how such a figure was achieved, by considering the possible limitations of the

analytical methods used to arrive upon it. The most likely source of 'error' that could lead to an overestimation of PHA yield seems to be the gravimetric method used to calculate CDW. Given the very low concentration of the growth medium, required by the VFA-sensitivity of *C. necator*, and the volume constraints imposed by flask size and incubator space, the samples taken at each timepoint were limited to 10 mL of liquid culture. These yielded cell pellets of just several milligrams, at the low end of what the available analytical balance could reliably measure. While the PHA titre data, calculated by GC-FID, may be considered highly robust - the CDW numbers used for calculation of PHA yield are perhaps less reliable.

However, even the least charitable interpretation must admit that the differences between individual treatment group means can be statistically resolved with high confidence, even if the validity of these numbers in an absolute sense is perhaps less certain. Returning to the central hypothesis: these data strongly support the hypothesis of an improvement in PHA yields from *C. necator* upon zeolite treatment for both the light ($p=0.0379$) and heavy zeolite treatments ($p<0.0001$) tested. Caution should however be exercised when using these yield numbers as absolute values.

Unlike the results with *P. putida*, in which moderate C:N ratios were found to give higher PHA production than very high values, this experiment was operated within a narrower range of C:N values, which in large part arise from limitations with the fermentation which have been extensively discussed. The highest production values were found in this experiment at the highest C:N ratio tested (C:N 67), though it is possible that the true optimum for PHA production in *C. necator* lies beyond this value. It is thus not possible to say that the value of C:N 67 represents any sort of global maximum in PHA production values with the data available.

Any future experiment investigating this question would do well to take two lessons from this experiment, **1.** It should include a broad enough range of C:N values as to go beyond the optimum C:N, and **2.** It should significantly increase liquid sample volumes to ensure cell pellets are large enough to derive credible CDW numbers to confidently determine yield values.

7.2.5 Conclusion

Bioproduction of PHA (PHB-co-PHV) in *C. necator* was measured on an acidogenic fermentate produced from molasses, which had been subjected to various zeolite treatments to increase its C:N ratio. An untreated negative control medium with a C:N of 12 was compared to two zeolite-treated media with C:N ratios of 31 and 67. Both titres and yields of PHA were

maximal in heavily treated media with a C:N of 67, strongly indicating that zeolite treatment of acidogenic fermentates is a feasible strategy to improve bioproduction of PHAs in *C. necator*. These results provide the first evidence of this zeolite treatment effect in the production of short-chain polyhydroxyalkanoates, suggesting this as a possible route for their production from low-cost carbon sources.

Chapter 8. Future directions

Over the course of the preceding five chapters, multiple issues and areas of possible future investigation were identified. These questions were either not pursued within the scope of this thesis, were attempted, but failed for one or more reasons, or are being actively pursued at the time of writing. These may broadly be grouped into two areas: short-term lab-scale experiments arising directly from the studies in this thesis, which might reasonably be pursued by a future doctoral student, and questions arising in the field not directly related to the research herein, but from whose solution the field would nonetheless benefit. Both are covered in the following section and could provide starting points for future experimentation in the field for researchers wishing to build on the findings of this thesis.

8.1.1 Chapter 3 and the "Acetate Parabola"

Chapter 3 "Anaerobic co-digestion of *Euphorbia tirucalli* with pig blood for volatile fatty acid production" explored the production of VFA from *Euphorbia tirucalli* through addition of various concentrations of blood as a high-nitrogen co-substrate. A key finding of this experiment was that titres of acetic acid were maximal in co-digestions containing either 50 or 75% of substrate as blood. When graphed against co-substrate loading, this gave a broadly parabolic trend in acetate titres. This parabolic relationship was found to become more pronounced at higher substrate concentrations, and to decay to approximate linearity at low concentrations. It is unknown from this experiment whether this interesting observation is unique to the specific feedstocks and parameters explored in this one experiment, or whether it represents a more generalisable principle governing interactions between feedstocks.

An experiment established in collaboration with Dr. Laura Martin is currently attempting to explore this question. This experiment replicates the experimental setup of **Chapter 3** but uses Agave as the low-nitrogen feedstock in place of *Euphorbia*. It then employs three different protein sources as high-nitrogen co-substrates (blood, whey, and soy protein – selected as approximations of wastes from the meat, dairy, and tofu industries, respectively) to identify whether a similar parabolic response can be observed in co-digestions of Agave with these three protein sources.

One hypothesis as to the underlying mechanism of this 'acetate parabola' is that it is driven at least in part by the accumulation of ammonium, which occurs to a higher degree at higher substrate concentrations. To address this, a fourth condition is included in this experiment

in which the entire agave-blood co-fermentation experiment is replicated but with the addition of zeolite directly to the reaction mix, to absorb ammonium as it is released. The hypothesis here is that if the addition of zeolite reduces the magnitude of the parabolic response, then this will provide evidence to implicate ammonium concentrations as a likely causative variable.

8.1.2 Matters arising from Chapter 4

The experiments in **Chapter 4** explored several CAM and non-CAM crops as feedstocks for acidogenic fermentation using two distinct microbial communities – AD sludge and rumen fluid. The findings of this experiment largely corroborate arguments in the literature for the relatively high degradability of CAM biomass, as compared to non-CAM. However, contrary to these studies, this outperformance was not found to be explained by the low lignin content of the CAM biomass, but rather by its lower fibre content (as measured by NDF), or the corollary of this measure – a higher content of soluble organic material.

8.1.2.1 Expansion of the CAM question – Employing a targeted "biorefinery" approach

The panel of feedstocks investigated in this experiment was somewhat limited, covering three CAM and three non-CAM feedstocks. This is insufficient to make general statements about the preferability of CAM crops to non-CAM as the "CAM" category alone contains over 16,000 distinct species. Despite this, several key principles were salient, namely that CAM biomass appeared less fibrous than non-CAM and that this appears to have been correlated with higher VFA yields upon fermentation.

The treatment given to Agave within this chapter represents, perhaps, a template for how future investigations of CAM might proceed. Both whole Agave leaves and the pulp remaining after fibre extraction were explored as AF substrates. In this latter example, AF is envisaged as a secondary stage in Agave valorisation after fibre extraction, seating it within the context of a broader cascade of products derived from the initial feedstock. This both allows the isolation of the high-value fibre fractions prior to fermentation, improving overall process economics, but also removes the least degradable fractions from the feedstock prior to fermentation. Placing AF studies within such a biorefinery context allows these inter-process synergies to be more deeply explored. Thus, perhaps the path forward for CAM-based AF is to focus more on deep process optimisation around key target crops (such as Agave, pineapple, and *Opuntia*), rather than to attempt to identify general principles around broad classes such as "CAM". One could envisage, for example, a similar, integrated biorefinery system for the processing of pineapple waste. This could make use of the 'piña' cloth, produced in the

Philippines from pineapple leaf fibres as a secondary product, whose extraction from pineapple leaves renders the remaining biomass yet more amenable to AF. The optimisation of the following value chain could provide a valuable avenue of research:

Pineapple fruit harvested → Piña cloth from leaf waste → AF of leaf pulp → PHA from VFA

8.1.2.2 Exploring the basis of observed yield differences between inocula

This work also identified a considerable difference in degradation kinetics between the two microbial communities tested, in particular finding yields of VFA in sludge to be higher than in rumen fluid. This finding was perhaps slightly contrary to expectation, as rumen fluid might reasonably be expected to show better performance on fibrous lignocellulosic substrates, which closely mirror its natural substrate. No explanation for this divergent performance was forthcoming from metagenomic analyses, and future work should be undertaken to explore two points: **1.** Whether AD sludge consistently outperforms rumen fluid in AF experiments, and **2.** The basis of this divergence.

Perhaps the most likely explanation for this observation is a difference in the absolute abundance of microbes in each community. While the doses of each inoculum were normalised on a volatile solids basis, it is possible that absolute microbial abundance per unit of VS was not equal between the two. The VS-normalisation approach employed here may thus not have provided an equally abundant microbiome to each condition. The ideal solution would be to perform either a replication of the experiment in this chapter, or at least some type of pairwise comparison between the two inocula, in which initial inoculum dose was normalised to absolute microbial abundance. This easier said than done, as anaerobic microbes are not particularly amenable to culturing for plate-count methods, though NGS methods do exist which could permit this normalisation [183].

A simpler alternative could be to analyse the degradation of a given dose of substrate at a range of inoculum loadings with each inoculum. Presumably, such an approach would permit the identification of the absolute yield maxima permitted by each inoculum without requiring prior knowledge of microbial abundance. Care would have to be taken to account for the introduction of additional volatiles at higher inoculum loadings, though this could be achieved through the use of appropriate controls, or by standardising the dose of inoculum volatiles in each condition through the addition of carefully calibrated doses of sterilised inoculum.

It is important that an explanation for this yield divergence be found, as the lower VFA yields seen in rumen fluid provide a strong argument against its use as an inoculum for AF purposes.

8.1.3 Exploring *Asparagopsis* inhibition of sludge methanogenesis

The experiments in **Chapter 5** explored the use of the seaweed *Asparagopsis taxiformis* as a possible methanogenesis inhibitor for application in industrial biorefinery. Much as in **Chapter 4**, the results here were found to depend heavily on the choice of inoculum, with *Asparagopsis* providing effective inhibition of methanogenesis in rumen fluid but not in AD sludge. These results suggested *Asparagopsis* could provide effective inhibition in rumen-driven reactor conditions. However, the significance of this conclusion for the industrial biorefinery is somewhat limited when taken together with the results of **Chapter 4**, which showed poor VFA yields in rumen-driven configurations. If the yield differential between rumen and sludge reactors in **Chapter 4** can be explained and resolved as proposed, this will automatically have implications for the applicability of *Asparagopsis* to industrial biorefinery.

The difference in inoculum sensitivity to *Asparagopsis* might however also be explained through comparison of the findings of **Chapters 4** and **5**. If the hypothesis of a difference in absolute microbial abundance explains the higher yields seen with sludge in **Chapter 4**, this may also explain the lower sensitivity of sludge to *Asparagopsis* treatment seen in **Chapter 5**, especially as both experiments were designed along similar lines, with inoculum doses standardised on a VS basis. Bromoform is understood to represent the active ingredient in *Asparagopsis*, and to inhibit methanogenic mechanisms universal across methanogens. Thus, it seems less likely that *Asparagopsis* inhibition is specific to rumen microbes, and more likely that its minimal inhibitory concentration varies between the two inocula.

The next experiment to run would thus be to identify the dose at which *Asparagopsis* can effectively inhibit methanogenesis in sludge. Treatment doses were capped at 10% of substrate volatiles in the **Chapter 5** experiments, and future experiments should explore a wider range of concentrations. It would also be valuable to vary inoculum concentrations to understand the relationship, if any between *Asparagopsis* dose and inoculum concentration, on the efficacy of *Asparagopsis* as an inhibitor; if microbial abundance explains the higher MIC of *Asparagopsis* in sludge, then this may be resolved through simple dilution of the sludge. It should be mentioned that Gompertz models of gas production in rumen fluid showed a slight shift in lag phase at sub-inhibitory *Asparagopsis* concentrations. In sludge conditions treated at

the maximum dose (10% of substrate vs), AD sludge conditions also showed a similar slight shift in lag phase which suggests that the inhibitory concentration may lie just beyond the maximum concentration tested in this study. Experimentally validating the efficacy of *Asparagopsis* in sludge would immediately broaden its possible applicability to a range of industrial biorefinery applications and it is very important that this experiment be run to validate the possibility of its use as a methanogenesis inhibitor in sludge.

Experiments should also be conducted to identify the tendency of initially *Asparagopsis*-responsive inocula to acclimate to its presence over time, as this would inform the design of strategies for its use in industrial applications. This might take the form of a batch experiment in which the *Asparagopsis*-acclimated community of one batch fermentation provides the inoculum for a subsequent batch fermentation or could take the form of a fed-batch experiment, in which *Asparagopsis* and substrate are co-fed, and inhibition quantified against an appropriate control over time.

Even if inocula demonstrate a tendency to acclimate, a possible strategy is suggested in **Chapter 5** to combat this. This involves the use of *Asparagopsis* only as a transient inhibitor used to initiate acidogenic fermentation, after which point methanogenesis is controlled through the accumulation of VFA. A fed-batch experiment could be run to validate such a system before its wider use at scale.

8.1.4 Matters arising from Chapter 6

Chapter 6 analysed the application of zeolites to remove ammonium from acidogenic fermentates and thereby induce an increase in their C:N ratios to enable bioproduction of high-value storage lipids. Zeolites were highly effective at removing ammonium from fermentates, and showed great specificity for the ammonium ion, with no depletion of the VFA carbon source observed. The nitrogen depletion provided by zeolite thus manifested as an increase in C:N ratio.

Both batch and continuous zeolite treatment systems were explored, and the preliminary efficacy of a zeolite chromatography system was demonstrated. Promising as these results are, they leave considerable room for future process optimisation as explored below.

8.1.4.1 Identifying the source of zeolite inhibition by fermentate

Zeolites were observed to provide more effective ammonium depletion in pure ammonium chloride solution than in fermentates of equivalent ammonium concentration. This is suggestive of undefined inhibitory processes, which are hypothesised to take one of two forms: **1.** The presence of other (primarily metal) cations in solution which compete for ammonium binding sites, or **2.** Biofouling or blockage of the microporous structure of the zeolites, reducing their effective surface area. This problem was also identified by Farkaš et al. [155], who analysed the exchange of ammonium onto clinoptilolite in both a landfill leachate and a model ammonium solution of equal concentration. Ammonium binding capacities of 4.2 mg/g and 17.7 mg/g zeolite were registered in the leachate and model solution, respectively. Bolan et al. [161] similarly reported zeolites with a high cation exchange capacity (of up to 20.4 mg NH_4^+/g) to bind significantly less than this theoretical maximum in wastewaters containing competing cations.

Small particulates in the fermentate may additionally clog the microporous structure of the zeolites, effectively reducing their surface area. This was suggested by Farkaš et al. [155] as possibly explaining some of the observed underperformance of zeolites in wastewaters. Future experimentation might investigate whether the biofouling issue could be managed through either filtration or flocculation of the fermentate, to remove particulates prior to zeolite treatment.

8.1.4.2 Zeolite reusability

It would be valuable, having acknowledged the biofouling concerns raised above, to test the reusability of zeolites used to treat fermentates. A sequential batch binding experiment could be performed in which zeolites are used to deplete a fermentate of ammonium, are re-equilibrated with NaCl and again used to deplete a fermentate. This process could be repeated several times and the ammonium depletion kinetics measured in each batch to determine the binding capacity and association rate per gram of zeolite, from which it could be determined if any degradation in binding capacity was evident. Evidence from Bolan et al. [161] is quite promising on this question. This study applied zeolites to remove ammonium from fellmongery (tannery) wastewaters and found leaching with 0.5 M HCl to completely restore the NH_4^+ binding capacity of the zeolite, with no detectable reduction in binding capacity even after 12 cycles of regeneration.

Not all wastewaters are equivalent however, and if biofouling is found to be a problem for zeolites in fermentate, several approaches may be tested as possible solutions. Zeolite recovery/ ammonium elution under either acidic or basic conditions (using perhaps HCl, NaOH, or KOH) may allow removal of contaminants in parallel with binding site recovery. Alternatively, fermentate pre-treatments, as introduced above may be tested. In a continuous, or chromatography-style system a sacrificial guard column could be added, with the obvious caveat that such interventions entail increased process costs.

8.1.4.3 Testing various zeolites for their binding capacity in fermentate

Experiments in **Chapter 6** and **7** were conducted using a naturally occurring clinoptilolite zeolite, selected for its abundance and low cost. A binding capacity of 4.9 mg NH_4^+-N (or 6.3 mg NH_4^+) per gram of zeolite was calculated in Agave digestate. A comparable binding capacity of 4.2 mg NH_4^+/g zeolite was identified by Farkaš et al. [155] when treating landfill leachates with clinoptilolite. Literature values exist suggesting much higher binding capacities to be possible, with selected studies reviewed in Wang and Peng [184] reporting values as high as 22.9, 26.3, and 30.6 mg NH_4^+ /g zeolite. These higher numbers typically derive from studies under more 'ideal' conditions in which the effect of competitor ions and biofouling were minimal.

Nonetheless, multiple natural, and yet more synthetic zeolite frameworks exist [150] and these should be evaluated for their binding capacity and more general suitability to ammonium depletion of fermentates. Overcoming the issue of zeolite underperformance in fermentates may simply be a case of sampling the available frameworks and selecting those zeolites for which their performance in fermentate most closely matches their performance in a model solution.

An alternative solution to increasing ammonium removal in fermentates is proposed by Watanabe et al. [185], who used hydrothermal modification of naturally occurring mordenite and clinoptilolite zeolites to roughly double the binding capacity of these materials. The same approach was successfully used by Bolan et al. [161]. It would be valuable for future investigations to evaluate these modification processes on zeolites for use in anaerobic fermentates, as these offer a simple route to greatly improve process efficiency. Because this treatment is required just once to increase media binding capacity, it has an economic advantage over fermentate pre-treatments in that its fixed cost can be amortized over many cycles of

fermentate treatment. This is particularly the case if the high reusability figures of Bolan et al. [161] can be validated in fermentates.

8.1.4.4 Alternative eluents

The final section of **Chapter 6** raised the question of recovering zeolite-bound ammonium in a usable and marketable form. A solution was proposed in which potassium salts act as the eluent to produce a solution which might find a market as (potassium/ammonium phosphate) fertiliser. Moreover, it was suggested that the potassium (or cations more generally) for this elution process might be provided by the inorganic fraction of the undigested biomass waste produced by the AF process, a fraction which currently sees little use beyond its use as compost. While a preliminary, proof-of-concept experiment was performed with pure chemicals, this question was not explored experimentally in any detail and significant room remains here for process optimisation.

Biomass ash varies considerably in its composition and will depend on such parameters as the composition of the original biomass, the treatments (such as AF) to which it is subjected, and the temperature at which it is combusted [168, 186]. It would be valuable to isolate the solid waste fraction produced from fermentate clarification, subject it to combustion at various temperatures, and analyse the resultant ash (through either flame photometry, or inductively coupled plasma mass spectrometry) for its content of metal cations. Once this is understood an assessment may be made as to whether this, once appropriately solubilised, may provide a useful and cost-effective eluent.

8.1.4.5 Zeolite chromatography optimisations

Experiments with a novel zeolite chromatography system detailed in **Chapter 6** demonstrated the principle of zeolite-based ion-exchange chromatography for ammonium removal from fermentates. Here too, significant room for improvement exists. In chromatography both the binding capacity and binding rate of the stationary phase are of importance, as faster rates of ammonium association with, and disassociation from, the zeolite medium will permit increased fermentate flow rates and increase overall system processivity.

It is likely that zeolite particle size plays a significant role in defining this binding rate, as smaller particles could be expected to saturate more quickly as diffusion into the internal space of the particles would be more rapid. This should be explored in detail experimentally.

Modifications to the system which permit a sharper (and therefore more concentrated) ammonium elution peak to be obtained will significantly improve the economics of ammonium recovery from the zeolite column, as this will minimise volume of eluent to be concentrated. Experimental modifications of zeolite particle size, microporous structure, and binding capacity, as well as analysis of column flow dynamics should all be investigated for their ability to improve elution peak resolution.

8.1.5 Matters arising from Chapter 7

Chapter 7 combined both the acidogenic fermentation covered in **Chapters 3-5**, and the zeolite treatment of **Chapter 6**, into an integrated system for polyhydroxyalkanoate production. The primary aim of the experiments in this chapter was to experimentally test the hypothesis that zeolite treatment of fermentates could allow for increased production of PHA bioplastics in pure culture systems. Experiments in *P. putida* KT2440 and *C. necator* H16 successfully demonstrated this principle, with both microbes demonstrating significant increases in both yields and titres of PHA with zeolite treatment. This successful proof of concept now opens a range of avenues for investigation, which could bring this concept closer to actualisation as a novel industrial process for renewable bioplastic production. These are detailed below.

8.1.5.1 Systematic evaluation of three key PHA species (*P. putida, C. necator, V. natriegens*)

Experiments with both *P. putida* and *C. necator* successfully demonstrated the benefits of zeolite treatment of fermentate media for increasing PHA production. However, both experiments have identifiable limitations which leave room for future approaches to optimise.

Firstly, both experiments tested a limited range of C:N ratios. In *P. putida*, the fermentate blending approach used meant that range of C:N from 10-45 was well covered, but the range between 50 and 100 was not. It is thus not clear whether the C:N optimum seen in the 25-45 range is a global maximum, or whether further improvement might be achieved by moving into the 50-100 range. Importantly, PHA production in C:N 93.5 was significantly worse than in the optimal (25-45) range, suggesting that future experiments need not test ratios above this value.

The *C. necator* experiment was similarly limited in the C:N ratios covered. This experiment was designed with a more limited scope than that for *P. putida* and was intended simply to demonstrate the benefit of zeolite treatment in *C. necator* rather than to identify the

C:N optimum for the species. These experiments, the first of their kind in each species, lay a foundation upon which a more detailed characterisation of the relationship between PHA production and zeolite treatment in each species can be built.

A third species, *Vibrio natriegens*, had been intended for inclusion, but these experiments were ultimately not performed. The high growth rate of this PHA-accumulating species raises unique possibilities for a non-sterile bioproduction process which are covered in more detail below. But a prerequisite to these experiments is to demonstrate that it responds to zeolite treatment as do *P. putida* and *C. necator*.

Future work in sterile, zeolite-treated media should focus on the detailed characterisation of these three species as a strong foundation for pure-culture PHA bioproduction optimisation, with *P. putida* as the model mc-PHA accumulator, *C. necator* as the sc-PHA hyperaccumulator, and *V. natriegens* as a sc-PHA accumulator with extremely high growth rates.

8.1.5.2 Expansion to alternative MSL species

Storage lipid accumulation under conditions of nitrogen limitation goes well beyond PHAs, with accumulation of oils, waxes, and triacylglycerides all being well documented in the literature. This suggests that the success seen in **Chapter 7** with PHA production may also generalise to production of these other industrially relevant chemicals and could offer a route for their efficient production on cheap carbon sources such as fermentate.

Some preliminary experiments have been performed in collaboration with Dr. Laura Martin on the application of zeolites to wax production in *Acinetobacter baylyi* ADP1, and this work is ongoing. Given the promise of the PHA results in **Chapter 7**, and given the magnitude of the treatment effect seen with PHA, the extension of this experimental approach to oil, wax and TAG-accumulating species could be a fruitful area for future investigation.

8.1.5.2 Cation sensitivity of MSL accumulation – toward a two-directional zeolite process

The accumulation of some storage lipids has been shown to be sensitive to the concentration of common cations [167]. Zeolite-based ammonium depletion is an ion-exchange process, in which the removal of ammonium from the fermentate occurs alongside a release of the ion with which the zeolite was initially equilibrated. In **Chapter 7**, this ion was sodium, and its increased concentration does not appear to have significantly impeded PHA accumulation. Martin et al. [167] found evidence that common cations can both increase and decrease wax

accumulation by *A. baylyi* ADP1. This suggests that the selection of the eluent salt used in ammonium recovery from zeolites might also need to also consider the cation sensitivity of the storage lipid accumulator to be grown in the treated fermentate. However, it also raises a possibility for yet further process optimisation, as the equilibration of zeolite with an ion, the presence of which increases storage lipid production, could further raise production levels above those attainable by ammonium removal alone.

A thorough investigation of the effect of different cations on storage lipid accumulation in various species offers the possibility of turning zeolite-treatment into a two-directional process – by coupling the removal of inhibitory ammonium to the release of an accumulation-inducing ion.

8.1.5.3 Utilising Vibrio natriegens for a non-sterile 'pure culture' bioproduction process.

The PHA-accumulating marine bacterium *Vibrio natriegens* is notable both for its extremely fast doubling rate and for its high salt tolerance [187]. These features suggest it may offer further room for process optimisation in the production of PHA from zeolite-treated fermentates. The bioproduction experiments in **Chapter 7** were performed in autoclave-sterilised fermentates, to ensure a pure culture of the PHA-accumulating species of interest. It is possible, given the fast growth rate of *V. natriegens*, that if inoculated into a non-sterile fermentate, it might rapidly come to dominate the medium – suggesting the possibility for its use in a non-sterile process, which would enjoy significantly reduced process costs. An experiment to this effect had been planned, but was ultimately not undertaken due to time constraints, and is detailed here in the hope that it might be taken up by a future reader:

This experiment involved inoculating both sterile and non-sterile, zeolite-treated and non-treated fermentates to an initial OD_{600} of 0.1 with *C. necator*, *P. putida*, and *V. natriegens* and running the respective growth curves to plateau, with regular sampling.

These samples would be analysed for PHA titres, as performed in **Chapter 7**, but importantly would also be submitted for metagenomic sequencing in order to determine the community composition in each condition over time. The hypothesis here is that *C. necator* and *P. putida*, with their relatively long doubling times would be largely outcompeted by other fermentate microbes, while *V. natriegens* would come to dominate the microbial population of fermentates into which it was inoculated. Because the microbial population against which these three microbes would be competing was largely anaerobic, the mere presence of oxygen in the aerobic culture would alone provide a considerable competitive advantage to the species of

interest. In the case of *V. natriegens*, a marine organism, an increase in media salinity could be used to further skew the culture conditions in its favour.

If verified, finding that *V. natriegens* can rapidly colonise a non-sterile fermentate could possibly allow a *V. natriegens* "pure-culture" PHA bioproduction system to be established without the need for fermentate sterilisation. This would significantly reduce process costs and bring PHA production yet closer to cost parity with its fossil-carbon competitors.

8.1.6 Unifying these processes

The experiments in this thesis cover a wide range of topics, from the analysis of CAM feedstocks as AF substrates, the inclusion of high-protein co-substrates on AF efficiency, the possible potential of *Asparagopsis taxiformis* as a methanogenesis inhibitor in AF, the use of zeolites to strip ammonium from fermentates, and the production of PHA on these fermentates. The unifying thread across these disparate topics is the attempt in each case to propose process improvements that might contribute to the realisation of a cost-effective, renewable paradigm for plastic production that might compete with the fossil carbon status quo.

The ideal conclusion to this thesis would have been to be able to unify these disparate sections into an integrated biorefinery process combining the findings of all five results chapters. In such a system, the production of VFA from biomass would be performed under conditions of *Asparagopsis*-based methanogenesis inhibition, achieving VFA production while minimising the cost represented by conventional small-molecule methanogenesis inhibitors. Zeolite-treatment of the digestate would then be used to achieve maximal PHA titres in pure cultures of either *C. necator* or *P. putida*.

This system would have two "control levers" allowing both customisation of PHA titre and of the composition of the PHA produced. Titres would be under the control of zeolite-treatment, which allows optimisation of C:N ratio of the medium according to the calculated maximum for the accumulator species. PHA composition, i.e., the relative abundance of the individual monomers within the PHA polymer would be controlled by manipulation of the C:N ratio of the substrate used in the initial acidogenic fermentation. This would allow customisation of the VFA profile of the fermentate, which would lead to unique PHA polymer compositions and tailored physical and mechanical properties.

This thesis was partially successful in delivering this biorefinery system, though two of the major innovations proposed above remain unachieved due to their inconsistency with the conclusions of several key experiments. These are:

1. The use of *Asparagopsis* as the methanogenesis inhibitor.
2. The customisation of PHA composition through tailored fermentate VFA profiles.

Asparagopsis provided effective inhibition in rumen fluid but not sludge, suggesting a rumen based VFA production system could be used. However, rumen fluid was also found to yield less VFA in acidogenic fermentations than AD sludge. While *Asparagopsis* is a far cheaper methanogenesis inhibitor than BES, this cost advantage does not justify accepting the significantly reduced VFA yields that a shift to a rumen-based AF system would entail. Accordingly, PHA bioproduction experiments in **Chapter 7** were performed using fermentates inoculated with AD sludge and with methanogenesis inhibition provided by BES. If issues around inoculum activity and the efficacy of Asparagopsis in AD sludge can be resolved, this *Asparagopsis*-based system may yet be achievable.

Manipulation of the co-substrate ratio between (high-carbon) *E. tirucalli* and (high-nitrogen) blood co-substrates in AF was shown in **Chapter 3** to allow customisation of the VFA produced. Taken together with the results of Dartiailh et al. [79], which showed the composition of PHA produced by *P. putida* to respond to changes in substrate composition, this suggested that customised AF parameters could allow for control of PHA composition. Zeolite plays a key role here too, in ensuring that the excess ammonium added to the fermentates by addition of protein can be removed before the PHA bioproduction step. It was however found in **Chapter 7** that PHA produced on protein-derived fermentates differed only very slightly in its monomer composition, due to the very narrow (C2-C6) range of the product spectrum achievable through AF.

References

1. Larsen, C.S. 2006. The agricultural revolution as environmental catastrophe: Implications for health and lifestyle in the Holocene. Quaternary International **150**, 12-20.

2. Takada, A. and A. Takada. 2020. The Last Hunter-Gatherers of the Kalahari. The Ecology of Playful Childhood: The Diversity and Resilience of Caregiver-Child Interactions among the San of Southern Africa, 21-37.

3. Flückiger, J., E. Monnin, B. Stauffer, J. Schwander, T.F. Stocker, J. Chappellaz, D. Raynaud, and J.M. Barnola. 2002. High-resolution Holocene N2O ice core record and its relationship with CH4 and CO2. Global Biogeochemical Cycles **16**, 10-1-10-8.

4. Kelley, C.P., S. Mohtadi, M.A. Cane, R. Seager, and Y. Kushnir. 2015. Climate change in the Fertile Crescent and implications of the recent Syrian drought. Proceedings of the national Academy of Sciences **112**, 3241-3246.

5. Fourier, J. 1824. Remarques générales sur les températures du globe terrestre et des espaces planétaires. Annales de Chemie et de Physique **27**.

6. Foote, E. 1856. ART. XXXI.—Circumstances Affecting the Heat of the Sun's Rays. American Journal of Science and Arts (1820-1879) **22**, 382.

7. Tyndall, J. 1861. I. The Bakerian Lecture.—On the absorption and radiation of heat by gases and vapours, and on the physical connexion of radiation, absorption, and conduction. Philosophical transactions of the royal society of London, 1-36.

8. *Coal Consumption Affecting Climate*, in *Rodney and Otamatea Times, Waitemata and Kaipara Gazette*. 1912. p. 7.

9. Supran, G., S. Rahmstorf, and N. Oreskes. 2023. Assessing ExxonMobil's global warming projections. Science **379**, eabk0063.

10. UNFCCC, *United Nations framework convention on climate change*. 1992, UNFCCC.

11. UNFCCC, *Paris Agreement to the United Nations Framework Convention on Climate Change, Dec. 12, 2015, TIAS No. 16–1104*. 2015.

12. Etheridge, D., L. Steele, R. Langenfelds, R. Francey, J. Barnola, and V. Morgan, *Historical CO2 Records from the Law Dome DE08, DE08-2, and DSS ice cores (1006 AD-1978 AD)*. 1998, Environmental System Science Data Infrastructure for a Virtual Ecosystem ….

13. Lan, X. and R. Keeling, *NOAA/GML (gml. noaa. gov/ccgg/trends/) and Dr Ralph Keeling, Scripps Institution of Oceanography (scrippsco2. ucsd. edu/)*, NOAA/GML, Editor. 2022.

14. NASA/GISS, *Global Land-Ocean Temperature Index*, N.s.G.I.f.S. Studies, Editor. 2023.

15. IEA, *Renewables 2023*. 2023, IEA: Paris.

16. IEA, *Global EV Outlook 2024*. 2024, IEA: Paris.

17. Geyer, R., J.R. Jambeck, and K.L. Law. 2017. Production, use, and fate of all plastics ever made. Science advances **3**, e1700782.

18. Whistance, J., D. Debnath, and W. Thompson. 2024. A biofuels outlook for the US and Brazil and what it might mean for sustainable development goal 7. Frontiers in Chemical Engineering **5**, 1290763.

19. Mason, P.M., K. Glover, J.A.C. Smith, K.J. Willis, J. Woods, and I.P. Thompson. 2015. The potential of CAM crops as a globally significant bioenergy resource: moving from 'fuel or food' to 'fuel and more food'. Energy Environ. Sci. **8**, 2320-2329.

20. Tenci, N.A., F. Ammam, W.E. Huang, and I.P. Thompson. 2023. Anaerobic co-digestion of *Euphorbia tirucalli* with pig blood for volatile fatty acid production. Bioresource Technology Reports **21**, 101333.

21. Tenci, N.A., F. Ammam, N. Austen, W.E. Huang, and I.P. Thompson. 2024. Red seaweed as an abundant, natural methanogenesis inhibitor for industrial biorefinery. Journal of Cleaner Production **454**, 142166.

22. IARC, *Occupational exposures in petroleum refining: crude oil and major petroleum fuels*, in *Occupational exposures in petroleum refining: crude oil and major petroleum fuels*. 1989, International Agency for Research on Cancer. p. 322-322.

23. Hawley, G.G., *The Condensed Chemical Dictionary*. 10th ed. ed. 1981, New York: Van Nostrand Reinhold Co. 1135.

24. Faramawy, S., T. Zaki, and A.-E. Sakr. 2016. Natural gas origin, composition, and processing: A review. Journal of Natural Gas Science and Engineering **34**, 34-54.

25. EIA. *How much oil is used to make plastic?* 2024 10/09/2024].

26. Sicotte, D.M. 2020. From cheap ethane to a plastic planet: Regulating an industrial global production network. Energy Research & Social Science **66**, 101479.

27. Klemm, D., B. Heublein, H.P. Fink, and A. Bohn. 2005. Cellulose: fascinating biopolymer and sustainable raw material. Angewandte chemie international edition **44**, 3358-3393.

28. Chen, H. 2014. Biotechnology of lignocellulose. Theory and Practice.

29. Rao, J., Z. Lv, G. Chen, and F. Peng. 2023. Hemicellulose: Structure, chemical modification, and application. Progress in Polymer Science, 101675.

30. Korányi, T.I., B. Fridrich, A. Pineda, and K. Barta. 2020. Development of 'Lignin-First'approaches for the valorization of lignocellulosic biomass. Molecules **25**, 2815.

31. Rabemanolontsoa, H. and S. Saka. 2013. Comparative study on chemical composition of various biomass species. RSC advances **3**, 3946-3956.

32. Lueangwattanapong, K., F. Ammam, P.M. Mason, C. Whitehead, S.J. McQueen-Mason, L.D. Gomez, A.C. Smith, and I.P. Thompson. 2020. Anaerobic digestion of

Crassulacean Acid Metabolism plants: Exploring alternative feedstocks for semi-arid lands. Bioresour. Technol. **297**, 122262.

33. Liu, W.-J. and H.-Q. Yu. 2021. Thermochemical conversion of lignocellulosic biomass into mass-producible fuels: emerging technology progress and environmental sustainability evaluation. ACS Environmental Au **2**, 98-114.

34. Duong, T.H., K. Grolle, T.T.V. Nga, G. Zeeman, H. Temmink, and M. Van Eekert. 2019. Protein hydrolysis and fermentation under methanogenic and acidifying conditions. Biotechnology for biofuels **12**, 1-10.

35. Costa, J., S. Barbosa, and D. Sousa. 2012. Effects of pre-treatment and bioaugmentation strategies on the anaerobic digestion of chicken feathers. Bioresource technology **120**, 114-119.

36. Gujjala, L.K., S.J. Kumar, B. Talukdar, A. Dash, S. Kumar, K.C. Sherpa, and R. Banerjee. 2019. Biodiesel from oleaginous microbes: opportunities and challenges. Biofuels **10**, 45-59.

37. Astals, S., D.J. Batstone, J. Mata-Alvarez, and P.D. Jensen. 2014. Identification of synergistic impacts during anaerobic co-digestion of organic wastes. Bioresour. Technol. **169**, 421-427.

38. Jensen, P.D., T. Sullivan, C. Carney, and D.J. Batstone. 2014. Analysis of the potential to recover energy and nutrient resources from cattle slaughterhouses in Australia by employing anaerobic digestion. Appl. Energ. **136**, 23-31

.

39. Anderson, D. 2006. Rendering operations. Essential rendering all about the animal by-products industry. Alexandria (VA): National Renderers Association, 31-52.

40. Li, Y., R. Zhang, G. Liu, C. Chen, Y. He, and X. Liu. 2013. Comparison of methane production potential, biodegradability, and kinetics of different organic substrates. Bioresour. Technol. **149**, 565-569.

41. APHA, *Standard Methods for the Examination of Water and Wastewater*. 1998, American Water Works Association and Water Environment Federation: Washington DC.

42. Fahmy, T.Y., Y. Fahmy, F. Mobarak, M. El-Sakhawy, and R.E. Abou-Zeid. 2020. Biomass pyrolysis: past, present, and future. Environment, Development and Sustainability **22**, 17-32.

43. Staš, M., J. Chudoba, D. Kubička, J. Blažek, and M. Pospíšil. 2017. Petroleomic characterization of pyrolysis bio-oils: a review. Energy & Fuels **31**, 10283-10299.

44. Ryue, J., L. Lin, F.L. Kakar, E. Elbeshbishy, A. Al-Mamun, and B.R. Dhar. 2020. A critical review of conventional and emerging methods for improving process stability in thermophilic anaerobic digestion. Energy for Sustainable development **54**, 72-84.

45. De Clercq, D., Z. Wen, O. Gottfried, F. Schmidt, and F. Fei. 2017. A review of global strategies promoting the conversion of food waste to bioenergy via anaerobic digestion. Renewable and Sustainable Energy Reviews **79**, 204-221.

46. Nguyen, V.K., D.K. Chaudhary, R.H. Dahal, N.H. Trinh, J. Kim, S.W. Chang, Y. Hong, D.D. La, X.C. Nguyen, and H.H. Ngo. 2021. Review on pretreatment techniques to improve anaerobic digestion of sewage sludge. Fuel **285**, 119105.

47. Sun, H., E. Wang, X. Li, X. Cui, J. Guo, and R. Dong. 2021. Potential biomethane production from crop residues in China: Contributions to carbon neutrality. Renewable and Sustainable Energy Reviews **148**, 111360.

48. Kang, A.J. and Q. Yang, *Enhanced Anaerobic digestion of Organic Waste*, in *Solid Waste Management in Rural Areas*, F.-C. Mihai, Editor. 2017, IntechOpen: Rijeka. p. 123-142.

49. Tait, S., S. Astals, S.D. Yap, P. Jensen, and D. Batstone. 2017. Enhanced methane production from pig manure in covered lagoons and digesters. Final Report: Pork CRC 4C-109.(Australia).

50. Sharma, P., A.A. Khardenavis, and H.J. Purohit. 2015. Metabolism of long-chain fatty acids (LCFAs) in methanogenesis. Microbial Factories: Biofuels, Waste treatment: Volume 1, 279-291.

51. Shi, J., R. Zhang, W. Liao, C.L. Hansen, and Y. Li, *Module B7 - Anaerobic Digestion*, in *Biobased Energy Education Material exchange System (BEEMS)*. 2012, American Society for Agricultural and Biological Engineers (ASABE). p. BEEMS.OSU.EDU.

52. Menzel, T., P. Neubauer, and S. Junne. 2020. Role of microbial hydrolysis in anaerobic digestion. Energies **13**, 5555.

53. Ning, T., H. Wang, M. Zheng, D. Niu, S. Zuo, and C. Xu. 2017. Effects of microbial enzymes on starch and hemicellulose degradation in total mixed ration silages. Asian-Australasian journal of animal sciences **30**, 171.

54. Wang, X., S. Cheng, Z. Li, Y. Men, and J. Wu. 2020. Impacts of cellulase and amylase on enzymatic hydrolysis and methane production in the anaerobic digestion of corn straw. Sustainability **12**, 5453.

55. Sanders, W.T.M., *Anaerobic hydrolysis during digestion of complex substrates*. 2001: Wageningen University and Research.

56. Angelidaki, I. and W. Sanders. 2004. Assessment of the anaerobic biodegradability of macropollutants. Rev. Environ. Sci. Biotechnol. **3**, 117-129.

57. Dai, X., Y. Hua, L. Dai, and C. Cai. 2019. Particle size reduction of rice straw enhances methane production under anaerobic digestion. Bioresource technology **293**, 122043.

58. Zhang, Y. and C.J. Banks. 2013. Impact of different particle size distributions on anaerobic digestion of the organic fraction of municipal solid waste. Waste management **33**, 297-307.

59. Solé-Bundó, M., H. Carrère, M. Garfí, and I. Ferrer. 2017. Enhancement of microalgae anaerobic digestion by thermo-alkaline pretreatment with lime (CaO). Algal Research **24**, 199-206.

60. Başar, İ.A., Ö. Çoban, M.Y. Göksungur, Ç. Eskicioğlu, and N.A. Perendeci. 2021. Enhancement of lignocellulosic biomass anaerobic digestion by optimized mild alkaline hydrogen peroxide pretreatment for biorefinery applications. Journal of Environmental Management **298**, 113539.

61. Schwede, S., Z.-U. Rehman, M. Gerber, C. Theiss, and R. Span. 2013. Effects of thermal pretreatment on anaerobic digestion of Nannochloropsis salina biomass. Bioresource Technology **143**, 505-511.

62. Lee, K., P. Chantrasakdakul, D. Kim, M. Kong, and K.Y. Park. 2014. Ultrasound pretreatment of filamentous algal biomass for enhanced biogas production. Waste management **34**, 1035-1040.

63. Zhou, J., B. Yan, Y. Wang, X. Yong, Z. Yang, H. Jia, M. Jiang, and P. Wei. 2016. Effect of steam explosion pretreatment on the anaerobic digestion of rice straw. RSC advances **6**, 88417-88425.

64. Kijpornyongpan, T., A. Schwartz, A. Yaguchi, and D. Salvachúa. 2022. Systems biology-guided understanding of white-rot fungi for biotechnological applications: a review. Iscience **25**.

65. Vermaas, J.V., L. Petridis, X. Qi, R. Schulz, B. Lindner, and J.C. Smith. 2015. Mechanism of lignin inhibition of enzymatic biomass deconstruction. Biotechnology for biofuels **8**, 1-16.

66. Lourenço, A. and H. Pereira. 2018. Compositional variability of lignin in biomass. Lignin-trends and applications, 65-98.

67. Neutelings, G. 2011. Lignin variability in plant cell walls: contribution of new models. Plant Science **181**, 379-386.

68. Yue, Z.-B., J. Wang, X.-M. Liu, and H.-Q. Yu. 2012. Comparison of rumen microorganism and digester sludge dominated anaerobic digestion processes for aquatic plants. Renewable Energy **46**, 255-258.

69. Yue, Z.-B., W.-W. Li, and H.-Q. Yu. 2013. Application of rumen microorganisms for anaerobic bioconversion of lignocellulosic biomass. Bioresource Technology **128**, 738-744.

70. Vavilin, V., B. Fernandez, J. Palatsi, and X. Flotats. 2008. Hydrolysis kinetics in anaerobic degradation of particulate organic material: an overview. Waste management **28**, 939-951.

71. Saritpongteeraka, K., P. Boonsawang, S. Sung, and S. Chaiprapat. 2014. Co-fermentation of oil palm lignocellulosic residue with pig manure in anaerobic leach bed reactor for fatty acid production. Energy Convers. Manag. **84**, 354-362.

72. Babel, S., K. Fukushi, and S. Bunpot. 2004. Effect of acid speciation on solid waste liquefaction in an anaerobic acid digester. Water Res. **38**, 2417-2423.

73. Chen, J.L., R. Ortiz, T.W. Steele, and D.C. Stuckey. 2014. Toxicants inhibiting anaerobic digestion: a review. Biotechnology advances **32**, 1523-1534.

74. Breure, A. and J. Van Andel. 1984. Hydrolysis and acidogenic fermentation of a protein, gelatin, in an anaerobic continuous culture. Applied Microbiology and Biotechnology **20**, 40-45.

75. Wang, X., Y. Zhang, Y. Li, Y.-L. Luo, Y.-R. Pan, J. Liu, and D. Butler. 2021. Alkaline environments benefit microbial K-strategists to efficiently utilize protein substrate and promote valorization of protein waste into short-chain fatty acids. Chemical Engineering Journal **404**, 127147.

76. Ramos-Suarez, M., Y. Zhang, and V. Outram. 2021. Current perspectives on acidogenic fermentation to produce volatile fatty acids from waste. Reviews in Environmental Science and Bio/Technology **20**, 439-478.

77. Christophe, G., J. Lara Deo, V. Kumar, R. Nouaille, P. Fontanille, and C. Larroche. 2012. Production of oils from acetic acid by the oleaginous yeast *Cryptococcus curvatus*. Appl. Biochem. Biotechnol. **167**, 1270-1279.

78. Mengmeng, C., C. Hong, Z. Qingliang, S.N. Shirley, and R. Jie. 2009. Optimal production of polyhydroxyalkanoates (PHA) in activated sludge fed by volatile fatty acids (VFAs) generated from alkaline excess sludge fermentation. Bioresour. Technol. **100**, 1399-1405.

79. Dartiailh, C., W. Blunt, P.K. Sharma, S. Liu, N. Cicek, and D.B. Levin. 2021. The thermal and mechanical properties of medium chain-length polyhydroxyalkanoates produced by *Pseudomonas putida* LS46 on various substrates
. Frontiers in Bioengineering and Biotechnology **8**, 617489.

80. Zhou, M., B. Yan, J.W.C. Wong, and Y. Zhang. 2018. Enhanced volatile fatty acids production from anaerobic fermentation of food waste: A mini-review focusing on acidogenic metabolic pathways. Bioresour. Technol. **248**, 68-78.

81. Ramsay, I.R. and P.C. Pullammanappallil. 2001. Protein degradation during anaerobic wastewater treatment: derivation of stoichiometry. Biodegradation **12**, 247-257.

82. Weng, C.-n. and J.S. Jeris. 1976. Biochemical mechanisms in the methane fermentation of glutamic and oleic acids. Water Research **10**, 9-18.

83. Liu, H., J. Wang, A. Wang, and J. Chen. 2011. Chemical inhibitors of methanogenesis and putative applications. Applied Microbiology and Biotechnology **89**, 1333-1340.

84. Stams, A.J. and X. Dong. 1995. Role of formate and hydrogen in the degradation of propionate and butyrate by defined suspended cocultures of acetogenic and methanogenic bacteria. Antonie Van Leeuwenhoek **68**, 281-284.

85. Siriwongrungson, V., R.J. Zeng, and I. Angelidaki. 2007. Homoacetogenesis as the alternative pathway for H2 sink during thermophilic anaerobic degradation of butyrate under suppressed methanogenesis. Water research **41**, 4204-4210.

86. Dong, W., Y. Yang, C. Liu, J. Zhang, J. Pan, L. Luo, G. Wu, M.K. Awasthi, and B. Yan. 2023. Caproic acid production from anaerobic fermentation of organic waste-Pathways and microbial perspective. Renewable and Sustainable Energy Reviews **175**, 113181.

87. Baleeiro, F.C.F., S. Kleinsteuber, and H. Sträuber. 2022. Recirculation of H2, CO2, and ethylene improves carbon fixation and carboxylate yields in anaerobic fermentation. ACS Sustainable Chemistry and Engineering **10**, 4073-4081.

88. Veluswamy, G., K. Shah, A. Ball, A. Guwy, and R. Dinsdale. 2021. A techno-economic case for volatile fatty acid production for increased sustainability in the wastewater treatment industry. Environmental Science: Water Research & Technology **7**, 927-941.

89. Dahiya, S., O. Sarkar, Y. Swamy, and S.V. Mohan. 2015. Acidogenic fermentation of food waste for volatile fatty acid production with co-generation of biohydrogen. Bioresource technology **182**, 103-113.

90. Kinley, R.D., R. de Nys, M.J. Vucko, L. Machado, and N.W. Tomkins. 2016. The red macroalgae *Asparagopsis taxiformis* is a potent natural antimethanogenic that reduces methane production during
in vitro fermentation with rumen fluid. Animal Production Science **56**, 282-289.

91. Li, X., H.C. Norman, R.D. Kinley, M. Laurence, M. Wilmot, H. Bender, R. de Nys, and N. Tomkins. 2016. *Asparagopsis taxiformis* decreases enteric methane production from sheep. Animal Production Science, 681-688.

92. Machado, L., M. Magnusson, N.A. Paul, R. Kinley, R. de Nys, and N. Tomkins. 2016. Dose-response effects of *Asparagopsis taxiformis* and *Oedogonium* sp. on in vitro fermentation and methane production. Journal of Applied Phycology **28**, 1443-1452.

93. Machado, L., M. Magnusson, N.A. Paul, R. Kinley, R. de Nys, and N. Tomkins. 2016. Identification of bioactives from the red seaweed *Asparagopsis taxiformis* that promote antimethanogenic activity *in vitro*. Journal of Applied Phycology **28**, 3117-3126.

94. Machado, L., N. Tomkins, M. Magnusson, D.J. Midgley, R. de Nys, and C.P. Rosewarne. 2018. *In vitro* response of rumen microbiota to the antimethanogenic red macroalga *Asparagopsis taxiformis*. Microbial Ecology **75**, 811-818.

95. Gírio, F., S. Marques, F. Pinto, A.C. Oliveira, P. Costa, A. Reis, and P. Moura. 2017. Biorefineries in the World. Biorefineries: targeting energy, high value products and waste valorisation, 227-281.

96. Carriquiry, M.A., X. Du, and G.R. Timilsina. 2011. Second generation biofuels: Economics and policies. Energy policy **39**, 4222-4234.

97. Borland, A.M., H. Griffiths, J. Hartwell, and A.C. Smith. 2009. Exploiting the potential of plants with crassulacean acid metabolism for bioenergy production on marginal lands. Journal of Experimental Botany **60**, 2879-2896.

98. Davis, S.C., J. Simpson, K.d.C. Gil-Vega, N.A. Niechayev, E.v. Tongerlo, N.H. Castano, L.V. Dever, and A. Búrquez. 2019. Undervalued potential of crassulacean acid metabolism for current and future agricultural production. Journal of Experimental Botany **70**, 6521-6537.

99. Krümpel, J., T. George, B. Gasston, G. Francis, and A. Lemmer. 2020. Suitability of *Opuntia ficus-indica* (L) Mill. and *Euphorbia tirucalli* L. as energy crops for anaerobic digestion. J. Arid Environ. **174**, 104047.

100. Edwards, E.J. 2019. Evolutionary trajectories, accessibility and other metaphors: the case of C4 and CAM photosynthesis. New Phytologist **223**, 1742-1755.

101. Borland, A.M., H. Griffiths, J. Hartwell, and A.C. Smith. 2009. Exploiting the potential of plants with crassulacean acid metabolism for bioenergy production on marginal lands. Journal of Experimental Botany **60**, 2879-2896.

102. Lueangwattanapong, K., *Potential of crassulacean acid metabolism (CAM) plants as biomass for bioenergy and biorefinery*. 2020, University of Oxford.

103. Schmidt, A., S. Lemaigre, T. Ruf, P. Delfosse, and C. Emmerling. 2018. Miscanthus as biogas feedstock: Influence of harvest time and stand age on the biochemical methane potential (BMP) of two different growing seasons. Biomass Conversion and Biorefinery **8**, 245-254.

104. Nefzaoui, A. and H. Ben Salem, *Opuntia: a strategic fodder and eficient tool to combat desertification in the wana region*. 2001.

105. Yang, L., M. Lu, S. Carl, J.A. Mayer, J.C. Cushman, E. Tian, and H. Lin. 2015. Biomass characterization of Agave and Opuntia as potential biofuel feedstocks. Biomass and Bioenergy **76**, 43-53.

106. Álvarez-Chávez, J., M. Villamiel, L. Santos-Zea, and A.K. Ramírez-Jiménez. 2021. Agave by-products: An overview of their nutraceutical value, current applications, and processing methods. Polysaccharides **2**, 720-743.

107. Huang, Y., F. Li, J. Meng, and W. Chen. 2018. Lignin content of agro-forestry biomass negatively affects the resultant biochar pH. BioResources **13**, 5153-5163.

108. Kim, S.J., M.Y. Kim, S.J. Jeong, M.S. Jang, and I.M. Chung. 2012. Analysis of the biomass content of various Miscanthus genotypes for biofuel production in Korea. Industrial Crops and Products **38**, 46-49.

109. Chávez-Rosales, J.S., L.F. Pintor-Ibarra, N. González-Ortega, R. Orihuela-Equihua, F. Ruiz-Aquino, C. Lujan-Álvarez, and J.G. Rutiaga-Quiñones. 2021. Basic chemical composition of Pinus spp. sawdust from five regions of Mexico, for bioenergetic purposes. BioResources **16**, 816.

110. Panizio, R.M., L.F.d.C. Calado, G. Lourinho, P.S.D. de Brito, and J.B. Mees. 2020. Potential of biogas production in anaerobic co-digestion of *Opuntia ficus-indica* and slaughterhouse wastes. Waste Biomass Valorization **11**, 4639-4647.

111. *Fatty Acid Industry Overview*. 2022 [cited 2024 19/09]; Available from: https://www.emergenresearch.com/industry-report/fatty-acid-market.

112. Caporusso, A., A. Capece, and I. De Bari. 2021. Oleaginous yeasts as cell factories for the sustainable production of microbial lipids by the valorization of agri-food wastes. Fermentation **7**, 50.

113. Chintagunta, A.D., G. Zuccaro, M. Kumar, S.J. Kumar, V.K. Garlapati, P.D. Postemsky, N.S. Kumar, A.K. Chandel, and J. Simal-Gandara. 2021. Biodiesel production from lignocellulosic biomass using oleaginous microbes: prospects for integrated biofuel production. Frontiers in Microbiology **12**, 658284.

114. Martin, L.K., W.E. Huang, and I.P. Thompson. 2021. Bacterial wax synthesis. Biotechnology Advances **46**, 107680.

115. Alves, A.A., E.C. Siqueira, M.P.S. Barros, P.E.C. Silva, and L.M. Houllou. 2023. Polyhydroxyalkanoates: a review of microbial production and technology application. International Journal of Environmental Science and Technology **20**, 3409-3420.

116. Yang, Y., F. Heidari, and B. Hu. 2019. Fungi (Mold)-based lipid production. Microbial lipid production: methods and protocols, 51-89.

117. Papanikolaou, S. and G. Aggelis. 2002. Lipid production by Yarrowia lipolytica growing on industrial glycerol in a single-stage continuous culture. Bioresource technology **82**, 43-49.

118. Choi, S.Y., I.J. Cho, Y. Lee, Y.J. Kim, K.J. Kim, and S.Y. Lee. 2020. Microbial polyhydroxyalkanoates and nonnatural polyesters. Advanced Materials **32**, 1907138.

119. Fernandes, M., A. Salvador, M.M. Alves, and A.A. Vicente. 2020. Factors affecting polyhydroxyalkanoates biodegradation in soil. Polymer Degradation and Stability **182**, 109408.

120. Jo, J., H. Kim, S.-Y. Jeong, C. Park, H.S. Hwang, and B. Koo. 2021. Changes in mechanical properties of polyhydroxyalkanoate with double silanized cellulose nanocrystals using different organosiloxanes. Nanomaterials **11**, 1542.

121. Anjum, A., M. Zuber, K.M. Zia, A. Noreen, M.N. Anjum, and S. Tabasum. 2016. Microbial production of polyhydroxyalkanoates (PHAs) and its copolymers: A review of recent advancements. International journal of biological macromolecules **89**, 161-174.

122. Reddy, C., R. Ghai, and V.C. Kalia. 2003. Polyhydroxyalkanoates: an overview. Bioresource technology **87**, 137-146.

123. Meng, D.-C. and G.-Q. Chen. 2018. Synthetic biology of polyhydroxyalkanoates (PHA). Synthetic biology–metabolic engineering, 147-174.

124. Passanha, P., S.R. Esteves, G. Kedia, R.M. Dinsdale, and A.J. Guwy. 2013. Increasing polyhydroxyalkanoate (PHA) yields from *Cupriavidus necator* by using filtered digestate liquors. Bioresour. Technol. **147**, 345-352.

125. Byrom, D. 1987. Polymer synthesis by microorganisms: technology and economics. Trends in biotechnology **5**, 246-250.

126. Morlino, M.S., R.S. García, F. Savio, G. Zampieri, T. Morosinotto, L. Treu, and S. Campanaro. 2023. Cupriavidus necator as a platform for PHA production: An overview of strains, metabolism, and modeling approaches. Biotechnology Advances, 108264.

127. Wen, Q., Z. Chen, T. Tian, and W. Chen. 2010. Effects of phosphorus and nitrogen limitation on PHA production in activated sludge. Journal of environmental sciences **22**, 1602-1607.

128. Zhang, L., Z. Jiang, T.-H. Tsui, K.-C. Loh, Y. Dai, and Y.W. Tong. 2022. A review on enhancing Cupriavidus necator fermentation for poly (3-hydroxybutyrate)(PHB)

production from low-cost carbon sources. Frontiers in Bioengineering and Biotechnology **10**, 946085.

129. de Mello, A.F.M., L.P. de Souza Vandenberghe, C.M.B. Machado, K.K. Valladares-Diestra, J.C. de Carvalho, and C.R. Soccol. 2023. Polyhydroxybutyrate production by Cupriavidus necator in a corn biorefinery concept. Bioresource Technology **370**, 128537.

130. Ahn, J., E.H. Jho, and K. Nam. 2015. Effect of C/N ratio on polyhydroxyalkanoates (PHA) accumulation by Cupriavidus necator and its implication on the use of rice straw hydrolysates. Environmental Engineering Research **20**, 246-253.

131. Martin, L.K., W.E. Huang, and I.P. Thompson. 2023. The effect of nutrient limitation on bacterial wax ester production. Bioresource Technology Reports **22**, 101423.

132. Korkakaki, E., M.C. van Loosdrecht, and R. Kleerebezem. 2017. Impact of phosphate limitation on PHA production in a feast-famine process. Water research **126**, 472-480.

133. Straathof, A., *The proportion of downstream costs in fermentative production processes*, in *Comprehensive biotechnology*. 2011, Elsevier. p. 811-814.

134. Wei, P., A. Xia, Q. Liao, C. Sun, Y. Huang, Q. Fu, X. Zhu, and R. Lin. 2018. Enhancing fermentative hydrogen production with the removal of volatile fatty acids by electrodialysis. Bioresource technology **263**, 437-443.

135. Rebecchi, S., D. Pinelli, L. Bertin, F. Zama, F. Fava, and D. Frascari. 2016. Volatile fatty acids recovery from the effluent of an acidogenic digestion process fed with grape pomace by adsorption on ion exchange resins. Chemical Engineering Journal **306**, 629-639.

136. Bekatorou, A., A. Dima, P. Tsafrakidou, K. Boura, K. Lappa, P. Kandylis, K. Pissaridi, M. Kanellaki, and A.A. Koutinas. 2016. Downstream extraction process development for recovery of organic acids from a fermentation broth. Bioresource technology **220**, 34-37.

137. Palakodeti, A., S. Azman, R. Dewil, and L. Appels. 2022. Ammonia Recovery from Organic Waste Digestate via Gas–Liquid Stripping: Application of the Factorial Design of Experiments and Comparison of the Influence of the Stripping Gas. Sustainability **14**, 17000.

138. Törnwall, E., H. Pettersson, E. Thorin, and S. Schwede. 2017. Post-treatment of biogas digestate–an evaluation of ammonium recovery, energy use and sanitation. Energy Procedia **142**, 957-963.

139. Dai, Z., C. Chen, Y. Li, H. Zhang, J. Yao, M. Rodrigues, P. Kuntke, and L. Han. 2023. Hybrid Donnan dialysis–electrodialysis for efficient ammonia recovery from anaerobic digester effluent. Environmental Science and Ecotechnology **15**, 100255.

140. Ferrari, F., M. Pijuan, S. Molenaar, N. Duinslaeger, T. Sleutels, P. Kuntke, and J. Radjenovic. 2022. Ammonia recovery from anaerobic digester centrate using onsite pilot scale bipolar membrane electrodialysis coupled to membrane stripping. Water Research **218**, 118504.

141. Petrovič, A., M. Simonič, and L. Čuček. 2021. Nutrient recovery from the digestate obtained by rumen fluid enhanced anaerobic co-digestion of sewage sludge and cattail: Precipitation by MgCl2 and ion exchange using zeolite. Journal of Environmental Management **290**, 112593.

142. Martin-Ryals, A.D., *Advancing wastewater valorization using anaerobic membrane bioreactors with bioaugmentation and ion-exchange, and bio-plastic production*. 2017, University of Illinois at Urbana-Champaign.

143. Petracchini, F., F. Liotta, V. Paolini, M. Perilli, D. Cerioni, F. Gallucci, M. Carnevale, and A. Bencini. 2018. A novel pilot scale multistage semidry anaerobic digestion reactor to treat food waste and cow manure. International Journal of Environmental Science and Technology **15**, 1999-2008.

144. Kocatürk-Schumacher, N.P., S. Bruun, K. Zwart, and L.S. Jensen. 2017. Nutrient recovery from the liquid fraction of digestate by clinoptilolite. CLEAN–Soil, Air, Water **45**, 1500153.

145. Huang, J.-C. and C. Shang, *Air stripping*, in *Advanced physicochemical treatment processes*. 2006, Springer. p. 47-79.

146. Rashid, S.S., Y.-Q. Liu, and C. Zhang. 2020. Upgrading a large and centralised municipal wastewater treatment plant with sequencing batch reactor technology for integrated nutrient removal and phosphorus recovery: Environmental and economic life cycle performance. Science of the Total Environment **749**, 141465.

147. Almoalimi, K. and Y.-Q. Liu. 2022. Enhancing ammonium rejection in forward osmosis for wastewater treatment by minimizing cation exchange. Journal of Membrane Science **648**, 120365.

148. Ryu, H.-D., D.Y. Lim, S.-J. Kim, U.-I. Baek, E.G. Chung, K. Kim, and J.K. Lee. 2020. Struvite precipitation for sustainable recovery of nitrogen and phosphorus from anaerobic digestion effluents of swine manure. Sustainability **12**, 8574.

149. Otieno, B., C.K. Funani, S.M. Khune, J. Kabuba, and P. Osifo. 2023. Struvite recovery from anaerobically digested waste-activated sludge: A short review. Journal of Materials Research **38**, 3815-3826.

150. Pérez-Botella, E., S. Valencia, and F. Rey. 2022. Zeolites in adsorption processes: State of the art and future prospects. Chemical Reviews **122**, 17647-17695.

151. Hedström, A. 2001. Ion exchange of ammonium in zeolites: a literature review. Journal of environmental engineering **127**, 673-681.

152. Seruga, P., M. Krzywonos, J. Pyz ̇anowska, A. Urbanowska, H. Pawlak-Kruczek, and Ł. Niedz ́wiecki. 2019. Removal of ammonia from the municipal waste treatment effluents using natural minerals. Molecules **24**, 3633.

153. Wan, C., S. Ding, C. Zhang, X. Tan, W. Zou, X. Liu, and X. Yang. 2017. Simultaneous recovery of nitrogen and phosphorus from sludge fermentation liquid by zeolite adsorption: Mechanism and application. Separation and Purification Technology **180**, 1-12.

154. Millini, R. and G. Bellussi. 2017. Zeolite science and perspectives.

155. Farkaš, A., M. Rožić, and Ž. Barbarić-Mikočević. 2005. Ammonium exchange in leakage waters of waste dumps using natural zeolite from the Krapina region, Croatia. Journal of Hazardous Materials **117**, 25-33.

156. Tada, C., Y. Yang, T. Hanaoka, A. Sonoda, K. Ooi, and S. Sawayama. 2005. Effect of natural zeolite on methane production for anaerobic digestion of ammonium rich organic sludge. Bioresource technology **96**, 459-464.

157. Kotsopoulos, T., X. Karamanlis, D. Dotas, and G. Martzopoulos. 2008. The impact of different natural zeolite concentrations on the methane production in thermophilic anaerobic digestion of pig waste. Biosystems engineering **99**, 105-111.

158. Alibaba.com. *Natural Zeolite Clinoptilolite for Animals- Pig*. 2024 [cited 2024 27/06/2024]; Available from: https://www.alibaba.com/product-detail/Natural-Zeolite-Clinoptilolite-For-Animals-Pig_1600495120953.html?spm=a2700.galleryofferlist.topad_classic.i4.73de4032ZgETly.

159. Wang, Q., Y. Yang, C. Yu, H. Huang, M. Kim, C. Feng, and Z. Zhang. 2011. Study on a fixed zeolite bioreactor for anaerobic digestion of ammonium-rich swine wastes. Bioresource Technology **102**, 7064-7068.

160. Wijesinghe, D.T.N., K.B. Dassanayake, P. Scales, and D. Chen. 2018. Developing an anaerobic digester with external Zeolite filled column for enhancing methane production from swine manure–A feasibility study. Journal of Environmental Science and Health, Part B **53**, 751-760.

161. Bolan, N.S., C. Mowatt, D. Adriano, and J. Blennerhassett. 2003. Removal of ammonium ions from fellmongery effluent by zeolite. Communications in soil science and plant analysis **34**, 1861-1872.

162. Comparetti, A., P. Febo, C. Greco, M.M. Mammano, and S. Orlando. 2017. Potential production of biogas from prickly pear (Opuntia ficus-indica L.) in Sicilian uncultivated areas. Chem. Eng **58**, 559-564.

163. Roque, B.M., M. Venegas, R.D. Kinley, R. de Nys, T.L. Duarte, X. Yiang, and E. Kebreab. 2021. Red seaweed (*Asparagopsis taxiformis*) supplementation reduces enteric methane by over 80 percent in beef steers. PLoS One **16**, e0247820.

164. Weatherburn, M. 1967. Phenol-hypochlorite reaction for determination of ammonia. Analytical chemistry **39**, 971-974.

165. Bower, C.E. and T. Holm-Hansen. 1980. A salicylate–hypochlorite method for determining ammonia in seawater. Canadian Journal of Fisheries and Aquatic Sciences **37**, 794-798.

166. Zhou, W., D.I. Colpa, B. Geurkink, G.-J.W. Euverink, and J. Krooneman. 2022. The impact of carbon to nitrogen ratios and pH on the microbial prevalence and polyhydroxybutyrate production levels using a mixed microbial starter culture. Science of the Total Environment **811**, 152341.

167. Martin, L.K., W.E. Huang, and I.P. Thompson. 2023. The effect of nutrient limitation on bacterial wax ester production. Bioresour. Technol. Rep. **22**, 101423.

168. Nunes, L., J. Matias, and J. Catalão. 2016. Biomass combustion systems: A review on the physical and chemical properties of the ashes. Renewable and Sustainable Energy Reviews **53**, 235-242.

169. Xu, K., J. Li, M. Zheng, C. Zhang, T. Xie, and C. Wang. 2015. The precipitation of magnesium potassium phosphate hexahydrate for P and K recovery from synthetic urine. Water Research **80**, 71-79.

170. Ji, Z.-Y., J.-S. Yuan, and X.-G. Li. 2007. Removal of ammonium from wastewater using calcium form clinoptilolite. Journal of Hazardous Materials **141**, 483-488.

171. Costa, P., M. Basaglia, S. Casella, and L. Favaro. 2022. Polyhydroxyalkanoate production from fruit and vegetable waste processing. Polymers **14**, 5529.

172. Andler, R., C. Valdés, V. Urtuvia, C. Andreeßen, and A. Díaz-Barrera. 2021. Fruit residues as a sustainable feedstock for the production of bacterial polyhydroxyalkanoates. Journal of Cleaner Production **307**, 127236.

173. Cruz-Rubio, J.M., M. Mueller, H. Viernstein, R. Loeppert, and W. Praznik. 2021. Prebiotic potential and chemical characterization of the poly and oligosaccharides present in the mucilage of Opuntia ficus-indica and Opuntia joconostle. Food Chemistry **362**, 130167.

174. Boutakiout, A., D. Elothmani, M. Mahrouz, and H. Hanine. 2015. Effect of season on proximate composition of cladode juice of two species of cactaceae. International Journal of Technology Enhancements and Emerging Engineering Reserch, New Delhi **3**, 3.

175. Vu, D.H., S. Wainaina, M.J. Taherzadeh, D. Åkesson, and J.A. Ferreira. 2021. Production of polyhydroxyalkanoates (PHAs) by Bacillus megaterium using food waste acidogenic fermentation-derived volatile fatty acids. Bioengineered **12**, 2480-2498.

176. Fukui, T. and Y. Doi. 1998. Efficient production of polyhydroxyalkanoates from plant oils by Alcaligenes eutrophus and its recombinant strain. Applied Microbiology and Biotechnology **49**, 333-336.

177. York, G.M., B.r.H. Junker, J. Stubbe, and A.J. Sinskey. 2001. Accumulation of the PhaP phasin of Ralstonia eutropha is dependent on production of polyhydroxybutyrate in cells. Journal of Bacteriology **183**, 4217-4226.

178. Huschner, F., E. Grousseau, C.J. Brigham, J. Plassmeier, M. Popovic, C. Rha, and A.J. Sinskey. 2015. Development of a feeding strategy for high cell and PHA density fed-batch fermentation of Ralstonia eutropha H16 from organic acids and their salts. Process Biochemistry **50**, 165-172.

179. Jia, Q., H. Wang, and X. Wang. 2013. Dynamic synthesis of polyhydroxyalkanoates by bacterial consortium from simulated excess sludge fermentation liquid. Bioresource Technology **140**, 328-336.

180. Bermúdez-Penabad, N., C. Kennes, and M.C. Veiga. 2017. Anaerobic digestion of tuna waste for the production of volatile fatty acids. Waste Manage. **68**, 96-102.

181. Liu, H., J. Wang, X. Liu, B. Fu, J. Chen, and H.-Q. Yu. 2012. Acidogenic fermentation of proteinaceous sewage sludge: Effect of pH. Water Research **46**, 799-807.

182. Massey, L.K., R.S. Conrad, and J.R. Sokatch. 1974. Regulation of leucine catabolism in Pseudomonas putida. Journal of Bacteriology **118**, 112-120.

183. Kallastu, A., E. Malv, V. Aro, A. Meikas, M. Vendelin, A. Kattel, R. Nahku, and J. Kazantseva. 2023. Absolute quantification of viable bacteria abundances in food by next-generation sequencing: quantitative NGS of viable microbes. Current Research in Food Science **6**, 100443.

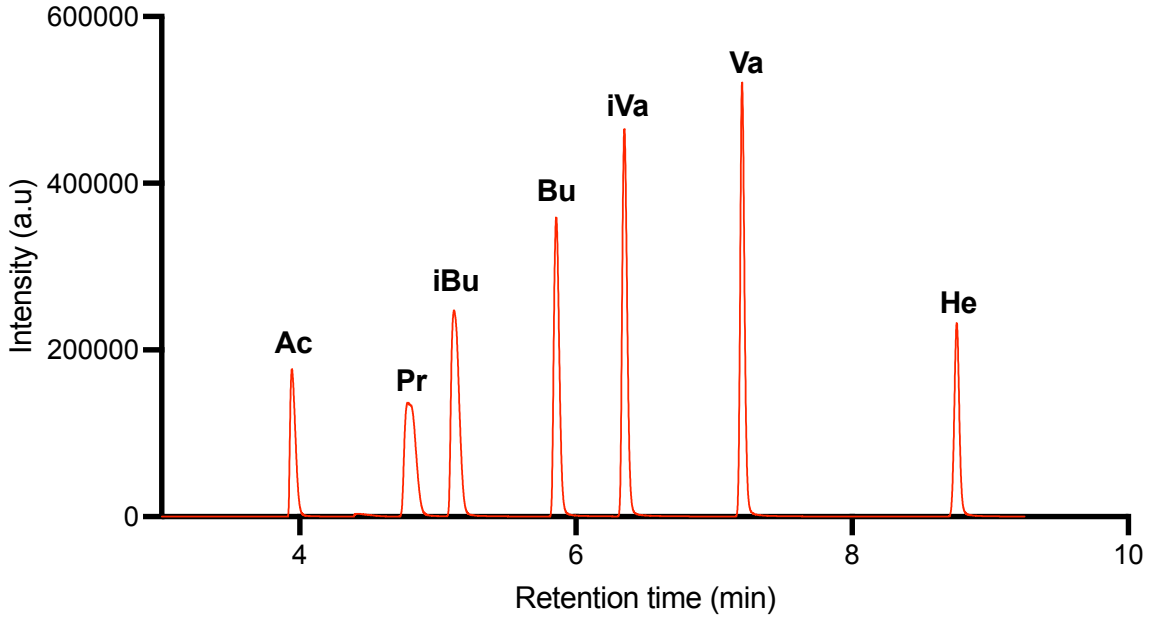
184. Wang, S. and Y. Peng. 2010. Natural zeolites as effective adsorbents in water and wastewater treatment. Chemical engineering journal **156**, 11-24.

185. Watanabe, Y., H. Yamada, J. Tanaka, and Y. Moriyoshi. 2005. Hydrothermal modification of natural zeolites to improve uptake of ammonium ions. Journal of Chemical Technology & Biotechnology: International Research in Process, Environmental & Clean Technology **80**, 376-380.

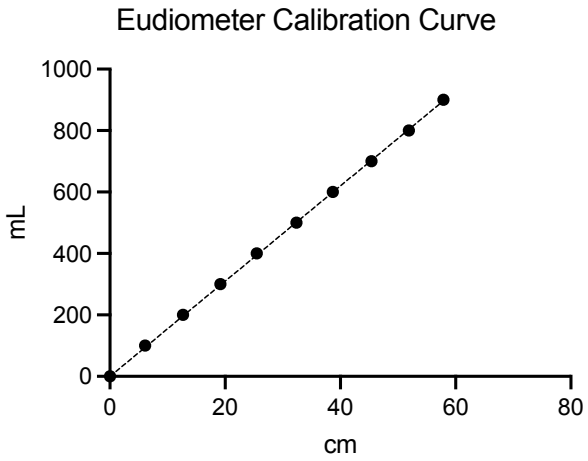
186. Zając, G., J. Szyszlak-Bargłowicz, W. Gołębiowski, and M. Szczepanik. 2018. Chemical characteristics of biomass ashes. Energies **11**, 2885.

187. Hoff, J., B. Daniel, D. Stukenberg, B.W. Thuronyi, T. Waldminghaus, and G. Fritz. 2020. Vibrio natriegens: an ultrafast-growing marine bacterium as emerging synthetic biology chassis. Environmental microbiology **22**, 4394-4408.

Appendices



Appendix 1.1: Exemplar of a typical GC-FID chromatogram from a mixed VFA standard solution as produced by the GC-FID method used across all results chapters in this thesis for the determination of VFA concentrations in samples. Peaks are shown for each of acetic (Ac), propionic (Pr), isobutyric (iBu), butyric (Bu), isovaleric (iVa), and valeric (Va) acid standards at a concentration of 12.5 g/L, and hexanoic acid (He) at 6.25 g/L.



Calibration curve gradient (mL/cm)	Regression R^2
15.494	1.0000

Appendix 1.5.: Experimentally determined calibration curve relating eudiometer height to volume to allow determination of gas production by gas displacement.

Appendix to Chapter 3

Certificate of Analysis

Sciantec
part of Cawood

University of Oxford, Engineering Science Department
Nicholas Tenci

Client Reference	LIGNIN CONTENT
Details	EUPHORBIA TIRUCALLI - SCREENED
Date Received	19-Aug-2022
Date Reported	6-Sep-2022
Lab Reference No	3237007
Order Number	DF2081943
Certificate No	s_3237007_LIGNIN CONTENT_1.pdf
Product	Miscellaneous - Feed Miscellaneous - Feed
Sampled Date	
Sample Source	

Method No		Test	Units	Result	Completed On
S1012		Neutral Detergent Fibre	%	35.4	25-Aug-2022
S1092	*	Cellulose	%	27.9	6-Sep-2022
S1092	*	Hemicellulose	%	3.8	31-Aug-2022
S1112	*	Acid Detergent Lignin	%	3.65	5-Sep-2022
S1129	*	Acid Detergent Fibre	%	31.59	31-Aug-2022

Unless otherwise stated results are expressed on an 'as received' basis.

Sciantec Analytical Services .
Stockbridge Technology Centre, Cawood, Yorkshire
YO8 3SD
t + 44 (0) 1757 242400
f + 44 (0) 1757 242401
www.sciantec.uk.com

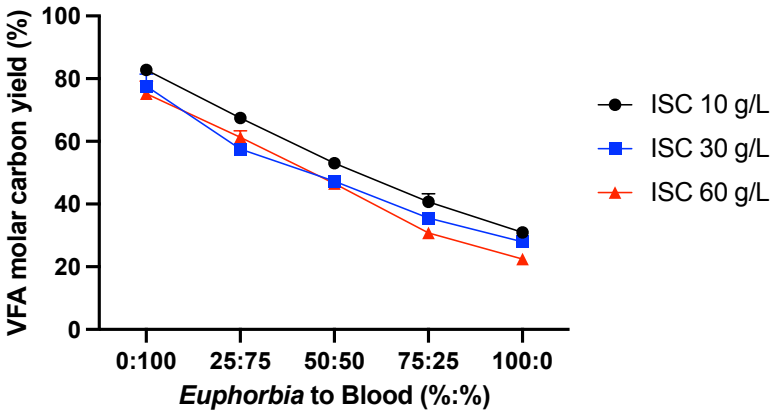
UKAS TESTING
2511

Alan Ash
Technical Support Manager

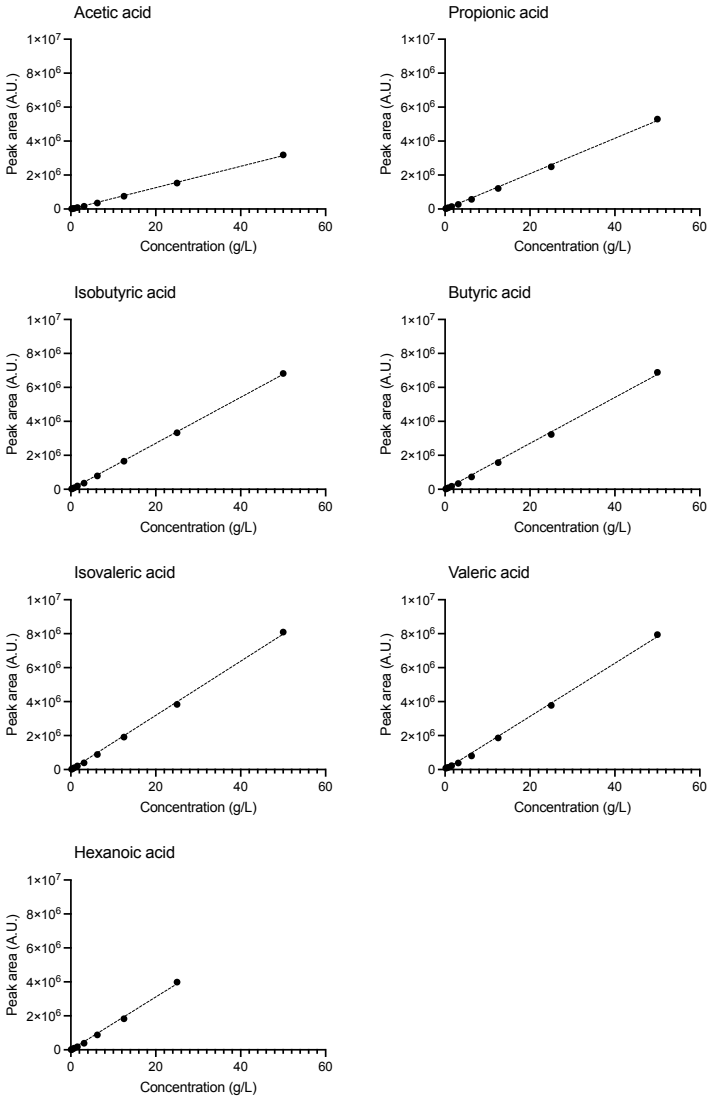
These results relate only to the sample(s) tested and do not guarantee the bulk of the material to be of equal quality. This report shall not be reproduced except in full, without the written approval of Sciantec Analytical Services . Sciantec Analytical Services. was not responsible for sampling and cannot be held liable in respect of the use to which information is put.
A certificate having a number with a suffix of _2 or greater is supplementary to the original report. Tests marked with # are subcontracted to a UKAS accredited laboratory. Tests marked "#are subcontracted to a non UKAS accredited laboratory. Tests marked with " are outside UKAS scope of accreditation. Microbiological assays marked with (p) are presumptive. Tests marked with ± are subcontracted to an ISO/IEC 17025:2017 accredited laboratory. Mycotoxin HPLC results have been corrected for recovery.

Sciantec Analytical Services is a division of the Cawood Scientific group. Registered Number: 5655711. Registered Office: Coopers Bridge, Brackens Lane, Bracknell, Berkshire RG42 6NS

Appendix 3.1: Certificate of analysis (by van Soest analysis) of the composition of *Euphorbia tirucalli* biomass used in experiments in **Chapter 3**.



Appendix 3.2: Linearity of VFA yield response to co-digestion on a carbon molar yield basis. Note that the three colours pertain to initial substrate loadings (ISC) of 10, 30, and 60 g/L, respectively.



Fatty acid	Standard curve gradient (Peak area/g/L)	Regression R^2
Acetic acid	62916	0.9994
Propionic acid	104108	0.9990
Isobutyric acid	135426	0.9997
Butyric acid	135222	0.9988
Isovaleric acid	159532	0.9992
Valeric acid	156480	0.9989
Hexanoic acid	155550	0.9977

Appendix 3.2: Standard curves and details of associated linear regressions used in **Chapter 3** for quantification of C2-C6 volatile fatty acids by GC-FID.

Appendix to Chapter 4

Certificate of Analysis

Sciantec

University of Oxford, Engineering Science Department
Accounts
Engineering Science Department
17 Park Road
OX1 3PJ

Client Reference	OFI (YOUNG)
Details	OPUNTIA FICUS INDICA-YOUNG CLADODE
Date Received	08-Feb-2023
Date Reported	23-Feb-2023
Lab Reference No	3381117
Order Number	
Certificate No	s_3381117_OFI (YOUNG)_1.pdf
Product	Miscellaneous - Feed Miscellaneous - Feed
Sampled Date	1-Feb-2023
Sample Source	

Method No		Test	Units	Result	Completed On
S1012		Neutral Detergent Fibre	%	21.6	14-Feb-2023
S1092	*	Cellulose	%	8.6	23-Feb-2023
S1092	*	Hemicellulose	%	6.4	15-Feb-2023
S1112	*	Acid Detergent Lignin	%	6.57	23-Feb-2023
S1129	*	Acid Detergent Fibre	%	15.20	12-Feb-2023

Unless otherwise stated results are expressed on an 'as received' basis.

Sciantec Analytical Services.
Stockbridge Technology Centre, Cawood, Yorkshire
YO8 3SD
t + 44 (0) 1757 242400
f + 44 (0) 1757 242401
www.sciantec.uk.com

Martin Dyer

Technical Function Manager

UKAS TESTING 2511

These results relate only to the sample(s) tested and do not guarantee the bulk of the material to be of equal quality. This report shall not be reproduced except in full, without the written approval of Sciantec Analytical Services . Sciantec Analytical Services. was not responsible for sampling and cannot be held liable in respect of the use to which information is put.
A certificate having a number with a suffix of _2 or greater is supplementary to the original report. Tests marked with # are subcontracted to a UKAS accredited laboratory. Tests marked '#' are subcontracted to a non UKAS accredited laboratory. Tests marked with * are outside UKAS scope of accreditation. Microbiological assays marked with (p) are presumptive. Tests marked with ± are subcontracted to an ISO/IEC 17025:2017 accredited laboratory. Mycotoxin HPLC results have been corrected for recovery.

Sciantec Analytical Services is a division of the Cawood Scientific group. Registered Number: 5655711. Registered Office: Coopers Bridge, Braziers Lane, Bracknell, Berkshire RG42 6NS

Certificate of Analysis

Sciantec

University of Oxford, Engineering Science Department
Accounts
Engineering Science Department
17 Park Road
OX1 3PJ

Client Reference	OFI (OLD)
Details	OPUNTIA FICUS INDICA-MATURE CLADODE
Date Received	08-Feb-2023
Date Reported	23-Feb-2023
Lab Reference No	3381118
Order Number	
Certificate No	s_3381118_OFI (OLD)_1.pdf
Product	Miscellaneous - Feed Miscellaneous - Feed
Sampled Date	1-Feb-2023
Sample Source	

Method No		Test	Units	Result	Completed On
S1012		Neutral Detergent Fibre	%	26.9	14-Feb-2023
S1092	*	Cellulose	%	12.6	23-Feb-2023
S1092	*	Hemicellulose	%	5.5	15-Feb-2023
S1112	*	Acid Detergent Lignin	%	8.73	23-Feb-2023
S1129	*	Acid Detergent Fibre	%	21.38	12-Feb-2023

Unless otherwise stated results are expressed on an 'as received' basis.

Sciantec Analytical Services.
Stockbridge Technology Centre, Cawood, Yorkshire
YO8 3SD
t + 44 (0) 1757 242400
f + 44 (0) 1757 242401
www.sciantec.uk.com

Martin Dyer

Technical Function Manager

UKAS TESTING 2511

These results relate only to the sample(s) tested and do not guarantee the bulk of the material to be of equal quality. This report shall not be reproduced except in full, without the written approval of Sciantec Analytical Services . Sciantec Analytical Services. was not responsible for sampling and cannot be held liable in respect of the use to which information is put.
A certificate having a number with a suffix of _2 or greater is supplementary to the original report. Tests marked with # are subcontracted to a UKAS accredited laboratory. Tests marked '#' are subcontracted to a non UKAS accredited laboratory. Tests marked with * are outside UKAS scope of accreditation. Microbiological assays marked with (p) are presumptive. Tests marked with ± are subcontracted to an ISO/IEC 17025:2017 accredited laboratory. Mycotoxin HPLC results have been corrected for recovery.

Sciantec Analytical Services is a division of the Cawood Scientific group. Registered Number: 5655711. Registered Office: Coopers Bridge, Braziers Lane, Bracknell, Berkshire RG42 6NS

Certificate of Analysis

Sciantec

University of Oxford, Engineering Science Department
Accounts
Engineering Science Department
17 Park Road
OX1 3PJ

Client Reference	PINEAPPLE
Details	ANANAS COSMOSUS LEAF
Date Received	08-Feb-2023
Date Reported	23-Feb-2023
Lab Reference No	3381121
Order Number	
Certificate No	s_3381121_PINEAPPLE_1.pdf
Product	Miscellaneous - Feed Miscellaneous - Feed
Sampled Date	1-Feb-2023
Sample Source	

Method No		Test	Units	Result	Completed On
S1012		Neutral Detergent Fibre	%	46.4	14-Feb-2023
S1092	*	Cellulose	%	10.1	23-Feb-2023
S1092	*	Hemicellulose	%	21.2	15-Feb-2023
S1112	*	Acid Detergent Lignin	%	15.08	23-Feb-2023
S1129	*	Acid Detergent Fibre	%	25.21	12-Feb-2023

Unless otherwise stated results are expressed on an 'as received' basis.

Sciantec Analytical Services.
Stockbridge Technology Centre, Cawood, Yorkshire
YO8 3SD
t + 44 (0) 1757 242400
f + 44 (0) 1757 242401
www.sciantec.uk.com

Martin Dyer

Technical Function Manager

UKAS TESTING 2511

These results relate only to the sample(s) tested and do not guarantee the bulk of the material to be of equal quality. This report shall not be reproduced except in full, without the written approval of Sciantec Analytical Services . Sciantec Analytical Services. was not responsible for sampling and cannot be held liable in respect of the use to which information is put.
A certificate having a number with a suffix of _2 or greater is supplementary to the original report. Tests marked with # are subcontracted to a UKAS accredited laboratory. Tests marked '#' are subcontracted to a non UKAS accredited laboratory. Tests marked with * are outside UKAS scope of accreditation. Microbiological assays marked with (p) are presumptive. Tests marked with ± are subcontracted to an ISO/IEC 17025:2017 accredited laboratory. Mycotoxin HPLC results have been corrected for recovery.

Sciantec Analytical Services is a division of the Cawood Scientific group. Registered Number: 5655711. Registered Office: Coopers Bridge, Braziers Lane, Bracknell, Berkshire RG42 6NS

Certificate of Analysis

Sciantec

University of Oxford, Engineering Science Department
Nicholas Tenci

Client Reference	AGAVE FIBRE
Details	AGAVE FIBRE
Date Received	24-Feb-2023
Date Reported	9-Mar-2023
Lab Reference No	3395275
Order Number	DF2086997
Certificate No	s_3395275_AGAVE FIBRE_1.pdf
Product	Miscellaneous - Feed Miscellaneous - Feed
Sampled Date	1-Feb-2023
Sample Source	

Method No		Test	Units	Result	Completed On
S1012		Neutral Detergent Fibre	%	71.1	3-Mar-2023
S1092	*	Cellulose	%	50.6	9-Mar-2023
S1092	*	Hemicellulose	%	17.4	8-Mar-2023
S1112	*	Acid Detergent Lignin	%	3.09	9-Mar-2023
S1129	*	Acid Detergent Fibre	%	53.73	8-Mar-2023

Unless otherwise stated results are expressed on an 'as received' basis.

Sciantec Analytical Services.
Stockbridge Technology Centre, Cawood, Yorkshire
YO8 3SD
t + 44 (0) 1757 242400
f + 44 (0) 1757 242401
www.sciantec.uk.com

Alan Ash

Technical Support Manager

UKAS TESTING 2511

These results relate only to the sample(s) tested and do not guarantee the bulk of the material to be of equal quality. This report shall not be reproduced except in full, without the written approval of Sciantec Analytical Services . Sciantec Analytical Services. was not responsible for sampling and cannot be held liable in respect of the use to which information is put.
A certificate having a number with a suffix of _2 or greater is supplementary to the original report. Tests marked with # are subcontracted to a UKAS accredited laboratory. Tests marked '#' are subcontracted to a non UKAS accredited laboratory. Tests marked with * are outside UKAS scope of accreditation. Microbiological assays marked with (p) are presumptive. Tests marked with ± are subcontracted to an ISO/IEC 17025:2017 accredited laboratory. Mycotoxin HPLC results have been corrected for recovery.

Sciantec Analytical Services is a division of the Cawood Scientific group. Registered Number: 5655711. Registered Office: Coopers Bridge, Braziers Lane, Bracknell, Berkshire RG42 6NS

Appendix 4.1: Certificates of analysis (by van Soest analysis) of the composition of biomass used in experiments in **Chapter 4**.

Certificate of Analysis

University of Oxford, Engineering Science Department
Accounts
Engineering Science Department
17 Park Road
OX1 3PJ

Client Reference	AGAVE (PULP)
Details	AGAVE ANGUSTIFOLIA DECORTICATED PULP
Date Received	08-Feb-2023
Date Reported	23-Feb-2023
Lab Reference No	3381120
Order Number	
Certificate No	s_3381120_AGAVE (PULP)_1.pdf
Product	Miscellaneous - Feed Miscellaneous - Feed
Sampled Date	1-Feb-2023
Sample Source	

Method No		Test	Units	Result	Completed On
S1012		Neutral Detergent Fibre	%	16.9	14-Feb-2023
S1092	*	Cellulose	%	9.0	23-Feb-2023
S1092	*	Hemicellulose	%	<0.1	15-Feb-2023
S1112	*	Acid Detergent Lignin	%	9.17	23-Feb-2023
S1129	*	Acid Detergent Fibre	%	18.19	12-Feb-2023

Unless otherwise stated results are expressed on an 'as received' basis.

Sciantec Analytical Services.
Stockbridge Technology Centre, Cawood, Yorkshire
YO8 3SD
t + 44 (0) 1757 242400
f + 44 (0) 1757 242401
www.sciantec.uk.com

Martin Dyer
Technical Function Manager

UKAS TESTING 2511

These results relate only to the sample(s) tested and do not guarantee the bulk of the material to be of equal quality. This report shall not be reproduced except in full, without the written approval of Sciantec Analytical Services . Sciantec Analytical Services. was not responsible for sampling and cannot be held liable in respect of the use to which information is put.
A certificate having a number with a suffix of _2 or greater is supplementary to the original report. Tests marked with # are subcontracted to a UKAS accredited laboratory. Tests marked "# are subcontracted to a non UKAS accredited laboratory. Tests marked with " are outside UKAS scope of accreditation. Microbiological assays marked with (p) are presumptive. Tests marked with ± are subcontracted to an ISO/IEC 17025:2017 accredited laboratory. Mycotoxin HPLC results have been corrected for recovery.

Sciantec Analytical Services is a division of the Cawood Scientific group. Registered Number: 5655711. Registered Office: Coopers Bridge, Braziers Lane, Bracknell, Berkshire RG42 6NS

Certificate of Analysis

University of Oxford, Engineering Science Department
Accounts
Engineering Science Department
17 Park Road
OX1 3PJ

Client Reference	AGAVE (WHOLE)
Details	AGAVE ANGUSTIFOLIA WHOLE LEAF
Date Received	08-Feb-2023
Date Reported	23-Feb-2023
Lab Reference No	3381119
Order Number	
Certificate No	s_3381119_AGAVE (WHOLE)_1.pdf
Product	Miscellaneous - Feed Miscellaneous - Feed
Sampled Date	1-Feb-2023
Sample Source	

Method No		Test	Units	Result	Completed On
S1012		Neutral Detergent Fibre	%	30.8	14-Feb-2023
S1092	*	Cellulose	%	18.0	23-Feb-2023
S1092	*	Hemicellulose	%	5.1	15-Feb-2023
S1112	*	Acid Detergent Lignin	%	7.69	23-Feb-2023
S1129	*	Acid Detergent Fibre	%	25.68	12-Feb-2023

Unless otherwise stated results are expressed on an 'as received' basis.

Sciantec Analytical Services.
Stockbridge Technology Centre, Cawood, Yorkshire
YO8 3SD
t + 44 (0) 1757 242400
f + 44 (0) 1757 242401
www.sciantec.uk.com

Martin Dyer
Technical Function Manager

UKAS TESTING 2511

These results relate only to the sample(s) tested and do not guarantee the bulk of the material to be of equal quality. This report shall not be reproduced except in full, without the written approval of Sciantec Analytical Services . Sciantec Analytical Services. was not responsible for sampling and cannot be held liable in respect of the use to which information is put.
A certificate having a number with a suffix of _2 or greater is supplementary to the original report. Tests marked with # are subcontracted to a UKAS accredited laboratory. Tests marked "# are subcontracted to a non UKAS accredited laboratory. Tests marked with " are outside UKAS scope of accreditation. Microbiological assays marked with (p) are presumptive. Tests marked with ± are subcontracted to an ISO/IEC 17025:2017 accredited laboratory. Mycotoxin HPLC results have been corrected for recovery.

Sciantec Analytical Services is a division of the Cawood Scientific group. Registered Number: 5655711. Registered Office: Coopers Bridge, Braziers Lane, Bracknell, Berkshire RG42 6NS

Certificate of Analysis

University of Oxford, Engineering Science Department
Accounts
Engineering Science Department
17 Park Road
OX1 3PJ

Client Reference	WHEAT
Details	TRITICUM AESTIVUM STRAW
Date Received	08-Feb-2023
Date Reported	23-Feb-2023
Lab Reference No	3381123
Order Number	
Certificate No	s_3381123_WHEAT_1.pdf
Product	Miscellaneous - Feed Miscellaneous - Feed
Sampled Date	1-Feb-2023
Sample Source	

Method No		Test	Units	Result	Completed On
S1012		Neutral Detergent Fibre	%	55.3	14-Feb-2023
S1092	*	Cellulose	%	17.2	23-Feb-2023
S1092	*	Hemicellulose	%	26.5	15-Feb-2023
S1112	*	Acid Detergent Lignin	%	11.60	23-Feb-2023
S1129	*	Acid Detergent Fibre	%	28.81	12-Feb-2023

Unless otherwise stated results are expressed on an 'as received' basis.

Sciantec Analytical Services.
Stockbridge Technology Centre, Cawood, Yorkshire
YO8 3SD
t + 44 (0) 1757 242400
f + 44 (0) 1757 242401
www.sciantec.uk.com

Martin Dyer
Technical Function Manager

UKAS TESTING 2511

These results relate only to the sample(s) tested and do not guarantee the bulk of the material to be of equal quality. This report shall not be reproduced except in full, without the written approval of Sciantec Analytical Services . Sciantec Analytical Services. was not responsible for sampling and cannot be held liable in respect of the use to which information is put.
A certificate having a number with a suffix of _2 or greater is supplementary to the original report. Tests marked with # are subcontracted to a UKAS accredited laboratory. Tests marked "# are subcontracted to a non UKAS accredited laboratory. Tests marked with " are outside UKAS scope of accreditation. Microbiological assays marked with (p) are presumptive. Tests marked with ± are subcontracted to an ISO/IEC 17025:2017 accredited laboratory. Mycotoxin HPLC results have been corrected for recovery.

Sciantec Analytical Services is a division of the Cawood Scientific group. Registered Number: 5655711. Registered Office: Coopers Bridge, Braziers Lane, Bracknell, Berkshire RG42 6NS

Certificate of Analysis

University of Oxford, Engineering Science Department
Accounts
Engineering Science Department
17 Park Road
OX1 3PJ

Client Reference	MAIZE
Details	ZEA MAYS STOVER
Date Received	08-Feb-2023
Date Reported	23-Feb-2023
Lab Reference No	3381124
Order Number	
Certificate No	s_3381124_MAIZE_1.pdf
Product	Miscellaneous - Feed Miscellaneous - Feed
Sampled Date	1-Feb-2023
Sample Source	

Method No		Test	Units	Result	Completed On
S1012		Neutral Detergent Fibre	%	52.2	14-Feb-2023
S1092	*	Cellulose	%	28.0	23-Feb-2023
S1092	*	Hemicellulose	%	21.0	15-Feb-2023
S1112	*	Acid Detergent Lignin	%	3.18	23-Feb-2023
S1129	*	Acid Detergent Fibre	%	31.20	12-Feb-2023

Unless otherwise stated results are expressed on an 'as received' basis.

Sciantec Analytical Services.
Stockbridge Technology Centre, Cawood, Yorkshire
YO8 3SD
t + 44 (0) 1757 242400
f + 44 (0) 1757 242401
www.sciantec.uk.com

Martin Dyer
Technical Function Manager

UKAS TESTING 2511

These results relate only to the sample(s) tested and do not guarantee the bulk of the material to be of equal quality. This report shall not be reproduced except in full, without the written approval of Sciantec Analytical Services . Sciantec Analytical Services. was not responsible for sampling and cannot be held liable in respect of the use to which information is put.
A certificate having a number with a suffix of _2 or greater is supplementary to the original report. Tests marked with # are subcontracted to a UKAS accredited laboratory. Tests marked "# are subcontracted to a non UKAS accredited laboratory. Tests marked with " are outside UKAS scope of accreditation. Microbiological assays marked with (p) are presumptive. Tests marked with ± are subcontracted to an ISO/IEC 17025:2017 accredited laboratory. Mycotoxin HPLC results have been corrected for recovery.

Sciantec Analytical Services is a division of the Cawood Scientific group. Registered Number: 5655711. Registered Office: Coopers Bridge, Braziers Lane, Bracknell, Berkshire RG42 6NS

Appendix 4.1 (Continued): Certificates of analysis (by van Soest analysis) of the composition of biomass used in experiments in **Chapter 4**.

Certificate of Analysis

University of Oxford, Engineering Science Department
Accounts
Engineering Science Department
17 Park Road
OX1 3PJ

Client Reference	MISCANTHUS
Details	MISCANTHUS SINENSIS WHOLE LEAF
Date Received	08-Feb-2023
Date Reported	23-Feb-2023
Lab Reference No	3381122
Order Number	
Certificate No	s_3381122_MISCANTHUS_1.pdf
Product	Miscellaneous - Feed Miscellaneous - Feed
Sampled Date	1-Feb-2023
Sample Source	

Method No		Test	Units	Result	Completed On
S1012		Neutral Detergent Fibre	%	72.6	14-Feb-2023
S1092	*	Cellulose	%	22.8	23-Feb-2023
S1092	*	Hemicellulose	%	37.6	15-Feb-2023
S1112	*	Acid Detergent Lignin	%	12.22	23-Feb-2023
S1129	*	Acid Detergent Fibre	%	35.04	12-Feb-2023

Unless otherwise stated results are expressed on an 'as received' basis.

Martin Dyer
Technical Function Manager

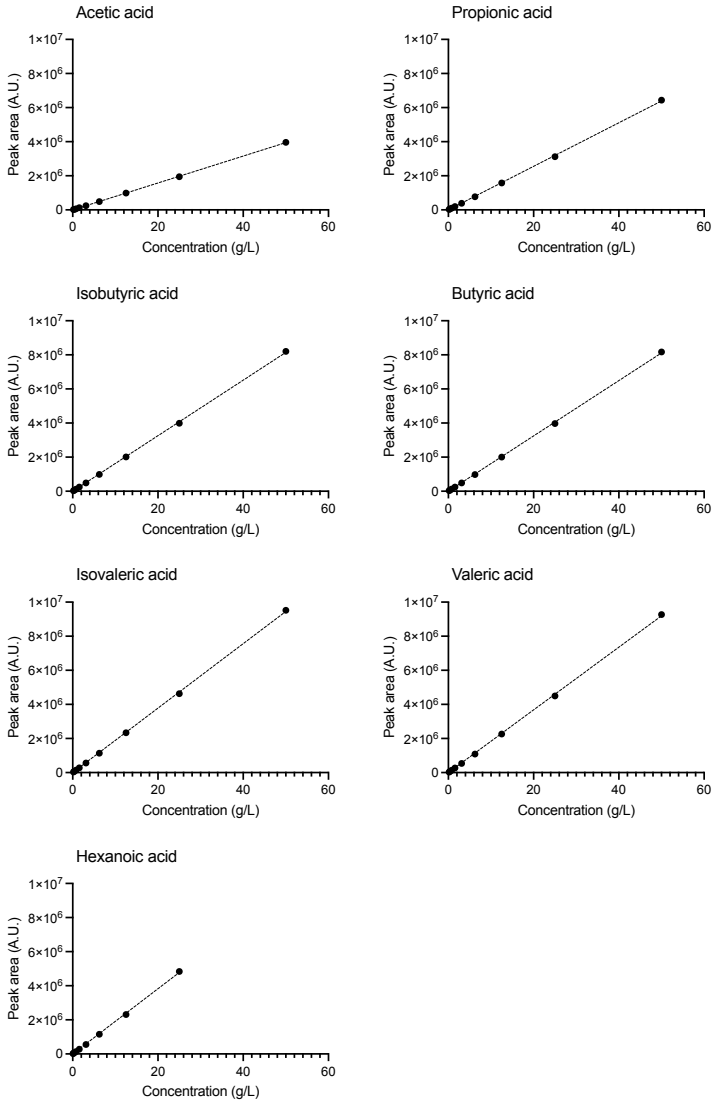
Sciantec Analytical Services.
Stockbridge Technology Centre, Cawood, Yorkshire
YO8 3SD
t + 44 (0) 1757 242400
f + 44 (0) 1757 242401
www.sciantec.uk.com

UKAS TESTING
2511

These results relate only to the sample(s) tested and do not guarantee the bulk of the material to be of equal quality. This report shall not be reproduced except in full, without the written approval of Sciantec Analytical Services . Sciantec Analytical Services. was not responsible for sampling and cannot be held liable in respect of the use to which information is put.
A certificate having a number with a suffix of _2 or greater is supplementary to the original report. Tests marked with # are subcontracted to a UKAS accredited laboratory. Tests marked "#' are subcontracted to a non UKAS accredited laboratory. Tests marked with * are outside UKAS scope of accreditation. Microbiological assays marked with (p) are presumptive. Tests marked with ± are subcontracted to an ISO/IEC 17025:2017 accredited laboratory. Mycotoxin HPLC results have been corrected for recovery.

Sciantec Analytical Services is a division of the Cawood Scientific group. Registered Number: 5655711. Registered Office: Coopers Bridge, Braziers Lane, Bracknell, Berkshire RG42 6NS

Appendix 4.1 (Continued): Certificates of analysis (by van Soest analysis) of the composition of biomass used in experiments in **Chapter 4**.



Fatty acid	Standard curve gradient (Peak area/g/L)	Regression R^2
Acetic acid	78930	0.9999
Propionic acid	127762	0.9998
Isobutyric acid	162885	0.9998
Butyric acid	162255	0.9998
Isovaleric acid	189076	0.9998
Valeric acid	183908	0.9998
Hexanoic acid	191181	0.9996

Appendix 4.2: Standard curves and details of associated linear regressions used in **Chapter 4** for quantification of C2-C6 volatile fatty acids by GC-FID.

Appendix to Chapter 5



Certificate of Analysis

University of Oxford, Engineering Science Department
Accounts
Engineering Science Department
17 Park Road
OX1 3PJ

Client Reference	ASPARAGOPSIS
Details	ASPARAGOPSIS TAXIFORMIS (WHOLE)
Date Received	08-Feb-2023
Date Reported	23-Feb-2023
Lab Reference No	3381125
Order Number	
Certificate No	s_3381125_ASPARAGOPSIS_1.pdf
Product	Miscellaneous - Feed Miscellaneous - Feed
Sampled Date	1-Feb-2023
Sample Source	

Method No		Test	Units	Result	Completed On
S1012		Neutral Detergent Fibre	%	19.2	14-Feb-2023
S1092	*	Cellulose	%	5.8	23-Feb-2023
S1092	*	Hemicellulose	%	12.1	15-Feb-2023
S1112	*	Acid Detergent Lignin	%	1.25	23-Feb-2023
S1129	*	Acid Detergent Fibre	%	7.03	12-Feb-2023

Unless otherwise stated results are expressed on an 'as received' basis.

Sciantec Analytical Services.
Stockbridge Technology Centre, Cawood, Yorkshire
YO8 3SD
t + 44 (0) 1757 242400
f + 44 (0) 1757 242401
www.sciantec.uk.com

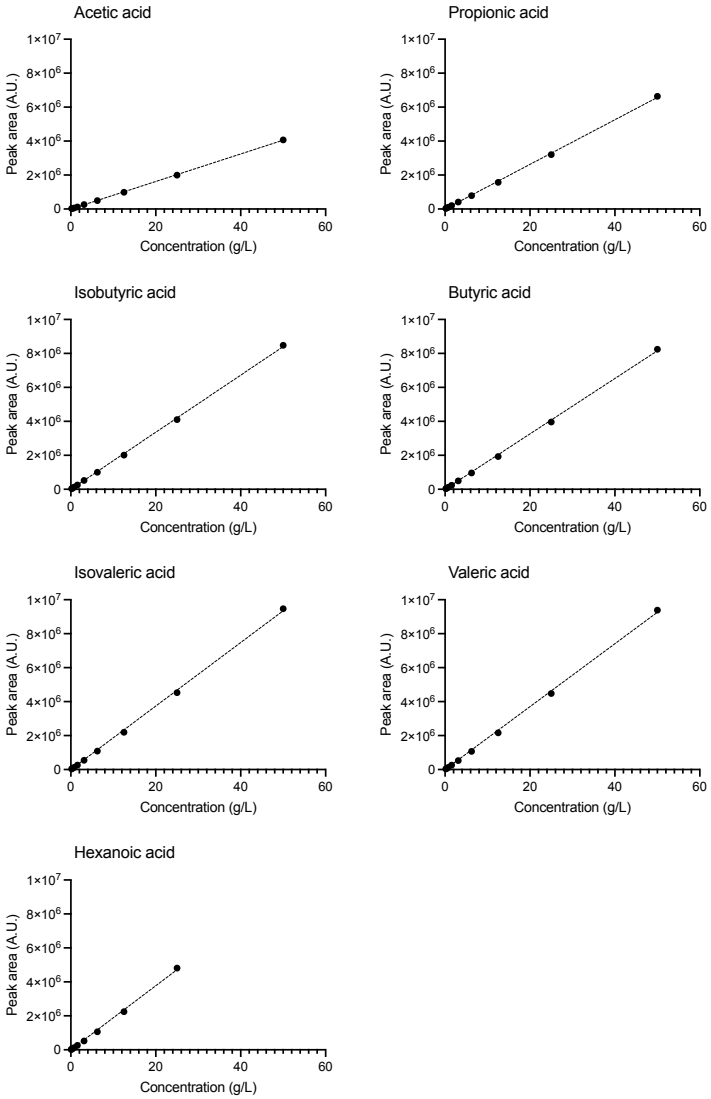
UKAS TESTING
2511

Martin Dyer
Technical Function Manager

These results relate only to the sample(s) tested and do not guarantee the bulk of the material to be of equal quality. This report shall not be reproduced except in full, without the written approval of Sciantec Analytical Services . Sciantec Analytical Services. was not responsible for sampling and cannot be held liable in respect of the use to which information is put.
A certificate having a number with a suffix of _2 or greater is supplementary to the original report. Tests marked with # are subcontracted to a UKAS accredited laboratory. Tests marked *# are subcontracted to a non UKAS accredited laboratory. Tests marked with * are outside UKAS scope of accreditation. Microbiological assays marked with (p) are presumptive. Tests marked with ± are subcontracted to an ISO/IEC 17025:2017 accredited laboratory. Mycotoxin HPLC results have been corrected for recovery.

Sciantec Analytical Services is a division of the Cawood Scientific group. Registered Number: 5655711. Registered Office: Coopers Bridge, Braziers Lane, Bracknell, Berkshire RG42 6NS

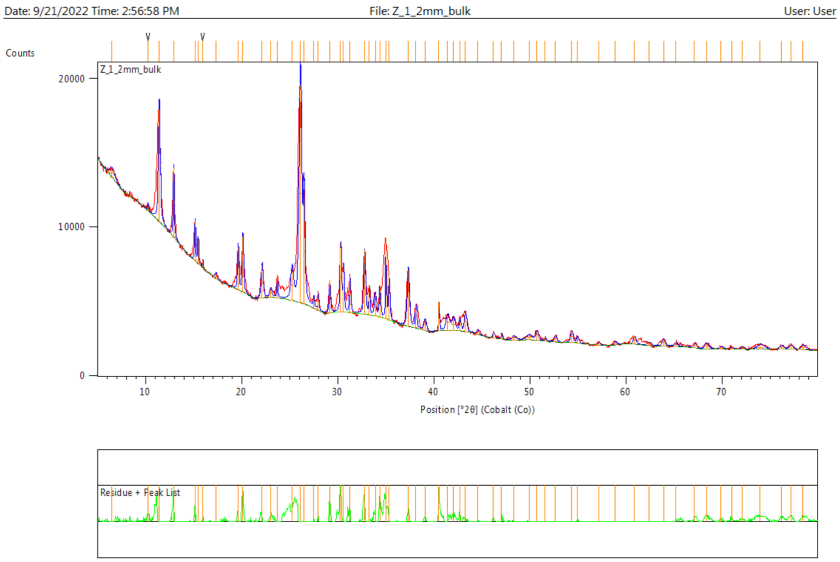
Appendix 5.1: Certificate of analysis (by van Soest analysis) of the composition of *Asparagopsis taxiformis* used in experiments in **Chapter 5**.



Fatty acid	Standard curve gradient (Peak area/g/L)	Regression R^2
Acetic acid	81081	0.9999
Propionic acid	131426	0.9997
Isobutyric acid	168021	0.9997
Butyric acid	163107	0.9996
Isovaleric acid	186961	0.9994
Valeric acid	185234	0.9994
Hexanoic acid	188617	0.9986

Appendix 5.1: Standard curves and details of associated linear regressions used in **Chapter 5** for quantification of C2-C6 volatile fatty acids by GC-FID.

Appendix to Chapter 6

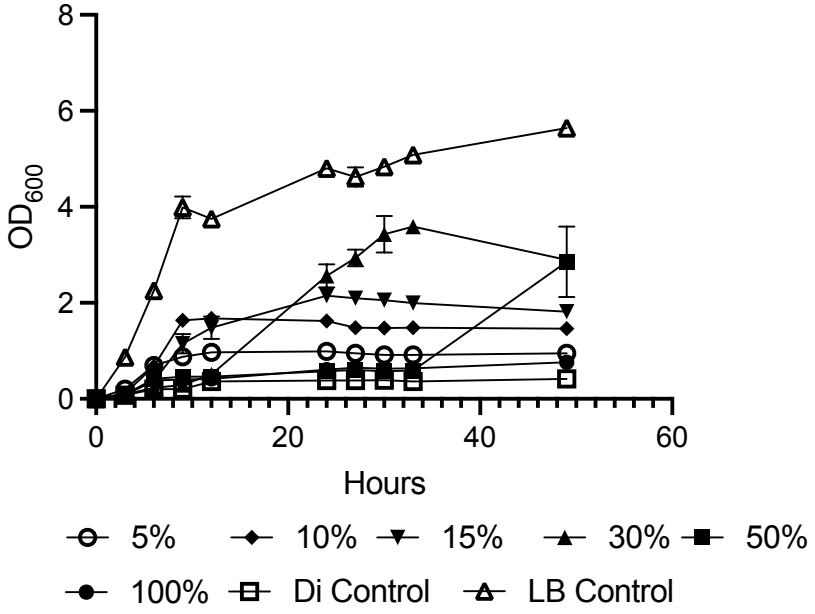


Pattern List

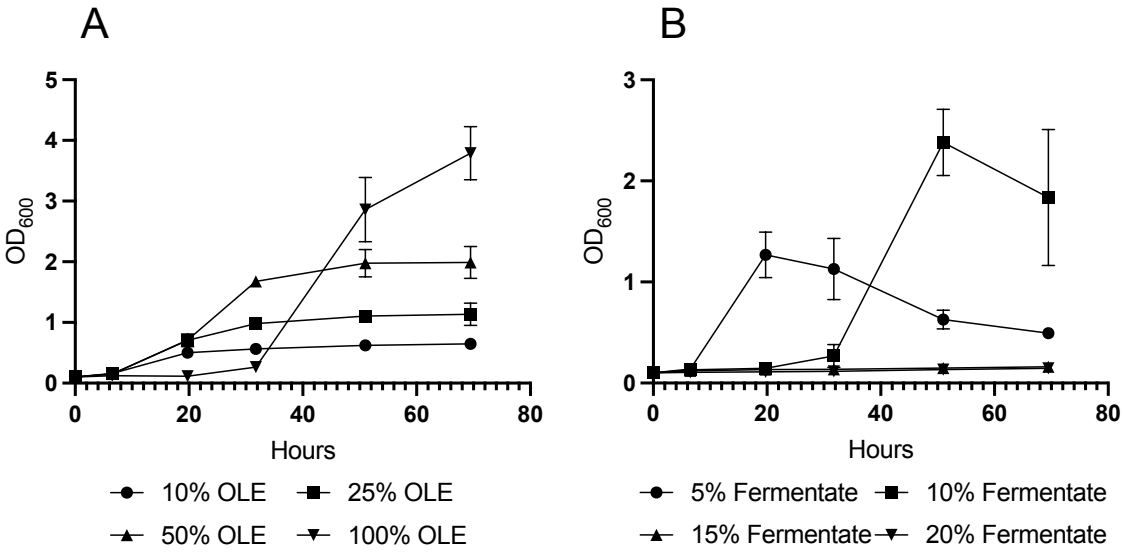
Ref.Code	Mineral Name	SemiQuant[%]	Score	Compound Name	Scale Fac.	Chem. Formula
01-081-8442		82	67	Potassium Hydronium Nickel Aluminum Silicate Hydrate	1.060	((H3 O)3.3 K0.3 Ni1.3) (Al6.2 Si29.8 O72) (H2 O)16.4
04-012-1134		12	17	Silicon Oxide	0.160	Si O2
04-013-3129	Taranakite, deuterated, syn	6	16	Deuterium Potassium Aluminum Phosphate Deuterate	0.139	D6 K3 Al5 (P O4)8 (D2 O)18

Appendix 6.1: Diffractogram obtained through x-ray powder diffraction analysis of zeolite used in **Chapter 6** and associated semi-quantitative assignment of composition. The most abundant phase (estimated at ~82% of the material) is represented by clinoptilolite, with smaller contributions by other phases.

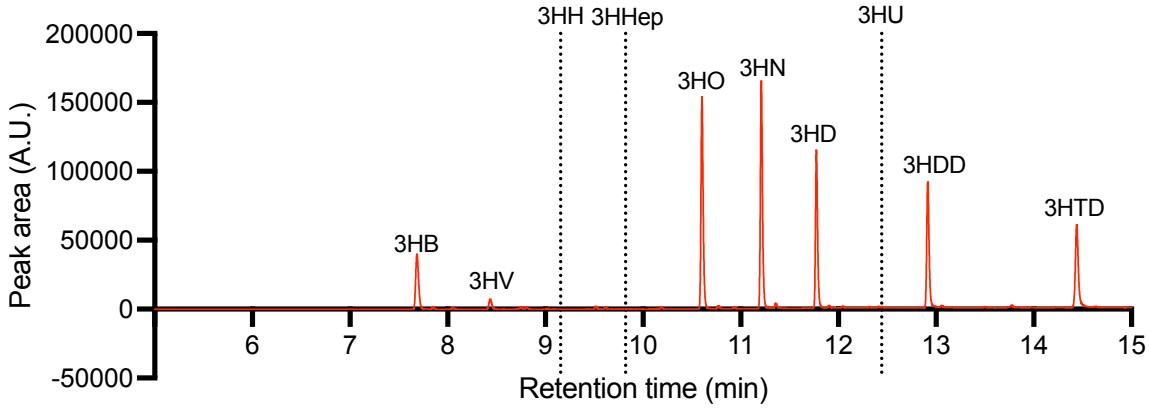
Appendix to Chapter 7



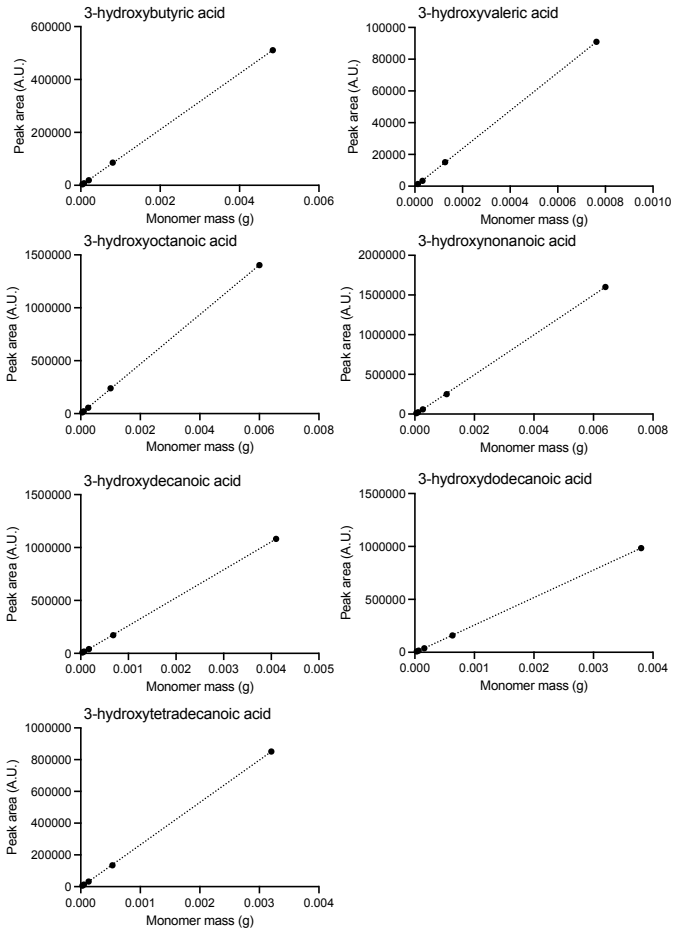
Appendix 7.1: Growth curves of *C. necator* on *Opuntia* fermentate used in calibration of media conditions in *P. putida* experiments. Di = Deionised water, LB = Lysogeny broth.



Appendix 7.2: Growth curves of *C. necator* on *Opuntia* Liquid Extract (OLE) and *Opuntia* fermentate used in calibration of media conditions in *C. necator* experiments. A) C. necator growth on OLE at various dilutions in deionised water. B) *C. necator* growth on various dilutions of fermentate in deionised water.



Appendix 7.3: Exemplar of a typical GC-FID chromatogram from a mixed PHA monomer standard solution as produced by the GC-FID method used in **Chapter 7** for the determination of VFA concentrations in samples. Several standards (3HH, 3HHep, 3HU) were unable to be obtained for experimental quantification and their response factors were determined by interpolation from adjacent standards. The positions of these missing peaks are indicated by vertical dotted lines.



Monomer	**Standard curve gradient** (Peak area/g)	**Regression R^2**
3HB	105622914	1.0000
3HV	119177716	1.0000
3HH*	157471737*	-
3HHep*	195765758*	-
3HO	234059779	1.000
3HN	249764157	1.000
3HD	263388719	1.000
3HU*	261167947*	-
3HDD	258947267	1.000
3HTD	265688510	1.000

Appendix 7.4: Standard curves and details of associated linear regressions used in **Chapter 7** for quantification of PHA monomers by GC-FID. Standard curves were calculated against total monomer mass per sample processed as per the standard protocols outlined in **Chapter 7**, hence the units of the x axes are grams. For several standards, the response factors were interpolated based on a weighted average of the response factors of adjacent standards. These are indicated by an asterisk.

Intellectual Property Office

Patents Form 1
Patents Act 1977 *(Rule 12)*

Request for grant of a patent

Concept House
Cardiff Road
Newport
South Wales
NP10 8QQ

Application number

1.	Your reference	**N429556GB**
2.	Full name, address and postcode of the applicant or of each applicant Patents ADP number *(if you know it)*	**Oxford University Innovation Limited** **Buxton Court** **3 West Way** **Oxford OX2 0JB** **United Kingdom**
3.	Title of the invention	**BACTERIAL PROCESS FOR PREPARATION OF MICROBIAL STORAGE LIPIDS**
4.	Name of your agent *(if you have one)* "Address for service" to which all correspondence should be sent. This may be in the United Kingdom, the Channel Islands or Gibraltar (see warning note below) *(including the postcode)* Patents ADP number *(if you know it)*	**J A Kemp LLP** **J A Kemp LLP** **80 Turnmill Street** **London EC1M 5QU** **Greater London** **United Kingdom**
5.	Priority declaration: Are you claiming priority from one or more earlier-filed patent applications? If so, please give details of the application(s)	

Country	Application number	Date of filing	PDAS Access Code

6.	Divisionals etc: Is this application a divisional application, or being made following resolution of an entitlement dispute about an earlier application. If so, please give the application number and filing date of the earlier application	Number of earlier UK application	Date of filing *(day / month / year)*
7.	Inventorship: (Inventors must be individuals not companies) Are all the applicants named above also inventors?	**No**	
8.	Are you paying the application fee with this form?	**Yes**	

(REV JAN21)
Intellectual Property Office is an operating name of the Patent Office

Patents Form 1(e)
https://www.gov.uk/ipo

Appendix 7.5: Application for grant of patent for zeolite-mediated modulation of fermentate C:N ratios for microbial storage lipid production.